Application of Amine Transaminases in the Chemoenzymatic Synthesis of Chiral Amines using Isopropylamine as Amine Donor

I n a u g u r a l d i s s e r t a t i o n

zur

Erlangung des akademischen Grades eines

Doktors der Naturwissenschaften (Dr. rer. nat.)

der

Mathematisch-Naturwissenschaftlichen Fakultät

der

Universität Greifswald

vorgelegt von

Ayad Dawood

Greifswald, November 2018

Dekan: Prof. Dr. Werner Weitschies

1. Gutachter : Prof. Dr. Uwe T. Bornscheuer

2. Gutachter: Dr. Florian Rudroff

Tag der Promotion: 07.02.2019

Table of contents

Scope and outline

Amine transaminases are versatile biocatalysts for the production of pharmaceutically and agrochemically relevant chiral amines. They represent an environmentally benign alternative to waste intensive transition metal catalysed synthesis strategies, especially because of their high stereoselectivity and robustness. Therefore, they have been frequently used in the (chemo)enzymatic synthesis of amines and/or became attractive targets for enzyme engineering especially in the last decade, mainly in order to enlarge their substrate scope. Certainly, one of the most notable examples of amine transaminase engineering is the manufacturing of the anti-diabetic drug Sitagliptin in large scale after several rounds of protein engineering. Thereby, the target amine was produced in asymmetric synthesis mode which is the most convenient and favored route to a target chiral amine, starting from the corresponding ketone. The choice of the amine donor is highly relevant for reaction design in terms of economical and thermodynamic considerations. For instance, the use of alanine as the natural amine donor is one of the most common strategies for the amination of target ketones but needs the involvement of auxiliary enzymes to shift the reaction equilibrium towards product formation. In fact, isopropylamine is probably one of the most favored donor molecules since it is cheap and achiral but it is supposed to be accepted only by a limited number of amine transaminases.

This thesis focusses on the optimization and application of amine transaminases for asymmetric synthesis reactions *en route* to novel target chiral amines using isopropylamine as the preferred amine donor.

In **Article I** the production of various halogen substituted chiral amines is presented. Suitable enantiocomplementary amine transaminases were identified via molecular docking experiments and were applied in asymmetric synthesis mode with isopropylamine as donor.

Article II aims the better understanding and consistency in usage of isopropylamine. Structural properties in the amine transaminase from *Ruegeria* sp. TM1040 were identified, which are responsible for isopropylamine acceptance. Furthermore, a systematic investigation of the pH-value, donor-acceptor ratio and stability effects was conducted for several amine transaminases with the aim to find a more general guidance for reaction engineering using isopropylamine.

In **Article III** the combination of amine transaminase activity with a chemical cross-coupling reaction of aryl compounds in chemoenzymatic one-pot fashion was demonstrated. The engineering of the transaminase from *Aspergillus fumigatus* was performed to generate the better acceptance of biaryl ketones. Isopropylamine was used as the amine donor. The immobilization of amine transaminases for the application in (proof-of-concept) continuous flow systems was subject of **Articles III** and **IV**.

Publication list

Article I	**Ayad W. H. Dawood**, Rodrigo O. M. A. de Souza, Uwe T. Bornscheuer, **Asymmetric Synthesis of Chiral Halogenated Amines using Amine Transaminases**, *ChemCatChem* **2018**, *10*, 951–955.
Article II	**Ayad W. H. Dawood**, Martin S. Weiß, C. Schulz, Ioannis V. Pavlidis, Hans Iding, Rodrigo O. M. A. de Souza, Uwe T. Bornscheuer, **Isopropylamine as Amine Donor in Transaminase-Catalyzed Reactions: Better Acceptance through Reaction and Enzyme Engineering**, *ChemCatChem* **2018**, *10*, 3943–3949.
Article III	**Ayad W. H. Dawood**, Jonathan Bassut, Rodrigo O. M. A. de Souza, Uwe T. Bornscheuer, **Combination of the Suzuki-Miyaura Cross-Coupling Reaction with Engineered Transaminases**, *Chem. Eur. J.* **2018**, *24*, 16009–16013.
Article IV	Stefania P. de Souza, Ivaldo I. Junior, Guilherme M. A. Silva, Leandro S. M. Miranda, Marcelo F. Santiago, Frank Leung-Yuk Lam, **Ayad Dawood**, Uwe T. Bornscheuer, Rodrigo O. M. A. de Souza, **Cellulose as an efficient matrix for lipase and transaminase immobilization**, *RSC Adv.* **2016**, *6*, 6665–6671.

1. Transaminases, members of PLP-dependent enzymes

The majority of enzyme activity depends on co-factors, which are either inorganic ions or small organic compounds.[1] Pyridoxal-5'-phosphate (PLP) as derivative of the B_6 vitamin (pyridoxamine) is considered to be one of the most relevant co-factors in nature. It plays a significant role in a great number of cellular processes in terms of anabolic or catabolic amino acid metabolism or even the biosynthesis of amino sugars.[2–4] The physiological importance of PLP-dependent enzymes is underlined by the fact that several drugs target the malfunction of PLP-enzymes in the therapy of e.g. epilepsy,[5] the African sleeping sickness[6] or even some kinds of cancer.[7] The utilization of PLP was found in various enzyme classes (see enzyme commission numbers, E.C.) including lyases, isomerases, hydrolases, oxidoreductases and transferases catalysing more than 200 distinct chemical reactions. This makes PLP certainly the most versatile co-factor.[1,2,8] Prominent examples for PLP-catalysed reactions are the transamination, decarboxylation, racemisation, α-β-elimination and retro-aldol cleavage reaction.[9,10] All of these mentioned reactions have one underlying principle of PLP-catalysed chemistry in common, namely the resonance stabilization of the formed carbanion intermediate. After Michaelis-complex formation the next intermediate is called external aldimine (Figure 1) in which one part of reaction specificity control of PLP-dependent enzymes lies. The appropriate coordination of the external aldimine forces an σ-π-orbital overlapping between the bond which has to be cleaved and the pyridine ring of the PLP by an orthogonal orientation.[1,11] That allows the subsequent stabilization of the formed negative charge by the co-factor after C-bond cleavage (Dunathan principle).[2,8,9,11,12] Thereby, the enzyme scaffold defines significantly which bond is going to be broken by the active site architecture as derived from crystallographic studies of PLP-enzymes.[13–15] For example, decarboxylases coordinate their substrate accordingly to mediate a Cα-carboxyl bond cleavage and lyases (like threonine-aldolase) focus on the Cα-Cβ or Cβ-Cγ bond.

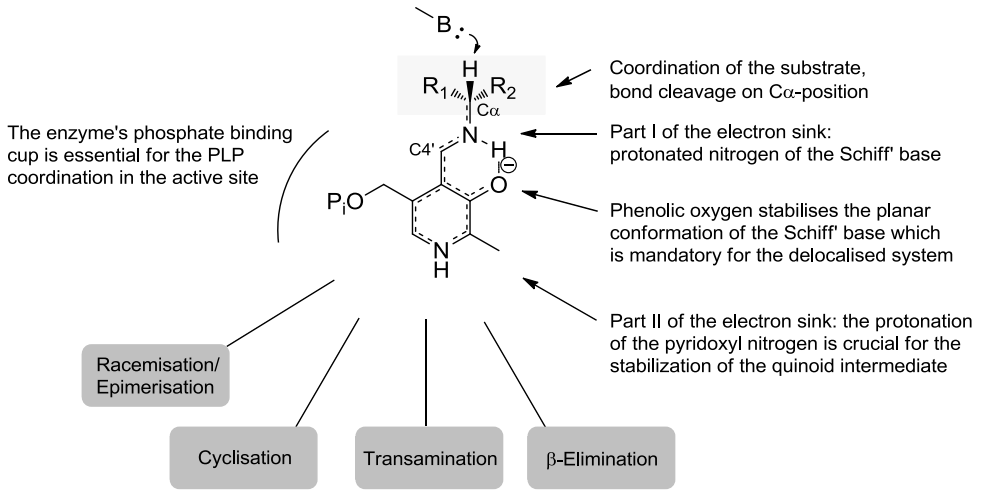

Figure 1. Illustration of the external aldimine, modified after reference[9]. The targeted bond for cleavage is weakened by the PLP π-electron system which is perpendicular orientated. The two nitrogens in the intermediate act as 'electron sink' and are responsible for the charge delocalization of the formed carbanion. For transaminases, acidic amino acids in proximity of the pyridine nitrogen are highly conserved for the control of its protonation state.[8] P_i = phosphate group.

In contrast, a large number of PLP-catalysed reactions are initiated by Cα-proton abstraction which is also crucial for the transamination, racemization and α-β-elimination reaction (Figure 1).[9] The actual degree of resonance stabilisation is the other determining part for reaction specificity control and separates the latter reaction types as well. In literature, the term *electron sink*[1] has been established to address the mechanistic reason for the charge delocalisation effect. Here, the involvement of two nitrogens in the intermediate molecule – the protonated imine nitrogen of the Schiff' base and the (protonated or not) pyridine nitrogen – is relevant. The phenolic oxygen of PLP interferes with the Schiff' base nitrogen via a keto-enol-tautomerism and favours the ketoenamine form as well as planarity of the imine and pyridine ring.[16] So, the protonated form of the imine maintaines the electron sink character of the Schiff' base and therefore is capable to stabilize reaction transition states. The protonation state of the pyridine nitrogen modulates the electrophilic strength of the Schiff' base-pyridine-π-electron system and determines the actual reaction type significantly. In racemases the pyridine nitrogen is uncharged, limiting the carbanion intermediate stabilisation via the Schiff' base nitrogen only. If however the pyridine nitrogen is kept protonated (and therefore charged) by acidic amino acid residues, the stabilisation of the carbanion over the entire molecule becomes possible and allows the formation of the quinoid intermediate which is the key intermediate step in e.g. transamination and α-β-elimination reactions.[9] Again, the enzyme scaffold determines the actual reaction type by controlling the pyridine protonation state.[8,11] However, despite the multitude of reaction types PLP-enzymes can catalyse, they are solely grouped in seven fold classes based on their three-dimensional structures.[10,17] In these fold types of PLP-dependent enzymes, transaminases (TA, E.C. 2.6.1.x) are members of the fold types I and IV and are additionally divided into six subclasses based on sequence homologies.[8,18] TAs (or synonymously called aminotransferases) catalyse the transfer of an amine group from an amine donor to an acceptor molecule, following a Ping-Pong Bi-Bi-reaction mechanism (Scheme 1A, see Chapter 1.1 for more details). They are sharing an overall quaternary protein structure consisting of a functional homo dimer (or sometimes even higher-ordered oligomers) and often a small and large domain per monomer.[2,12] The active site is located at the interface between both subunits, composed of amino acids from each monomer.

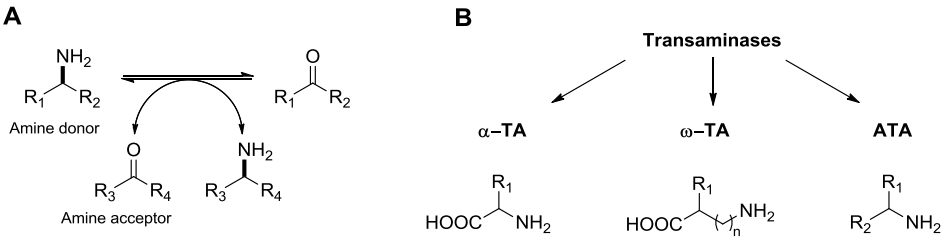

Scheme 1. **A** Scheme of a transaminase catalysed reaction. **B** Illustration of the different classes of transaminases with their natural substrates. Redrawn from reference[19].

The substrate scope of TAs is another approach for a classification, mainly referring to the presence and position of the transferred amine group and/or carboxyl moiety of natural substrates (Scheme 1B).[19] Due to the latter classification α-TAs, ω-TAs and Amine-TAs (ATA) are categorized. ATAs (subclass II

and III of the transaminase family) are of special interest for the (chemo)enzymatic application, since they tolerate substrates without a carboxyl moiety and therefore a wide range of amines, ketones or aldehydes.[8,17] The ATA from the bacteria *Vibrio fluvialis* was first described[20,21] and became one of the best investigated representatives of this enzyme class through the years.[22–25]

1.1. Transamination reaction mechanism

The reaction chemistry of PLP-dependent transamination was extensively studied on aspartate amino transferases and aromatic amino acid transferases[26,27] by crystallographic investigations of enzyme-substrate complexes. Recently, Cassimjie et al. proposed a detailed mechanism of the deamination of 1-phenylethylamine on the basis of simulation aided quantum mechanical studies using an active site model of the ATA from *Chromobacterium violaceum*.[28] However, generally all TAs are supposed to follow the same reaction mechanism but differing drastically in substrate specificity.[29] TAs catalyse the oxidative deamination of an amine donor and the reductive amination of an amine acceptor in two distinct half reactions.[2,12,19,26] The first one consists of the conversion of the amine donor to its corresponding ketone whereas in the second half-reaction the (ketone) amine acceptor is converted to the final amine product. During one complete cycle of transamination the co-factor PLP alters between its aldehyde and amine form (pyridoxamine-5'-phosphate – PMP), respectively and acts as an 'amine group shuttle'. Due to the regeneration of PLP by a second substrate (and because dealing with in total four substrates/products), TAs exhibit a Ping-Pong Bi-Bi reaction mechanism.[19] In the enzyme resting state the co-factor is bound covalently to the ε-amino group of the highly conserved catalytic lysine forming the internal aldimine (or internal Schiff' base). As first step of the catalytic cycle the amino group of the donor molecule undertakes a nucleophilic attack at the iminium carbon (C4', see Figure 1) of PLP and undergoes a transaldimination reaction with a geminal diamine intermediate (Michaelis-complex).[30] Thereby, a coordinated water molecule in the active site is supposed to take the role of a proton shuttle during attack from the substrate amino group to the phenolic oxygen of PLP. The subsequently formed PLP-substrate complex is called external aldimine and is common for all PLP-dependent enzymes.[1] As described above, substrate coordination defines significantly the following reaction type by the principle of stereoelectronic control (Dunathan principle): By the perpendicular orientation of the Cα-H bond of the bound substrate (Figure 1) and the π-electron system of PLP an σ-π-orbital overlapping is forced in order to weaken the bond of interest by lowering the pKa of the α-carbon and so facilitating proton abstraction by the catalytic lysine. The proton abstraction on Cα causes the planar quinoid intermediate in which the formed carbanion is resonance stabilized over the entire intermediate molecule (electron sink effect), dispending electrons for the formulation of new bonds.[1] Here, this new bond is formed with an incoming proton at C4', transferred by the catalytic lysine and resulting in the ketimine intermediate. This proton transfer (from Cα to C4') is characteristic for enzymatic transamination and at the same time the rate-limiting step.[31–34] This makes the resonance stabilization character of the pyridine/Schiff' base system the key feature in the transamination reaction and thus the tautomeric conversion of the aldimine to the ketimin via the quinoid intermediate becomes possible (Scheme 2).[31]

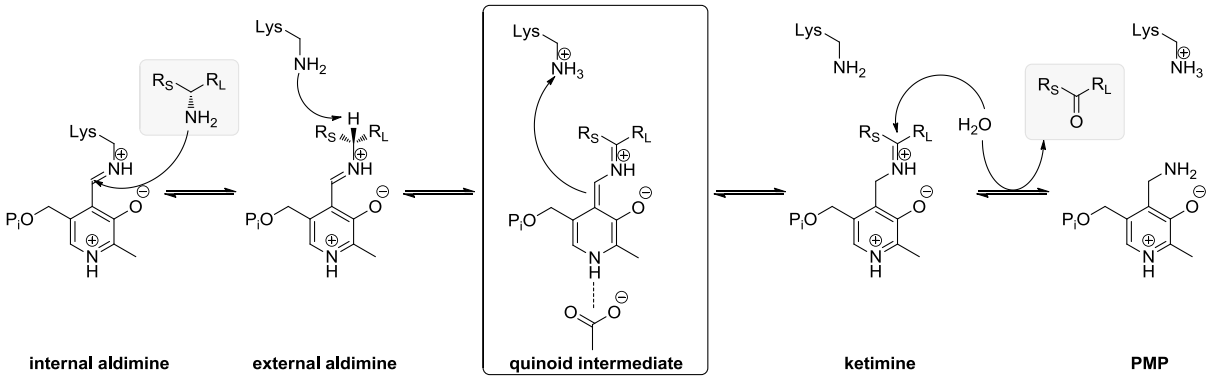

Scheme 2. Schematic overview of the first transamination half-reaction. The geminal diamine and the carbinolamine intermediate are omitted for clarity. After forming the external aldimine as first intermediate after substrate binding, a proton transfer occurs by the catalytic lysine from the Cα of the bound substrate to C4' of the co-factor PLP (see Figure 1). The formed carbanion after proton abstraction is resonance stabilized via the planar quinoid intermediate. This quinoid intermediate is central for each half-reaction, since the dearomatized character of the pyridine ring generates a charge delocalization effect over the entire molecule which is significantly mediated by the protonated pyridine nitrogen. The protonation state is controlled by conserved acidic amino acid residues in the active site. This overall constellation therefore allows hydration at C4' and subsequently rearomatization of the pyridine ring. After hydrolysis of the following ketimine intermediate the ketone product releases and PMP is formed. P_i = phosphate group.

Notably, the keto-enol-tautomerism between the imine nitrogen and the phenolic oxygen of PLP is also supposed to have an influence on quinoid reactivity.[16,28] Finally, the ketimine intermediate is hydrolysed to PMP and the ketone product is released via a carbinolamine intermediate step. Again, the catalytic lysine is supposed to have its participation as proton carrier during hydrolysis.[28] Thus, one half-reaction is complete, followed by the second consisting of the same intermediates in reversed order and yielding the amine product as well as the regenerated co-factor.

1.2. Amine Transaminases (ATAs) generate enantioselectivity by a two-pocket-active site

The excellent enantioselectivity of ATAs is certainly one of their most significant features.[26] Depending on the accepted enantiomer of a regarded substrate (*S*)-selective ATAs (fold class I of PLP-dependent enzymes) and (*R*)-selective ATAs (fold class IV) are distinguishable. Up to 2010 a large number of (*S*)-selective ATAs had been identified but only two (*R*)-selective ones.[35,36] Then, Höhne et al.[37] were able to mine putative (*R*)-ATA candidate protein sequences from databases by identification of sequence motives for ATA activity. The discovery of 17 novel (*R*)-ATAs revealed that all are belonging to the subclass IV of the transaminase family (D-amino acid aminotransferase superfamily).[12,38] The high enantioselectivity of ATAs already has been noticed from substrate scope investigations at a stage when no structural information about this enzyme group existed (e.g.[22,23,39]). From those experiments active site models for a few ATAs were concluded. The postulated two-pocket-model – consisting of a small and a large binding pocket – was later confirmed by various crystal structures[40,41] proving that the small binding pocket naturally accommodates only a methyl or ethyl group relating to the Cα atom of the substrate. In contrast, the large one has space for a phenyl or a carboxyl moiety. Thus, an inverted

substrate would not fit appropriately in the active site. This strict allocation of substrate moieties is considered as fundamental basis for the excellent ATA stereoselectivity (Figure 2A). Besides that, the mirrored active site architecture of these enantiocomplementary enzymes on the one hand forces the coordination of the small substituent of the substrate to the *P-side* of PLP and the large one to the *O-side* (referring to the phosphate group and phenolic oxygen of PLP).[42] Additionally, the topographical arrangement of the catalytic lysine in (*S*)- and (*R*)-selective ATAs allows the proton transfer from C4' to Cα during catalysis only from opposite sites, respectively (see Figure 2B and C).[30,43] In (*R*)-ATAs the catalytic lysine is located at the *re*-face of the intermediate, relating to the PLP-C4', so the *si*-face is solvent exposed, and vice versa in (*S*)-ATAs. Only with the 'right' enantiomer a productive binding mode and therefore chiral product formation is achievable. Consequently, the inclusion of PLP coordination and the topology of catalytically key amino acid residues play an important role in determining chirality of the newly formed product.

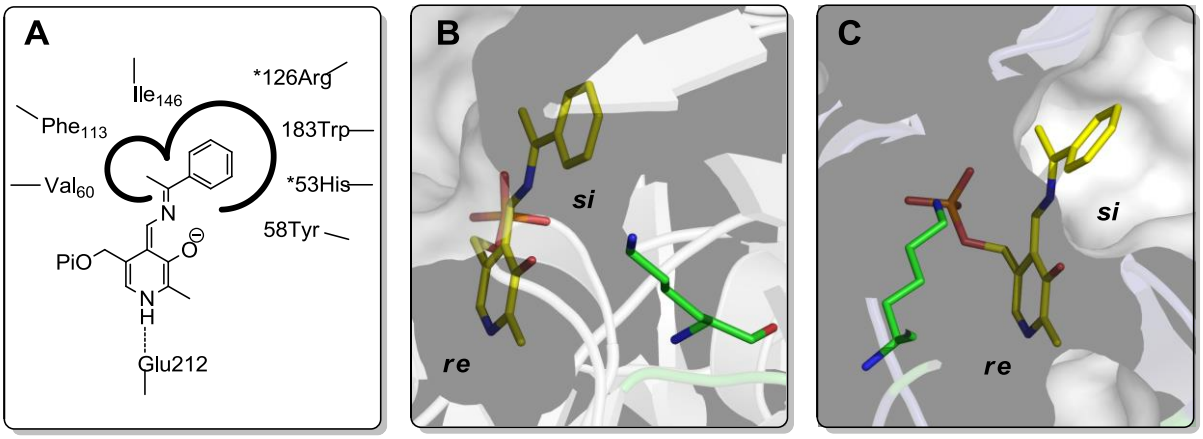

Figure 2. **A** Schematic presentation of the two-binding pocket model. The active site of *Aspergillus fumigatus'* ATA was taken as example.[38] Stars indicate the contribution of the other monomer. The catalytic lysine is omitted for clarity. **B** and **C** Active sites of the two enantiocomplementary ATAs from *Silicibacter pomeroyi*[44] (**B**) and *Aspergillus fumigatus* (**C**). The catalytic lysine (green sticks) is located at two different sides of the intermediate molecule in both ATAs and conducts the characteristic suprafacial proton transfer[30] on either the *re* or *si* side, respectively. The quinoid intermediate consisting of 1-phenylethylamine is shown (yellow sticks). P_i = phosphate group.

2. Application of enzymes in organic chemistry – biocatalytic versus chemical synthesis

In the last few decades, enzymes in general have been established as considerable catalysts in organic synthesis and industrial processes for the production of a broad range of pharmaceuticals, fine chemicals, food additives or polymers.[45,46] Indeed, a large number of compounds in the pharmaceutical or agrochemical field, which were marketed since years, contain key intermediates produced by biocatalysts.[47] While in the 1990s, biocatalysis was narrowed to a couple of reaction types using hydrolases and a few reductases[45,48] meanwhile science in the field of (industrial) application of enzymes created a huge number of organic synthesis processes including alcohol dehydrogenases, lyases, Baeyer-Villiger monooxygenases (BVMO) and transferases for the synthesis of alcohols, amines, amides, amino acids and carboxylic acids, to name only a few.[48,49] Undoubtedly, the driving force for this enormous progress was the influence of several factors, like meaningful achievements in molecular biology, biotechnology, bioinformatics, enzyme discovery and engineering (see Chapter 3) as well as high-throughput screenings.[46,50] Biocatalysed reactions have indeed several strengths over their chemical counterparts, for instance the high reaction specificity of enzymes, the fact of less waste production or the operation under mild reaction conditions in terms of temperature and pH, but not least due to the ability of enzymes to introduce chirality into molecules with very high regio- and enantioselectivity.[51,52] Around 80% of all commercialized compounds are chiral with rising trend[53] and chemical synthesis strategies for chiral compounds usually utilize toxic transition or heavy metals in conjunction with chiral ligands or protection/de-protection strategies under harsh reaction conditions. And finally the chiral product is often obtained in moderate yield and enantiomeric excess what entails further purification steps.[26,46,54–57] Thus, the scientific community claimed alternative strategies for synthetic routes to optically active compounds or building blocks, also against the background of increasing regulations by government institutions regarding environmental protection and product impurities after downstream processing.[46,47,53,54,58] One particular example for the latter was the announcement of European and American drug regulation instances in 1992 which approved strict limits regarding racemic mixtures of pharmaceutical compounds, since the physiological activity is often linked to the absolute configuration of a molecule.[53,59] Consequently, biocatalysis gained increasing attraction over the last years and became more and more a considerable and environmentally benign alternative to classic chemical routes, especially when a high chemo-, regio- and enantioselectivity is demanded.[45,48,50,52,60,61] Over time milestones in the field of biocatalysis were achieved by the production of several active pharmaceutical ingredients (APIs, or intermediates thereof) in large scale and high yield utilizing various enzyme classes, for instance by marketing of pregabaline and psymberin (anti-epilepsy and cytotoxin, lipase-catalysed), montelukast and pseudoephedrine (anti-asthma and sympathomimetica, reductase-catalysed), telaprevir (anti-hepatitis C, mono amine oxidase-catalysed), armodafinil (psychostimulant, BVMO-catalysed) or sitagliptin (diabetes type II treatment, TA-catalysed).[45,62] Certainly, in some cases one of the main enhancements was the significant shortened synthesis route by introduction of biocatalytic steps. Additionally, biocatalytic routes sometimes even facilitate the operation in one-pot fashion which avoids chromatography steps and often means higher overall yield, like it was shown for the synthesis of ε-caprolactam when employing an alcohol

dehydrogenase, a BVMO, a TA and an esterase in a sequential multi-enzyme cascade reaction.[63] The given examples show insistently that the access to a number of relevant compounds in agrochemical, food and pharmaceutical industry by biocatalysis is a considerable alternative. In order to generate and maintain the industrial relevance of a biocatalyst, in some of the mentioned cases enzyme-characteristic limitations in stereo-/regioselectivity, substrate scope, product or substrate inhibition and process stability had to be overcome. Protein engineering became a highly relevant field in the biocatalytic application of enzymes to address those limitations.

3. Protein engineering

Protein engineering is a valuable tool for biocatalyst improvement, especially when alteration of reaction conditions or the identification of new, more suitable enzymes failed.[56] The advances in recombinant DNA technology were certainly the major driving force for developing of innovative techniques in protein engineering.[45] Essentially, there are two main strategies in enzyme engineering, the rational design and directed evolution. Rational design highly depends on information about the protein structure and catalytic mechanism in order to predict changes in protein structure or amino acid sequence to induce or alter a certain enzyme activity or property.[64] Herein, certain strategically crucial points or regions of the protein are targeted in order to achieve significant improvements within a few steps of site-directed mutagenesis. In rational design the availability of protein crystal structures play a special role, which are a fundamental basis of the scientist's knowledge about the protein. Indeed, the early works of rational design were hampered by the limited amount of published crystal structures.[65] However, in the last decade rational design got a massive input by the rising number of published protein crystal structures and the intensive development of a vast number of *in silico* tools.[45,56,66] Meanwhile, a large number of software supports the scientist in creation and evaluation of protein variants which increased the probability of beneficial mutations significantly.[65,67,68] Molecular modelling emerged to a very powerful tool in rational design.[64] It mimics protein behaviour *in silico* on the bases of experimental data and therefore aims a more precise prediction of mutational effects.[69–71] Incidentally, a very interesting and promising approach is the *de novo* enzyme design, therefore the introduction of a novel enzyme activity, very often without a starting sequence scaffold.[65] A deep knowledge of the desired reaction and transition states is mandatory for a prediction of a possible active site by molecular modelling or a library based search for appropriate protein scaffolds via fitting algorithms.[72] A few reports are known in which enzyme activity is *de novo* generated by computational design catalysing for instance a Kemp elimination,[73] a Diels-Alder reaction[74] or a Retro-Aldol reaction[75] but at extremely low reaction rates. In contrast to the distinct structure-function analysis by rational design, directed evolution bases on random mutagenesis. The pioneer work was performed by Stemmer and Arnold,[76–79] introducing the basis of a necessary repertoire of molecular biology methods in order to modify the respective biocatalyst via an *in vitro* version of evolution.[45] Regarding a certain DNA sequence the random introduction of mutations is nowadays accomplished by e.g. using a DNA polymerase with significantly increased error-rate by applying non-optimal reaction conditions (error-prone PCR, epPCR). Usually, the *Taq* DNA polymerase is used because it lacks proofreading. The major advantage of direct evolution is that no (structural) information about the protein is required. Changes are rather made over the entire gene sequence which generates an enormous amount of protein variants (which are obtained in libraries). Those variants are screened towards the desired activity or property to identify a beneficial mutation which itself serves as template of the next round of mutagenesis.[64,65] This iterative character makes directed evolution a very time and labor intensive technique with high demand of satisfying high-throughput methods, especially when various positions are mutated in parallel. Several works addressed the issue of a large library size to make the screening of enzyme variants 'smarter'.[45,56] One very effective way is the elimination of unnecessary codons. The principle of mutagenesis with these degenerated codons was presented by the Reetz group by introducing NNK (N stands for any nucleic

base, K for guanine or thymine) and NDT codons (D stands for adenine, guanine and thymine).[80] In the meantime, enzyme engineering was developed into a combination of both, rational design and directed evolution.[81–85] This form of complementary mutagenesis scientists call semi-rational protein design.[86] CASTing[87] (combinatorial active site saturation test) is one of the most prominent examples for a semi-rational design, which constitutes of the identification of crucial amino acids residues (mostly by rational design) which are then mutated by the means of random or site-directed mutagenesis.[66] The key selling point of this method is the simultaneous mutagenesis of a few amino acid residues in proximity in order to investigate cooperative mutational effects. Furthermore, other semi-rational design approaches target the identification of relevant positions from databases by searching for natural diversity and/or conservation.[65] An example is 3DM,[88] a commercial structure-based sequence alignment and analysis tool, which identifies the distribution of amino acids within a protein superfamily at a certain (structurally unique 3DM) position. Additionally, it mines literature data for 3DM-positions and analyses the connectivity between residues to highlight correlative mutations. Though, as every structure-guided (consensus) approach also 3DM bases on the idea that consensus amino acid sequences (or 3DM core regions) of an alignment are the 'enzyme fitness' determining regions.[65] But fulfilling this requirement, 3DM allows the design of significantly reduced libraries with focus on hot spot amino acid positions which are characteristic for a specific property for a specific enzyme family what was successfully demonstrated by the Bornscheuer group.[89]

However, as result of the discussed techniques (and combinations thereof) a series of advances in the improvement of biocatalysts could be generated which are reviewed regularly (for the most recent examples see[61,90–92]). In the field of ATA engineering the acceptance of sterically demanding substrates was the main focus of engineering efforts in the last decade rather than improvements in enantioselectivity or towards substrate and product inhibition.[61,90] The manufacture of Sitagliptin was an impressive example for a substrate walking approach in a two-step fashion. First (semi-)rational alteration of a binding pocket of the ATA from *Arthrobacter* sp. (Arth-TA) using molecular docking techniques and second, a direct evolution approach to make the selected ATA fully accept the prositagliptin ketone and additionally the desired reaction conditions.[93] The best variant (Arthmut11-TA) contained 27 mutations after 11 rounds of mutagenesis. Other more recent achievements were given for example by the Bornscheuer group in which the ATAs from *Vibrio fluvialis* (Vfl-TA) and *Ruegeria sp.* were engineered to accommodate bulky substrates with high demand on the small binding pocket.[94–98] In these works methods of both, pure directed evolution and semi-rational design were used and led to a 8,900-fold improvement in activity in the best case.[97] In contrast, Dourado et al. used molecular docking and molecular dynamic simulation experiments (therefore only rational design) to create a variant of Vfl-TA which was able to convert a biphenyl compound[99] (see Chapter 6). As implied with the few examples mentioned, protein engineering significantly influenced the landscape of the pharmaceutical industry or fine chemical production and contributed to the maturation process of biocatalysis.[45,59,100]

3.1. High-throughput assays for ATAs

The choice of the assay is a crucial and efficiency determining step in the identification of enzymes with desired activity.[3,90] Especially, when scientists are facing large libraries either from enrichment cultivations or mutagenesis studies, the utilization of instrumental analytic like high performance liquid chromatography, gas chromatography, mass spectrometry or nuclear magnetic resonance spectroscopy is very time and labor consuming, so therefore not practical.[101] In the last two decades various high-throughput assays for the fast, easy and often sensitive determination of TA activity were developed.[90,102] In such cases a range of different substrates were tested to prove a high flexibility and adaptability of the presented assay. Nevertheless, at the route to Arthmut11-TA for instance Savile et al.[93] decided 'to screen' towards the target reaction under target conditions using low throughput analysis, presumably keeping the words from Frances Arnold in mind "*you get what you screen for*".[103] Since amino acids and keto acids are the natural substrates of TAs they were widely used in screening assays, in particular because of the favored reaction equilibrium when using pyruvate as amine acceptor in the screening towards target amines. The co-product alanine is the key compound for several high-throughput assays (Scheme 3A). For instance, Yun et al. published the quantification of amino acids using $CuSO_4$ under monitoring at 595 nm for the determination of TA activity.[104] Major drawbacks of this method are the detrimental effect of $CuSO_4$/MeOH on enzyme activity and the high background signal, especially when whole cells or crude lysate were used.[90,102] The Turner group presented the detection of alanine by coupling with D- or L-amino acid oxidases (AAO), respectively.[105] Hydrogen peroxide is formed during alanine oxidation which itself is detected via the activity of the horse radish peroxidase in combination with pyrogallol as colored indicator which is observable at 540 nm. Also in the glycine oxidase assay[106] (GO-assay), published by the Bornscheuer group, the activity of the horse radish peroxidase is used for detection of H_2O_2. Glyoxylate is supposed to be equally accepted by TAs like pyruvate.[44,107,108] After transamination glycine is going to be converted back to glyoxylate by a thermostable glycine oxidase from *Geobacillus kaustophilus*[109] under hydrogen peroxide formation. In turn, the hydrogen peroxide is incorporated into the oxidation of phenol to benzoquinone which forms a colored quinone based imine dye. The GO-assay is applicable as both, a solid phase and a liquid-phase version. The latter is feasible in a microtiter plate fashion under monitoring via UV-Vis spectroscopy. The toxicity of phenol, the necessity of basic pH values for the oxidation of phenol and a moderate linear range in signal response for the liquid-phase version are considerable drawbacks.[106] Nevertheless, the solid phase GO-assay is very attractive for the screening of large mutant libraries. Indeed, several directed evolution approaches were conducted with solid phase assays dealing with e.g. esterases, oxidases or racemases.[110–113] However, also the formation of pyruvate can be detected in a coupled enzyme assay (Scheme 3B). In this way the target amine is produced during the assay using alanine as amine donor.[90] Thereby, the enzyme cascade reaction with lactate dehydrogenases (LDH) and glucose dehydrogenases (GDH) aims the *in situ* removal of pyruvate in order to drive the reaction towards product formation (for detailed information see Chapter 5.1). A modification of this LDH/GDH system[114] includes the detection of gluconic acid via an pH indicator (phenol red, observable at 560 nm).[115,116]

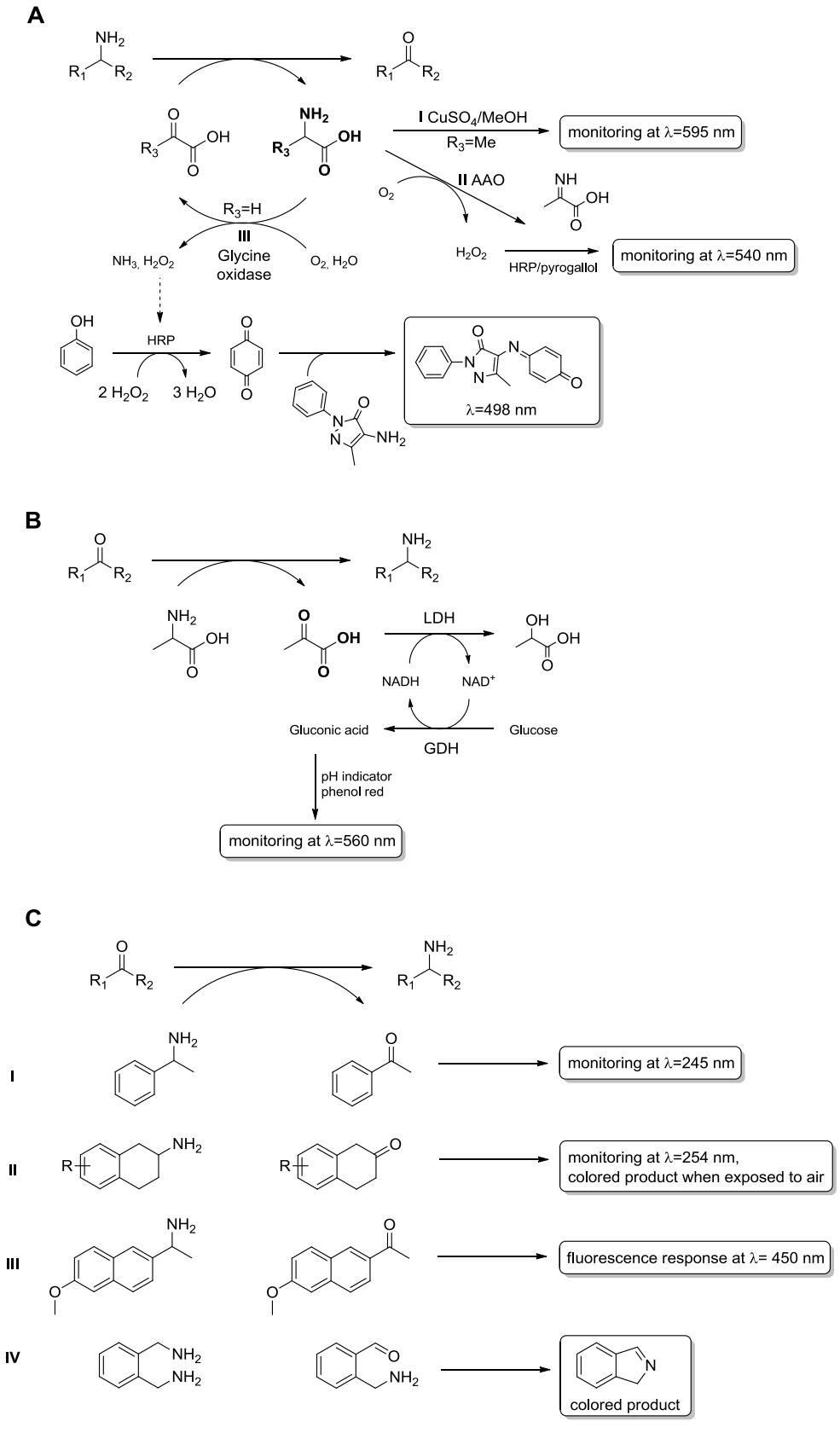

Scheme 3. High-throughput assays for the detection of ATA activity. AAO = amino acid oxidase, HRP = horse radish peroxidase, LDH = lactate dehydrogenase, GDH = glucose dehydrogenase, NAD = nicotinamide adenine dinucleotide, Me = methyl group.

A couple of other assays are based on the application of certain amine donors whose corresponding ketone is (in contrast to the described reactions so far) directly detected (Scheme 3C). The acetophenone assay[117] for example, developed by the Bornscheuer group, is a very powerful high-throughput assay which allows the sensitive and quantitative analysis of TA activity (Scheme 3C I).[90,118] Starting with 1-phenylethylamine as amine donor, the formation of acetophenone can be monitored at 245 nm with significant absorption intensity (ε= 12 mM^{-1} cm^{-1}). Furthermore, this assay is highly adaptable regarding the choice of the amine acceptor and reaction conditions.[119] Martin et al. reported the application of aminotetraline (and substituted derivatives) in the first directed evolution approach targeting the activity and thermostability of the ATA from *Arthrobacter citreus*.[120] The signal of the corresponding ketone is detectable at 254 nm but remains not stable since a change in color occurs when the compound is exposed to air (Scheme 3C II). The group of Berglund developed an assay in which the fluorophore acetonaphthone is produced (Scheme 3C III).[121] The intensive fluorescence signal can be monitored at 450 nm with a very low background response. Interestingly, Green et al. published the concept of a 'smart' amine donor, *ortho*-xylylenediamine.[122] After transamination the co-product undergoes an intramolecular imine formation which is followed by a spontaneous 1,5-hydrid shift forming the more favored aromatic isoindole which additionally polymerizes and forms a black precipitate (Scheme 3C IV). Therefore, by this *in situ* co-product removal the reaction is 'pulled' towards product formation (for an explanation see Chapter 5.1). So, Green et al. provided a promising approach if the choice of the ketone substrate is thermodynamically not favored. Unfortunately, a strong background in color formation was observed which increases the chance of false-positive hits.[90] Interestingly, this assay is also applicable in solid phase. Following this example Baud et al. have shown a similar 'smart' amine donor with an option for solid phase screening based on 2-phenylethylamine derivatives.[123]

However, in summary the application of natural substrates like pyruvate or alanine ensures a generality regarding substrate acceptance but makes auxiliary enzymes and reagents necessary for signal detection what could hamper the assay if e.g. low expression levels or an insufficient compatibility in terms of reaction conditions are achievable.[106] On the other side the direct detection of a certain ketone product provides a higher grade of 'freedom-to-operate'[124] but scientists should take a low substrate acceptance and a considerable chance for side reactions into account.

4. Chiral amines

Like no other substance class amines are prevalent in natural chemical products and pharmaceutical or agrochemical active ingredients.[61] Many physiologically important substances are nitrogen containing, for example natural macromolecules or alkaloids from plant secondary metabolism or building blocks in drugs or drug candidates including primary, secondary and tertiary amines.[54,124] At the same time the N-C bond is often a stereogenic element in such molecules.[26] Roughly one third of the top 200 pharmaceutical products in 2014 are actually chiral amines (Figure 3). Since primary amines serve as convenient starting materials for the synthesis of higher substituted ones via alkylation reactions, as a consequence, α-chiral primary amines are of special interest in organic chemistry.[125,126]

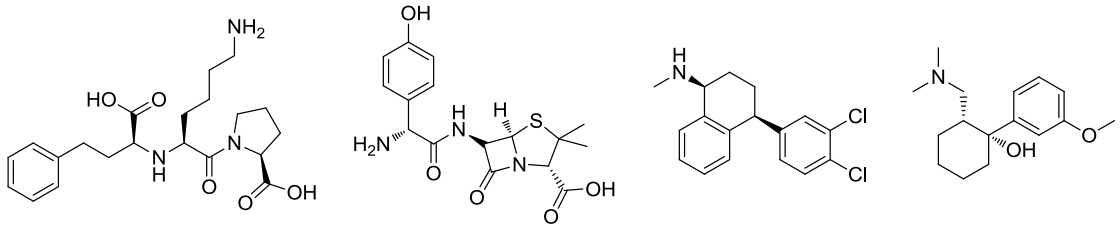

Figure 3. Examples of the top 200 pharmaceuticals.[127]

4.1. Chemical synthesis strategies

Although the chemical point of view is not the focus of this thesis, a few methods will be described briefly to give an overview to the reader. If more information are desired, further reading is recommended.[125,126] However, when starting from racemic mixtures of amines the most applied method for large scale productions is still a resolution process via crystallisation of the desired enantiomer by diastereomeric salt formation using resolving agents, mostly chiral carboxylic acids.[53,124] Quite often this method is combined with a continuous chiral chromatography step to supply the 'right' enantiomer for further reactions and additionally a racemisation unit is introduced to maximize yield.[124] Alternatively, ketones and aldehydes are used as cheap, achiral and easy accessible starting materials in asymmetric reductive amination. Most important methods here are the asymmetric hydrogenation and addition in which the educts are converted to ketimines, enamides or aldimines, respectively (Scheme 4). Chirality is accomplished under employment of chiral auxiliaries (R_1 and R_3 in Scheme 4) or chiral ligands, either by sterical hindrance effects in the chirality-introducing step or by favouring the one enantiomer over the other during product formation.[54,59,125] However, in both cases a protected secondary amine is formed from which an α-chiral primary amine is obtainable as final product via deprotection reactions. Obviously, both methods in Scheme 4 are differing in the range of accessible products, since the asymmetric addition for instance enables the synthesis of amines with a tertiary carbon in α-position by addition of carbanions or radicals to the aldimine.[125]

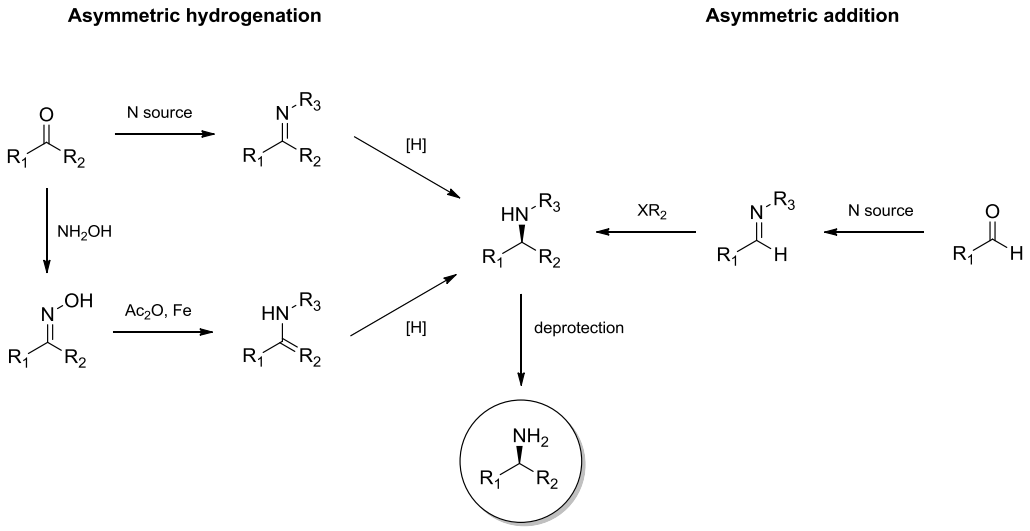

Scheme 4. Commonly used strategies for the chemical synthesis of primary chiral amines (redrawn from reference[54]). During asymmetric hydrogenation a proton insertion takes place at the stereo-differentiating step. This method was honoured with the Nobel Prize in 2001. In asymmetric addition the production of an aldimine from a carbanion occurs. Even combinations of both strategies are conceivable.[128]

Still, chemical synthesis strategies for stereospecific introduction of nitrogen are challenging in the light of avoidance of harsh and waste intensive reaction conditions and the assurance of high chemo-, regio-, and especially enantioselectivity.[53,54,125,126] Even recent chemical synthesis approaches which involve high temperatures, high pressure, exclusion of air and water, (toxic) reaction auxiliaries (which entail additional steps for attaching, cleavage and purification from by-products) and transition metals (like in ruthenium-catalysts which usually are not reusable) are far from perfect enantioselectivities. Therefore it is not surprising that the convenient and environmentally benign production of optically pure amines is still subject of ongoing investigations.[54] As stated above enzymatic routes to optically pure amines bear a great potential in organic chemistry and thus gained much attention in the past.

4.2. Enzymatic routes to primary chiral amines – kinetic resolution and asymmetric synthesis

Comparable with their chemical counterpart enzymatic approaches for chiral amine synthesis have been developed based on resolution mode (kinetic resolution) and the asymmetric synthesis.[129] The kinetic resolution can be used for the production of enantio-enriched compounds starting from the racemic mixture of an amine. The used enzyme is applied here as the resolving agent according to its enantiopreference.[130,131] Some drawbacks are associated with this method like the low atom efficiency with a highest theoretical yield of 50% or the product inhibition by the formed ketone, but on the other side only stoichiometric amounts of substrates are needed.[54,59,132,133] The direct asymmetric synthesis of a chiral amine from its corresponding ketone (or aldehyde) does not have the mentioned intrinsic limitation in theoretical maximum yield but usually the unfavored reaction equilibrium has to be overcome, for instance with an excess of one of the employed substrates.[90,91,134–136] Nevertheless, the asymmetric synthesis is one of the central topics in both, chemical synthesis and biocatalysis and

therefore highly preferred in academia as well as pharmaceutical manufacture, if not the access to the racemic amine is more oppertune.[18,58,62,136–138] In the last several years a couple of enzymes belonging to the classes of hydrolases, oxidoreductases, lyases and transferases have been discovered for catalysing the production of the desired chiral amine in one of the modes mentioned above (Scheme 5).[26,54,59,129,137,139] Lipases, for instance, as members of the hydrolase enzyme class, are widely used biocatalysts for the formation and cleavage of esters and amides.[140] They are remarkable not only for their process robustness (since they are e.g. operable in pure organic solvents) and broad substrate scope but also for the high regio- and enantioselectivity which made them to the *best friend* of organic chemists.[140]

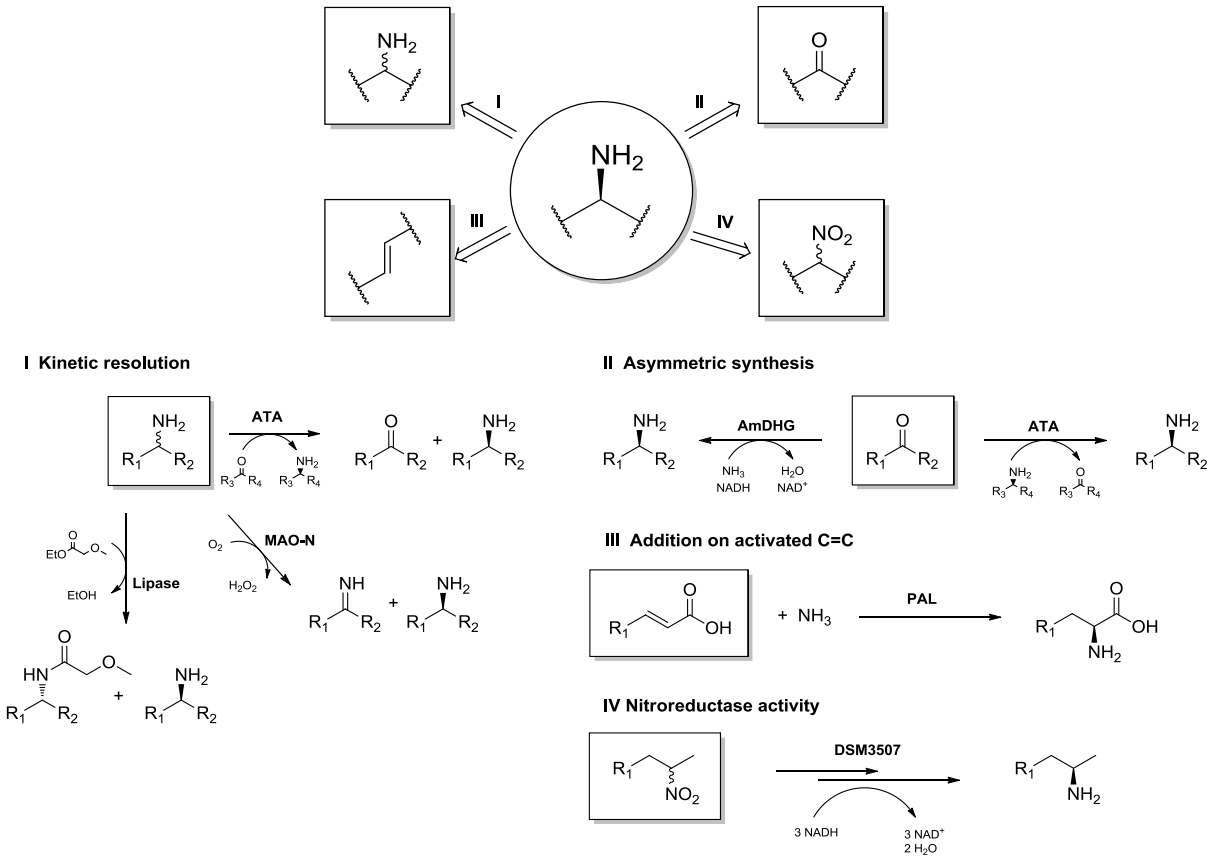

Scheme 5. Enzymatic routes to optically active primary amines. MAO = monoamine oxidase, AmDHG = amine dehydrogenase, PAL = phenylalanine ammonia lyase, NAD = nicotinamide adenine dinucleotide.

The lipase catalysed kinetic resolution of 1-phenylethylamine by enantioselective amide formation was initially investigated by companies like Shell and Bayer in the beginning of the 1990s.[53] BASF further optimized this process by a careful selection of the acyl donor (ethyl methoxyacetate, Scheme 5 I) and enzyme immobilization, leading to the preparation of enantiopure (*R*)-1-phenylethylamine via extraction/distillation of the acetylated product and basic hydrolysis of the amide bond.[141] In order to maximize the final product yield an *in situ* racemization was successfully involved either by imine formation and non-selective hydrogenation via palladium[142] or ruthenium (Shvo's)[143] catalysts or via radical induced racemization.[144,145] Despite the fact that those dynamic kinetic resolution methods could

be applied to several benzylic and aliphatic amines and improved the final isolated yield to 95% in the best case the possibility of undesired side reactions are obvious, if not the racemization catalyst itself affected enzyme activity.[54,131]

Besides lipases, mono amine oxidases (MAO) can be utilized in kinetic resolution mode as well (Scheme 5 I). Two types of MAO enzymes exists with different co-factor dependencies.[59] Solely type II (FAD-dependent type) is suitable for application as biocatalyst, since the members of type II release the imine product during catalytic cycle. MAOs catalyse the enantioselective oxidation of amines to imines by the simultaneous reduction of molecular oxygen to hydrogen peroxide. Again, the desired enantiomer can be obtained in a theoretical yield of 100% by a dynamic kinetic resolution mode when the formed imine was subjected to chemical reduction what leads to racemization. This was investigated by the Turner group while using the MAO from *Aspergillus niger* (MAO-N).[146] MAO-N is certainly the best studied amine oxidase and became object of several protein engineering approaches using a combination of directed evolution techniques and rational design.[147] The result was a set of MAO-N variants with complementary enantioselectivities and an enlarged substrate scope including complex secondary and tertiary amines.[54,148] Prominent examples for API production with MAO-N are for instance telaprevir, boceprevir, levocetirizine and solifenacin.[59,62,149,150]

Transaminases are usable in kinetic resolution and asymmetric synthesis mode (Scheme 5 I and II) what was their unique feature among all mentioned enzyems for long time.[26] Initially, most of the applications using TAs were following the kinetic resolution approach. The company Celgene first employed an (*S*)-selective TA in a large process in a kinetic resolution of various aliphatic and aromatic amines.[59,151] Shin and Kim et al. started to do academic research on this enzyme class to minimize product inhibition during kinetic resolution. Significant advances were achieved using bi-phasic systems[20,152], membrane reactors[153] or packed bed reactors.[154] Through the years scientists were paying more attention to the catalytic abilities of TAs and started an intensive research field in chiral amines synthesis.

Amine dehydrogenases (AmDHG) are a quite recently created group of enzymes.[148] They catalyse the asymmetric reductive amination of a keton or aldehyde moiety in presence of ammonia and using NAD(P)H (nicotinamide adenine dinucleotide) as hydride source (Scheme 5 II). While amino *acid* dehydrogenases were known before, Itoh et al.[155] presented in 2000 an AmDHG from *Streptomyces virginiae* capable to catalyse the reductive amination of a range of aliphatic and aromatic ketones although with low enantiopreference.[59] However, that expanded the enzymatic toolbox for chiral amine production since beforehand TAs reserved the ability to perform a reductive amination from achiral ketones.[26] Extensive engineering of amino acid dehydrogenases from *Bacillus stearothermophilus* (a leucine dehydrogenase), *Bacillus badius* and *Rhodococcus* sp. (both phenylalanine dehydrogenases) allowed the enantioselective conversion of a wide range of (bulky) ketones by these enzymes.[156–159] Another highly desired reaction using ammonia as nitrogen source is the stereoselective hydroamination of alkenes (Scheme 5 III).[148] Some amino acid lyses are literature known to catalyse this reaction, unfortunately limited to amino acid products.[139] Nevertheless, the ACE inhibitor Indolapril was successfully synthesised under involvement of the phenylalanine ammonia lyase (PAL).[160,161] Through engineering of the 3-methylaspartate lyase either non-canonical amino acids are achievable and additionally the nucleophile specificity could be broadened from ammonia to small amines (like

methylamine) to access secondary amines.[162,163] The reduction of the nitro group is rather known to be a chemical synthetic route to a number of APIs (Scheme 5 IV).[164] However, several microorganisms can catalyse this reaction under amine formation and oxidation of NADH.[165] But besides a few aromatic nitro compounds the accessible scope of target molecules is limited.[166]

More recently, further enzymes were identified for amine synthesis although primary amines not seem to be their main substrate scope.[167] Imine reductases and (the recently discovered) reductive aminases were tested towards a couple of ketone compounds revealing that cyclohexanone could be successfully converted into cyclohexylamine by both enzyme types.[168,169]

The majority of the presented biocatalytic routes suffers from significant bottlenecks like limited substrate scope, kinetic resolution as sole possible reaction type or the dependence on a co-factor recycling system. The latter in particular regards to all mentioned oxidoreductases.[148] Conclusively, TAs have a special status in the synthesis of chiral amines since they show an immense potential in utilization for the preparation of a broad spectrum of amines – either in kinetic resolution or asymmetric synthesis mode – and their co-factor PLP is regenerated during the second half of the catalytic cycle without need of an external regeneration system.[1]

4.2.1. Enzyme cascades involving Transaminases

The establishment of enzyme cascades achieved major advances in the production of several compounds of interest, mainly because much more versatility in the choice of the starting material is given and simultaneously the isolation of possible unstable intermediates is avoided.[91,138,170,171] Indeed, deracemization through enzymatic dynamic kinetic resolution becomes possible in cascade reactions. By the combination of two enantiocomplementary TAs the first one in the cascade is acting in kinetic resolution mode providing the ketone substrate for the subsequent asymmetric amination catalysed by the other TA.[133] Using this method the APIs Mexiletine[172–174] (an anti-arrhythmic drug) and Niraparib[175,176] (potential anti-cancer drug in the treatment of leukemia, under patent to Pfizer) were efficiently produced. Another example for deracemization is given by combining of the (*S*)-selective MAO-N with a (*R*)-selective TA in order to yield the (*R*)-amine.[177,178] Deracemization is supposed to be highly recommended when the corresponding ketone is not accessible or expensive[179–181] but usually a two step-fashion under inactivation or removal of the prior enzyme in the cascade is needed especially when the substrate scope of the used enzymes is overlapping.[174,182]

A wide range of further cascade reactions involving TAs are literature known, like the combination with a lyase (acetohydroxyacid synthase I) to get access to both enantiomers of norephedrine and norpseudoephedrine[183,184] or the setup with an alcohol dehydrogenase when alcohols are the starting material for the preparation of primary amines. An elegant approach was published by Sattler et al. and Pickl et al. showing a complex reaction setup with intermediate oxidation reactions and asymmetric amination on the way to aliphatic (di)amines.[185,186] The basis for that functional group interconversion is the same oxidation state of both moieties which makes an electron borrowing mechanism[187] and co-factor regeneration possible under employment of another alanine dehydrogenase for TA amine acceptor regeneration. The Bornscheuer and the Höhne group presented cascade reactions on manipulating of two stereocenters via the combination of (either wild-type or engineered) TAs with

enoate reductases or keto reductases, respectively and provided a route to several diastereomers of the respective amine.[188–190]

For further reading regarding recent achievements in TA-mediated cascade reactions the following reviews are recommended.[90–92,133,191]

4.3. Amine Transaminases in asymmetric synthesis of chiral amines

As mentioned before, asymmetric catalysis is considered generally to be the most important method to introduce chiralitiy into pharmaceutically and agrochemically active molecules.[124,135,192] Especially for chiral amine synthesis the start from achiral ketones and aldehydes makes the cost and waste intensive synthesis of racemic amine mixtures obsolete what is of course highly desired in pharmaceutical and agrochemical manufacture. Up into the 2000 years, in biocatalysis applications the asymmetric synthesis was less attractive because of major obstacles in reaction equilibrium and so, kinetic resolution reactions were predominant on the route to chiral amines (see Chapter 4.2). The first asymmetric synthesis of amines using ATAs was described by Shin and Kim et al.[193] claiming the excellent enantioselectivity of ATAs and the first example of reaction equilibrium shifting in TA reactions. This initial development of an ISPR-techniques in asymmetric synthesis (*in situ* (co-)product removal) in order to prevent the accumulation of inhibitory co-products, definitively paved the way for this branch of ATA-mediated catalysis (see Chapter 5.1).[60,136]

In recent years, numerous research groups in academia and industry applied ATAs in the synthesis of a range of pharmaceutically active compounds or intermediates thereof under consideration of a broad range of starting materials including linear, cyclic and aromatic ketones (e.g. [60–62,91,92,139]). Additionally, one pushing effect was the easy and rapid availability of (wild-type and engineered) ATAs in the form of commercial ready-to-use screening kits offered by Codexis and other companies.[90] However, the production of various APIs has been realized on larger scale using ATAs. The manufacturing of the diabetes-drug Sitagliptin (the active ingredient of Januvia®, Table 1, entry 1) was already mentioned before. [93] With the engineered Arthmut11-TA, the product was obtained in 92% yield and 99.5%*ee* in a reaction with 200 g/L substrate concentration, 6 g/L enzyme load, 50% co-solvent concentration at 50°C with isopropylamine (IPA) as the amine donor. The co-product acetone could easily be stripped off the reaction continuously by a nitrogen flow. Notably, enzyme engineering led to a higher tolerance towards higher concentrations of DMSO and IPA and higher temperatures. In comparison to the chemical counterpart of Sitagliptin manufacture, which employed an asymmetric hydrogenation under high pressure and usage of a chiral Rh-catalyst,[194] the biocatalytic reaction system resulted in a 13% higher overall yield and 19% reduction of total waste.[195] The same enzyme was later applied in the asymmetric synthesis of the aminated precursor of the drug Ramatroban, a thromboxane receptor antagonist for the treatment of asthma or coronary artery diseases (Table 1, entry 2).[196] The utilization of IPA as the 'ideal amine donor' was tried but caused side reactions in the form of enolate or enamine formation what was avoided by 1-phenylethylamine (PEA) as amine donor. The amine product of the transamination reaction was obtained in 96% yield and >97%*ee* without any final purification step. The authors compared the advantages over the chemical process and claimed a higher yield as well as

shorter reaction sequence and reaction time for the final product. The beneficial thermodynamic properties of PEA were also used for the synthesis of the amine precursor of the Janus kinase 2 inhibitor (JAK2 inhibitor, Table 1, entry 3) after identification of Vfl-TA (ATA from *Vibrio fluvialis*) as suitable biocatalyst.[197,198] The multi-gram preparation (500 g, 0.35 M substrate concentration) was implemented into a chemoenzymatic route to the final product with 97% yield and 99%*ee* for the transamination product (*S*)-1-(5-fluoropyrimidin-2-yl)-ethanamine. In order to avoid co-product inhibition by the formed acetophenone a bi-phasic system with 20% toluene was installed. Rivastigmine (Table 1, entry 4), a cholinesterase inhibitor for the treatment of Alzheimer's or Parkinson's disease,[60,199,200] was one of the first reactions processes with an ATA (Vfl-TA) involved leading to the preparation of the primary amine precursor as synthetic key step in 100 mg scale, 71% yield and 99%*ee*.[201] However, in many other examples ATAs show potential in API (precursor) production. Relevant (final) products are for instance Dilevalol[202] (Table 1, entry 5), Formoterol[202] (entry 6), Imagabaline[24] and Ivabradine[203] emphasising the value of enzymes in the future synthesis process development.

Table 1. Biocatalytic application of ATAs for the synthesis of pharmaceutically active compounds.

Entry	Reaction	Ref.
1	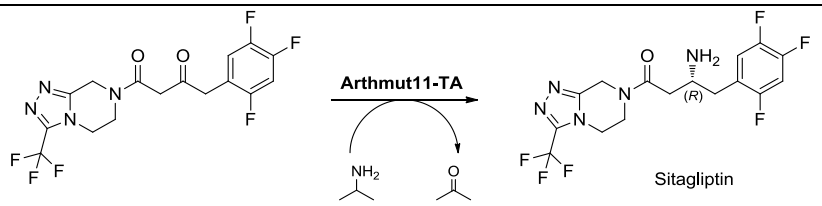	[93]
2	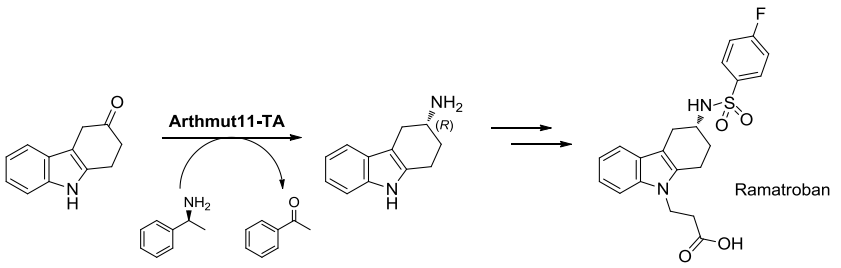	[196]
3	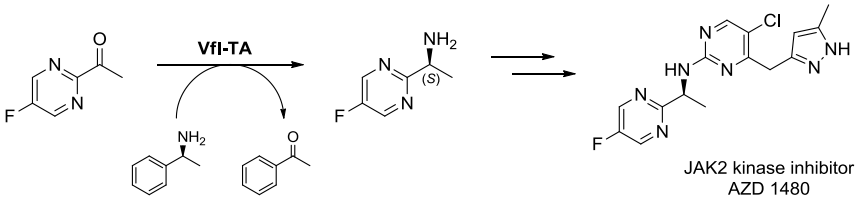	[197,198]
4[a]	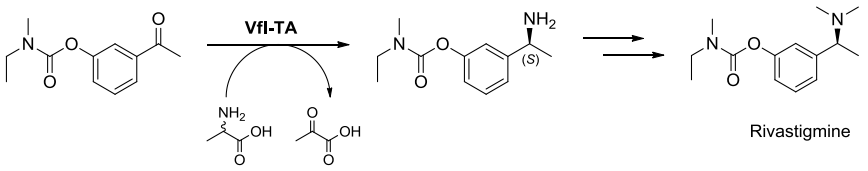	[199,201]
5[a]	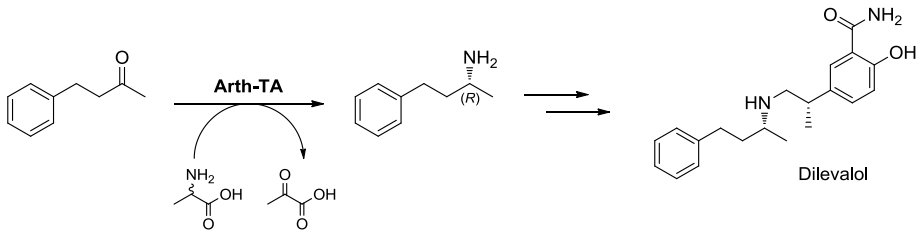	[202]
6[a]	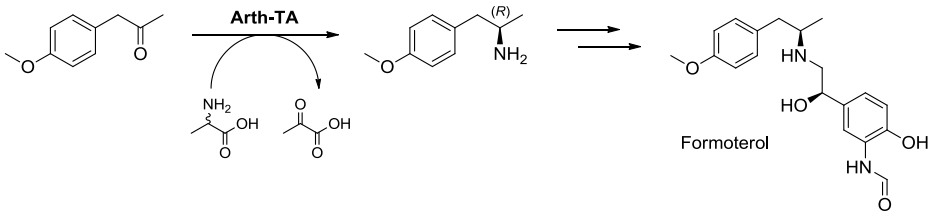	[202]
7	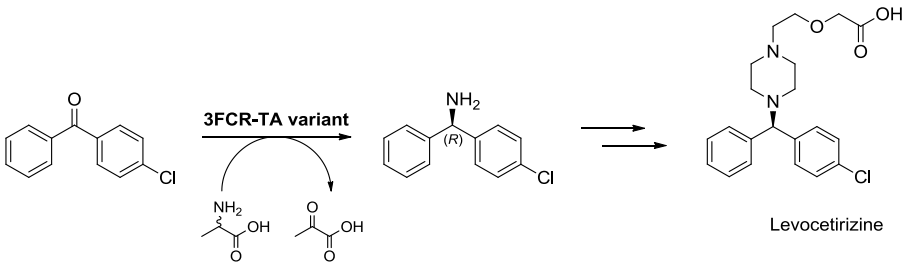	[94,204]

[a] If alanine was used as the amine donor a pyruvate removal system was applied to shift the equilibrium towards the product side.

4.4. The synthesis of halogenated arylalkyl amines (Article I)

Halogenated amine compounds are routinely found in natural and pharmaceutically relevant compounds with outstanding physiological activity.[205] They often show potent effects e.g. in the treatment of a number of diseases.[206] A similar status applies for pyridine derivatives[207] and additionally, pyridine amines are attractive chelating ligands in organic chemistry for several metal ions especially when a high variety of coordination geometries is needed.[208]

A couple of reports are known for the asymmetric amination of halogenated ketones or aldehydes using TAs. They are mainly dealing with halogenated acetophenone derivatives[206,209,210] or fluorinated phenylacetone in order to investigate the substrate scope of several ATAs.[211–213] The asymmetric synthesis of 3,4-dimethoxyamphetamine (DMA) using Arth-TA was also described.[35,36] Other relevant citations refer to the production of fluorinated and chlorinated derivatives of 1-(pyridinyl)ethanamine for the production of API intermediates.[197,198,214,215] Subject of **Article I** is the asymmetric synthesis of various brominated and chlorinated 1-phenyl-2-propanamine, 4-phenylbutan-2-amine, and 1-(3-pyridinyl)ethanamine derivatives whose enantioselective amination by ATAs was not described yet (Scheme 6). For instance, enantiomers of substituted amphetamine derivatives (**1b**-**6b** Scheme 6) have distinct pharmacological properties, e.g. affect neuroreceptors like serotonin or dopamine receptors or having drug potential in obesity diseases, also as halogenated derivatives.[216,217] Moreover, the halogen moiety is quite often the basis for the synthesis of more complex compounds so that the target amines shown in Scheme 6 possibly bear building block functionality for a number of pharmaceutically and agrochemically active molecules (Figure 4).[53,125,166] Initially, the choice of the four ATA candidates with complementary enantioselectivity was guided by literature search[44,114,202,209,218–222] and ligand-docking experiments in which strategically chosen quinoid intermediates were modelled (Figure 5). One of the main aspects of **Article I** was the utilization of IPA as the apparently ideal amine donor (see Chapter 5). Model reactions were performed to test IPA acceptance (and especially the right donor-acceptor-ratio) revealing the ATAs from *Silicibacter pomeroyi*[44] (Spo-TA) and *Aspergillus fumigtus*[37,38] (Afu-TA) as final biocatalysts (Figure 5).

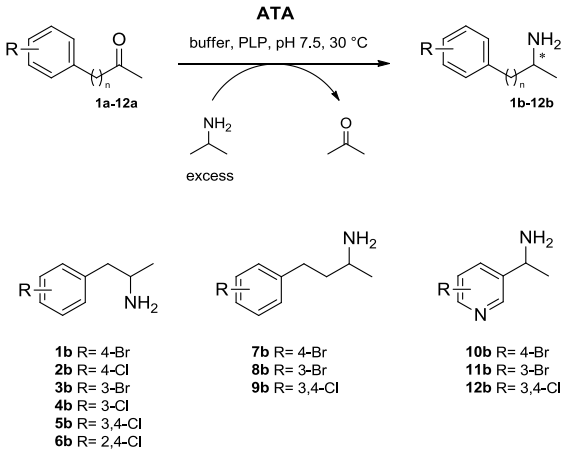

Scheme 6. Amine products (bottom) obtained by the asymmetric synthesis (top) from the corresponding prochiral ketones (**1a**-**12a**) using ATAs from *Silicibacter pomeroyi* and *Aspergillus fumigtus* as biocatalysts.

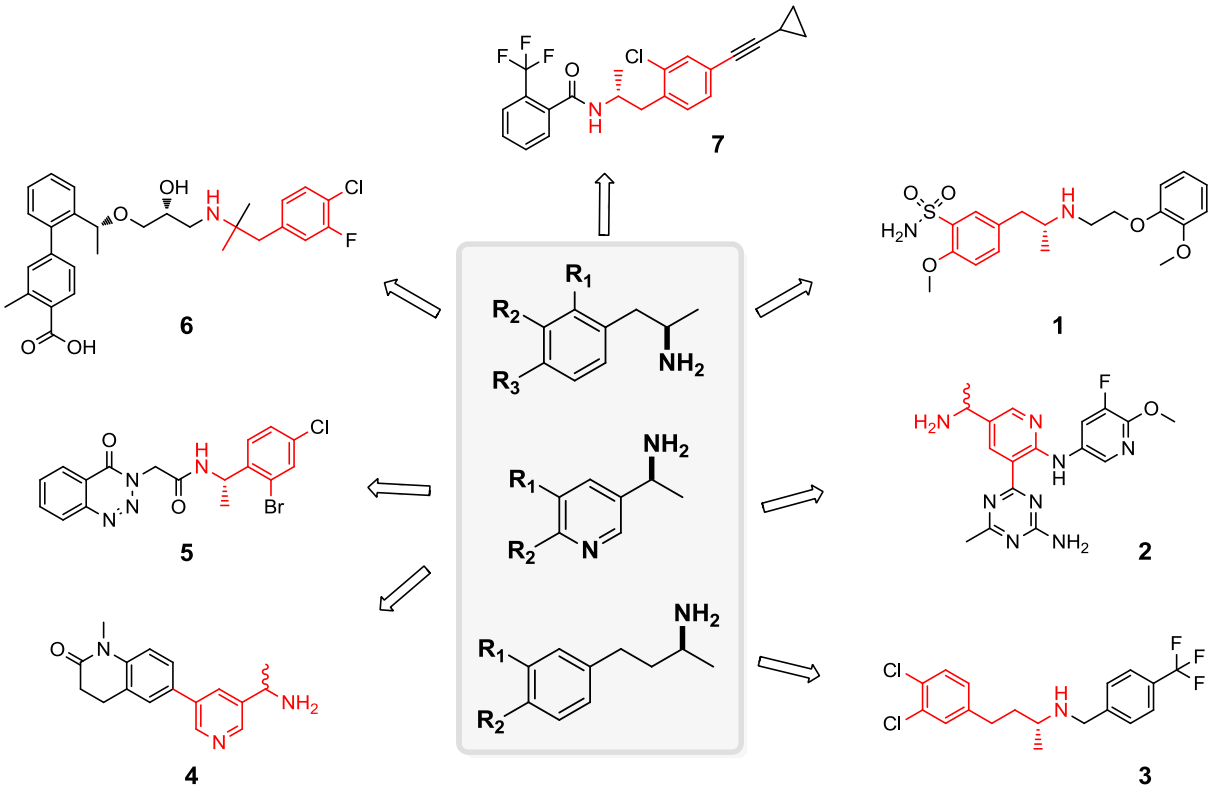

Substance	Physiological activity / Application	Ref.
1	Tamsulosin; prostata hyperplasy drug	[223]
2	PI3K kinase inhibitor, cancer drug; lipid-kinases are ubiquitous and associated with signal transduction mechanisms; they are supposed to be related with some kind of cancer (PI3K-mediated cancer)	[224]
3	Sigma2-receptor antagonist with effect against amyloid-beta induced diseases, e.g. Alzheimer	[225]
4	Dihydroquinolin-2-one derivatives show effects at chronic disorders like kidney disorders or hypertension	[226]
5	GPR139 (G-protein) agonist; GPR139 is highly produced in the habenulae of the brain; the habenulae has strong effect at the limbic system with their dopamine and serotonin receptors and is responsible for sensation of pain, sleep disorders, depression, shizophrenia and other disorders of the central nerve system	[227]
6	Encaleret; osteoporosis drug	[228]
7	Pesticide/Biocidal	[229]

Figure 4. Compilation of pharmaceutically and agrochemically active compounds derivable from the chiral amines obtained in **Article I**.

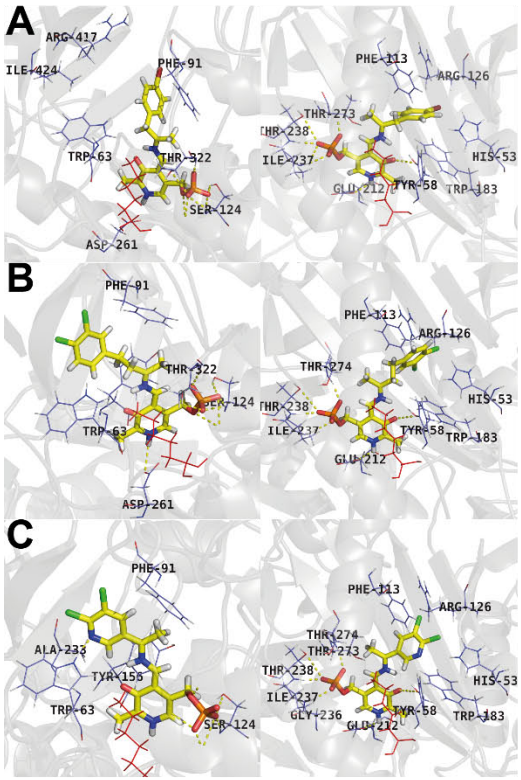

Pymol illustration of the docking experiments with Spo-TA (left) and Afu-TA (right). The PDB IDs are 3HMU and 4CHI, respectively. The catalytic lysine is indicated in red, hydrogen bonds are indicated with yellow dash lines. The quinoid intermediates (yellow) of (see Scheme 6) **1b** (A), **9b** (B) and **12b** (C) were docked into the active site of both ATAs. The involved amino acid residues for coordination of the PLP as well as those for pocket formation were verified with literature. Some residues were omitted for clarity. The overall result of all docking experiments gave a strong indication of a correct substrate coordination.

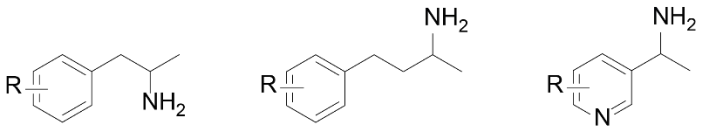

1. Indication by Molecular Docking

3. Biocatalysis

2. Optimization of the donor-acceptor-ratio

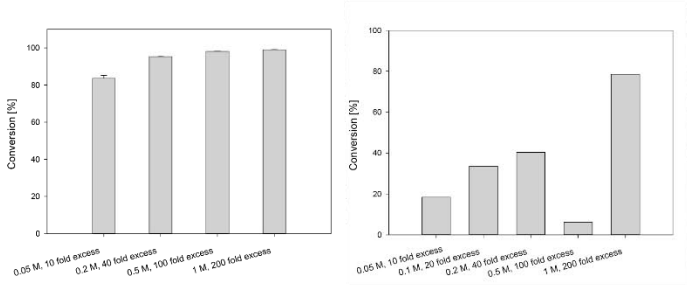

Conversion of 1-(4-bromophenyl)propan-2-one **1a** (Scheme 6) in dependence of the excess of isopropylamine using Spo-TA (left) and Afu-TA (right). In case of Spo-TA a relative low excess of 10-fold was already sufficient to observe high conversion (>80 %). The reaction with Afu-TA reached the same value only at 1 M IPA (a 200-fold excess). General procedure: 5 mM of **1a**, 10 % DMF, IPA as indicated, HEPES buffer (50 mM, pH 7–7.5), 30 °C for 18 h. The conversion was analyzed via gas chromatography.

Figure 5. Experimental concept of **Article I**. **1.** After identification of suitable ATA candidates by literature search, ligand-docking experiments were performed to strengthen those indications by checking of plausible substrate coordination *in silico*. **2.** The optimal donor-acceptor-ratio was determined by applying different IPA concentrations while keeping the amount of the ketone fixed. This knowledge was mandatory to achieve quantitative conversion in the following biocatalysis **3**. For identification of substrates **1**, **9**, **12** see Scheme 6.

With the optimal reaction conditions in hand the production of the target amines **1b**-**12b** was conducted (Table 2). Predominantly, excellent conversion and enantiomeric excess (*ee*) values were obtained with minor exceptions. Particularly, using Spo-TA the *ee* values of the 4-phenylbutan-2-amines (especially **7b** and **9b**) were relatively divergent indicating a certain degree of flexibility of the formed intermediate in the active site. Those observations correspond with former reports when benzylic ketones with longer alkyl chain were aminated with (*S*)-selective ATAs, also indicating an impact of the substituent on the benzene ring.[44,230] However, preparative scale reactions were performed using both enantiocomplementary ATAs with substrate **1a** as representative model substrate. The identity and absolute configuration of the amine product **1b** was confirmed via chiral gas chromatography (GC) analysis, ^{1}H-NMR, ^{13}C-NMR spectroscopy and optical rotation values,[231] respectively.

Table 2. Conversion and enantiomeric excess values of the amine products **1b**–**12b** (see Scheme 6) obtained by asymmetric synthesis using IPA as donor and crude cell lysate containing overexpressed Spo-TA or Afu-TA.

	Spo-TA			Afu-TA		
Substrate	*c* [%][a,b]		ee_P [%][b]	*c* [%][a,b]		ee_P [%][b]
1a	95.6	± 3.0	>99	96.2	± 0.3	>99
2a	96.6	± 0.8	>99	96.1	± 0.4	>99
3a	91.4	± 0.4	98	95.0	± 0.3	>99
4a	97.6	± 1.3	>99	95.9	± 0.5	>99
5a	96.3	± 2.9	98	93.4	± 1.1	>99
6a	97.1	± 2.2	>99	91.1	± 0.4	>99
7a	93.3	± 2.8	80	93.9	± 0.4	>99
8a	95.9	± 1.9	95	84.5	± 4.1	>99
9a	88.0	± 6.0	73	95.6	± 0.7	>99
10a	88.8	± 5.0	>99	78.4	± 2.3	>99
11a	93.9	± 4.7	>99	91.4	± 0.4	>99
12a	90.7	± 8.3	>99	86.4	± 2.9	>99

[a] Reaction conditions: HEPES buffer (50 mM) pH 7.5, 5 mM ketone, isopropylamine (0.25 M for Spo-TA, 1 M for Afu-TA) , 10 % DMF, 30°C, 18 h. [b] Conversion and enantiomeric excess was determined via chiral GC analysis.

5. The choice of the amine donor

Using TAs, the introduction of chirality makes the asymmetric syntheses the most attractive route, but at the same time this mode is often hampered by low conversion values because of unfavorable thermodynamic situations.[54,90,193,232] Shin and Kim et al. initially investigated the field of reductive amination using ATAs and claimed from the beginning that the choice of respective couples of substrates (amine donor and acceptor, product and co-product) is crucial in TA-catalysed reactions.[193] In most cases the equilibrium can be considered far on the reactant's side and therefore a technique for equilibrium displacement is needed.[54,132,230] So alanine – as natural amine donor – indeed has been proven as one of the most popular amine donors but at the same time its utilization bears the most unfavored reaction equilibrium.[91,139] For instance, Höhne et al. observed a maximum conversion of 6% in the asymmetric synthesis of 1-*N*-Boc-3-aminopyrrolidine using alanine in equimolar ratio.[230] An excess of alanine usually does not lead to more favorable situation with one exception so far when the amination of 4'-methoxyphenylacetone in 94% yield with a 16-fold excess of alanine was reported.[233] In turn, aliphatic and especially benzylic amines are supposed to be thermodynamically more suitable donor molecules.[234,235] Isopropylamine – IPA – is a promising amine donor since it is cost-effective, readily obtainable, excellently water soluble and the co-product acetone can be easily removed in terms of equilibrium displacement if necessary (see Chapter 5.1).[91,93,135,219,236–238] Also, because IPA is achiral, the enantioselectivity of the respective ATA has not to be considered. From the industrial point of view IPA is certainly the most favored amine donor for TA-mediated reactions[239] but although IPA is ranked as the 'better' donor than alanine[90] still a high excess is needed to drive the desired reaction to completeness.[61,236] And more important, a limited number of ATAs are known to accept IPA.[90,92,136,240] Affirmatively, solely five wild-type ATAs from *Arthrobacter citreus*,[219] *Halomonas elongata*,[241] *Orchobactrum anthropi*,[235] *Silicibacter pomeroyi*,[242] *Pseudomonas putida*[243] and *Arthrobacter* sp. KNK168[243] were already literature known to achieve excellent conversion in respective reactions with IPA. Interestingly, those observations were mainly made for (*S*)-selective ATAs. Nevertheless, IPA was increasingly used in recent years in academia and industry for the synthesis of a broad range of target amines.[62,95,96,99,139,202,206,239,244–249] In fact, besides alanine, IPA became one of the most applied amine donors for ATA reactions.[61,91,92,132,139]

5.1. Techniques for equilibrium displacement

Several techniques have been discovered or developed to efficiently shift the equilibrium on the desired product side to give higher conversion and enhanced yield. Fundamentally, those techniques can be divided into two main approaches, on the one side the application of the donor in large excess and on the other side the *in situ* removal of the formed (co-)product (IS(c)PR technique), inclusive combination of both.[132] In terms of the latter an immense scientific effort was made in the last decade mostly relying on alanine as amine donor with followed degradation or conversion of the co-product pyruvate in order to pull the reaction into the desired direction (Scheme 7A).[90] Hence, (multi-)enzyme cascades emerged to valuable tools in asymmetric synthesis in order to enable thermodynamic unfavored amination reactions of a broad range of target compounds.[136] For instance, the application of a lactate

dehydrogenase (LDH) in terms of converting pyruvate to lactate under consumption of NADH was already investigated when the first asymmetric synthesis using Vfl-TA was reported even if a co-factor recycling was omitted.[20,136] Koszelewski et al. later involved a glucose dehydrogenase (GDH) under employment of glucose as reducing agent and therefore created a self-sufficient and effective system for pyruvate removal.[114]

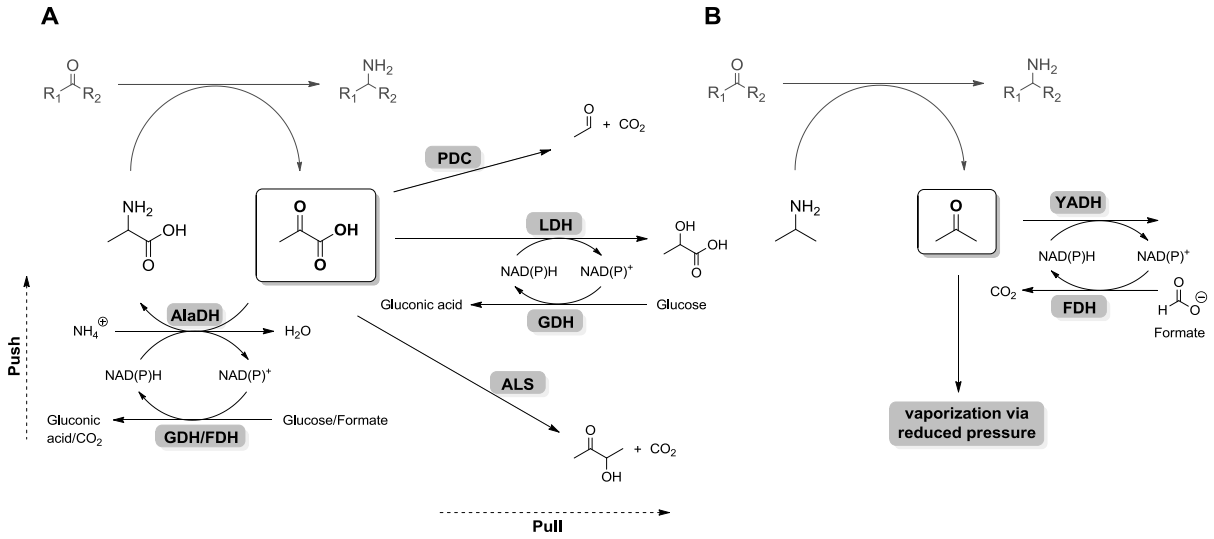

Scheme 7. Illustration of co-product removal systems using **A** alanine or **B** isopropylamine as amine donor. AlaDH = alanine dehydrogenase, LDH = lactate dehydrogenase, GDH = glucose dehydrogenase, FDH = formate dehydrogenase, PDC = pyruvate decarboxylase, ALS = acetolactat synthase, YADH = yeast alcohol dehydrogenase, NAD = nicotinamide adenine dinucleotide.

Many research groups incorporated the LDH/GDH system for the production of their target amines with mostly excellent yield and enantiomeric excess using (*R*)- and (*S*)-selective TAs.[116,136,202,218,222,250,251] Alternatively, when an alanine dehydrogenase (AlaDH) is applied, the recycling of pyruvate back into alanine becomes possible, having a push effect towards reductive amination. Simultaneously, this system allows lower concentrations of the starting material.[252] Again, the presence of the reducing equivalent NADH is mandatory which gets recycled in similar way like mentioned previously. A slight modification of the AlaDH system uses a formate dehydrogenase (FDH) under carbon dioxide formation and reduction of NAD^+. The practicability was demonstrated several times.[132,136,221] Höhne et al. and Yun et al. published decarboxylation approaches of pyruvate using either a pyruvate decarboxylase (PDC) or acetolactate synthase (ALS).[230,253] The advantages of both systems is the omission of a co-factor recycling system and the equilibrium is efficiently shifted through the formation of carbon dioxide, although an excess of alanine still seems to be necessary.[132] Nevertheless, an unwanted feature of the PDC system is the function of the formed acetaldehyde as amine acceptor in the TA reaction forming ethanamine and constantly consuming the amine donor.[230] However, despite the wide diversity in pyruvate removal systems equilibrium shifting using enzyme cascades possibly remains challenging especially regarding an overall accordance in reaction conditions, either in one-pot or sequential setup.[238] When using IPA as amine donor, acetone is formed as the co-product. A very convenient

method is the removal of acetone by a mild vacuum distillation because acetone is rather volatile and has a lower boiling point than the majority of other reactants (Scheme 7B). Additionally, a nitrogen flow strongly supports the discharge of acetone. This was initially presented for the production of Sitagliptin[93] and has been taken up for the synthesis of the herbicides metolachlor for instance.[254] The elimination of acetone via physical separation has the significant advantage that solely one enzyme is involved.[255] Notably, this system is not suitable in every case since it depends drastically on the actual properties of the substrate of interest. Tufvesson et al. and Satyawali et al. addressed the general validity of the vaporization technique and compared for instance prositagliptin and ketones with lower molecular weight. Compounds like acetophenone and some specific substituted derivatives are supposed to be highly effected by vaporisation strategies causing a blind ketone loss over reaction time.[256,257] As alternative strategy acetone could also be converted enzymatically by coupling with an alcohol dehydrogenase from *Saccharomyces cerevisiae* (YADH).[258] Here, one of the key features is the narrowed substrate scope of this ADH discriminating ketones larger than a C3 backbone achieving an acetone removal system with significant specificity. However, applying IPA in high excess is from the practical point of view the most simple, most convenient and most employed method for equilibrium shifting using this amine donor.[3,90,236,238,239] Thus, the fact that a single-enzyme system can be performed opens up possibilities for a higher degree of 'freedom to operate'[124] in terms of reaction conditions, experimental setup and effort as well as formulation of the biocatalyst,[90,259] among other aspects.

A number of further IS(c)PR techniques was reviewed intensively over the entire timespan of ATA investigation,[60,90,136] for instance the simultaneous extraction of one of the formed ketone products through bi-phasic systems[260–262] or the spontaneous tautomerization, oligomerization or cyclization of sacrificial ketone co-products to a thermodynamically stable compound (so called 'smart' donors).[209,211–213,263,264] For IPA application the chemoenzymatic combination with an aluminum isopropoxide catalysed Oppenauer oxidation was presented in which acetone was chemically reduced to isopropanol.[265] The selling-point in the latter example was the synthesis of the ketone substrate as 'side product' in order to simultaneously pull and push the reaction towards product formation. Recently, a novel technique was presented in which the selective *in situ* crystallization of the desired amine product occurs.[266] Also these examples have limitations and drawbacks, for example poor distinction between substrate or product and inactivation of the biocatalyst during *in situ* extraction in a bi-phasic system, a questionable acceptance of the alternative 'smart' donors by various ATAs and a high screening effort to find a suitable counterion for the *in situ* crystallization of the desired amine product.[60,90,266]

5.2. Understanding isopropylamine (IPA) as the amine donor (Article II)

5.2.1. Engineering of IPA acceptance

During investigations in this thesis with different ATAs, significant differences in IPA acceptance were observed. For instance, Spo-TA (ATA from *Silicibacter pomeroyi*) generally showed high reactivity with IPA towards several amine acceptors with quite low molar excess (see Chapter 4.4) and in contrast the

ATA from *Ruegeria* sp. TM1040 (3FCR-TA) did not exceed 10% conversion in the best case during preliminary tests for **Article II**. With the best knowledge only a few publications can be found in literature in which the engineering to a higher reactivity using IPA was aimed and reported.[93,255] Again, the manufacture of Sitagliptin has to be cited as example. Here, enzyme engineering resulted not only in a better substrate acceptance or higher temperature and solvent stability, but also in an enhanced IPA acceptance. Arthmut11-TA as best variant contained 27 mutations, many of them globally distributed over the entire protein with the effect to ensure acceptance or tolerance of IPA, respectively. Due to the increased ability to accept IPA this and other variants from this substrate-walking-approach were commercialized and then further used for various applications with IPA (see Chapter 4.3), for instance the production of unnatural amino acids.[235] Interestingly, Han et al. discovered one key residue for apparent better IPA acceptance in the (*S*)-selective ATA from *Ochrobactrum anthropi* (named as OATA).[255] In this study, position 58 in OATA (according to the Protein Data Bank numbering) has been identified as promising active site residue for site directed mutagenesis after *in silico* studies in order to improve the activity towards several ketones significantly (in total nine arylalkyl ketones and six alkyl ketones). The mutation OATA-W58L did not only lead to a better conversion of the investigated (bulky) ketones, however, at the same time this mutation was obviously responsible for a higher binding affinity towards IPA. This was proven by determination of a 9-fold lower K_M value towards IPA via a pseudo-one-substrate kinetic model which meant that the IPA concentration was altered while keeping the concentration of the co-substrate (pyruvate) fixed. According to the authors, that effect could be explained structurally when a possible steric interference of (wild-type) tryptophan 58 with one of the methyl groups of IPA is eliminated after mutagenesis. The variant OATA-W58L was interestingly compared with Arthmut11-TA in the amination of acetophenone under reduced pressure and showed indeed a 5-fold higher formation of 1-phenylethylamine (PEA) than Arthmut11-TA. Position 58 was further investigated by subsequent mutagenesis studies to examine its influence on the substrate scope of OATA.[249,267,268] However, the authors claimed that OATA was chosen in the beginning due to its relative high starting activity towards IPA.[235] But is this improvement in IPA related activity transferable to another scaffolds, maybe with lower starting activity?

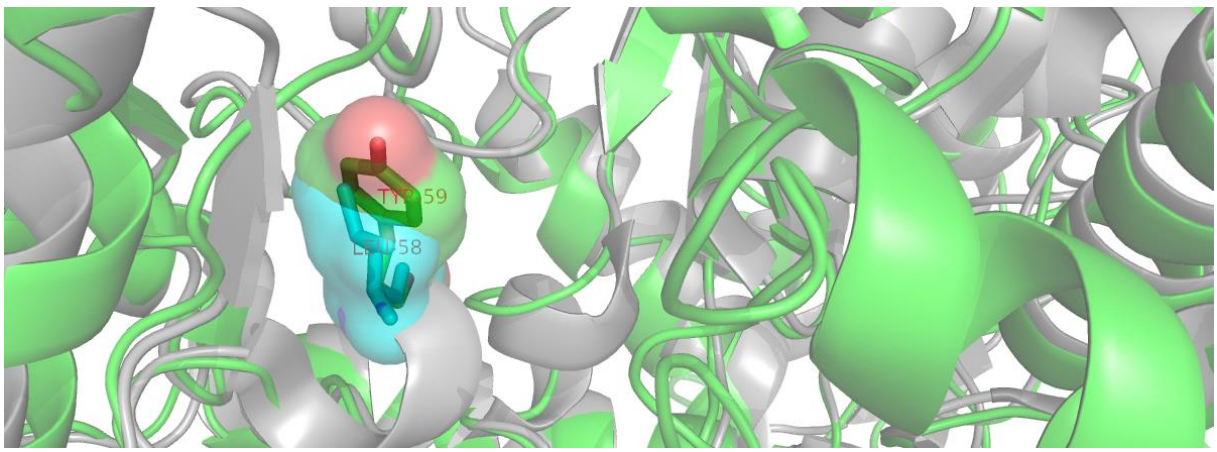

Figure 6. Superimposed structures of 3FCR-TA (PDB-ID 3FCR, green) and OATA-W58L (PDB-ID 5GHG, grey). The homologous positions tyrosine 59 in 3FCR-TA (green/red) and leucine 58 in OATA (cyan) are highlighted. The sequence identity between both TAs is 43%.

Recently, the engineering of 3FCR-TA (ATA from *Ruegeria* sp. TM1040) for the acceptance of bulky ketones was reported whose corresponding amines predominantly have pharmaceutical relevance (see Table 1, entry 7).[94–96] The best variants from this approach (especially one quadruple mutant 3FCR-Y59W-Y87F-Y152F-T231A, 3FCR-QM) did not accept IPA well as the amine donor which for instance was observed in the asymmetric synthesis of exo-3-amino-8-aza-bicyclo[3.2.1]oct-8-yl-phenyl-methanone.[95] Remarkably, position 59 in 3FCR-TA (according to PDB numbering) is the homologous position of 58 in OATA after structure superposing (Figure 6) and both were reported to be very crucial for the activity towards aromatic and bulky substrates.[94,269] Additionally, a comparable cross-link of key residues was seen in the 'flipping arginine' which mediates dual substrate recognition of ATAs and is highly conserved in e.g. amino acid transaminases, ornithine transaminases and amine transaminases.[8,269] This flexible arginine residue facilitates the required flexibility in accepting substrates with two different chemical groups like a phenyl (e.g. PEA) and carboxyl moiety (e.g. pyruvate). This is facilitated by a salt bridge formation between the guanidine group of the arginine and the carboxylate function of the respective substrate and by a 'flip out' in order to provide space for bulky and hydrophobic moieties. The position of this arginine residue at the entrance of the active site is predestined for this role in substrate binding. Though, the TA from *Bacillus anthracis* (Ban-TA) represents an exception as the 'flipping arginine' is replaced by a glycine which means that no movement of an amino acid residue is required for substrate recognition.[270] Interestingly, Ban-TA showed reasonable activity towards IPA. A possible hypothesis here could be that a strong positive charge at the entrance of the active site tunnel was considered to be detrimental for the accessibility of IPA on the PLP molecule.

However, the motive of the investigations in **Article II** was to prove or disprove the role of both mentioned positions in IPA acceptance for the 3FCR scaffold. The variant 3FCR-QM from previous engineering approaches was chosen as template to enable the synthesis of pharmaceutically relevant amines using IPA and therefore to further enhance the presented 3FCR-TA variants.

Table 3. Initial activity of purified 3FCR variants determined via the glycine oxidase assay[106] towards two concentrations of IPA as the amine donor. Measurements were performed in triplicate.

Transaminase / variant	**Activity [mU/mg]**		**Fold increase in activity**
	IPA 0.05 M	**IPA 0.2 M**	
3FCR-QM	3.64 ± 0.15	8.55 ± 1.28	2.3
3FCR-QM-W59L	16.8 ± 1.13	39.04 ± 0.17	2.3
Fold increase in activity	4.6	4.5	

Reaction conditions: CHES buffer (2-(Cyclohexylamino)ethanesulfonic acid), pH 9.5 (50 mM), 2 mM glyoxylate, IPA concentration as indicated, 37 °C.

Following the procedure which was described before in 3FCR-TA engineering, position 59 was saturated via site directed mutagenesis using degenerative codons and the resulting library was screened via the glycine oxidase (GO) assay against IPA.[94,106] Indeed, the only variant with significant improved activity towards IPA contained the mutation W59L which led to a 4.6-fold higher activity compared to the

template (Table 3). Noteworthy, a direct transfer of the mutation 59L caused an improving effect in activity towards IPA with glyoxylate as amine acceptor, even though the fold in increase is lower here. Also the mutation of the 'flipping arginine' (position 420 in 3FCR-TA) had a promoting effect on IPA acceptance in this scaffold. Since the GO-assay was not suitable for this mutagenesis study (because this assay demands coordination of the carboxylate moiety of glyoxylate) the R420 variants of 3FCR-QM were interrogated in the chosen asymmetric synthesis model reactions (Table 4). Several amino acids were introduced at position 420 with different characteristics (hydrophobic, basic and acidic) revealing the mutation to tryptophan as the best (for more information see **Article II**). This finding would support the hypothesis of a detrimental and flexibly mounted positive charge at the active site tunnel since already the swap into histidine caused a slight improvement. Both variations (W59L and R420W) were introduced into 3FCR-QM and tested in asymmetric synthesis (Table 4). The respective W59L-R420A variant was inducted into the experiments in order to provide the maximum space and possibly the lowest interference at this position. It could be demonstrated that both positions (59 and 420) are important key positions for IPA activity in the 3FCR scaffold. Through combination of the best amino acid variations for both positions the conversion in the chosen model reactions could be increased substantially in comparison to the starting scaffold, although differences for each ketone substrate could be seen. Finally, with the variant 3FCR-QM-W59L-R420W a general approach for an improved IPA acceptance for the investigated reactions was identified, achieving conversion values higher than 83%.

Table 4. Comparison of the presented variants of 3FCR-TA in asymmetric synthesis of the illustrated amines using IPA as the amine donor. * n.d.: not detectable

ATA variant	**Conversion [%]**			
	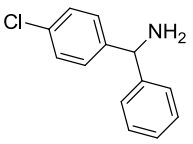	ee_P [%]	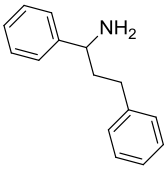	ee_P [%]
3FCR-QM	12.8 ± 1.2	> 99 (*R*)	n.d.*	-
3FCR-QM-W59L	6.8 ± 1.5	86 (*R*)	8.9 ± 1.8	> 99 (*S*)
3FCR-QM-W59L-R420A	50.6 ± 3.6	91 (*R*)	23.8 ± 2.5	> 99 (*S*)
3FCR-QM-W59L-R420W	83.5 ± 4.0	80 (*R*)	85.8 ± 3.5	> 99 (*S*)

Reaction conditions for the asymmetric synthesis: 2 mM ketone, 0.5 M IPA, 30 % (v/v) DMSO, CHES buffer pH 10 (50 mM), 0.1 mM PLP, 0.89 - 1.2 mg mL^{-1} purified enzyme, 30 °C. Conversion was determined after 20 h via chiral gas chromatography. Samples were taken in triplicate from three parallel reactions.

5.2.2. Reaction engineering for a better reactivity with IPA

Generally, only a few reports are given in which the influence of reaction parameters (like temperature and pH) on the degree of TA-mediated product formation was investigated.[256] Moreover those studies were predominantly done for PEA and alanine as donor molecules.[271,272] In turn, a set of different reaction conditions were reported when IPA was used, referring to variations in donor-acceptor-ratio or pH value. So far, there has been no experimental study which aimed the identification of optimal reaction conditions (in terms of donor concentration and final pH) and investigation of the enzyme stability in presence of IPA. Thus, in **Article II** the ketones acetophenone and 2'-bromoacetophenone were subjected for this study as two common aromatic benchmark substrates for the evaluation of amine donors.[206,209,211,212,258,263] This choice was made because a halogen substitution on the acetophenone substrate is supposed to have a promoting effect on reaction equilibrium.[234,258] On the other hand the amination of acetophenone is considered as very challenging due to the markedly unfavored equilibrium,[193,211,238] so significant effects were expected here after reaction engineering. In the presented experiments a molar IPA excess range of 5-fold to 100-fold and a pH range of 7.5 to 10 was investigated including a couple of ATAs which were commonly used in literature as well as the presented variants of 3FCR-QM. The results indicated that both aspects, pH influence and donor-acceptor-ratio, should be considered indeed as highly enzyme as well as substrate dependent (or a combination of both). Regarding each enzyme for itself no general trend could be seen over the entire pH range since reactivities in a predominantly similar order of magnitude were observable. The variation in the donor-acceptor-ratio only took significant effect in the amination of acetophenone as expected, in turn indicating a more favored equilibrium situation for 2'-bromoacetophenone as amine acceptor. The 3FCR-QM-W59L-R420X variants exhibited one of the best performance in all tested reactions what proved the expansion of an improved IPA acceptance to other ketone substrates than given in Table 4. Interestingly, the incubation with IPA did not have a significant detrimental effect on enzyme stability for any tested ATA which was tested via subsequent activity measurements (for more details see **Article II**). Therefore, a missing IPA tolerance was obviously not the reason in this case study for different reactivities. Apparently, every ATA reaction needs to be optimized relating to the mentioned aspects when IPA is to be used as amine donor.

The investigations in **Article II** did not include other critical reaction parameters like temperature or pressure as both factors are known to be supporting effects in acetone removal.[247,255,256] However, especially the application of an elevated temperature should be treated with caution because enzyme stability is most likely decreased what obviously has a significant counter-effect on conversion.[243] Moreover, a higher temperature does not mean that an excess of IPA and/or a nitrogen flow could be nevertheless necessary in any case. Presumably, a maintained enzyme activity is the 'better pushing effect' for a certain process even though a larger excess of the amine donor has to be applied.[273]

6. Combination of ATA activity with the Suzuki cross-coupling reaction

6.1. Biocatalysis combined with transition metal catalysis

One-pot cascade reactions are an established instrument for the finding of a suitable synthesis route to a target product.[138,274–276] Originally, the catalysts for these cascades belonged to the same 'type' since pure chemical or pure biocatalytic cascade reactions were focused on. In fact, the one-pot combination of these 'two-worlds'[275] of chemo- and biocatalysis is immense underrepresented and rather gained increased attraction in the recent years.[275,277] The major potential of such a chemoenzymatic reaction is the unification of different reaction types *en route* to a desired compound which usually is not achievable by means of a pure chemical or enzymatic reactions. From the economical point of view one-pot reactions are bearing convincing benefits over reactions with distinct reaction steps, like solvent or environmental contaminant reduction, the choice of more favored starting materials and the omission of (unstable) intermediate isolation, what often means significant increases in the overall product yield and thus in the space-time yield of a certain process.[274] Especially, when biocatalysts are involved this introduces characteristic enhancements, for instance mild operation conditions and water as the main solvent, as described in Chapter 2. Particularly, water as the 'natural' reaction medium came more and more into focus of chemists, not only in terms of environmentally aspects, rather because the full spectrum of enzymatic activity is accessible.[275] But unfortunately, water- (and oxygen-)free conditions were mostly required for the majority of metal (and organo-)catalysts and very often high temperatures as well.[278,279] Thus, although many possibilities would emerge when 'closing the gap' between chemo- and biocatalysis in general, realization was frequently hindered due to suffering from incompatibilities as mentioned. In order to achieve compatibility a careful adaption of reactants, catalysts and/or reaction conditions is needed and on the other side (or in combination), engineering of chemo- and biocatalysts has been conducted in chemobiocatalysis, mainly by making one catalyst accepting the conditions of the other.[45,277,280–283]

However, several pioneering works of combining transition metal- and biocatalysts have been published which were subject of several recent reviews.[274,275,278,279] For instance, the production of D-mannitol, combining a glucose isomerase and a platinum-catalysed hydrogenation, is certainly the most cited work in this context.[284] Furthermore, dynamic kinetic resolutions using chemical racemization are also initial approaches of chemobiocatalysis involving e.g. ruthenium, palladium, rhodium or vanadium catalysts (see Chapter 4.2). Here, the groups of Bäckvall, Williams, Reetz, Turner and Kim have done the pioneer work in the 90s and early 2000 years utilizing lipases or monoamine oxidases for the production of chiral alcohols or amines.[142,285–290] Apart from those 'early' works more recent examples emerged in which reaction types, like cross-coupling reactions (Pd-catalysed Heck- or Suzuki reaction),[291,292] metathesis (Ru-catalysed),[293,294] Wacker-oxidation (Pd-catalysed)[295] and hydrogenation (Rh-catalysed)[296–298] were combined with alcohol dehydrogenase, hydrolase or Baeyer-Villiger/P450 monooxygenase activity to obtain the respective desired alcohol, amino alcohol, amino acid or lactone in good to excellent yield, enantiomeric excess and diastereomeric ratio. In several of these cases the chemical reaction part benefited from intensive research in order to make the respective

catalyst or ligand compatible and/or stable in aqueous media and therefore to generate a basis for the chemoenzymatic application.[292,298] Among the given examples, Fink et al. applied compartmentalization and immobilisation of different reactions and catalysts in order to combine the chemical hydrogenation and enzymatic oxidation reaction.[297] Those are common techniques to generate compatibility when engineering or optimization of catalysts and/or reaction conditions only achieved partial compatibility.[274,278] Incidentally, this is not the only example for similar approaches with transition metal catalysts.[277,299,300]

6.2. The Suzuki-Miyaura cross-coupling reaction and its chemoenzymatic incorporation

Beside other palladium-catalysed cross-coupling reactions like the Heck, Stille or Nigishi reaction, the Suzuki cross-coupling in particular is one of the most powerful tools in the synthesis of biaryl compounds.[301] Since its discovery in 1979[302] (and especially over the last two decades) the Suzuki reaction has received massive attention and is still the focus of recent and fast-growing research. A considerable potential of this reaction is the high tolerance to a large range of reaction conditions (solvent and temperature) and functional groups paired with a great simplicity and reactivity in water.[301,303–306] The most described Suzuki reaction is the cross-coupling of C(sp^2)-halide (or -triflate) with a C(sp^2)-boronic acid.[307–311] The reaction mechanism can be described by three successive steps (Scheme 8). First, the oxidative addition of the aryl halide to the palladium catalyst starts the catalytic cycle and forms the palladium intermediate complex. Thereby, the oxidation state of Pd plays a crucial role because only Pd^0 is the reactive species which favors the oxidative addition reaction. Although Pd^{II} precatalysts are commonly used, the reduction to Pd^0 should occur first, either by ligands or *in situ*.[301] Besides that, this step is considered as rate limiting because the thermodynamics of this reaction is mainly determined by the halogen atom with a relative reactivity decreasing in the following order, I>Br>>Cl.[304] Additionally, the ligand structure has been proven to have a significant effect on reactant reactivity during oxidative addition with the result that intensive research was performed on different Pd-ligands.[301] Sterically hindered electron-rich ligands on phosphine basis were discovered to increase the reaction rate and finally emerged to one of the most popular ligand types for the Suzuki reaction.[312,313] The subsequent and central catalytic step is the transfer of the boron aryl substituent onto Pd. This transmetalation step is (in contrast to the others) specific for metal-catalysed cross-coupling reactions in general and at the same time the least understood one in the catalytic cycle.[301,314] The proposed mechanism of transmetalation contains the action of a base.[315,316] The utilized base activates the Pd intermediate complex which is further attacks by the aryl boronic acid. Sodium carbonate, potassium carbonate or caesium carbonate are reported to be the most applied bases in aqueous cross-coupling reactions.[301] It is also the base which mediates the final reductive elimination by addition and coordination to the biaryl-Pd-complex which causes a Pd anion and lowers the barrier for biaryl product release. Originally, the Suzuki-Miyaura reaction was performed in organic solvents to ensure the water/oxygen-free conditions which were often required for the phosphine ligands.[303,317,318]

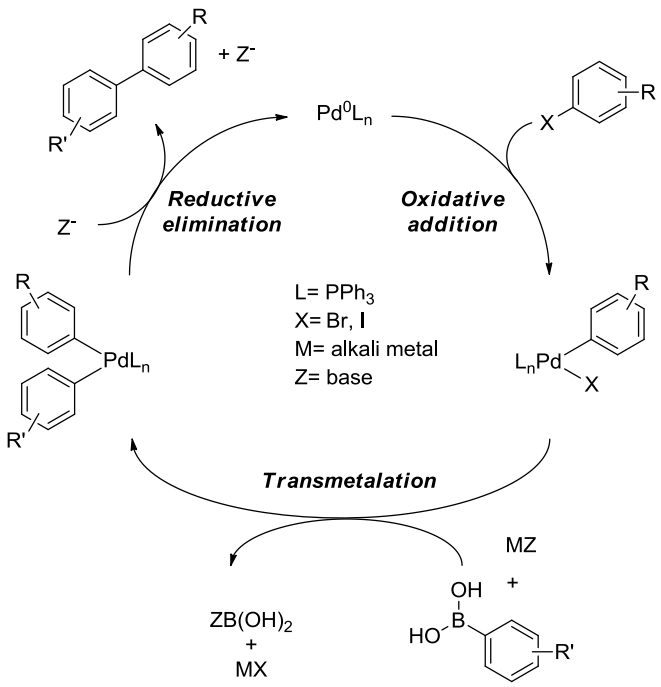

Scheme 8. Simplified mechanism of the Suzuki-Miyaura cross-coupling reaction (redrawn from references[315,316]). The major requirement is the reduction of palladium to the active Pd^0 species which is e.g. realized by ligand complexation. Therefore, phosphine ligands are used to be the most common ones. Starting from the activated Pd^0-catalyst the addition of the aryl halide generates a Pd^{II} intermediate complex. Central for all cross-coupling reactions is the transmetalation which occurs base catalysed and reveals the biaryl Pd^{II} intermediate under substitution of the halogen. The also base catalysed reductive elimination yields the final biaryl product. One significant advantage over other cross-coupling reactions is the low toxicity of the reactants. Besides the Heck- and Negishi reaction, the Suzuki-Miyaura cross-coupling was honoured with the Nobel Prize in 2010.

As previously mentioned very intensive research generated a great number of reports in which the Suzuki-Miyaura reaction could take place in phosphine-free and/or water-solvent systems in order to address the demands of green chemistry (e.g.[319–333]). Those reports contained for instance the introduction of water-soluble ligands on phosphine basis[292,334] or the replacement of the original ligand with other stabilizing additives or activating supports like palladium on carbon (Pd/C),[335] mesoporous silica[336] ethylene glycol and ethylenediaminetetraacetic acid (EDTA).[331,332,337] Interestingly, also ligand-free applications were presented.[333,335,338–341] In any case the authors emphasized the robustness of their method for the fast reaction of aryl bromides or iodides with arylboronic acids at ambient temperature and in the presence of water and air.

However, the very first successful chemoenzymatic combination of the Suzuki-Miyaura reaction and enzyme activity was reported by Burda et al.[291] A two-step-one-pot synthesis of 1-(4-biphenylyl)-1-ethanol was conducted in water-isopropanol mixture via enantioselective asymmetric reduction of the produced biaryl ketone by using the alcohol dehydrogenase (ADH) from *Rhodococcus* sp. The chiral biaryl-alcohol was obtained with very good conversion and enantiomeric excess (91%*c*, >99%*ee*). The authors underlined the necessity of a sequential two-step approach because for ADH activity a pH shift to pH 7 and a full conversion of the inhibitory boronic acid was mandatory.[275] This first successful example motivated the Cacchi group to focus on this chemoenzymatic combination and developed water-soluble palladium nanoparticles stabilized within the protein cavity of a thermostable DNA binding protein to obtain the actual catalyst for biaryl formation under elevated temperatures.[342] Furthermore,

Ahmed et al. produced bi-phenylalanine via the involvement of a phenylalanine ammonia lyase prior to the Suzuki cross-coupling reaction[343] and France et al. indeed included the enzymatic transamination (using ATA013 from Codexis) as well as Suzuki reaction to facilitate their route to dibenzazepines.[344] Both latter works contained intermediate isolation steps and solvent changes and therefore cannot be considered as compatible one-pot reaction setups.

6.3. The compatibility of the Suzuki reaction with ATA activity

Inspired from the previously discussed works, in this thesis the first chemoenzymatic combination of ATA activity with the Suzuki cross-coupling reaction in a one-pot fashion was aimed. According to the 'principles' of chemobiocatalysis an adaption of both reactions was mandatory. Regarding the cross-coupling reaction, the production of 4-acetylbiphenyl (using 4'-bromoacetophenone and phenylboronic acid as starting material) was chosen as model reaction for the examination of a suitable reaction setup or conditions, similar to almost all works cited in this chapter. Interestingly, several works demonstrated a simplified ligand-free application of this reaction without prior catalyst preparation in *N*,*N*-dimethylformamide (DMF)- or ethanol-water-mixtures in the presence of an inorganic base.[333,335] DMF-water-mixtures were considered as a good starting point since DMF was efficiently used as co-solvent for TA reactions previously in this thesis (see **Article I**). Unfortunately, attempts to conduct the chosen protocol[333] remained unsuccessful in the presence of buffer traces, PLP and IPA (as the desired amine donor for the TA reaction) and so the concept of performing a concurrent reaction setup[274] was dismissed. Also a sequential one-pot reaction running the enzymatic transamination *prior* to cross-coupling seemed not suitable.

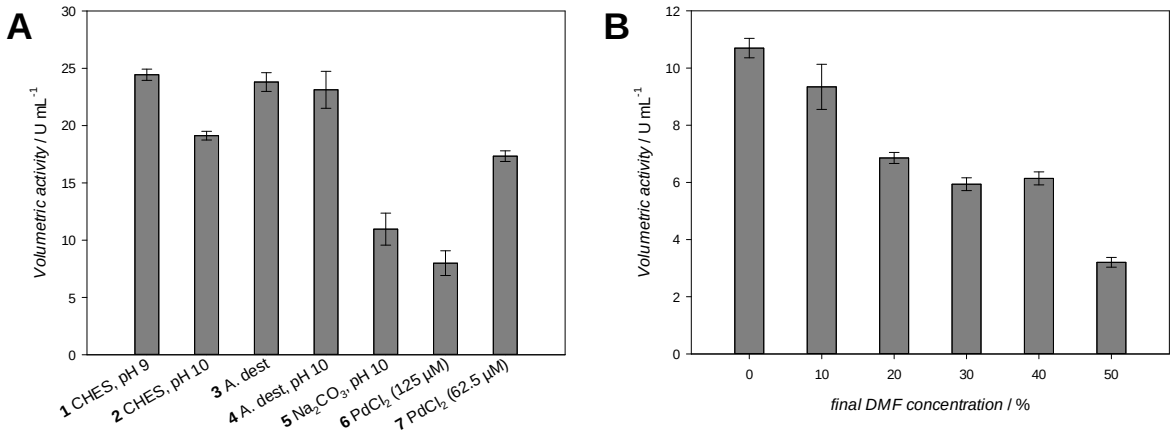

Figure 7. Verification of ATA compatibility with the Suzuki cross-coupling reaction. **A** Activity (U mL^{-1}) values were determined via modification of the acetophenone assay as indicated using crude lysate with overexpressed Afu-TA (ATA from *Aspergillus fumigatus*) wild-type. General reaction conditions were: 2 mM (*R*)-1-phenylethylamine, 2 mM pyruvate, 2% DMSO dissolved in **1** distilled water (A. dest.) and CHES (50 mM pH 9), **2** A. dest. and CHES (50 mM pH 10), **3** pure A. dest. (pH 7.4), **4** A. dest.-NaOH (pH 10), **5** 6 mM Na_2CO_3 in A. dest. (pH 10), **6** CHES (50 mM pH 9) and 125 µM $PdCl_2$, **7** CHES (50 mM pH 9) and 62.5 µM $PdCl_2$. One unit (U) of ATA activity was defined as the formation of 1 µmol of acetophenone per minute (ε= 12 $M^{-1}cm^{-1}$). Measurements were performed in triplicate. **B** Samples of crude lysate containing overexpressed Afu-TA were incubated with different concentrations of DMF at 30 °C for 20 h. Activity was measured via acetophenone assay.[117] For reaction conditions with CHES buffer see A. All measurements were performed in triplicate.

The reverse sequence is though not free from the possible complication of missing acceptance of sterically demanding biaryl ketones by the TA which makes protein engineering necessary. Indeed, already the acceptance of naphtyl compounds by TAs had to be engineered in some cases,[90] so a good conversion of biaryl substrates was not expectable, which was finally confirmed by pre-tests. Among the tested TAs, only Afu-TA (the ATA from *Aspergillus fumigatus*) showed moderate acceptance of 4-acetylbiphenyl in asymmetric synthesis mode (39%*c*, Table 5). However, key point of these investigations was that Afu-TA revealed as highly compatible with the demands of the Suzuki reaction (Figure 7) which is indeed the contrary scenario like in the case of Burda et al.[291] If engineering of Afu-TA would prove to be successful the high robustness of this TA would be the key point for the (sequential) one-pot combination of both reactions towards the production of biaryl amines.

6.4. The production of chiral biaryl amines using the engineered ATA from *Aspergillus fumigatus* in one-pot

Various biaryl amines were identified as target compounds with respect to cover different regioisomers and the presence of aryl substituents and/or heteroaromatics (Scheme 9, Table 5). All biaryl ketones could be synthesized with very good to excellent conversion with the chosen protocol for Suzuki cross-coupling starting from 4'-bromoacetophenone or 1-(5-bromopyridin-3-yl)ethanone, respectively (Scheme 9). With a promising ATA candidate in hand a mutagenesis approach was aimed in order to provide better conversions of the targeted biaryl ketones. Molecular docking studies were performed to identify possible amino acid residues around the active site which might hamper the acceptance of bulky biphenyls, namely His53, Phe113, Arg126 and Ile146 (according to the PDB numbering, Figure 8).

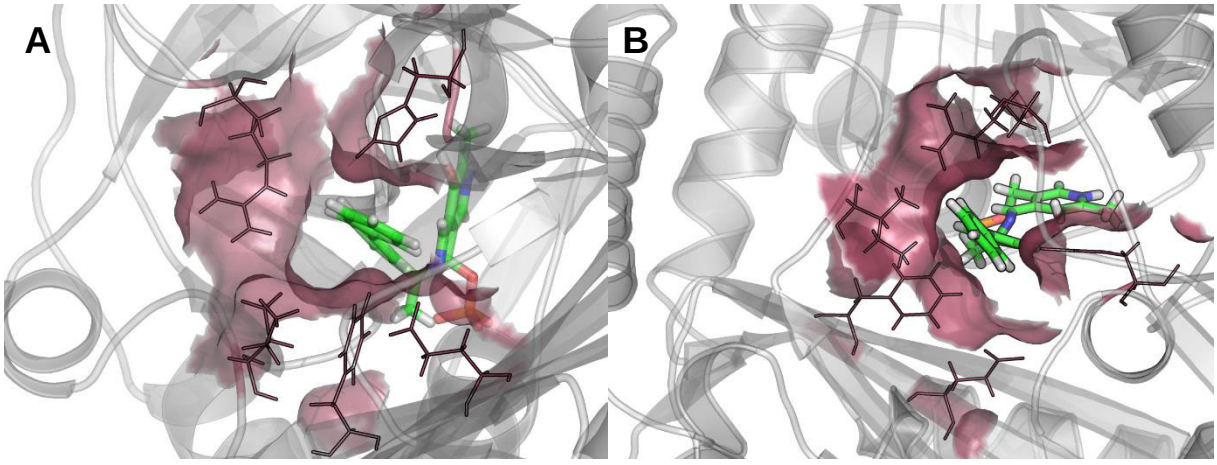

Figure 8. Output of the molecular docking experiments using the crystal structure of the ATA from *Aspergillus fumigatus* (Afu-TA, PDB-ID: 4CHI).[38,40] The quinoid intermediate of two representative substrates (**A** Table 5, entry 1 and **B** Table 5, entry 3) were docked into the active site of Afu-TA. The best and most plausible ligand-receptor complex was evaluated visually. The amino acid residues with a distance of <5 Å around the ligand (especially around the biphenyl moiety) were considered as possible interfering: His53, Phe113, Arg126 and Ile146 (according to the PDB numbering, given in red).

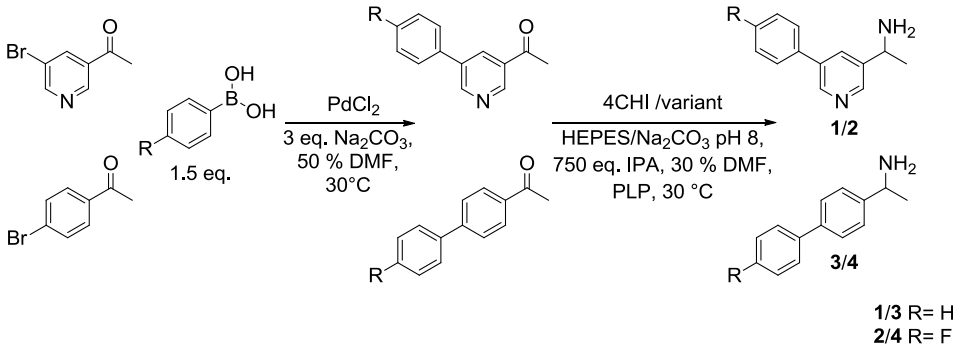

Scheme 9. One-pot synthesis of 1-(5-phenylpyridin-3-yl)ethanamine **1** and 1-(4-biphenyl)ethylamine **3** including fluorinated derivatives **2** and **4**. The numbering corresponds to the entries in Table 5. Starting from aryl halides chiral biaryl amines could be obtained by the sequential order of Suzuki–Miyaura and ATA reaction. The crude cross-coupling reaction product was diluted with an ATA/IPA/PLP-containing solution achieving the final conditions for the ATA reaction. Molar equivalents were given in relation to the brominated starting material.

For each amino acid residue alanine variants were produced and tested in the asymmetric synthesis of the every corresponding amine in Table 5. Indeed, the variants F113A and I146A performed very well keeping in mind that a single alanine mutation was sufficient in both cases to double total conversion (87%*c* in the best case, Table 5). The omission of the 'flipping arginine'[8,269] in Afu-TA, R126[345] obviously did not have any supporting impact on activity towards biaryl ketones with demand on the large binding pocket. Because of its great flexibility this residue is most likely capable to provide the space which is necessary for the accommodation of such substrates.

Table 5. Comparison of Afu-TA variants derived from rational design in the synthesis of biaryl amines (entry 1-4) with IPA as amine donor. The biaryl ketone substrates were previously synthesized starting from the corresponding bromo-ketones, the respective boronic acid derivative, sodium carbonate as activating base and ligand-free $PdCl_2$ as catalyst. The ATA reaction was initiated by adding of an ATA crude lysate and IPA/PLP-containing reaction solution. For further information see **Article III**.

ATA/ variant	**Substrate conversion [%]**			
	1	**2**	**3**	**4**
	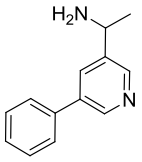	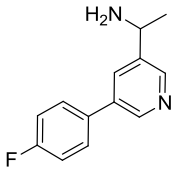	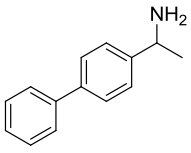	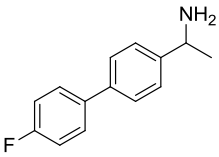
Afu-wild-type	38.5 ± 3.8	39.7 ± 4.2	38.9 ± 1.6	27.2 ± 2.4
Afu -H53A	45.6 ± 3.2	48.6 ± 3.1	21.6 ± 2.7	27.1 ± 2.5
Afu -F113A	72.5 ± 1.0	75.0 ± 2.6	19.2 ± 2.9	18.4 ± 2.5
Afu -R126A	37.6 ± 2.7	18.2 ± 2.8	46.8 ± 3.1	35.7 ± 2.8
Afu -I146A	87.5 ± 1.4	79.1 ± 3.7	23.6 ± 3.4	14.8 ± 2.0
Afu -F113A-I146A	83.8 ± 4.2	79.8 ± 3.5	17.4 ± 3.2	17.4 ± 4.2

Reaction conditions (final concentrations): 1 mM ketone (entry 1–4), 0.75M IPA, 30% (v/v) DMF, (4-(2-hydroxyethyl)-1-piperazineethanesulfonic acid)-HEPES/Na_2CO_3 buffer (27 mM) pH 10, 0.1 mM PLP, 30 °C. Samples were taken in triplicate from three parallel reactions. Conversion was determined after 20 h via gas chromatography (GC). Corresponding amines were identified via GCMS.

However, this residue was already subject in previous mutagenesis studies which also focused on generating acceptance of biarly ketones.[99] The (*S*)-selective ATA from *Vibrio fluvialis* (Vfl-TA) initially lacked any activity towards 2-acetylbiphenyl which was improved significantly by rational design. The authors' justification to mutate the 'flipping arginine' of Vfl-TA (R415) already in the first round of mutagenesis was a further enlargement of the active site and a decrease of the positive charge in order to increase the affinity to the hydrophobic substrate. The authors claimed that molecular docking and simulation studies showed a noticeable reduction of the distance between the ketone moiety of the biaryl ketone and the PMP nitrogen what increases the likelihood for a nucleophilic attack. Their best performing variant regarding this position was R415A. However, in response to the results for the positions 113 and 146 in Afu-TA a double mutant (F113A-I146A) was produced in the hope to further increase the conversion, but no significant difference was detectable. The maintenance of the variants' stereoselectivity was confirmed via the chiral analysis of 1-(1,1'-biphen-4-yl)-ethanamine (Table 5, entry 3), whereby for any variant enantiomeric excess values of >99%*ee* were detected (see **Article III**). This was indeed not unexpected because the shape of the small binding pocket was not changed and additionally the demand on the large binding pocket was even increased by the selected substrates.

6.5. ATA immobilisation for a (proof-of-concept) continuous flow application (Articles III and IV)

Continuous flow systems were already used in industry since the early 20th century, mainly in the production of petro- or bulk chemicals. The synthesis of fine chemicals in flow is relatively new but enjoys growing popularity especially in developing economies, for instance in modern API and agrochemical production.[346,347] The concept of a continuous flow process contains a starting material which is pumped through a chemical reactor, often in the form of a tubing or channel, and finally a continuous product stream results at the end of the flow setup. Notably, not only chemical transformations are possible and/or subject of flow techniques, also *in situ* crystallization or changes in product formulation could be integrated into the process what was demonstrated by Mascia et al.[348] In this work the *in continuo* production of aliskiren (an antihypertensiva) included catalysis, reaction quenching, product work-up and isolation in a fully automated process. Further, this is an excellent example for the efficient reduction of reaction time and solvent usage by flow techniques compared to the batch reaction analogue, namely 48 h single process time vs. 1 h and 1500 L solvent effort per year vs. 136 L. Thus, those aspects are the major characteristics of a flow system, because of the high surface-to-volume ratio[349] in such tubing a higher heat and mass transfer as well as the more precise control over pressure and flow rate occurs which finally cause short residence times of educts, smaller reaction volumes, reliable and reproducible processes.[350] This reflects the potential of flow chemistry regarding economics and environmental protection.[346,349,351] Another very important key aspect is compartmentalization which allows the combination of different reactions under different conditions in a cascade fashion.[352] However, according to Roberge et al. those properties of continuous flow systems consequently would have the capability to improve approx. 50% of all chemical reactions in industry (especially in API synthesis), not only in terms of productivity and space-time yield but also as platform for reaction engineering.[353] Recently, the latter was shown by Pfizer when in fact over 1500 reaction conditions for a Suzuki cross-

coupling reaction were evaluated before upscaling the desired reaction.[354] Indeed, continuous flow systems became an arising focus of chemical catalysis in academia and industry what is also indicated by an annually increasing number of publications, patents and reviews in this field.[346,355,356] In chemical synthesis, that very intensive and broad research led to a set of (multi-step) continuous flow setups, which for instance are conducting and combining several different reaction types like Grignard addition, Mannich reaction, Claisen condensation, Friedel-Crafts acylation, Buchwald-Hartwig coupling and Suzuki cross-coupling in conjunction with e.g. light or microwave irradiation *en route* to a lot of pharmaceutical relevant products.[346,352] It is noteworthy, that the intensive efforts over the last years in combining continuous flow chemistry and the Suzuki-Miyaura reaction has been reviewed recently with differentiating between homogeneous and heterogeneous catalysis.[357] Howsoever, in the last 20 years, also continuous flow biocatalysts emerged to an effective tool for chemists, using both, whole cells and free enzymes including e.g. lipase, lyase, monooxygenase, ketoreductase, phenylalanine ammonia lyase, glucosidase, aldolase, laccase, transketolase and transaminase activity in the synthesis of epoxides, peptides, amino acids, carboxylic acids, sugars, alcohols, amino alcohols and amines in single-reactor or multi-reactor chemoenzymatic approaches.[300,356,358] Thereby, enzyme immobilisation is a key topic in the establishment of a biocatalysis driven continuous flow setup. Immobilisation allows the specific localisation and provision of enzymes and whole cells at the desired place, in desired quantities, for a desired timespan and makes product isolation or purification easier.[356] Another considerable advantage is that enzyme stability and reactivity was improved in many cases when immobilisation was performed.[359,360] A large number of immobilization methods exist (e.g.[361–370]) which all can be grouped in three classes, binding to a carrier, entrapment and cross-linking.[362] Since the immobilisation is not main focus of this thesis a brief overview is supposed to be given. The carrier based technique additionally differentiate many types of immobilisation, e.g. adsorptive, covalent and affinity binding. Immobilisation via adsorption bases on hydrophobic, ionic and hydrogen bond interactions between the biocatalyst and the carrier. A number of adsorptive carrier has been used, like molecular sieves (Celite)[371,372] or silica.[364] The major issue of adsorptive immobilisation is certainly the relative high enzyme leaching during process which might not only be inefficient because of the low reusability but also hampers product purity.[360,368] The covalent immobilisation provides a massive improvement in this context but at the same time the suitability of this technique for the particular enzyme should be tested since enzyme deactivation occurs quite often.[362] Glutaraldehyde- or epoxy functionalized silica,[373,374] chitosan[242,375] and glass surfaces[376] are here known examples aiming the reaction with amino groups of the target protein, primary lysine residues. Affinity immobilisation bases on the high binding affinity of a target protein to a functional group or moiety at a certain carrier,[377] for instance the binding of a few amino acids (primary histidine) to chelated metal ions.[356] In fact, this type of immobilisation is very convenient because on the one hand the immobilisation procedure is fast and simple without need for pre-treatment with activating or cross-linking reagents and on the other side it allows a more specific loading with the recombinant and histidine-tag bearing target protein. The latter can be achieved without previous protein purification which is a major enhancement over the other described immobilisation methods. On the other side treatment with imidazole or low pH makes carrier regeneration easy and effective. However, in any case of carrier based immobilisation the desired enzyme carrier optimally has to fulfil several characteristics like large surface area, high density of

functional groups for enzyme attachment, water insolubility, inertness towards the desired reaction, as well as chemical, thermal and physical robustness.[356,378] Finally, the entrapment and cross-linking technique have in common that the respective biocatalyst is trapped in a network of a surrounding gel, membrane or by other enzymes, either non-covalently (e.g. in the case of calcium-alginate-beads)[369,379] or covalently (e.g. glutaraldehyde mediated cross-linked enzyme aggregates, CLEA).[380] Also combinations with covalent attachments are possible.[368] A serious disadvantage is the significant low process robustness.[362] In various works immobilized ATAs were applied using different supports, e.g. chitosan,[242,375] polystyrene,[244] silica monolith,[381] methacrylate beads[247] or affinity resins[382,383] including concepts for continuous flows systems in some cases. Therefore, Andrade et al.[247] used an immobilised whole cell system with overexpressed Arth-TA for the asymmetric synthesis of 1-methoxy-2-propylamin in flow with high conversion and enantiomeric excess (96%*c*, >99%*ee*). Recently, Biggelaar et al.[381] also immobilised Arthmut11-TA successfully on silica monolith via a combination of adsorptive and covalent immobilisation. This concept was not described yet for TAs. As model reaction the authors showed the kinetic resolution of 4-bromo-1-phenylethylamine *in continuo*.

A comparable approach was demonstrated in **Article IV** in which the covalent immobilisation of Vfl-TA (ATA from *Vibrio fluvialis*) on functionalized cellulose was presented. Also this type of carrier was not described before for the immobilisation and application of TAs in biocatalysis. Cellulose is supposed to be the most abundant biopolymer on earth and has been used for various applications in polymer science (e.g.[384–386]). As environmentally benign and readily available carrier it was widely used for enzyme immobilisation already 40 years ago even though via ionic interactions.[361]

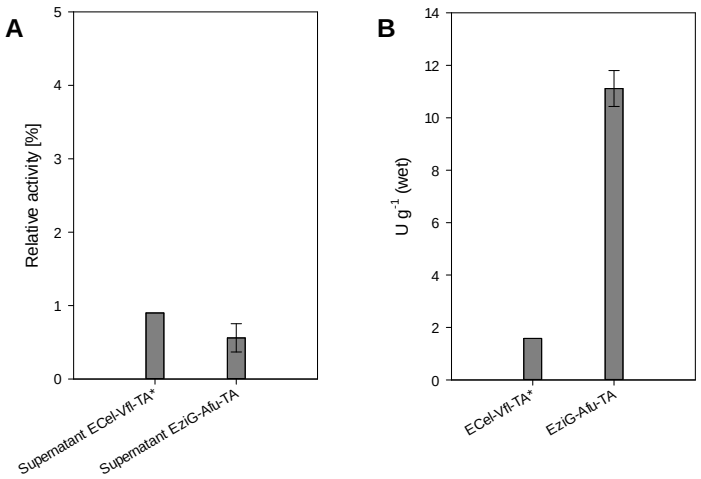

Figure 9. Evaluation of ATA immobilization from crude lysate on epoxy-functionalized cellulose (ECel) and EziG™ carrier (via His-tag immobilization) of Vfl-TA (ATA from *Vibrio fluvialis*) and Afu-TA (ATA from *Aspergillus fumigatus*), respectively. **A** The residual activity in the supernatant after immobilization procedure is given in relation to a respective blank experiment and was determined via the acetophenone assay.[117] The blank experiment contained crude lysate with overexpressed Vfl-TA or Afu-TA incubated under immobilization conditions but without carrier. **B** Amounts of U g^{-1} (wet) carrier determined via the modified acetophenone assay according to reference[375]. Values for Vfl-TA were took over from **Article IV** and were provided without standard deviation. One unit (U) of ATA activity was defined as the formation of 1 µmol of acetophenone per minute (ε=12 $M^{-1}cm^{-1}$).

The study shown in **Article IV** compared two reagents the cellulose raw material has been treated with, to provide the functional groups for protein attachment, either APTES ((3-Aminopropyl)trimethoxysilane) and glutaraldehyde in combination (to obtain an aldehyde function) or GLYMO ((3-Glycidyloxy-propyl)trimethoxysilane, to obtain an epoxy function). Both carriers were examined via activity measurements, solid state ^{13}C-NMR spectroscopy, confocal laser scanning microscopy and scanning electron microscopy. The interested reader is referred to **Article IV** for further information. However, the epoxy-functionalized cellulose (ECel) exhibited a roughly 63% higher immobilisation yield which was determined via a modified version of the acetophenone assay[375] and additionally substantiated by the confocal laser scanning microscopy. The Vfl-ECel immobilisate was taken for further studies, particularly in the asymmetric synthesis of 1-phenylethylamine with L-alanine as amine donor under continuous flow conditions yielding the product with 80% conversion (Scheme 10A). Also in **Article III** the idea of a continuous chemoenzymatic production of biaryl amines was followed in order to provide a proof-of-principle concept for this application. For this approach the immobilization with affinity resins was chosen, more specifically by using the EziG™ carrier[383] because first, this carrier has already been proven for the immobilisation of ATAs and second, the high specific loading with target protein was considered as highly desirable. Even though after immobilisation the residual ATA activity in the supernatant was comparably low, the immobilisation of Afu-TA on EziG™ revealed indeed a higher activity on carrier compared to the Vfl-TA-ECel immobilisate (Figure 9).

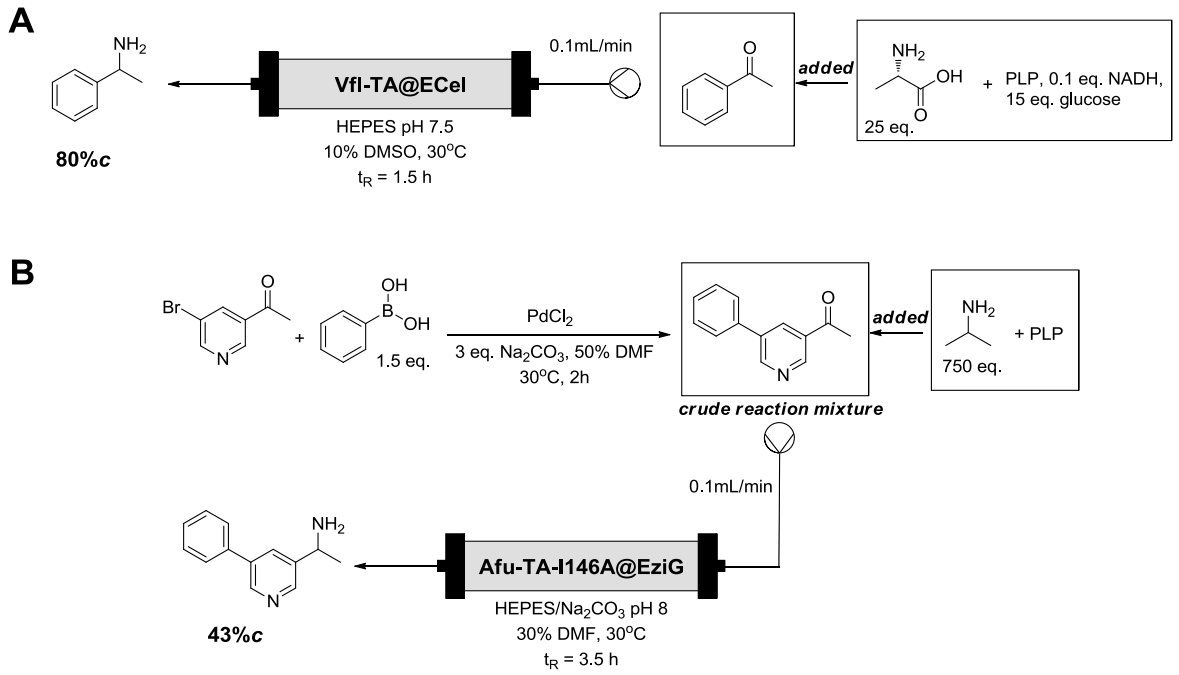

Scheme 10. Continuous flow reactions presented in **Article IV** (A) and **III** (B). **A** Synthesis of (*S*)-1-phenylethylamine with Vfl-TA immobilized on functionalized cellulose (**Article IV**). This was chosen as model reaction to characterize the presented enzyme carrier. Since alanine was used as the amine donor, the LDH/GDH system was used as equilibrium displacement technique. All auxiliary enzymes were supplied in the added reaction solution. **B** Chemoenzymatic synthesis of 1-(5-phenylpyridin-3-yl)ethanamine (Table 5, entry 1, **Article III**). The crude Suzuki-Miyaura reaction product was added in flow to an IPA (the used amine donor) and PLP containing solution and subsequently pumped through a column containing 0.5 g of the immobilized variant Afu-TA-I146A on EziG™ carrier. Conversions were determined via GC analysis. Molar equivalents are given in relation to the respective ketone.

The best performing reaction from the investigations in **Article III** (Table 5, entry 1, Afu-TA-I146A) was allocated for the experiment illustrated in Scheme 10B. The cross-coupling reaction occurred under optimal conditions as indicated; subsequently, the crude reaction mixture and the reaction solution for transamination were pumped synchronically through a column with immobilized Afu-TA-I146A variant obtaining the product 1-(5-phenylpyridin-3-yl)ethanamine with a conversion of 43%. The shown concept could be extended by a two-reactor setup conducting the biaryl formation by a heterogeneous Suzuki cross-coupling reaction beforehand. In such a case, the aspect of compartmentalization is certainly one of the most advantageous properties of continuous flow systems, especially if chemoenzymatic combinations with limited compatibility are aimed.

7. Summary and outlook

In asymmetric synthesis, the choice of the amine donor is crucial for reaction design since the majority of transaminase-catalysed reactions suffer from an unfavored thermodynamic equilibrium. Although IPA is considered as ideal amine donor, unfortunately many reactions in literature did not achieve full conversion. Keeping this in mind, scientists very often use alanine as the 'conceptional reliable' amine donor even though auxiliary enzymes for the equilibrium shift are required. In this work, the efficient utilization of IPA was aimed via reaction and enzyme engineering. A systematic investigation of different reaction condition effects was performed for a range of ATA, revealing that in the investigated reactions only the donor-acceptor ratio had a major influence on amine product formation. With a sufficient high excess of IPA even a range of wild-type enzymes achieved good conversion in model reactions with IPA. This concept was followed in the successful production of halogenated chiral amines using a wild-type (*R*)- and (*S*)-ATA, in many cases with quantitative conversion. However, for the engineered ATA from *Ruegeria* sp. (3FCR-QM) the identification of crucial amino acid residues for IPA acceptance around the active site was possible. Future experiments could reveal whether the presented mutations are transferable to other scaffolds but either way the engineering of IPA acceptance is a challenging topic since no obvious steric hindrance could be addressed as in the case of bulky substrates. Furthermore, in this thesis the access to chiral biarly amines in a two-step-one-pot fashion was presented via the combination of the Suzuki–Miyaura cross-coupling with a transaminase-catalysed reaction under ligand-free and mild conditions. Key points of this approach were the excellent compatibility of the selected transaminase with the demands of the chemical cross-coupling reaction and the engineering of a better acceptance of several biaryl ketones by the simple means of an alanine scanning study. In the shown case, the success in enzyme engineering avoided the necessity of amine group protection strategies if the cross-coupling reaction should have been carried out after transamination. In addition, a proof-of-concept continuous flow application was proven to produce biaryl amines *in continuo*.

8. References

[1] P. Christen, P. K. Mehta, *Chem. Rec.* **2001**, *1*, 436–447.
[2] A. C. Eliot, J. F. Kirsch, *Annu. Rev. Biochem.* **2004**, *73*, 383–415.
[3] I. Slabu, J. L. Galman, R. C. Lloyd, N. J. Turner, *ACS Catal.* **2017**, *7*, 8263–8284.
[4] X. M. He, H. Liu, *Annu. Rev. Biochem.* **2002**, *71*, 701–754.
[5] S. R. Kleppner, A. J. Tobin, *Emerg. Ther. Targets* **2001**, *5*, 219–239.
[6] C. C. Wang, *Annu Rev Pharmacol Toxicol* **1995**, *35*, 93–127.
[7] K. Snell, D. Riches, *Cancer Lett.* **1989**, *44*, 217–220.
[8] F. Steffen-Munsberg, C. Vickers, H. Kohls, H. Land, H. Mallin, A. Nobili, L. Skalden, T. van den Bergh, H.-J. Joosten, P. Berglund, *Biotechnol. Adv.* **2015**, *33*, 566–604.
[9] M. D. Toney, *Biochim. Biophys. Acta BBA-Proteins Proteomics* **2011**, *1814*, 1407–1418.
[10] R. Percudani, A. Peracchi, *BMC Bioinformatics* **2009**, *10*, 273–281.
[11] H. C. Dunathan, *Proc. Natl. Acad. Sci.* **1966**, *55*, 712–716.
[12] J. N. Jansonius, *Curr. Opin. Struct. Biol.* **1998**, *8*, 759–769.
[13] J. F. Kirsch, G. Eichele, G. C. Ford, M. G. Vincent, J. N. Jansonius, H. Gehring, P. Christen, *J. Mol. Biol.* **1984**, *174*, 497–525.
[14] M. Toney, E. Hohenester, S. Cowan, J. Jansonius, *Science* **1993**, *261*, 756–759.
[15] C. Momany, S. Ernst, R. Ghosh, N.-L. Chang, M. L. Hackert, *J. Mol. Biol.* **1995**, *252*, 643–655.
[16] S. D. Banik, A. Chandra, *J. Phys. Chem. B* **2014**, *118*, 11077–11089.
[17] N. V. Grishin, M. A. Phillips, E. J. Goldsmith, *Protein Sci.* **1995**, *4*, 1291–1304.
[18] B.-Y. Hwang, B.-K. Cho, H. Yun, K. Koteshwar, B.-G. Kim, *J. Mol. Catal. B Enzym.* **2005**, *37*, 47–55.
[19] M. Höhne, U. T. Bornscheuer, in *Enzyme Catal. Org. Synth.* (Eds.: K. Drauz, H. Gröger, O. May), Wiley-VCH, **2012**, pp. 779–820.
[20] J.-S. Shin, B.-G. Kim, *Biotechnol. Bioeng.* **1997**, *55*, 348–358.
[21] J.-S. Shin, H. Yun, J.-W. Jang, I. Park, B.-G. Kim, *Appl. Microbiol. Biotechnol.* **2003**, *61*, 463–471.
[22] J.-S. Shin, B.-G. Kim, *J. Org. Chem.* **2002**, *67*, 2848–2853.
[23] B.-K. Cho, H.-Y. Park, J.-H. Seo, J. Kim, T.-J. Kang, B.-S. Lee, B.-G. Kim, *Biotechnol. Bioeng.* **2008**, *99*, 275–284.
[24] K. S. Midelfort, R. Kumar, S. Han, M. J. Karmilowicz, K. McConnell, D. K. Gehlhaar, A. Mistry, J. S. Chang, M. Anderson, A. Villalobos, *Protein Eng. Des. Sel.* **2013**, *26*, 25–33.
[25] C. Rausch, A. Lerchner, A. Schiefner, A. Skerra, *Proteins Struct. Funct. Bioinforma.* **2013**, *81*, 774–787.
[26] M. S. Malik, E.-S. Park, J.-S. Shin, *Appl. Microbiol. Biotechnol.* **2012**, *94*, 1163–1171.
[27] K. Hirotsu, M. Goto, A. Okamoto, I. Miyahara, *Chem. Rec.* **2005**, *5*, 160–172.
[28] K. E. Cassimjee, B. Manta, F. Himo, *Org. Biomol. Chem.* **2015**, *13*, 8453–8464.
[29] P. K. Mehta, T. I. Hale, P. Christen, *Eur. J. Biochem.* **1993**, *214*, 549–561.
[30] K. Soda, T. Yoshimura, N. Esaki, *Chem. Rec.* **2001**, *1*, 373–384.
[31] R.-Z. Liao, W.-J. Ding, J.-G. Yu, W.-H. Fang, R.-Z. Liu, *J. Comput. Chem.* **2008**, *29*, 1919–1929.
[32] F. V. Pishchugin, I. T. Tuleberdiev, *Russ. J. Gen. Chem.* **2005**, *75*, 1465–1468.
[33] P. H. Yu, D. A. Durden, B. A. Davis, A. A. Boulton, *J. Neurochem.* **1987**, *48*, 440–446.
[34] S. Kuramitsu, K. Hiromi, H. Hayashi, Y. Morino, H. Kagamiyama, *Biochemistry* **1990**, *29*, 5469–5476.
[35] A. Iwasaki, Y. Yamada, Y. Ikenaka, J. Hasegawa, *Biotechnol Lett* **2003**, *25*, 1843–1846.
[36] A. Iwasaki, Y. Yamada, N. Kizaki, Y. Ikenaka, J. Hasegawa, *Appl Microbiol Biotechnol* **2006**, *69*, 499–505.
[37] M. Höhne, S. Schätzle, H. Jochens, K. Robins, U. T. Bornscheuer, *Nat. Chem. Biol.* **2010**, *6*, 807–813.
[38] M. Thomsen, L. Skalden, G. J. Palm, M. Höhne, U. T. Bornscheuer, W. Hinrichs, *Acta Crystallogr. D Biol. Crystallogr.* **2014**, *70*, 1086–1093.
[39] E.-S. Park, J.-Y. Dong, J.-S. Shin, *Appl. Microbiol. Biotechnol.* **2014**, *98*, 651–660.
[40] M. Thomsen, L. Skalden, G. J. Palm, M. Höhne, U. T. Bornscheuer, W. Hinrichs, *Acta Crystallograph. Sect. F Struct. Biol. Cryst. Commun.* **2013**, *69*, 1415–1417.
[41] M. S. Humble, K. E. Cassimjee, M. Haakansson, Y. R. Kimbung, B. Walse, V. Abedi, H.-J. Federsel, P. Berglund, D. T. Logan, *FEBS J.* **2012**, *279*, 779–792.

[42] G. G. Wybenga, C. G. Crismaru, D. B. Janssen, B. W. Dijkstra, *J. Biol. Chem.* **2012**, *287*, 28495–28502.
[43] P. Christen, P. Kasper, H. Gehring, M. Sterk, *FEBS Lett.* **1996**, *389*, 12–14.
[44] F. Steffen-Munsberg, C. Vickers, A. Thontowi, S. Schätzle, T. Tumlirsch, M. Svedendahl Humble, H. Land, P. Berglund, U. T. Bornscheuer, M. Höhne, *ChemCatChem* **2013**, *5*, 150–153.
[45] U. T. Bornscheuer, G. W. Huisman, R. J. Kazlauskas, S. Lutz, J. C. Moore, K. Robins, *Nature* **2012**, *485*, 185–194.
[46] M. D. Truppo, *ACS Med. Chem. Lett.* **2017**, *8*, 476–480.
[47] A. S. Wells, G. L. Finch, P. C. Michels, J. W. Wong, *Org. Process Res. Dev.* **2012**, *16*, 1986–1993.
[48] R. C. Simon, F. G. Mutti, W. Kroutil, *Drug Discov. Today Technol.* **2013**, *10*, 37–44.
[49] J. M. Woodley, *Curr. Opin. Chem. Biol.* **2013**, *17*, 310–316.
[50] N. J. Turner, R. Kumar, *Curr. Opin. Chem. Biol.* **2018**, *43*, A1–A3.
[51] G. Hughes, J. C. Lewis, *Chem. Rev.* **2018**, *118*, 1–3.
[52] B. M. Nestl, B. A. Nebel, B. Hauer, *Curr. Opin. Chem. Biol.* **2011**, *15*, 187–193.
[53] M. Breuer, K. Ditrich, T. Habicher, B. Hauer, M. Keßeler, R. Stürmer, T. Zelinski, *Angew. Chem. Int. Ed.* **2004**, *43*, 788–824.
[54] M. Höhne, U. T. Bornscheuer, *ChemCatChem* **2009**, *1*, 42–51.
[55] S. Wenda, S. Illner, A. Mell, U. Kragl, *Green Chem.* **2011**, *13*, 3007–3047.
[56] T. Davids, M. Schmidt, D. Böttcher, U. T. Bornscheuer, *Curr. Opin. Chem. Biol.* **2013**, *17*, 215–220.
[57] J.-H. Xie, D.-H. Bao, Q.-L. Zhou, *Synthesis* **2014**, *47*, 460–471.
[58] D. J. C. Constable, P. J. Dunn, J. D. Hayler, G. R. Humphrey, J. L. Leazer, Jr., R. J. Linderman, K. Lorenz, J. Manley, B. A. Pearlman, A. Wells, *Green Chem* **2007**, *9*, 411–420.
[59] D. Ghislieri, N. J. Turner, *Top. Catal.* **2014**, *57*, 284–300.
[60] M. Fuchs, J. E. Farnberger, W. Kroutil, *Eur. J. Org. Chem.* **2015**, *2015*, 6965–6982.
[61] A. Gomm, E. O'Reilly, *Curr. Opin. Chem. Biol.* **2018**, *43*, 106–112.
[62] G. W. Huisman, S. J. Collier, *Curr. Opin. Chem. Biol.* **2013**, *17*, 284–292.
[63] J. H. Sattler, M. Fuchs, F. G. Mutti, B. Grischek, P. Engel, J. Pfeffer, J. M. Woodley, W. Kroutil, *Angew. Chem. Int. Ed.* **2014**, *53*, 14153–14157.
[64] G. A. Behrens, A. Hummel, S. K. Padhi, S. Schätzle, U. T. Bornscheuer, *Adv. Synth. Catal.* **2011**, *353*, 2191–2215.
[65] K. Steiner, H. Schwab, *Comput. Struct. Biotechnol. J.* **2012**, *2*, 201209010.
[66] A. S. Bommarius, J. K. Blum, M. J. Abrahamson, *Curr. Opin. Chem. Biol.* **2011**, *15*, 194–200.
[67] J. Damborsky, J. Brezovsky, *Curr. Opin. Chem. Biol.* **2009**, *13*, 26–34.
[68] A. Romero-Rivera, M. Garcia-Borràs, S. Osuna, *Chem. Commun.* **2017**, *53*, 284–297.
[69] E. Krieger, K. Joo, J. Lee, J. Lee, S. Raman, J. Thompson, M. Tyka, D. Baker, K. Karplus, *Proteins Struct. Funct. Bioinforma.* **2009**, *77*, 114–122.
[70] E. Krieger, G. Koraimann, G. Vriend, *Proteins Struct. Funct. Bioinforma.* **2002**, *47*, 393–402.
[71] K. Arnold, L. Bordoli, J. Kopp, T. Schwede, *Bioinformatics* **2006**, *22*, 195–201.
[72] F. Richter, A. Leaver-Fay, S. D. Khare, S. Bjelic, D. Baker, *PLoS ONE* **2011**, *6*, 19230.
[73] D. Röthlisberger, O. Khersonsky, A. M. Wollacott, L. Jiang, J. DeChancie, J. Betker, J. L. Gallaher, E. A. Althoff, A. Zanghellini, O. Dym, *Nature* **2008**, *453*, 190–195.
[74] J. B. Siegel, A. Zanghellini, H. M. Lovick, G. Kiss, A. R. Lambert, J. L. St.Clair, J. L. Gallaher, D. Hilvert, M. H. Gelb, B. L. Stoddard, *Science* **2010**, *329*, 309–313.
[75] L. Jiang, E. A. Althoff, F. R. Clemente, L. Doyle, D. Rothlisberger, A. Zanghellini, J. L. Gallaher, J. L. Betker, F. Tanaka, C. F. Barbas, *Science* **2008**, *319*, 1387–1391.
[76] F. H. Arnold, *Nat. Biotechnol.* **1998**, *16*, 617–618.
[77] F. H. Arnold, *Acc. Chem. Res.* **1998**, *31*, 125–131.
[78] W. P. C. Stemmer, *Nature* **1994**, *370*, 389–391.
[79] W. P. Stemmer, *Proc. Natl. Acad. Sci.* **1994**, *91*, 10747–10751.
[80] M. T. Reetz, D. Kahakeaw, R. Lohmer, *ChemBioChem* **2008**, *9*, 1797–1804.
[81] B. D. Allen, A. Nisthal, S. L. Mayo, *Proc. Natl. Acad. Sci.* **2010**, *107*, 19838–19843.
[82] T. S. Chen, A. E. Keating, *Protein Sci.* **2012**, *21*, 949–963.
[83] S. M. Lippow, T. S. Moon, S. Basu, S.-H. Yoon, X. Li, B. A. Chapman, K. Robison, D. Lipovšek, K. L. J. Prather, *Chem. Biol.* **2010**, *17*, 1306–1315.
[84] T. P. Treynor, C. L. Vizcarra, D. Nedelcu, S. L. Mayo, *Proc. Natl. Acad. Sci.* **2007**, *104*, 48–53.
[85] S. Lutz, *Curr. Opin. Biotechnol.* **2010**, *21*, 734–743.
[86] R. A. Chica, N. Doucet, J. N. Pelletier, *Curr. Opin. Biotechnol.* **2005**, *16*, 378–384.
[87] M. T. Reetz, L.-W. Wang, M. Bocola, *Angew. Chem. Int. Ed.* **2006**, *45,* 1236–1241.

[88] R. K. Kuipers, H.-J. Joosten, W. J. H. van Berkel, N. G. H. Leferink, E. Rooijen, E. Ittmann, F. van Zimmeren, H. Jochens, U. Bornscheuer, G. Vriend, *Proteins* **2010**, *78*, 2101–2113.
[89] R. Kourist, H. Jochens, S. Bartsch, R. Kuipers, S. K. Padhi, M. Gall, D. Böttcher, H.-J. Joosten, U. T. Bornscheuer, *ChemBioChem* **2010**, *11*, 1635–1643.
[90] F. Guo, P. Berglund, *Green Chem.* **2017**, *19*, 333–360.
[91] S. A. Kelly, S. Pohle, S. Wharry, S. Mix, C. C. R. Allen, T. S. Moody, B. F. Gilmore, *Chem. Rev.* **2018**, *118*, 349–367.
[92] E. E. Ferrandi, D. Monti, *World J. Microbiol. Biotechnol.* **2018**, *34*, 13.
[93] C. K. Savile, J. M. Janey, E. C. Mundorff, J. C. Moore, S. Tam, W. R. Jarvis, J. C. Colbeck, A. Krebber, F. J. Fleitz, J. Brands, *Science* **2010**, *329*, 305–309.
[94] I. V. Pavlidis, M. S. Weiß, M. Genz, P. Spurr, S. P. Hanlon, B. Wirz, H. Iding, U. T. Bornscheuer, *Nat. Chem.* **2016**, *8*, 1076–1082.
[95] M. S. Weiß, I. V. Pavlidis, P. Spurr, S. P. Hanlon, B. Wirz, H. Iding, U. T. Bornscheuer, *Org. Biomol. Chem.* **2016**, *14*, 10249–10254.
[96] M. S. Weiß, I. V. Pavlidis, P. Spurr, S. P. Hanlon, B. Wirz, H. Iding, U. T. Bornscheuer, *ChemBioChem* **2017**, *18*, 1022–1026.
[97] A. Nobili, F. Steffen-Munsberg, H. Kohls, I. Trentin, C. Schulzke, M. Höhne, U. T. Bornscheuer, *ChemCatChem* **2015**, *7*, 757–760.
[98] M. Genz, O. Melse, S. Schmidt, C. Vickers, M. Dörr, T. van den Bergh, H.-J. Joosten, U. T. Bornscheuer, *ChemCatChem* **2016**, *8*, 3199–3202.
[99] D. F. Dourado, S. Pohle, A. T. Carvalho, D. S. Dheeman, J. M. Caswell, T. Skvortsov, I. Miskelly, R. T. Brown, D. J. Quinn, C. C. Allen, *ACS Catal.* **2016**, *6*, 7749–7759.
[100] A. S. Bommarius, *Annu. Rev. Chem. Biomol. Eng.* **2015**, *6*, 319–345.
[101] B.-Y. Hwang, B.-G. Kim, *Enzyme Microb. Technol.* **2004**, *34*, 429–436.
[102] S. Mathew, G. Shin, M. Shon, H. Yun, *Biotechnol. Bioprocess Eng.* **2013**, *18*, 1–7.
[103] H. Zhao, F. H. Arnold, *Curr. Opin. Struct. Biol.* **1997**, *7*, 480–485.
[104] H. Yun, B.-Y. Hwang, J.-H. Lee, B.-G. Kim, *Appl. Environ. Microbiol.* **2005**, *71*, 4220–4224.
[105] J. Hopwood, M. D. Truppo, N. J. Turner, R. C. Lloyd, *Chem Commun* **2010**, *47*, 773–775.
[106] M. S. Weiß, I. V. Pavlidis, C. Vickers, M. Höhne, U. T. Bornscheuer, *Anal. Chem.* **2014**, *86*, 11847–11853.
[107] J.-S. Shin, B.-G. Kim, *Biotechnol. Bioeng.* **2002**, *77*, 832–837.
[108] E.-S. Park, J.-Y. Dong, J.-S. Shin, *Appl. Microbiol. Biotechnol.* **2014**, *98*, 651–660.
[109] I. Martínez-Martínez, J. Navarro-Fernández, F. García-Carmona, H. Takami, Á. Sánchez-Ferrer, *Proteins Struct. Funct. Bioinforma.* **2007**, *70*, 1429–1441.
[110] U. T. Bornscheuer, J. Altenbuchner, H. H. Meyer, *Biotechnol. Bioeng.* **1998**, *58*, 554–559.
[111] S. Delagrave, D. J. Murphy, J. L. R. Pruss, A. M. Maffia, B. L. Marrs, E. J. Bylina, W. J. Coleman, C. L. Grek, M. R. Dilworth, M. M. Yang, *Protein Eng. Des. Sel.* **2001**, *14*, 261–267.
[112] S. C. Willies, J. L. White, N. J. Turner, *Tetrahedron* **2012**, *68*, 7564–7567.
[113] F. Escalettes, N. J. Turner, *ChemBioChem* **2008**, *9*, 857–860.
[114] D. Koszelewski, I. Lavandera, D. Clay, D. Rozzell, W. Kroutil, *Adv. Synth. Catal.* **2008**, *350*, 2761–2766.
[115] M. D. Truppo, J. D. Rozzell, J. C. Moore, N. J. Turner, *Org. Biomol. Chem.* **2009**, *7*, 395–398.
[116] M. D. Truppo, N. J. Turner, *Org. Biomol. Chem.* **2010**, *8*, 1280–1283.
[117] S. Schätzle, M. Höhne, E. Redestad, K. Robins, U. T. Bornscheuer, *Anal. Chem.* **2009**, *81*, 8244–8248.
[118] K. E. Cassimjee, M. S. Humble, V. Miceli, C. G. Colomina, P. Berglund, *ACS Catal.* **2011**, *1*, 1051–1055.
[119] M. Genz, C. Vickers, T. van den Bergh, H.-J. Joosten, M. Dörr, M. Höhne, U. T. Bornscheuer, *Int. J. Mol. Sci.* **2015**, *16*, 26953–26963.
[120] A. R. Martin, R. DiSanto, I. Plotnikov, S. Kamat, D. Shonnard, S. Pannuri, *Biochem. Eng. J.* **2007**, *37*, 246–255.
[121] T. Scheidt, H. Land, M. Anderson, Y. Chen, P. Berglund, D. Yi, W.-D. Fessner, *Adv. Synth. Catal.* **2015**, *357*, 1721–1731.
[122] A. P. Green, N. J. Turner, E. O'Reilly, *Angew. Chem. Int. Ed.* **2014**, *53*, 10714–10717.
[123] D. Baud, N. Ladkau, T. Moody, J. Ward, H. Hailes, *Chem. Commun.* **2015**, *51*, 17225–17228.
[124] J. M. Hawkins, T. J. N. Watson, *Angew. Chem. Int. Ed.* **2004**, *43*, 3224–3228.
[125] T. C. Nugent, M. El-Shazly, *Adv. Synth. Catal.* **2010**, *352*, 753–819.
[126] T. Nugent, S. Marinova, *Synthesis* **2013**, *45*, 153–166.
[127] F. Weber, G. Sedelmeier, *Nachr Chem* **2014**, *62*, 997–997.
[128] T. C. Nugent, A. K. Ghosh, V. N. Wakchaure, R. R. Mohanty, *Adv. Synth. Catal.* **2006**, *348*, 1289–1299.
[129] H. Gröger, *Bioorg. Med. Chem.* **2018**, *26*, 1239–1240.

[130] A. M. Bezborodov, N. A. Zagustina, *Appl. Biochem. Microbiol.* **2016**, *52*, 237–249.
[131] O. Verho, J.-E. Bäckvall, *J. Am. Chem. Soc.* **2015**, *137*, 3996–4009.
[132] D. Koszelewski, K. Tauber, K. Faber, W. Kroutil, *Trends Biotechnol.* **2010**, *28*, 324–332.
[133] M. D. Patil, G. Grogan, A. Bommarius, H. Yun, *Catalysts* **2018**, *8*, 254–279.
[134] J. Lalonde, *Curr. Opin. Biotechnol.* **2016**, *42*, 152–158.
[135] S. Mathew, H. Yun, *ACS Catal.* **2012**, *2*, 993–1001.
[136] R. C. Simon, N. Richter, E. Busto, W. Kroutil, *ACS Catal.* **2014**, *4*, 129–143.
[137] J. D. Stewart, *Curr. Opin. Chem. Biol.* **2001**, *5*, 120–129.
[138] E. Ricca, B. Brucher, J. H. Schrittwieser, *Adv. Synth. Catal.* **2011**, *353*, 2239–2262.
[139] H. Kohls, F. Steffen-Munsberg, M. Höhne, *Curr. Opin. Chem. Biol.* **2014**, *19*, 180–192.
[140] U. T. Bornscheuer, R. J. Kazlauskas, Wiley-VCH; Weinheim; **2006**.
[141] F. Balkenhohl, K. Ditrich, B. Hauer, W. Ladner, *J. Prakt. Chemie* **1997**, *339*, 381–384.
[142] M.-J. Kim, W.-H. Kim, K. Han, Y. K. Choi, J. Park, *Org. Lett.* **2007**, *9*, 1157–1159.
[143] J. Paetzold, J. E. Bäckvall, *J. Am. Chem. Soc.* **2005**, *127*, 17620–17621.
[144] S. Escoubet, S. Gastaldi, N. Vanthuyne, G. Gil, D. Siri, M. P. Bertrand, *Eur. J. Org. Chem.* **2006**, *2006*, 3242–3250.
[145] S. Escoubet, S. Gastaldi, N. Vanthuyne, G. Gil, D. Siri, M. P. Bertrand, *J. Org. Chem.* **2006**, *71*, 7288–7292.
[146] N. J. Turner, *Chem. Rev.* **2011**, *111*, 4073–4087.
[147] M. Alexeeva, A. Enright, M. J. Dawson, M. Mahmoudian, N. J. Turner, *Angew. Chem. Int. Ed.* **2002**, *41*, 3177–3180.
[148] G. Grogan, *Curr. Opin. Chem. Biol.* **2018**, *43*, 15–22.
[149] A. Znabet, M. M. Polak, E. Janssen, F. J. J. de Kanter, N. J. Turner, R. V. A. Orru, E. Ruijter, *Chem. Commun.* **2010**, *46*, 7918–7920.
[150] T. Li, J. Liang, A. Ambrogelly, T. Brennan, G. Gloor, G. Huisman, J. Lalonde, A. Lekhal, B. Mijts, S. Muley, *J. Am. Chem. Soc.* **2012**, *134*, 6467–6472.
[151] A. Iwasaki, N. Ito, Y. Yasohara, in *Microb. Prod.* (Eds.: H. Anazawa, S. Shimizu), Springer Japan, Tokyo, **2014**, pp. 121–129.
[152] J.-S. Shin, B.-G. Kim, *Enzyme Microb. Technol.* **1999**, *25*, 426–432.
[153] J.-S. Shin, B.-G. Kim, A. Liese, C. Wandrey, *Biotechnol. Bioeng.* **2001**, *73*, 179–187.
[154] J.-S. Shin, B.-G. Kim, D.-H. Shin, *Enzyme Microb. Technol.* **2001**, *29*, 232–239.
[155] N. Itoh, C. Yachi, T. Kudome, *J. Mol. Catal. B Enzym.* **2000**, *10*, 281–290.
[156] M. J. Abrahamson, E. Vázquez-Figueroa, N. B. Woodall, J. C. Moore, A. S. Bommarius, *Angew. Chem. Int. Ed.* **2012**, *51*, 3969–3972.
[157] M. J. Abrahamson, J. W. Wong, A. S. Bommarius, *Adv. Synth. Catal.* **2013**, *355*, 1780–1786.
[158] L. J. Ye, H. H. Toh, Y. Yang, J. P. Adams, R. Snajdrova, Z. Li, *ACS Catal.* **2015**, *5*, 1119–1122.
[159] T. Knaus, W. Böhmer, F. G. Mutti, *Green Chem.* **2017**, *19*, 453–463.
[160] B. de Lange, D. J. Hyett, P. J. D. Maas, D. Mink, F. B. J. van Assema, N. Sereinig, A. H. M. de Vries, J. G. de Vries, *ChemCatChem* **2011**, *3*, 289–292.
[161] N. J. Turner, E. O'Reilly, *Nat. Chem. Biol.* **2013**, *9*, 285–288.
[162] V. Puthan Veetil, H. Raj, M. de Villiers, P. G. Tepper, F. J. Dekker, W. J. Quax, G. J. Poelarends, *ChemCatChem* **2013**, *5*, 1325–1327.
[163] H. Raj, W. Szymański, J. de Villiers, H. J. Rozeboom, V. P. Veetil, C. R. Reis, M. de Villiers, F. J. Dekker, S. de Wildeman, W. J. Quax, *Nat. Chem.* **2012**, *4*, 478–484.
[164] K. Durchschein, B. Ferreira-da Silva, S. Wallner, P. Macheroux, W. Kroutil, S. M. Glueck, K. Faber, *Green Chem.* **2010**, *12*, 616–619.
[165] H. Korbekandi, P. Mather, J. Gardiner, G. Stephens, *Enzyme Microb. Technol.* **2008**, *42*, 308–314.
[166] R. O. M. A. de Souza, L. S. M. Miranda, U. T. Bornscheuer, *Chem. Eur. J.* **2017**, *23*, 12040–12063.
[167] M. Sharma, J. Mangas-Sanchez, N. J. Turner, G. Grogan, *Adv. Synth. Catal.* **2017**, *359*, 2011–2025.
[168] D. Wetzl, M. Gand, A. Ross, H. Müller, P. Matzel, S. P. Hanlon, M. Müller, B. Wirz, M. Höhne, H. Iding, *ChemCatChem* **2016**, *8*, 2023–2026.
[169] G. A. Aleku, S. P. France, H. Man, J. Mangas-Sanchez, S. L. Montgomery, M. Sharma, F. Leipold, S. Hussain, G. Grogan, N. J. Turner, *Nat. Chem.* **2017**, *9*, 961–969.
[170] P. A. Santacoloma, G. Sin, K. V. Gernaey, J. M. Woodley, *Org. Process Res. Dev.* **2011**, *15*, 203–212.
[171] I. Oroz-Guinea, E. García-Junceda, *Curr. Opin. Chem. Biol.* **2013**, *17*, 236–249.
[172] D. Koszelewski, D. Clay, D. Rozzell, W. Kroutil, *Eur. J. Org. Chem.* **2009**, *2009*, 2289–2292.
[173] D. Koszelewski, D. Pressnitz, D. Clay, W. Kroutil, *Org. Lett.* **2009**, *11*, 4810–4812.

[174] D. Koszelewski, B. Grischek, S. M. Glueck, W. Kroutil, K. Faber, *Chem. Eur. J.* **2011**, *17*, 378–383.
[175] C. K. Chung, P. G. Bulger, B. Kosjek, K. M. Belyk, N. Rivera, M. E. Scott, G. R. Humphrey, J. Limanto, D. C. Bachert, K. M. Emerson, *Org. Process Res. Dev.* **2014**, *18*, 215–227.
[176] Z. Peng, J. W. Wong, E. C. Hansen, A. L. A. Puchlopek-Dermenci, H. J. Clarke, *Org. Lett.* **2014**, *16*, 860–863.
[177] Y.-M. Seo, S. Mathew, H.-S. Bea, Y.-H. Khang, S.-H. Lee, B.-G. Kim, H. Yun, *Org. Biomol. Chem.* **2012**, *10*, 2482–2485.
[178] E. O'Reilly, C. Iglesias, N. J. Turner, *ChemCatChem* **2014**, *6*, 992–995.
[179] K. Faber, *Chem. Eur. J.* **2001**, *7*, 5004–5010.
[180] C. C. Gruber, I. Lavandera, K. Faber, W. Kroutil, *Adv. Synth. Catal.* **2006**, *348*, 1789–1805.
[181] N. J. Turner, *Curr. Opin. Chem. Biol.* **2010**, *14*, 115–121.
[182] D. Koszelewski, N. Müller, J. H. Schrittwieser, K. Faber, W. Kroutil, *J. Mol. Catal. B Enzym.* **2010**, *63*, 39–44.
[183] T. Sehl, H. C. Hailes, J. M. Ward, R. Wardenga, E. von Lieres, H. Offermann, R. Westphal, M. Pohl, D. Rother, *Angew. Chem. Int. Ed.* **2013**, *52*, 6772–6775.
[184] M. Müller, G. A. Sprenger, M. Pohl, *Curr. Opin. Chem. Biol.* **2013**, *17*, 261–270.
[185] J. H. Sattler, M. Fuchs, K. Tauber, F. G. Mutti, K. Faber, J. Pfeffer, T. Haas, W. Kroutil, *Angew. Chem. Int. Ed.* **2012**, *51*, 9156 – 9159.
[186] M. Pickl, M. Fuchs, S. M. Glueck, K. Faber, *ChemCatChem* **2015**, *7*, 3121–3124.
[187] G. Guillena, D. J. Ramón, M. Yus, *Chem. Rev.* **2010**, *110*, 1611–1641.
[188] L. Skalden, C. Peters, J. Dickerhoff, A. Nobili, H.-J. Joosten, K. Weisz, M. Höhne, U. T. Bornscheuer, *ChemBioChem* **2015**, *16*, 1041–1045.
[189] L. Skalden, C. Peters, L. Ratz, U. T. Bornscheuer, *Tetrahedron* **2016**, *72*, 7207–7211.
[190] H. Kohls, M. Anderson, J. Dickerhoff, K. Weisz, A. Córdova, P. Berglund, H. Brundiek, U. T. Bornscheuer, M. Höhne, *Adv. Synth. Catal.* **2015**, *357*, 1808–1814.
[191] J. Rudat, B. R. Brucher, C. Syldatk, *AMB Express* **2012**, *2*, 11.
[192] D. Zhu, L. Hua, *Biotechnol. J.* **2009**, *4*, 1420–1431.
[193] J. S. Shin, B. G. Kim, *Biotechnol. Bioeng.* **1999**, *65*, 206–211.
[194] K. B. Hansen, Y. Hsiao, F. Xu, N. Rivera, A. Clausen, M. Kubryk, S. Krska, T. Rosner, B. Simmons, J. Balsells, *J. Am. Chem. Soc.* **2009**, *131*, 8798–8804.
[195] A. A. Desai, *Angew. Chem. Int. Ed.* **2011**, *50*, 1974–1976.
[196] E. Busto, R. C. Simon, B. Grischek, V. Gotor-Fernández, W. Kroutil, *Adv. Synth. Catal.* **2014**, *356*, 1937–1942.
[197] R. E. Meadows, K. R. Mulholland, M. Schürmann, M. Golden, H. Kierkels, E. Meulenbroeks, D. Mink, O. May, C. Squire, H. Straatman, *Org. Process Res. Dev.* **2013**, *17*, 1117–1122.
[198] L. Frodsham, M. Golden, S. Hard, M. N. Kenworthy, D. J. Klauber, K. Leslie, C. Macleod, R. E. Meadows, K. R. Mulholland, J. Reilly, *Org. Process Res. Dev.* **2013**, *17*, 1123–1130.
[199] M. Fuchs, D. Koszelewski, K. Tauber, W. Kroutil, K. Faber, *Chem. Commun.* **2010**, *46*, 5500–5502.
[200] M. Rosler, R. Anand, A. Cicin-Sain, S. Gauthier, Y. Agid, P. Dal-Bianco, H. B. Stahelin, R. Hartman, M. Gharabawi, T. Bayer, *BMJ* **1999**, *318*, 633–640.
[201] M. Fuchs, D. Koszelewski, K. Tauber, J. Sattler, W. Banko, A. K. Holzer, M. Pickl, W. Kroutil, K. Faber, *Tetrahedron* **2012**, *68*, 7691–7694.
[202] F. G. Mutti, C. S. Fuchs, D. Pressnitz, J. H. Sattler, W. Kroutil, *Adv. Synth. Catal.* **2011**, *353*, 3227–3233.
[203] S. Pedragosa-Moreau, A. Le Flohic, V. Thienpondt, F. Lefoulon, A.-M. Petit, N. Ríos-Lombardía, F. Morís, J. González-Sabín, *Adv. Synth. Catal.* **2017**, *359*, 485–493.
[204] G. Li, J. Wang, M. T. Reetz, *Bioorg. Med. Chem.* **2018**, *26*, 1241–1251.
[205] N. J. Turner, M. D. Truppo, *Curr. Opin. Chem. Biol.* **2013**, *17*, 212–214.
[206] C. E. Paul, M. Rodrıguez-Mata, E. Busto, I. Lavandera, V. Gotor-Fernández, V. Gotor, S. Garcıa-Cerrada, J. Mendiola, Ó. de Frutos, I. Collado, *Org. Process Res. Dev.* **2014**, *18*, 788–792.
[207] O. Torre, E. Busto, V. Gotor-Fernández, V. Gotor, *Adv. Synth. Catal.* **2007**, *349*, 1481–1488.
[208] A. Rajput, R. Mukherjee, *Coord. Chem. Rev.* **2013**, *257*, 350–368.
[209] I. Slabu, J. L. Galman, C. Iglesias, N. J. Weise, R. C. Lloyd, N. J. Turner, *Catal. Today* **2018**, *306*, 96–101.
[210] K. E. Cassimjee, M. S. Humble, H. Land, V. Abedi, P. Berglund, *Org. Biomol. Chem.* **2012**, *10*, 5466–5470.
[211] A. Gomm, W. Lewis, A. P. Green, E. O'Reilly, *Chem. Eur. J.* **2016**, *22*, 12692–12695.
[212] A. P. Green, N. J. Turner, E. O'Reilly, *Angew. Chem. Int. Ed.* **2014**, *53*, 10714–10717.

[213] L. Martınez-Montero, V. Gotor, V. Gotor-Fernández, I. Lavandera, *Adv. Synth. Catal.* **2016**, *358*, 1618–1624.
[214] M. López-Iglesias, D. González-Martínez, V. Gotor, E. Busto, W. Kroutil, V. Gotor-Fernández, *ACS Catal.* **2016**, *6*, 4003–4009.
[215] M. López-Iglesias, D. González-Martínez, M. Rodríguez-Mata, V. Gotor, E. Busto, W. Kroutil, V. Gotor-Fernández, *Adv. Synth. Catal.* **2017**, *359*, 279–291.
[216] W. Xu, X. Wang, A. M. Tocker, P. Huang, M. E. Reith, L.-Y. Liu-Chen, A. B. Smith, S. Kortagere, *ACS Chem. Neurosci.* **2016**, *8*, 486–500.
[217] R. W. Fuller, *Ann. N. Y. Acad. Sci.* **1978**, *305*, 147–159.
[218] W. Kroutil, E.-M. Fischereder, C. S. Fuchs, H. Lechner, F. G. Mutti, D. Pressnitz, A. Rajagopalan, J. H. Sattler, R. C. Simon, E. Siirola, *Org. Process Res. Dev.* **2013**, *17*, 751–759.
[219] M. Svedendahl, C. Branneby, L. Lindberg, P. Berglund, *ChemCatChem* **2010**, *2*, 976–980.
[220] A. K. Holzer, K. Hiebler, F. G. Mutti, R. C. Simon, L. Lauterbach, O. Lenz, W. Kroutil, *Org. Lett.* **2015**, *17*, 2431–2433.
[221] D. Koszelewski, M. Göritzer, D. Clay, B. Seisser, W. Kroutil, *ChemCatChem* **2010**, *2*, 73–77.
[222] S. Schätzle, F. Steffen-Munsberg, A. Thontowi, M. Höhne, K. Robins, U. T. Bornscheuer, *Adv. Synth. Catal.* **2011**, *353*, 2439–2445.
[223] D. Acetti, E. Brenna, C. Fuganti, *Tetrahedron Asymmetry* **2007**, *18*, 488–492.
[224] K. Andrews, Y. Y. Bo, S. Booker, V. J. Cee, N. D'Angelo, B. J. Herberich, F. T. Hong, C. L. M. Jackson, B. A. Lanman, H. Liao, *Pat. US 20100273764 A1* **2010**.
[225] S. M. Catalano, G. Rishton, N. J. Izzo, *Pat. WO 2013029060 A2* **2013**.
[226] J. Aebi, K. Amrein, B. Hornsperger, H. Knust, B. Kuhn, Y. Liu, H. P. Maerki, A. V. Mayweg, P. Mohr, X. Tan, *Pat. WO 2013037779 A1* **2013**.
[227] S. Hitchock, B. Lam, H. Monenschein, H. Reichard, *Pat. WO 2016081736 A1* **2016**.
[228] P. Abrams, M. Speakman, M. Stott, D. Arkell, R. Pocock, *BJU Int.* **1997**, *80*, 587–596.
[229] M. Takeshi, Y. Tajima, Y. Yutaka, I. Motoyoshi, N. Yusuke, A. Miho, N. Kunimitsu, U. Yuki, *Pat. WO 2018 124088 A1* **2018**.
[230] M. Höhne, S. Kühl, K. Robins, U. T. Bornscheuer, *ChemBioChem* **2008**, *9*, 363–365.
[231] L. Munoz, A. M. Rodriguez, G. Rosell, M. P. Bosch, A. Guerrero, *Org. Biomol. Chem.* **2011**, *9*, 8171–8177.
[232] J. Lima-Ramos, W. Neto, J. M. Woodley, *Top. Catal.* **2014**, *57*, 301–320.
[233] K. Nakamichi, T. Shibatani, Y. Yamamoto, T. Sato, *Appl. Microbiol. Biotechnol.* **1990**, *33*, 637–640.
[234] M. T. Gundersen, R. Abu, M. Schürmann, J. M. Woodley, *Tetrahedron Asymmetry* **2015**, *26*, 567–570.
[235] E.-S. Park, J.-Y. Dong, J.-S. Shin, *Org. Biomol. Chem.* **2013**, *11*, 6929–6933.
[236] M. D. Truppo, J. D. Rozzell, J. C. Moore, N. J. Turner, *Org. Biomol. Chem.* **2009**, *7*, 395–398.
[237] M. E. B. Smith, B. H. Chen, E. G. Hibbert, U. Kaulmann, K. Smithies, J. L. Galman, F. Baganz, P. A. Dalby, H. C. Hailes, G. J. Lye, *Org. Process Res. Dev.* **2010**, *14*, 99–107.
[238] R. Abu, J. M. Woodley, *ChemCatChem* **2015**, *7*, 3094–3105.
[239] M. D. Truppo, J. D. Rozzell, N. J. Turner, *Org. Process Res. Dev.* **2009**, *14*, 234–237.
[240] G. Shin, S. Mathew, H. Yun, *J. Ind. Eng. Chem.* **2015**, *23*, 128–133.
[241] L. Cerioli, M. Planchestainer, J. Cassidy, D. Tessaro, F. Paradisi, *J. Mol. Catal. B Enzym.* **2015**, *120*, 141–150.
[242] H. Mallin, M. Höhne, U. T. Bornscheuer, *J. Biotechnol.* **2014**, *191*, 32–37.
[243] N. Richter, R. Simon, H. Lechner, W. Kroutil, J. Ward, H. Hailes, *Org. Biomol. Chem.* **2015**, *13*, 8843–8851.
[244] W. Neto, M. Schürmann, L. Panella, A. Vogel, J. M. Woodley, *J. Mol. Catal. B Enzym.* **2015**, *117*, 54–61.
[245] A. Cuetos, M. Garcıa-Ramos, E.-M. Fischereder, A. Dıaz-Rodrıguez, G. Grogan, V. Gotor, W. Kroutil, I. Lavandera, *Angew. Chem. Int. Ed.* **2016**, *55*, 3144–3147.
[246] M. Truppo, J. M. Janey, B. Grau, K. Morley, S. Pollack, G. Hughes, I. Davies, *Catal Sci Technol* **2012**, *2*, 1556–1559.
[247] L. H. Andrade, W. Kroutil, T. F. Jamison, *Org. Lett.* **2014**, *16*, 6092–6095.
[248] J. Ryan, M. Šiaučiulis, A. Gomm, B. Maciá, E. O'Reilly, V. Caprio, *J. Am. Chem. Soc.* **2016**, *138*, 15798–15800.
[249] S.-W. Han, J. Kim, H.-S. Cho, J.-S. Shin, *ACS Catal.* **2017**, *7*, 3752–3762.
[250] F. G. Mutti, C. S. Fuchs, D. Pressnitz, N. G. Turrini, J. H. Sattler, A. Lerchner, A. Skerra, W. Kroutil, *Eur. J. Org. Chem.* **2012**, *2012*, 1003–1007.
[251] D. Pressnitz, C. S. Fuchs, J. H. Sattler, T. Knaus, P. Macheroux, F. G. Mutti, W. Kroutil, *ACS Catal.* **2013**, *3*, 555–559.

[252] D. Koszelewski, I. Lavandera, D. Clay, G. M. Guebitz, D. Rozzell, W. Kroutil, *Angew. Chem. Int. Ed.* **2008**, *47*, 9337–9340.
[253] H. Yun, B.-G. Kim, *Biosci. Biotechnol. Biochem.* **2008**, *72*, 3030–3033.
[254] G. Matcham, M. Bhatia, W. Lang, C. Lewis, R. Nelson, A. Wang, W. Wu, *Chim. Int. J. Chem.* **1999**, *53*, 584–589.
[255] S.-W. Han, E.-S. Park, J.-Y. Dong, J.-S. Shin, *Adv. Synth. Catal.* **2015**, *357*, 1732–1740.
[256] P. Tufvesson, C. Bach, J. M. Woodley, *Biotechnol. Bioeng.* **2014**, *111*, 309–319.
[257] Y. Satyawali, D. F. del Pozo, P. Vandezande, I. Nopens, W. Dejonghe, *Biotechnol. Prog.* **2018**, DOI 10.1002/btpr.2731.
[258] K. E. Cassimjee, C. Branneby, V. Abedi, A. Wells, P. Berglund, *Chem. Commun.* **2010**, *46*, 5569–5571.
[259] P. Tufvesson, J. Lima-Ramos, J. S. Jensen, N. Al-Haque, W. Neto, J. M. Woodley, *Biotechnol. Bioeng.* **2011**, *108*, 1479–1493.
[260] G. Rehn, P. Adlercreutz, C. Grey, *J. Biotechnol.* **2014**, *179*, 50–55.
[261] G. Rehn, B. Ayres, P. Adlercreutz, C. Grey, *J. Mol. Catal. B Enzym.* **2016**, *123*, 1–7.
[262] T. Börner, G. Rehn, C. Grey, P. Adlercreutz, *Org. Process Res. Dev.* **2015**, *19*, 793–799.
[263] J. L. Galman, I. Slabu, N. J. Weise, C. Iglesias, F. Parmeggiani, R. C. Lloyd, N. J. Turner, *Green Chem.* **2017**, *19*, 361–366.
[264] B. Wang, H. Land, P. Berglund, *Chem Commun* **2013**, *49*, 161–163.
[265] T. Esparza-Isunza, M. González-Brambila, R. Gani, J. M. Woodley, F. López-Isunza, *Chem. Eng. J.* **2015**, *259*, 221–231.
[266] D. Hülsewede, M. Tänzler, P. Süss, A. Mildner, U. Menyes, J. von Langermann, *Eur. J. Org. Chem.* **2018**, *2018*, 2130–2133.
[267] S.-W. Han, E.-S. Park, J.-Y. Dong, J.-S. Shin, *Appl. Environ. Microbiol.* **2015**, *81*, 6994–7002.
[268] S.-W. Han, E.-S. Park, J.-Y. Dong, J.-S. Shin, *Adv. Synth. Catal.* **2015**, *357*, 2712–2720.
[269] F. Steffen-Munsberg, C. Vickers, A. Thontowi, S. Schätzle, T. Meinhardt, M. Svedendahl Humble, H. Land, P. Berglund, U. T. Bornscheuer, M. Höhne, *ChemCatChem* **2013**, *5*, 154–157.
[270] F. Steffen-Munsberg, P. Matzel, M. A. Sowa, P. Berglund, U. T. Bornscheuer, M. Höhne, *Appl. Microbiol. Biotechnol.* **2016**, *100*, 4511–4521.
[271] M. Voges, F. Schmidt, D. Wolff, G. Sadowski, C. Held, *Fluid Phase Equilibria* **2016**, *422*, 87–98.
[272] M. Voges, R. Abu, M. T. Gundersen, C. Held, J. M. Woodley, G. Sadowski, *Org. Process Res. Dev.* **2017**, *21*, 976–986.
[273] P. Kelefiotis-Stratidakis, T. Tyrikos-Ergas, I. V. Pavlidis, *Org. Biomol. Chem.* **2018**, DOI 10.1039/C8OB02342E.
[274] F. Rudroff, M. D. Mihovilovic, H. Gröger, R. Snajdrova, H. Iding, U. T. Bornscheuer, *Nat. Catal.* **2018**, *1*, 12–22.
[275] H. Gröger, *Curr. Opin. Chem. Biol.* **2014**, *19*, 171–179.
[276] P. Zajkoska, M. Cárdenas-Fernández, G. J. Lye, M. Rosenberg, N. J. Turner, M. Rebroš, *J. Chem. Technol. Biotechnol.* **2017**, *92*, 1558–1565.
[277] M. Heidlindemann, G. Rulli, A. Berkessel, W. Hummel, H. Gröger, *ACS Catal.* **2014**, *4*, 1099–1103.
[278] J. Muschiol, C. Peters, N. Oberleitner, M. D. Mihovilovic, U. T. Bornscheuer, F. Rudroff, *Chem. Commun.* **2015**, *51*, 5798–5811.
[279] C. A. Denard, J. F. Hartwig, H. Zhao, *ACS Catal.* **2013**, *3*, 2856–2864.
[280] R. J. Kazlauskas, U. T. Bornscheuer, *Nat. Chem. Biol.* **2009**, *5*, 526–529.
[281] J. Tomasek, J. Schatz, *Green Chem.* **2013**, *15*, 2317–2338.
[282] V. Köhler, Y. M. Wilson, M. Dürrenberger, D. Ghislieri, E. Churakova, T. Quinto, L. Knörr, D. Häussinger, F. Hollmann, N. J. Turner, *Nat. Chem.* **2013**, *5*, 93–99.
[283] A. Corma, *J. Catal.* **2003**, *215*, 294–304.
[284] M. Makkee, A. P. G. Kieboom, H. Van Bekkum, J. A. Roels, *J. Chem. Soc. Chem. Commun.* **1980**, *0*, 930–931.
[285] J. V. Allen, J. M. J. Williams, *Tetrahedron Lett.* **1996**, *37*, 1859–1862.
[286] P. M. Dinh, J. A. Howarth, A. R. Hudnott, J. M. J. Williams, W. Harris, *Tetrahedron Lett.* **1996**, *37*, 7623–7626.
[287] M.-J. Kim, Y. Ahn, J. Park, *Curr. Opin. Biotechnol.* **2002**, *13*, 578–587.
[288] A. L. E. Larsson, B. A. Persson, J.-E. Bäckvall, *Angew. Chem. Int. Ed.* **1997**, *36*, 1211–1212.
[289] R. Carr, M. Alexeeva, M. J. Dawson, V. Gotor-Fernández, C. E. Humphrey, N. J. Turner, *ChemBioChem* **2005**, *6*, 637–639.
[290] M. T. Reetz, K. Schimossek, *Chim. Int. J. Chem.* **1996**, *50*, 668–669.
[291] E. Burda, W. Hummel, H. Gröger, *Angew. Chem. Int. Ed.* **2008**, *47*, 9551–9554.

[292] S. Borchert, E. Burda, J. Schatz, W. Hummel, H. Gröger, *J. Mol. Catal. B Enzym.* **2012**, *84*, 89–93.
[293] K. Tenbrink, M. Seßler, J. Schatz, H. Gröger, *Adv. Synth. Catal.* **2011**, *353*, 2363–2367.
[294] C. A. Denard, H. Huang, M. J. Bartlett, L. Lu, Y. Tan, H. Zhao, J. F. Hartwig, *Angew. Chem. Int. Ed.* **2014**, *53*, 465–469.
[295] I. Schnapperelle, W. Hummel, H. Gröger, *Chem. Eur. J.* **2012**, *18*, 1073–1076.
[296] C. Simons, U. Hanefeld, I. W. C. E. Arends, T. Maschmeyer, R. A. Sheldon, *Top. Catal.* **2006**, *40*, 35–44.
[297] M. J. Fink, M. Schön, F. Rudroff, M. Schnürch, M. D. Mihovilovic, *ChemCatChem* **2013**, *5*, 724–727.
[298] J. H. Schrittwieser, F. Coccia, S. Kara, B. Grischek, W. Kroutil, N. d'Alessandro, F. Hollmann, *Green Chem.* **2013**, *15*, 3318–3331.
[299] S. Suljić, J. Pietruszka, *Adv. Synth. Catal.* **2014**, *356*, 1007–1020.
[300] R. Yuryev, S. Strompen, A. Liese, *Beilstein J. Org. Chem.* **2011**, *7*, 1449–1467.
[301] P. Loxq, E. Manoury, R. Poli, E. Deydier, A. Labande, *Coord. Chem. Rev.* **2016**, *308*, 131–190.
[302] N. Miyaura, A. Suzuki, *J. Chem. Soc. Chem. Commun.* **1979**, *0*, 866–867.
[303] R. Franzén, Y. Xu, *Can. J. Chem.* **2005**, *83*, 266–272.
[304] N. Miyaura, A. Suzuki, *Chem. Rev.* **1995**, *95*, 2457–2483.
[305] C. Bolm, *Org. Lett.* **2012**, *14*, 2925–2928.
[306] C.-J. Li, *Chem. Rev.* **2005**, *105*, 3095–3166.
[307] A. Suzuki, *J. Organomet. Chem.* **1999**, *576*, 147–168.
[308] S. Kotha, K. Lahiri, D. Kashinath, *Tetrahedron Lett.* **2002**, *58*, 9633–9695.
[309] F. Bellina, A. Carpita, R. Rossi, *Synthesis* **2004**, *2004*, 2419–2440.
[310] J.-P. Corbet, G. Mignani, *Chem. Rev.* **2006**, *106*, 2651–2710.
[311] H. Doucet, *Eur. J. Org. Chem.* **2008**, *2008*, 2013–2030.
[312] T. E. Barder, S. D. Walker, J. R. Martinelli, S. L. Buchwald, *J. Am. Chem. Soc.* **2005**, *127*, 4685–4696.
[313] R. Martin, S. L. Buchwald, *Acc. Chem. Res.* **2008**, *41*, 1461–1473.
[314] A. J. J. Lennox, G. C. Lloyd-Jones, *Angew. Chem. Int. Ed.* **2013**, *52*, 7362–7370.
[315] C. Amatore, A. Jutand, G. Le Duc, *Chem. Eur. J.* **2011**, *17*, 2492–2503.
[316] C. Amatore, G. Le Duc, A. Jutand, *Chem. Eur. J.* **2013**, *19*, 10082–10093.
[317] J. P. Wolfe, R. A. Singer, B. H. Yang, S. L. Buchwald, *J. Am. Chem. Soc.* **1999**, *121*, 9550–9561.
[318] L. Wu, Z.-W. Li, F. Zhang, Y.-M. He, Q.-H. Fan, *Adv. Synth. Catal.* **2008**, *350*, 846–862.
[319] G. A. Grasa, A. C. Hillier, S. P. Nolan, *Org. Lett.* **2001**, *3*, 1077–1080.
[320] C. W. K. Gstöttmayr, V. P. W. Böhm, E. Herdtweck, M. Grosche, W. A. Herrmann, *Angew. Chem. Int. Ed.* **2002**, *41*, 1363–1365.
[321] N. Shahnaz, B. Banik, P. Das, *Tetrahedron Lett.* **2013**, *54*, 2886–2889.
[322] D. Badone, M. Baroni, R. Cardamone, A. Ielmini, U. Guzzi, *J. Org. Chem.* **1997**, *62*, 7170–7173.
[323] N. A. Bumagin, D. N. Korolev, *Tetrahedron Lett.* **1999**, *40*, 3057–3060.
[324] N. A. Bumagin, *Catal. Commun.* **2016**, *79*, 17–20.
[325] T. I. Wallow, B. M. Novak, *J. Org. Chem.* **1994**, *59*, 5034–5037.
[326] T. Huang, C.-J. Li, *Tetrahedron Lett.* **2002**, *43*, 403–405.
[327] S. Venkatraman, T. Huang, C.-J. Li, *Adv. Synth. Catalyis* **2002**, *344*, 399–405.
[328] P. Sharma, A. Singh, *Catal. Sci. Technol.* **2014**, *4*, 2978–2989.
[329] S. Jindabot, K. Teerachanan, P. Thongkam, S. Kiatisevi, T. Khamnaen, P. Phiriyawirut, S. Charoenchaidet, T. Sooksimuang, P. Kongsaeree, P. Sangtrirutnugul, *J. Organomet. Chem.* **2014**, *750*, 35–40.
[330] C. A. Fleckenstein, H. Plenio, *Chem. Eur. J.* **2008**, *14*, 4267–4279.
[331] D. N. Korolev, N. A. Bumagin, *Tetrahedron Lett.* **2005**, *46*, 5751–5754.
[332] J. Zhang, W. Zhang, Y. Wang, M. Zhang, *Adv. Synth. Catal.* **2008**, *350*, 2065–2076.
[333] C. Liu, Q. Ni, F. Bao, J. Qiu, *Green Chem.* **2011**, *13*, 1260–1266.
[334] V. Polshettiwar, A. Decottignies, C. Len, A. Fihri, *ChemSusChem* **2010**, *3*, 502–522.
[335] G. Zhang, *Synthesis* **2005**, *2005*, 537–542.
[336] Q. Yang, S. Ma, J. Li, F. Xiao, H. Xiong, *Chem. Commun.* **2006**, 2495–2497.
[337] T. Maegawa, Y. Kitamura, S. Sako, T. Udzu, A. Sakurai, A. Tanaka, Y. Kobayashi, K. Endo, U. Bora, T. Kurita, *Chem. Eur. J.* **2007**, *13*, 5937–5943.
[338] J. Qiu, L. Wang, M. Liu, Q. Shen, J. Tang, *Tetrahedron Lett.* **2011**, *52*, 6489–6491.
[339] Z. Li, C. Gelbaum, W. L. Heaner, J. Fisk, A. Jaganathan, B. Holden, P. Pollet, C. L. Liotta, *Org. Process Res. Dev.* **2016**, *20*, 1489–1499.

[340] Z. Li, C. Gelbaum, J. S. Fisk, B. Holden, A. Jaganathan, G. T. Whiteker, P. Pollet, C. L. Liotta, *J. Org. Chem.* **2016**, *81*, 8520–8529.
[341] N. A. Bumagin, V. V. Bykov, *Tetrahedron* **1997**, *53*, 14437–14450.
[342] A. Prastaro, P. Ceci, E. Chiancone, A. Boffi, R. Cirilli, M. Colone, G. Fabrizi, A. Stringaro, S. Cacchi, *Green Chem.* **2009**, *11*, 1929–1932.
[343] S. T. Ahmed, F. Parmeggiani, N. J. Weise, S. L. Flitsch, N. J. Turner, *ACS Catal.* **2015**, *5*, 5410–5413.
[344] S. P. France, G. A. Aleku, M. Sharma, J. Mangas-Sanchez, R. M. Howard, J. Steflik, R. Kumar, R. W. Adams, I. Slabu, R. Crook, *Angew. Chem. Int. Ed.* **2017**, *56*, 15589–15593.
[345] L. Skalden, M. Thomsen, M. Höhne, U. T. Bornscheuer, W. Hinrichs, *FEBS J.* **2015**, *282*, 407–415.
[346] R. Porta, M. Benaglia, A. Puglisi, *Org. Process Res. Dev.* **2016**, *20*, 2–25.
[347] R. O. M. A. de Souza, P. Watts, *J. Flow Chem.* **2017**, *7*, 146–150.
[348] S. Mascia, P. L. Heider, H. Zhang, R. Lakerveld, B. Benyahia, P. I. Barton, R. D. Braatz, C. L. Cooney, J. M. B. Evans, T. F. Jamison, *Angew. Chem. Int. Ed.* **2013**, *52*, 12359–12363.
[349] T. Razzaq, C. O. Kappe, *Chem. Asian J.* **2010**, *5*, 1274–1289.
[350] H. Wu, M. A. Khan, A. S. Hussain, *Chem. Eng. Commun.* **2007**, *194*, 760–779.
[351] P. Plouffe, A. Macchi, D. M. Roberge, *Org. Process Res. Dev.* **2014**, *18*, 1286–1294.
[352] F. G. Finelli, L. S. M. Miranda, R. O. M. A. de Souza, *Chem. Commun.* **2015**, *51*, 3708–3722.
[353] D. M. Roberge, L. Ducry, N. Bieler, P. Cretton, B. Zimmermann, *Chem. Eng. Technol.* **2005**, *28*, 318–323.
[354] D. Perera, J. W. Tucker, S. Brahmbhatt, C. J. Helal, A. Chong, W. Farrell, P. Richardson, N. W. Sach, *Science* **2018**, *359*, 429–434.
[355] L. Tamborini, P. Fernandes, F. Paradisi, F. Molinari, *Trends Biotechnol.* **2018**, *36*, 73–88.
[356] J. Britton, S. Majumdar, G. A. Weiss, *Chem. Soc. Rev.* **2018**, *47*, 5891–5918.
[357] C. Len, S. Bruniaux, F. Delbecq, V. Parmar, *Catalysts* **2017**, *7*, 146.
[358] J. Wachtmeister, D. Rother, *Curr. Opin. Biotechnol.* **2016**, *42*, 169–177.
[359] R. C. Rodrigues, C. Ortiz, Á. Berenguer-Murcia, R. Torres, R. Fernández-Lafuente, *Chem Soc Rev* **2013**, *42*, 6290–6307.
[360] U. T. Bornscheuer, *Angew. Chem. Int. Ed.* **2003**, *42*, 3336–3337.
[361] R. A. Sheldon, *Adv. Synth. Catal.* **2007**, *349*, 1289–1307.
[362] R. A. Sheldon, S. van Pelt, *Chem. Soc. Rev.* **2013**, *42*, 6223–6235.
[363] S. Datta, L. R. Christena, Y. R. S. Rajaram, *3 Biotech* **2013**, *3*, 1–9.
[364] E. Magner, *Chem. Soc. Rev.* **2013**, *42*, 6213–6222.
[365] A. Liese, L. Hilterhaus, *Chem. Soc. Rev.* **2013**, *42*, 6236–6249.
[366] M. Hartmann, X. Kostrov, *Chem. Soc. Rev.* **2013**, *42*, 6277–6289.
[367] Z. Zhou, M. Hartmann, *Chem. Soc. Rev.* **2013**, *42*, 3894–3912.
[368] D. Brady, J. Jordaan, *Biotechnol. Lett.* **2009**, *31*, 1639–1650.
[369] L. Cao, *Curr. Opin. Chem. Biol.* **2005**, *9*, 217–226.
[370] U. Hanefeld, L. Gardossi, E. Magner, *Chem Soc Rev* **2009**, *38*, 453–468.
[371] A.-X. Yan, X.-W. Li, Y.-H. Ye, *Appl. Biochem. Biotechnol.* **2002**, *101*, 113–130.
[372] A. Vinu, V. Murugesan, M. Hartmann, *J. Phys. Chem. B* **2004**, *108*, 7323–7330.
[373] D. Zhang, H. E. Hegab, Y. Lvov, L. Dale Snow, J. Palmer, *SpringerPlus* **2016**, *5*, 48.
[374] H.-Z. Ma, X.-W. Yu, C. Song, Q. Xue, B. Jiang, *J. Mol. Catal. B Enzym.* **2016**, *127*, 76–81.
[375] H. Mallin, U. Menyes, T. Vorhaben, M. Höhne, U. T. Bornscheuer, *ChemCatChem* **2013**, *5*, 588–593.
[376] J. Britton, C. L. Raston, G. A. Weiss, *Chem. Commun.* **2016**, *52*, 10159–10162.
[377] M. Oshige, K. Yumoto, H. Miyata, S. Takahashi, M. Nakada, K. Ito, M. Tamegai, H. Kawaura, S. Katsura, *Open J. Polym. Chem.* **2013**, *3*, 6–10.
[378] J. C. S. dos Santos, O. Barbosa, C. Ortiz, A. Berenguer-Murcia, R. C. Rodrigues, R. Fernandez-Lafuente, *ChemCatChem* **2015**, *7*, 2413–2432.
[379] Q. Shen, R. Yang, X. Hua, F. Ye, W. Zhang, W. Zhao, *Process Biochem.* **2011**, *46*, 1565–1571.
[380] L. Cao, F. van Rantwijk, R. A. Sheldon, *Org. Lett.* **2000**, *2*, 1361–1364.
[381] L. van den Biggelaar, P. Soumillion, D. P. Debecker, *Catalysts* **2017**, *7*, 54.
[382] M. Planchestainer, M. L. Contente, J. Cassidy, F. Molinari, L. Tamborini, F. Paradisi, *Green Chem.* **2017**, *19*, 372–375.
[383] K. Engelmark Cassimjee, M. Kadow, Y. Wikmark, M. Svedendahl Humble, M. L. Rothstein, D. M. Rothstein, J.-E. Bäckvall, *Chem. Commun. Camb. Engl.* **2014**, *50*, 9134–9137.
[384] S. J. Eichhorn, A. Dufresne, M. Aranguren, N. E. Marcovich, J. R. Capadona, S. J. Rowan, C. Weder, W. Thielemans, M. Roman, S. Renneckar, *J. Mater. Sci.* **2010**, *45*, 1–33.
[385] Y. Habibi, L. A. Lucia, O. J. Rojas, *Chem. Rev.* **2010**, *110*, 3479–3500.

[386] N. Lavoine, I. Desloges, A. Dufresne, J. Bras, *Carbohydr. Polym.* **2012**, *90*, 735–764.

Affirmation

Hiermit erkläre ich, dass diese Arbeit bisher von mir weder an der Mathematisch-Naturwissenschaftlichen Fakultät der Universität Greifswald noch einer anderen wissenschaftlichen Einrichtung zum Zwecke der Promotion eingereicht wurde. Ferner erkläre ich, dass ich diese Arbeit selbstständig verfasst und keine anderen als die darin angegebenen Hilfsmittel und Hilfen benutzt und keine Textabschnitte eines Dritten ohne Kennzeichnung übernommen habe.

_____

Ayad Dawood, M.Sc.

Curriculum vitae

The curriculum vitae has been removed in the published version.

Publications

Articles

S. Schaller, D. Latowski, M. Jemiola-Rzeminska, **A. Dawood**, C. Wilhelm, K. Strzalka, R. Goss, Regulation of LHCII aggregation by different thylakoid membrane lipids, *Biochim. Biophys. Acta* **2011**, *1807*, 326-335

S. P. de Souza, I. I. Junior, G. M. Silva, L. S. Miranda, M. F. Santiago, F. L.-Y. Lam, **A. Dawood**, U. T. Bornscheuer, R. O. M. A. de Souza, Cellulose as an efficient matrix for lipase and transaminase immobilization, *RSC Adv.* **2016**, *6*, 6665–6671

D. Last, J. Müller, **A. W. H. Dawood**, E. J. Moldenhauer, I. V. Pavlidis, U. T. Bornscheuer, Highly efficient and easy protease-mediated protein purification, *Appl. Microbiol. Biotechnol.* **2016**, *100*, 1945-1953

A. W. H. Dawood, R. O. M. A. de Souza, U. T. Bornscheuer, Asymmetric Synthesis of Chiral Halogenated Amines using Amine Transaminases, *ChemCatChem* **2018**, *10*, 951–955

A. W. H. Dawood, M. S. Weiß, C. Schulz, I. V. Pavlidis, H. Iding, R. O. M. A. de Souza, U. T. Bornscheuer, Isopropylamine as Amine Donor in Transaminase-Catalyzed Reactions: Better Acceptance through Reaction and Enzyme Engineering, *ChemCatChem* **2018**, *10*, 3943–3949

A. W. H. Dawood, J. Bassut, R. O. M. A. de Souza, U. T. Bornscheuer, Combination of the Suzuki–Miyaura Cross-Coupling Reaction with Engineered Transaminases, *Chem. Eur. J.* **2018**, *24*, 16009–16013.

Conference contributions

A. W. H. Dawood, M. Genz, I. V. Pavlidis, M. Höhne, R. O. M. A. de Souza, U. T. Bornscheuer, Engineering and Immobilization of Transaminases for Continuous-flow Process Applications, poster presentation at Transam 2.0 - Chiral Amines Through (Bio)Catalysis, March 2015, Greifswald

A. W. H. Dawood, J. Bassut, R. O. M. A. de Souza, U. T. Bornscheuer, Synthesis of chiral amines by utilizing ω–transaminases in a coupled chemoenzymatic reaction, poster presentation at the 13th International Symposium on Biocatalysis and Biotransformations, July 2017, Budapest

A. W. H. Dawood, R. O. M. A. de Souza, U. T. Bornscheuer, Asymmetric synthesis of chiral halogenated amines using amine transaminases, poster presentation at the Amine Biocat 3.0, December 2017, Manchester

_____

Ayad Dawood, M.Sc.

Acknowledgements

Zuerst will ich mich beim Bundesministerium für Bildung und Forschung für die finanzielle Unterstützung bedanken. Den größten Dank jedoch möchte ich dir, Uwe, aussprechen und dies nicht nur, weil du mir dieses Projekt gegeben und mich zu jedem Zeitpunkt fachlich unterstützt hast. Vielmehr auch, weil du mir Raum für Ideen gegeben und mich vor allen Dingen (und insbesondere in diesem Jahr) menschlich aufgebaut hast. Danke auch, dass du dich für meine Vertragsverlängerung stark gemacht hast, die genau zur richtigen Zeit kam.

I would like to thank you, Rodrigo, for the nice support in our project and for the very warm welcome in Rio de Janeiro.

Matthias, ich bedanke mich sehr bei dir für all die Diskussionen und Unterhaltungen in deinem Büro. Du hast mir eingängig gezeigt, wo ich und meine Arbeit Optimierungsbedarf haben. Dies hat mich nicht nur inspiriert, sondern auch charakterlich vorangebracht.

Gottfried, dir möchte ich ebenfalls dafür danken, dass du zu jeder Zeit ein offenes Ohr für mich hattest und dies auch zu menschenunwürdigen Uhrzeiten im PC-Pool. Deine Begeisterung für die Wissenschaft war förmlich als Aura zu spüren und diese war es auch, die mich sehr oft beflügelte.

Dem gesamten Arbeitskreis möchte ich für die freundliche Aufnahme sowie für die nette und aufgeschlossene Atmosphäre danken. Bei nahezu allen Fragen und Problemen konnte man bei euch und in euch eine Lösung finden.

Dominique, dir will ich danken, dass du mich in ausgesprochen vielen Belangen beraten konntest oder mir auch einfach nur zugehört hast. Ich bin dir auch dankbar, dass du mich an einem verregneten Tag im Oktober 2017 ins Krankenhaus *getragen* hast, im wahrsten Sinne des Wortes.

Mark, dir will ich dafür danken, dass du mich u.a. an Python herangeführt hast, sodass ich eigene Schritte im Programmieren machen konnte. Dies hat mir besonders in meiner Endphase geholfen, weil irgendwann die Probenvorbereitung und GC-Messzeit zu den einzigen zeitlich limitierenden Faktoren in meiner Analytik wurden.

Apropos Analytik: Hier warst du, Ina, eine große Unterstützung, nicht nur wenn es um die GCMS-Wartung und Säulenwechsel ging. Immer wenn etwas Unvorhergesehenes geschah, warst du erreichbar, oft auch an Freitagabenden. Außerdem bin ich dir dankbar, dass du mir tatkräftig *meine* GCMS 6 freigehalten hast, damit ich meine Biokatalysen messen konnte. Für jene hast du, Angelika, jederzeit die entsprechenden Substrate bestellt, auch dann wenn es zwischenzeitlich überhandnahm mit den Bestellungen. Dafür danke ich dir.

Dir Christian, auch liebevoll CSC genannt, danke ich für die nette Zusammenarbeit im IPA-Projekt. *Figure 1* im IPA-Paper war im Wesentlichen deiner Hände Arbeit und dafür hast du dir Lob und Dank verdient.

Lisa, du hattest in den letzten 3,5 Jahren eine sehr besondere Stellung. Wir konnten uns (fast) immer alles sagen, uns über alles austauschen, alles miteinander *durchmachen*. Dabei war es deine offene und hilfsbereite Art, die Eindruck hinterlassen hat. Und du hast auch stets für Pausenverpflegung gesorgt. Du hast sehr viel gegeben, auch manchmal mehr als mir lieb war, ich denke da an die ungefähr 20 Spitznamen für mich. Ich habe es schon mal gesagt und ich sage es wieder: Es war ein großes Glück, dass wir beide zusammen mit dem Doktor angefangen haben!

Lukas! Dir will ich für einen sehr interessanten Austausch danken, kurzweilige Abende in C211, immer was zu lachen, die spannenden Wetten mit Suchtpotential, Trailerpark und für das Gefühl, nach 20 Uhr nicht nur der einzige im Labor zu sein. Auch außerhalb des Labors warst du ein guter Freund und eine Unterstützung, nur mit dir konnte ich so viel beim Bankdrücken stemmen!

Miriam, es war immer eine Freude dein *liebliches Antlitz* in C211 zu sehen. Du hast mich oft (gewollt und ungewollt) zum Lachen gebracht, auch wenn mir manchmal zu selbigem nicht recht zumute war. Ebenso haben die langen Telefonate sowie die Sushi- und Filmabende sehr viel Spaß gemacht.

Dir, Florian, will ich Danke sagen, weil man mit dir immer diskutieren konnte, über fachliche, praktische, philosophische und private Sachen. Deswegen wurdest du wahrscheinlich nicht nur von mir so geschätzt... und außerdem noch für deine Begabung, mit einem Feuerzeug, Ethanol und Trockeneis ganz wunderbare Dinge zu *zaubern*.

Moritz, dir danke ich für die netten und sehr anregenden Unterhaltungen über Transaminasen, Jagdsport und auch viele andere Dinge! Nicht nur der Flug nach Manchester ging auf die Art sehr schnell rum.

Bei Katja, Vishnu und Eva bedanke ich mich für die lustige Zeit und die gute Freundschaft mit vielen aufbauenden Worten. Das gilt auch für Thomas (Bayer), der durch seinen Witz und Charme *für immer einen Platz in meinem Herzen* haben wird.

Henrik, dir will ich sagen, dass ich wirklich froh bin, das gefunden zu haben, was uns beide verbindet..Gauloises red.

I want to thank you, Kathleen, Isabel, Chris and Ingrid for all of your advice, help and encouragement!

Sascha, Andy, Askin, Marcus und Lorna will ich für die gute und auch witzige Zeit danken.

Saskia, bei dir bedanke ich mich für die netten Gespräche im DNA-Labor und für dein freundliches Angebot an meinem letzten Arbeitstag, ein paar meiner Proben mit auf dein Gel aufzutragen.

Meiner Familie danke ich ganz herzlich für die Hilfestellung. Ihr habt zu jeder Zeit Anteil an der Zeit in Greifswald genommen und mir immer einen *Heimathafen* geboten, wenn es nötig war.

Und meiner Frieda möchte ich zu guter Letzt für die wunderschöne Zeit hier in Greifswald und die unendliche Geduld sowie Unterstützung danken, die du mir zu Teil kommen ließest. Ich kann mir vorstellen, dass vieles nicht immer einfach war in den letzten Jahren. Aber deine aufmunternde, liebevolle und aufopferungsvolle Art hat mich durch meinen Doktor getragen und mir auch das Gefühl gegeben, dass ich immer auf dich zählen kann.

Author contributions

Article I	**Ayad W. H. Dawood**, Rodrigo O. M. A. de Souza, Uwe T. Bornscheuer, **Asymmetric Synthesis of Chiral Halogenated Amines using Amine Transaminases**, *ChemCatChem* **2018**, *10*, 951–955.

UTB, ROMAS and AWHD initiated the project; AWHD designed and conducted the experiments; AWHD drafted the manuscript; UTB revised the manuscript; All authors read and approved the manuscript

Article II	**Ayad W. H. Dawood**, Martin S. Weiß, C. Schulz, Ioannis V. Pavlidis, Hans Iding, Rodrigo O. M. A. de Souza, Uwe T. Bornscheuer, **Isopropylamine as Amine Donor in Transaminase-Catalyzed Reactions: Better Acceptance through Reaction and Enzyme Engineering**, *ChemCatChem* **2018**, *10*, 3943–3949.

UTB and HI initiated the project; AWHD and MSW designed and conducted the experiments with the help of CS; AWHD drafted the manuscript; All authors read and revised the manuscript

Article III	**Ayad W. H. Dawood**, Jonathan Bassut, Rodrigo O. M. A. de Souza, Uwe T. Bornscheuer, **Combination of the Suzuki-Miyaura Cross-Coupling Reaction with Engineered Transaminases**, *Chem. Eur. J.* **2018**, *24*, 16009–16013.

UTB and ROMAS initiated the project; AWHD designed and conducted the experiments; JB performed experiments on cross-coupling compatibility; AWHD drafted the manuscript; All authors read and approved the manuscript

Article IV	Stefania P. de Souza, Ivaldo I. Junior, Guilherme M. A. Silva, Leandro S. M. Miranda, Marcelo F. Santiago, Frank Leung-Yuk Lam, **Ayad Dawood**, Uwe T. Bornscheuer, Rodrigo O. M. A. de Souza, **Cellulose as an efficient matrix for lipase and transaminase immobilization**, *RSC Adv.* **2016**, *6*, 6665–6671.

UTB and ROMAS initiated the project; AWHD performed the transaminase production and a part of the immobilization experiments; FLYL synthesized the immobilization support; SPS, IIJ, GMAS, LSMM, MFS worked on the lipase catalysed reactions; All authors read and approved the manuscript

_____ _____

Ayad Dawood, M.Sc. Uwe T. Bornscheuer, Prof. Dr.

Articles

Article I

ChemPubSoc Europe

DOI: 10.1002/cctc.201701962

CHEMCATCHEM Communications

Asymmetric Synthesis of Chiral Halogenated Amines using Amine Transaminases

Ayad W. H. Dawood,[a] Rodrigo O. M. A. de Souza,[b] and Uwe T. Bornscheuer*[a]

Amine transaminases (ATAs) are versatile and industrially relevant biocatalysts that catalyze the transfer of an amine group from a donor to an acceptor molecule. Asymmetric synthesis from a prochiral ketone is the most preferred route to the desired amine product, as it is obtainable in a theoretical yield of 100%. In addition to the requirement of active and enantioselective ATAs, the choice of a suitable amine donor is also important to save costs and to avoid additional enzymes to shift the equilibrium and/or to recycle the cofactors. In this work, we identified suitable (*R*)- and (*S*)-ATAs from *Aspergillus fumigatus* and *Silicibacter pomeroyi*, respectively, to afford a set of halogen-substituted derivatives of brominated or chlorinated 1-phenyl-2-propanamine, 4-phenylbutan-2-amine, and 1-(3-pyridinyl)ethanamine. Optimization of the donor–acceptor ratio enabled application of isopropylamine as an amine donor, which resulted in high conversions and amines with 73–99% *ee*.

Optically pure amines are important and versatile building blocks for the pharmaceutical and agrochemical industries. Chemical synthesis strategies are usually waste intensive, and the formation of chiral amines requires the use of transition metals and chiral auxiliaries.[1] Enzymatic routes to chiral compounds are an environmentally benign alternative because of mild operating conditions and the intrinsic selectivity of the biocatalysts.

One strategy to access primary chiral amines is the utilization of amine transaminases (ATAs). ATAs are pyridoxal-5′-phosphate (PLP)-dependent enzymes and belong to PLP fold classes I and IV. They catalyze the transfer of a primary amine group from a donor molecule to an acceptor molecule through a ping-pong–Bi-Bi mechanism with the use of PLP as a co-factor. Substrate recognition is ensured by two binding pockets: a small one only able to accommodate a methyl group, and a large one with space for a group such as phenyl or a carboxyl moiety. Asymmetric synthesis is the most convenient and economically favored route to a target amine, as it starts from a prochiral ketone and results in the desired chiral product with a theoretical yield of 100%.[2–4] The first asymmetric synthesis of (*S*)-1-phenylethylamine (1-PEA) utilizing the ATA from *Vibrio fluvialis* JS17 was reported by Shin and Kim, who applied several amine donors, for example, 1-PEA, 1-aminoindane, and 1-aminotetralin.[5] Those amine donors are favored in a thermodynamic manner, as the corresponding ketones show drastically lower reactivity in terms of the reverse reaction, which makes them interesting for a biocatalytic approach.[5–8] However, the use of alanine—a natural amine donor—is one of the most common strategies for the amination of target ketones.[9–11] The major drawback is the necessity to remove the coproduct pyruvate by additional enzymes, as a large excess of alanine does not lead to a thermodynamically more favorable situation.[12] For this purpose, pyruvate decarboxylase,[2] alanine dehydrogenase, or, most commonly, a combination of lactate dehydrogenase and glucose dehydrogenase (LDH/GDH system)[13,14] are applied to drive the desired transamination reaction to completeness. More recently, aliphatic diamines were reported as effective amine donors.[15–20]

An interesting, alternative amine donor is isopropylamine (IPA), as it is cheap and achiral and its acetone byproduct can be stripped off the reaction continuously, as demonstrated by the industrial-scale synthesis of (*S*)-sitagliptin by using an engineered (*R*)-ATA.[21] The only downside of this system is the necessity of a large excess amount of IPA to drive the equilibrium to the desired product side, which might hamper the stability and activity of the ATAs.[9,12,19,21]

To the best of our knowledge, there are only a few reports dealing with the acceptance of halogenated ketones by amine transaminases.[15–17,19,20,22–31] For instance, Slabu et al.,[19] Cassimjee et al.,[22] and Paul et al.[24] investigated halogenated acetophenone derivatives. López-Iglesias et al.[27] successfully produced fluorinated 1-(3-pyridinyl)ethanamine, and Meadows et al.[28] and Frodsham et al.[29] reported the synthesis of (*S*)-1-(5-fluoropyrimidin-2-yl)ethylamine. Gomm et al.,[15] Green et al.,[16] and Martínez-Monteroet al.[17] subjected 4-fluorophenylacetone to the asymmetric synthesis of the corresponding amine. Finally, Schmidt et al.[30] focused on halogenated propargylamines. However, the compounds described in this work were not yet investigated. We thus herein report the asymmetric synthesis of chlorinated and brominated 1-phenyl-2-propanamine, 4-phenylbutan-2-amine, and 1-(3-pyridinyl)ethanamine derivatives (Scheme 1) by using different ATAs and isopropylamine as the amine donor.

[a] *A. W. H. Dawood, Prof. Dr. U. T. Bornscheuer*
Department of Biotechnology & Enzyme Catalysis
Institute of Biochemistry
Greifswald University
Felix-Hausdorff-Str. 4, 17487 Greifswald (Germany)
Web: http://biotech.uni-greifswald.de
E-mail: uwe.bornscheuer@uni-greifswald.de

[b] *Prof. Dr. R. O. M. A. de Souza*
Biocatalysis and Organic Synthesis Group
Institute of Chemistry
Federal University of Rio de Janeiro
(Brazil)

Supporting Information and the ORCID identification number(s) for the author(s) of this article can be found under https://doi.org/10.1002/cctc.201701962.

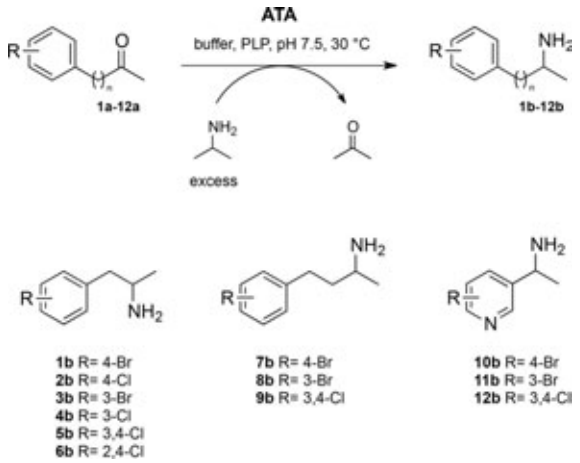

Scheme 1. Amine products (bottom) obtained by asymmetric synthesis (top) from corresponding prochiral ketones **1a**–**12a** by using isopropylamine as the amine donor and different amine transaminases.

The choice of suitable amine transaminases was mainly guided by a literature search, for which similar but usually non-halogenated ketones served as substrates.[9,10,13,19,23,24,32–35] For instance, ATA-117 was used to make (*R*)-1-(4-methoxyphenyl)propan-2-amine,[13] the ATA from *Chromobacterium violaceum* (Cvi-TA) catalyzed the conversion of 1-(4-methoxyphenyl)propan-2-one and 3-acetylpyridine,[33] the ATAs from *Silicibacter pomeroyi*[32] (Spo-TA) and *Aspergillus fumigatus* (Afu-TA)[35] were utilized for the synthesis of both enantiomers of 4-phenylbutane-2-amine. Hence, for our investigations we chose the (*S*)-selective ATAs Spo-TA and Cvi-TA, and as a result of structural similarities to the enzymes mentioned above, the ATA from *Vibrio fluvialis* (Vfl-TA) as well as the (*R*)-selective ATA from *Aspergillus fumigatus* (Afu-TA) were also examined.[32,36–38] Of particular interest was the reported IPA acceptance by Spo-TA and Afu-TA.[39]

To get additional indicators for successful catalysis, docking experiments with representatives of the three substrate groups (Scheme 1) were performed in silico to strengthen the choice of the focused ATAs. Quinonoid intermediates of **1b**, **9b**, and **12b** were docked into the active sites of Spo-TA (PDB ID: 3HMU), Afu-TA (PDB ID: 4CHI), Cvi-TA (PDB ID: 4A6T), and Vfl-TA (PDB ID: 4E3Q). The result showed plausible coordination of all docked intermediate complexes for every considered ATA (Figure S1, Supporting Information).

For preliminary test purposes, we decided to use the reaction with 1-(4-bromophenyl)propan-2-one (**1a**) as a model reaction to investigate several reaction conditions. Initially, we tested the ATAs for activity towards **1a** by using various amine donors. By application of the alanine/LDH/GDH system or by using 1-PEA in a slight excess amount (fivefold), very good conversion of **1a** into **1b** was observed by using Cvi-TA (LDH/GDH system: 99%; 1-PEA: no conversion), Afu-TA (LDH/GDH system: 99%; 1-PEA: 98%), and Spo-TA (1-PEA: 95%; Table S1). Vfl-TA did not convert **1a** at all. However, as 1-PEA is rather expensive[6] and the alanine/LDH/GDH system requires the involvement of additional enzymes, isopropylamine as a donor was investigated (especially the donor–acceptor ratio) by using model substrate **1a** with Spo-TA and Afu-TA. In the case of Spo-TA, a relatively low 10-fold excess amount of IPA was sufficient to observe high conversion (>80%). The reaction with Afu-TA reached the same value only at 1 M IPA (a 200-fold excess; Figure S5). Consequently, Spo-TA and Afu-TA were used for the asymmetric synthesis of all substrates with the use of IPA as the amine donor (Scheme 1, Table 1). Both Spo-TA and Afu-TA showed excellent conversions (>90%) with minor exceptions (see substrates **8a**–**10a** and **12a**, ≈78–88% conversion). The optical purities of the chiral amine products were predominantly excellent (>95% *ee*, with two exceptions, amines **7b** and **9b**, 73–80% *ee*; Table 1) as determined by chiral-phase gas chromatography (GC) analysis (see the Supporting Information for chromatograms and retention times, Table S4). Preparative-scale reactions (50 or 100 mg **1a**) with the use of Spo-TA or Afu-TA confirmed the identity of 1-(4-bromophenyl)-2-propanamine (**1b**) after GC–MS analysis and ^{1}H NMR and ^{13}C NMR spectroscopy (see the Supporting Information). The absolute configuration of each enantiomer was verified by literature data by using optical rotation values.[40]

Table 1. Conversion and enantiomeric excess values of amine products **1b**–**12b** obtained by asymmetric synthesis by using IPA as the donor and crude cell lysate containing overexpressed Spo-TA (0.75 U) or Afu-TA (0.5 U).

Substrate	Conversion [%][a,b] Spo-TA	ee_P [%][b]	Conversion [%][a,b] Afu-TA	ee_P [%][b]
1a	95.6±3.0	>99	96.2±0.3	>99
2a	96.6±0.8	>99	96.1±0.4	>99
3a	91.4±0.4	98	95.0±0.3	>99
4a	97.6±1.3	>99	95.9±0.5	>99
5a	96.3±2.9	98	93.4±1.1	>99
6a	97.1±2.2	>99	91.1±0.4	>99
7a	93.3±2.8	80	93.9±0.4	>99
8a	95.9±1.9	95	84.5±4.1	>99
9a	88.0±6.0	73	95.6±0.7	>99
10a	88.8±5.0	>99	78.4±2.3	>99
11a	93.9±4.7	>99	91.4±0.4	>99
12a	90.7±8.3	>99	86.4±2.9	>99

[a] Reaction conditions: HEPES buffer (50 mM, pH 7.5), 5 mM ketone, IPA (0.25 M for Spo-TA, 1 M for Afu-TA), 10% DMF, 30 °C, 18 h. [b] Conversion and enantiomeric excess were determined by chiral-phase GC analysis by using a Hydrodex-β-TBDAc column (Macherey & Nagel). All measurements were performed in triplicate.

Thus, we demonstrated the enzymatic synthesis of a set of halogen-substituted chiral benzylamines derived from 1-phenyl-2-propanamine, 4-phenylbutan-2-amine, and 1-(3-pyridinyl)ethanamine with isopropylamine as a cheap and convenient amine donor. The use of the amine transaminases from *Silicibacter pomeroyi* (Spo-TA) and *Aspergillus fumigatus* (Afu-TA) enabled mostly quantitative conversions of compounds **1a**–**12a** to yield the desired amines with excellent optical purities (mostly >99% *ee*).

Experimental Section

All chemicals were purchased from Sigma–Aldrich (Darmstadt, Germany), Roth (Karlsruhe, Germany), Acros/Thermofisher Scientific (Waltham, USA), or Enamine (Monmouth, USA) in analytical grade.

Enzyme expression and cell lysis

Genes encoding the ATAs from *Silicibacter pomeroyi* and *Aspergillus fumigatus* were subcloned into the pET22b vector with a C-terminal His-tag and were transformed into *E. coli* BL21 (DE3) as described previously.[32] ATAs from *Chromobacterium violaceum* and *Vibrio fluvialis* were available in pET24b and pET28a vectors containing a C-terminal and N-terminal His-tag, respectively. Protein expression was done in Terrific Broth (TB) media with 100 μg mL^{-1} ampicillin or 50 μg mL^{-1} kanamycin at 160 rpm and 20 °C. After the optical density at $\lambda = 600$ nm (OD_{600}) reached 0.7, expression was induced by adding 0.2 mM isopropyl β-D-1-thiogalactopyranoside (final concentration). After 18 h, the cultures were centrifuged (4000×*g*, 15 min, 4 °C) and washed with lysis buffer [4-(2-hydroxyethyl)-1-piperazineethanesulfonic acid (HEPES, 50 mM pH 7.5), pyridoxal-5′-phosphate (PLP, 0.1 mM), 300 mM NaCl]. Cell disruption was performed by sonication by using the Bandelin Sonoplus HD 2070 (8 min, 50% pulsed cycle, 50% power) on ice followed by centrifugation to remove cell debris (12000×*g*, 45 min, 4 °C, Sorvall centrifuge). The supernatant containing the crude ATA was stored at 4 °C until use.

Determination of transaminase activity

Characterization of the ATAs was done by the acetophenone assay according to Schätzle et al.[41] with slight modifications. As all used ATAs showed their optimum at basic pH values, the assay was performed in *N*-cyclohexyl-2-aminoethanesulfonic acid (CHES) buffer (50 mM pH 9). In the reaction solution, the concentrations of the amine donor [(*R*)- or (*S*)-1-PEA] and the acceptor pyruvate were set to 1.25 mM in 0.25% (*v*/*v*) DMSO. Briefly, a prediluted ATA solution (10 μL) was mixed with buffer, and the reaction was initiated by the addition of the reaction solution. The formation of acetophenone was quantified at $\lambda = 245$ nm by using a Tecan Infinite M200 Pro (Crailsheim, Germany) at 30 °C. One unit (U) of ATA activity was defined as the formation of 1 μmol acetophenone per minute ($\varepsilon =$ 12 mM^{-1} cm^{-1}). All measurements were performed in triplicate.

Asymmetric synthesis of chiral amines 1 b–12 b

Biotransformations of ketones **1 a**–**12 a** were performed in triplicate on a 0.25 mL scale by using 1.5 mL glass vials at 30 °C and 950 rpm shaking. The mixtures contained ATA crude lysate (9–14 U mL^{-1}, 50 μL), 5 mM ketone, 10% DMF as cosolvent, and 250 mM IPA in 50 mM HEPES (pH 7.5–8). After incubation for 24 h, the reaction was quenched by adding 3 M NaOH (resulting in pH ≥ 13). Samples for gas chromatography (GC) analysis were taken immediately after this quenching.

GC analysis

Samples (30–40 μL) were taken for chiral-phase GC analysis and were extracted with ethyl acetate (250 μL) containing 1 mM 4′-iodoacetophenone as an internal standard for quantification. The organic layer was dried (anhydrous $MgSO_4$) and derivatized with *N*-methyl-bis-trifluoroacetamide (MBTFA) by adding a commercial stock solution (7.5 μL) to the organic layer (100 μL) and incubating at 60 °C for 30 min. Afterwards, the samples were analyzed immediately by using a chiral Hydrodex-β-TBDAc column (Macherey & Nagel). For analysis of all ketones, the following temperature gradient program was established: initial temperature 80 °C, kept for 10 min, linear gradient to 175 °C with a slope of 4 °C min^{-1}, kept for 13 min, linear gradient to 220 °C with a slope of 20 °C min^{-1}, kept for 5 min. The conversion of each compound was determined by quantification of substrate consumption by calculating the response factor. Each sample included an internal standard and was set in relation to control experiments in each batch experiment with known substrate concentration. The linearity of the response factor over a certain range was verified by a calibration curve. Chiral analysis of the amine products was done either as described above or with the following temperature profile: 60 °C, kept for 35 min, linear gradient to 165 °C with a slope of 2 °C min^{-1}, kept for 20 min, linear gradient to 220 °C with a slope of 5 °C min^{-1}, kept for 10 min.

Preparative-scale synthesis of 1 b

The conversion of 1-(4-bromophenyl)propan-2-one (**1 a**) into 1-(4-bromophenyl)-2-propanamine (**1 b**) was performed on a preparative scale with crude cell lysate containing Spo-TA or Afu-TA. The following conditions were applied: **1 a** (50 mg if using Spo-TA; 100 mg if using Afu-TA) was added to an Erlenmeyer flask and mixed with DMF (12% final concentration), HEPES buffer (50 mM final, pH 7.5), and isopropylamine (850 mM final concentration). The pH was adjusted with aqueous HCl. In the end, 15 vol% of crude cell lysate was added, which led to a final working volume of 30 mL in the case of Spo-TA and 50 mL in the case of Afu-TA. The reaction mixture was incubated at 30 °C under agitation for 72 h. For quantification of the conversion, samples were taken and extracted as described above. The reaction was stopped if no further conversion was observed during reaction monitoring (for Spo-TA, 98%; for Afu-TA, 62%). The reaction workup was done as follows: After acidification with 3 M aq. HCl to pH 1, extraction with ethyl acetate (2×30 mL) was performed in a separation funnel. The aqueous layer was basified with 3 M aq. NaOH solution to pH 11–12 and was extracted with methyl *tert*-butyl ether (5×15 mL). The combined organic layer was washed with saturated brine solution (2×15 mL), dried (anhydrous $MgSO_4$), and concentrated under vacuum. The amine product was obtained as a yellow oil. Each product was confirmed by GC–MS, and a sample (10–12 mg) was subjected to ^{1}H NMR and ^{13}C NMR spectroscopy. A racemic standard was synthesized for comparison reasons according to the literature[42] (for the ^{1}H NMR and ^{13}C NMR spectra, see the Supporting Information).

The absolute configuration was determined by optical rotation data by using a Polar-L polarimeter from IBZ Messtechnik. A solution of each enantiomer in chloroform was prepared (concentration as indicated). The specific optical rotation data of each enantiomer was verified with literature values.[40]

(*S*)-1-(4-Bromophenyl)-2-propanamine [(*S*)-**1 b**]: Yield: 25% (not optimized), >99% *ee*, $[\alpha]_D^{20} = +20.8$ ($c = 0.9$, $CHCl_3$).

(*R*)-1-(4-Bromophenyl)-2-propanamine [(*R*)-**1 b**]: Yield: 27% (not optimized), >99% *ee*, $[\alpha]_D^{20} = -25.9$ ($c = 1.2$, $CHCl_3$).

Bioinformatic analyses

Docking studies were done by using YASARA Structure (v.17.1.28).[43] The quinonoid intermediate (the reactive intermedi-

ate in the ATA reaction) consisting of PLP and **1b**/**9b**/**12b** was modeled by a combination of ChemDraw (v.11) and YASARA followed by energy minimization. Prior to the docking experiments, refinement of the lowest energy ligand conformation and all used crystal structures from the PDB was performed with the built-in macro (YAMBER3 force field at 298 K for 500 ps, standard settings). As Spo-TA (PDB ID: 3HMU) was crystallized in the apo form, the position of the PLP cofactor had to be determined first, as its position was crucial for visual evaluation of the docking result (mainly by superimposing the docked ligand–receptor complex with the refined, PLP-containing crystal structure and checking the coverage of the pyridine ring of the PLP). A PDB-BLAST search was done, which revealed the best result in sequence identity of 53% with the ATA from *Chromobacterium violaceum* (PDB ID: 4A6T; for BLAST results, see the Supporting Information). Both structures were superimposed, and the position of the PLP was transferred from one structure to another. Because of plausibility reasons, the surrounding binding residues of the phosphate group and the nitrogen atom of the PLP pyridine ring were confirmed with the literature data.[44] The applied docking method was the implemented AutoDock VINA algorithm with standard settings, which comprised 100 runs in total and subsequent clustering to give distinct complex conformations. The output was evaluated visually. Usually, the best conformation revealed by this way was one of those with the highest binding energy and the lowest dissociation constant according to the docking log file. All illustrations were made with PyMOL (v.1.7).

Acknowledgements

We thank the Bundesministerium für Bildung und Forschung (Grant 01DN14016) for financial support. R.O.M.A.d.S. thanks the Alexander-von-Humboldt foundation for a Capes-Humboldt research fellowship. We are also grateful to Prof. Dr. Bednarski and Patrick Werth (Pharmazeutische/Medizinische Chemie, Institut für Pharmazie, Greifswald) for assisting with some equipment.

Conflict of interest

The authors declare no conflict of interest.

Keywords: amines · asymmetric synthesis · biocatalysis · chirality · molecular docking

[1] M. Höhne, U. T. Bornscheuer, *ChemCatChem* **2009**, *1*, 42 – 51.
[2] M. Höhne, S. Kühl, K. Robins, U. T. Bornscheuer, *ChemBioChem* **2008**, *9*, 363 – 365.
[3] A. Iwasaki, Y. Yamada, Y. Ikenaka, J. Hasegawa, *Biotechnol. Lett.* **2003**, *25*, 1843 – 1846.
[4] A. Iwasaki, Y. Yamada, N. Kizaki, Y. Ikenaka, J. Hasegawa, *Appl. Microbiol. Biotechnol.* **2006**, *69*, 499 – 505.
[5] J. S. Shin, B. G. Kim, *Biotechnol. Bioeng.* **1999**, *65*, 206 – 211.
[6] P. Tufvesson, M. Nordblad, U. Krühne, M. Schürmann, A. Vogel, R. Wohlgemuth, J. M. Woodley, *Org. Process Res. Dev.* **2015**, *19*, 652 – 660.
[7] J.-H. Seo, D. Kyung, K. Joo, J. Lee, B.-G. Kim, *Biotechnol. Bioeng.* **2011**, *108*, 253 – 263.
[8] U. Kaulmann, K. Smithies, M. E. Smith, H. C. Hailes, J. M. Ward, *Enzyme Microb. Technol.* **2007**, *41*, 628 – 637.
[9] F. G. Mutti, C. S. Fuchs, D. Pressnitz, J. H. Sattler, W. Kroutil, *Adv. Synth. Catal.* **2011**, *353*, 3227 – 3233.
[10] W. Kroutil, E.-M. Fischereder, C. S. Fuchs, H. Lechner, F. G. Mutti, D. Pressnitz, A. Rajagopalan, J. H. Sattler, R. C. Simon, E. Siirola, *Org. Process Res. Dev.* **2013**, *17*, 751 – 759.
[11] A. Nobili, F. Steffen-Munsberg, H. Kohls, I. Trentin, C. Schulzke, M. Höhne, U. T. Bornscheuer, *ChemCatChem* **2015**, *7*, 757 – 760.
[12] D. Koszelewski, K. Tauber, K. Faber, W. Kroutil, *Trends Biotechnol.* **2010**, *28*, 324 – 332.
[13] D. Koszelewski, I. Lavandera, D. Clay, D. Rozzell, W. Kroutil, *Adv. Synth. Catal.* **2008**, *350*, 2761 – 2766.
[14] P. Tufvesson, J. Lima-Ramos, J. S. Jensen, N. Al-Haque, W. Neto, J. M. Woodley, *Biotechnol. Bioeng.* **2011**, *108*, 1479 – 1493.
[15] A. Gomm, W. Lewis, A. P. Green, E. O'Reilly, *Chem. Eur. J.* **2016**, *22*, 12692 – 12695.
[16] A. P. Green, N. J. Turner, E. O'Reilly, *Angew. Chem. Int. Ed.* **2014**, *53*, 10714 – 10717; *Angew. Chem.* **2014**, *126*, 10890 – 10893.
[17] L. Martínez-Montero, V. Gotor, V. Gotor-Fernández, I. Lavandera, *Adv. Synth. Catal.* **2016**, *358*, 1618 – 1624.
[18] S. E. Payer, J. H. Schrittwieser, W. Kroutil, *Eur. J. Org. Chem.* **2017**, 2553 – 2559.
[19] I. Slabu, J. L. Galman, C. Iglesias, N. J. Weise, R. C. Lloyd, N. J. Turner, *Catal. Today* **2018**, DOI: 10.1016/j.cattod.2017.01.025.
[20] J. L. Galman, I. Slabu, N. J. Weise, C. Iglesias, F. Parmeggiani, R. C. Lloyd, N. J. Turner, *Green Chem.* **2017**, *19*, 361 – 366.
[21] C. K. Savile, J. M. Janey, E. C. Mundorff, J. C. Moore, S. Tam, W. R. Jarvis, J. C. Colbeck, A. Krebber, F. J. Fleitz, J. Brands, *Science* **2010**, *329*, 305 – 309.
[22] K. E. Cassimjee, M. S. Humble, H. Land, V. Abedi, P. Berglund, *Org. Biomol. Chem.* **2012**, *10*, 5466 – 5470.
[23] M. Svedendahl, C. Branneby, L. Lindberg, P. Berglund, *ChemCatChem* **2010**, *2*, 976 – 980.
[24] C. E. Paul, M. Rodriguez-Mata, E. Busto, I. Lavandera, V. Gotor-Fernández, V. Gotor, S. Garcia-Cerrada, J. Mendiola, Ó. de Frutos, I. Collado, *Org. Process Res. Dev.* **2014**, *18*, 788 – 792.
[25] S.-W. Han, E.-S. Park, J.-Y. Dong, J.-S. Shin, *Adv. Synth. Catal.* **2015**, *357*, 2712 – 2720.
[26] A. Cuetos, M. Garcia-Ramos, E.-M. Fischereder, A. Diaz-Rodriguez, G. Grogan, V. Gotor, W. Kroutil, I. Lavandera, *Angew. Chem. Int. Ed.* **2016**, *55*, 3144 – 3147; *Angew. Chem.* **2016**, *128*, 3196 – 3199.
[27] M. López-Iglesias, D. González-Martínez, M. Rodríguez-Mata, V. Gotor, E. Busto, W. Kroutil, V. Gotor-Fernández, *Adv. Synth. Catal.* **2017**, *359*, 279 – 291.
[28] R. E. Meadows, K. R. Mulholland, M. Schürmann, M. Golden, H. Kierkels, E. Meulenbroeks, D. Mink, O. May, C. Squire, H. Straatman, *Org. Process Res. Dev.* **2013**, *17*, 1117 – 1122.
[29] L. Frodsham, M. Golden, S. Hard, M. N. Kenworthy, D. J. Klauber, K. Leslie, C. Macleod, R. E. Meadows, K. R. Mulholland, J. Reilly, *Org. Process Res. Dev.* **2013**, *17*, 1123 – 1130.
[30] N. G. Schmidt, R. C. Simon, W. Kroutil, *Adv. Synth. Catal.* **2015**, *357*, 1815 – 1821.
[31] M. L. Contente, M. Planchestainer, F. Molinari, F. Paradisi, *Org. Biomol. Chem.* **2016**, *14*, 9306 – 9311.
[32] F. Steffen-Munsberg, C. Vickers, A. Thontowi, S. Schätzle, T. Tumlirsch, M. Svedendahl Humble, H. Land, P. Berglund, U. T. Bornscheuer, M. Höhne, *ChemCatChem* **2013**, *5*, 150 – 153.
[33] A. K. Holzer, K. Hiebler, F. G. Mutti, R. C. Simon, L. Lauterbach, O. Lenz, W. Kroutil, *Org. Lett.* **2015**, *17*, 2431 – 2433.
[34] D. Koszelewski, M. Göritzer, D. Clay, B. Seisser, W. Kroutil, *ChemCatChem* **2010**, *2*, 73 – 77.
[35] S. Schätzle, F. Steffen-Munsberg, A. Thontowi, M. Höhne, K. Robins, U. T. Bornscheuer, *Adv. Synth. Catal.* **2011**, *353*, 2439 – 2445.
[36] M. Höhne, S. Schätzle, H. Jochens, K. Robins, U. T. Bornscheuer, *Nat. Chem. Biol.* **2010**, *6*, 807 – 813.
[37] M. Thomsen, L. Skalden, G. J. Palm, M. Höhne, U. T. Bornscheuer, W. Hinrichs, *Acta Crystallogr. Sect. D* **2014**, *70*, 1086 – 1093.
[38] L. Skalden, M. Thomsen, M. Höhne, U. T. Bornscheuer, W. Hinrichs, *FEBS J.* **2015**, *282*, 407 – 415.
[39] H. Mallin, M. Höhne, U. T. Bornscheuer, *J. Biotechnol.* **2014**, *191*, 32 – 37.
[40] L. Muñoz, A. M. Rodriguez, G. Rosell, M. P. Bosch, A. Guerrero, *Org. Biomol. Chem.* **2011**, *9*, 8171 – 8177.
[41] S. Schätzle, M. Höhne, E. Redestad, K. Robins, U. T. Bornscheuer, *Anal. Chem.* **2009**, *81*, 8244 – 8248.

[42] R. Laufer, G. Ng, Y. Liu, N. K. B. Patel, L. G. Edwards, Y. Lang, S.-W. Li, M. Feher, D. E. Awrey, G. Leung, *Bioorg. Med. Chem.* **2014**, *22*, 4968 – 4997.
[43] E. Krieger, G. Koraimann, G. Vriend, *Proteins Struct. Funct. Bioinf.* **2002**, *47*, 393 – 402.
[44] M. S. Humble, K. E. Cassimjee, M. Haakansson, Y. R. Kimbung, B. Walse, V. Abedi, H.-J. Federsel, P. Berglund, D. T. Logan, *FEBS J.* **2012**, *279*, 779 – 792.

Manuscript received: December 9, 2017
Revised manuscript received: January 6, 2018
Accepted manuscript online: January 9, 2018
Version of record online: February 6, 2018

Heterogeneous & Homogeneous & Bio- & Nano-
CHEMCATCHEM
CATALYSIS

Supporting Information

Asymmetric Synthesis of Chiral Halogenated Amines using Amine Transaminases

Ayad W. H. Dawood,[a] Rodrigo O. M. A. de Souza,[b] and Uwe T. Bornscheuer*[a]

cctc_201701962_sm_miscellaneous_information.pdf

Table of content

Molecular Docking

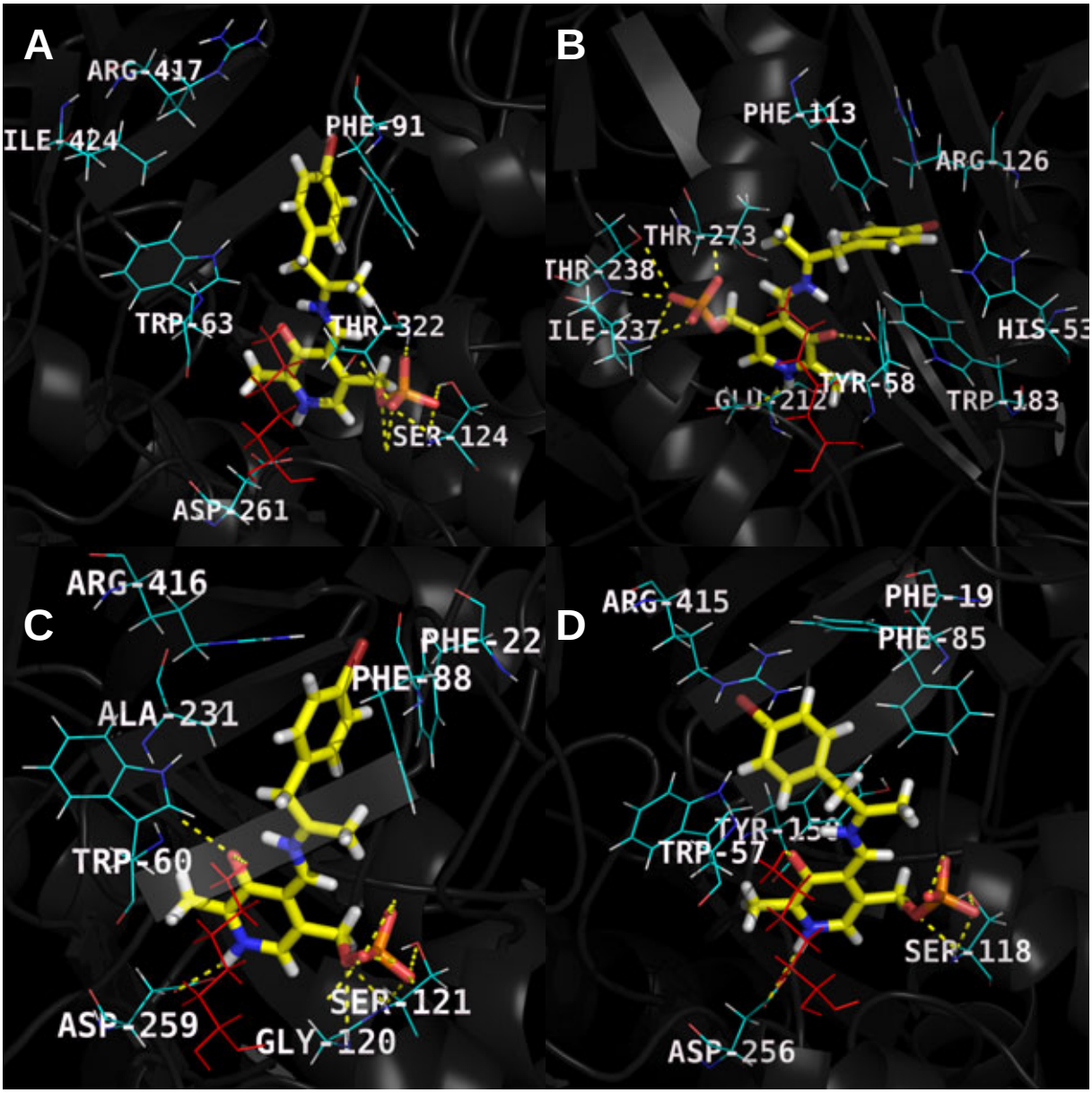

Figure S1. *Pymol* illustration of the docking experiments with Spo-TA (A), Afu-TA (B), Cvi-TA (C) and Vfl-TA (D). The PDB IDs for all ATAs were 3HMU, 4CHI, 4A6T and 4E3Q, respectively. The catalytic lysine is indicated in red, hydrogen bonds are indicated with yellow dash lines. The quinoid intermediate of **1b** (yellow) was docked into the active site of all four ATAs according to the procedure described in the Experimental Section. After docking the output was checked for plausibility by coverage with the position of the original PLP molecule (contained in the PDB file, for the procedure in case of Spo-TA (3HMU) see Experimental Section). The involved amino acid residues for coordination of the PLP as well as those for pocket formation were additionally verified with literature.[1–4] Some residues were omitted for clarity. The overall result of all docking experiments gave a strong indication of a correct substrate coordination thus each provided binding pocket was hosting the respective part of the docked molecule in a reasonable angle to the pyridine ring of the PLP.

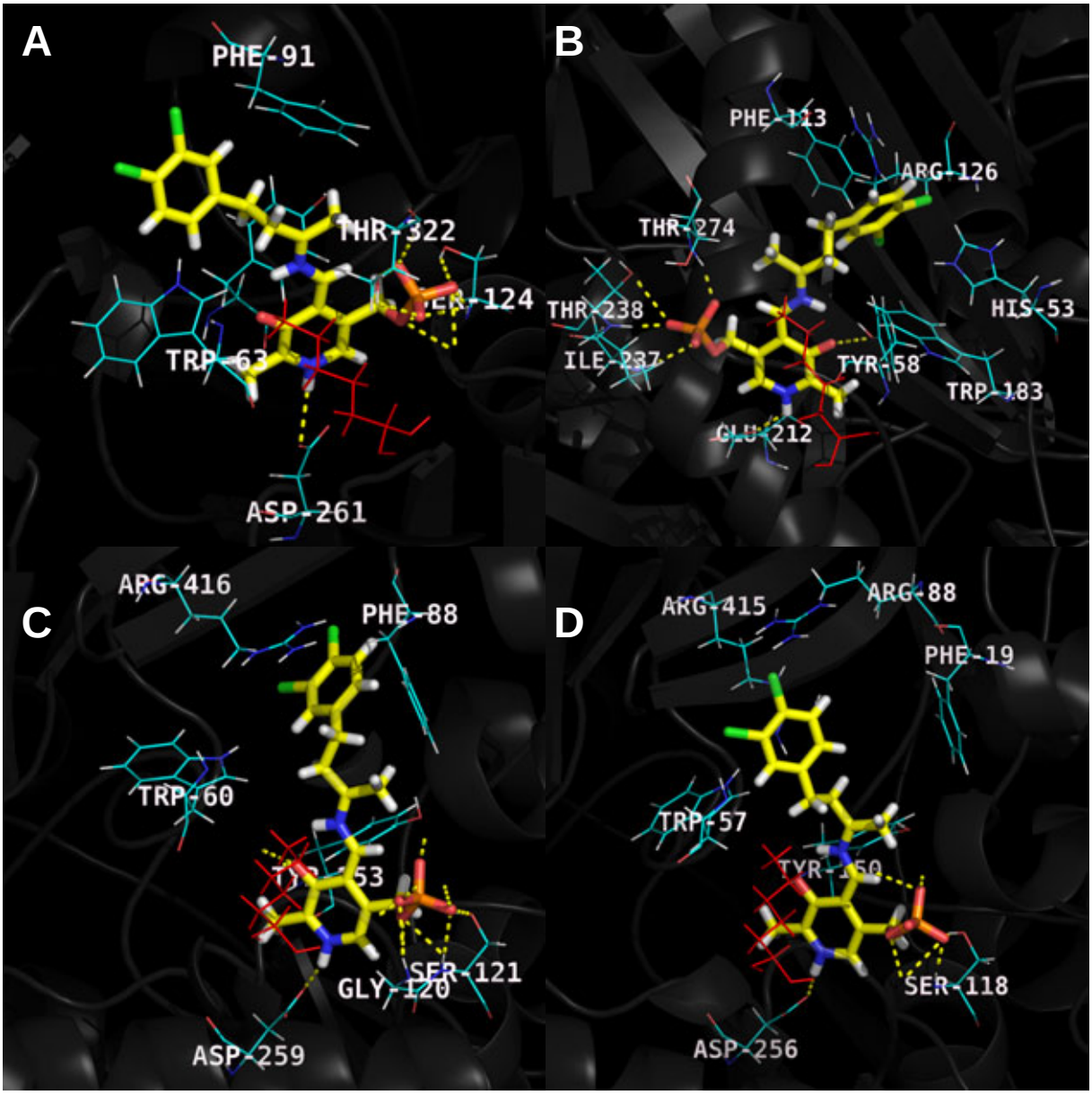

Figure S2. *Pymol* illustration of the docking experiments with Spo-TA (A), Afu-TA (B), Cvi-TA (C) and Vfl-TA (D). The PDB IDs for all ATAs were 3HMU, 4CHI, 4A6T and 4E3Q, respectively. The catalytic lysine is indicated in red, hydrogen bonds are indicated with yellow dash lines. The quinoid intermediate of **9b** was docked into the active site of all four ATAs according to the procedure described in the Experimental Section. For details see caption of Figure S1.

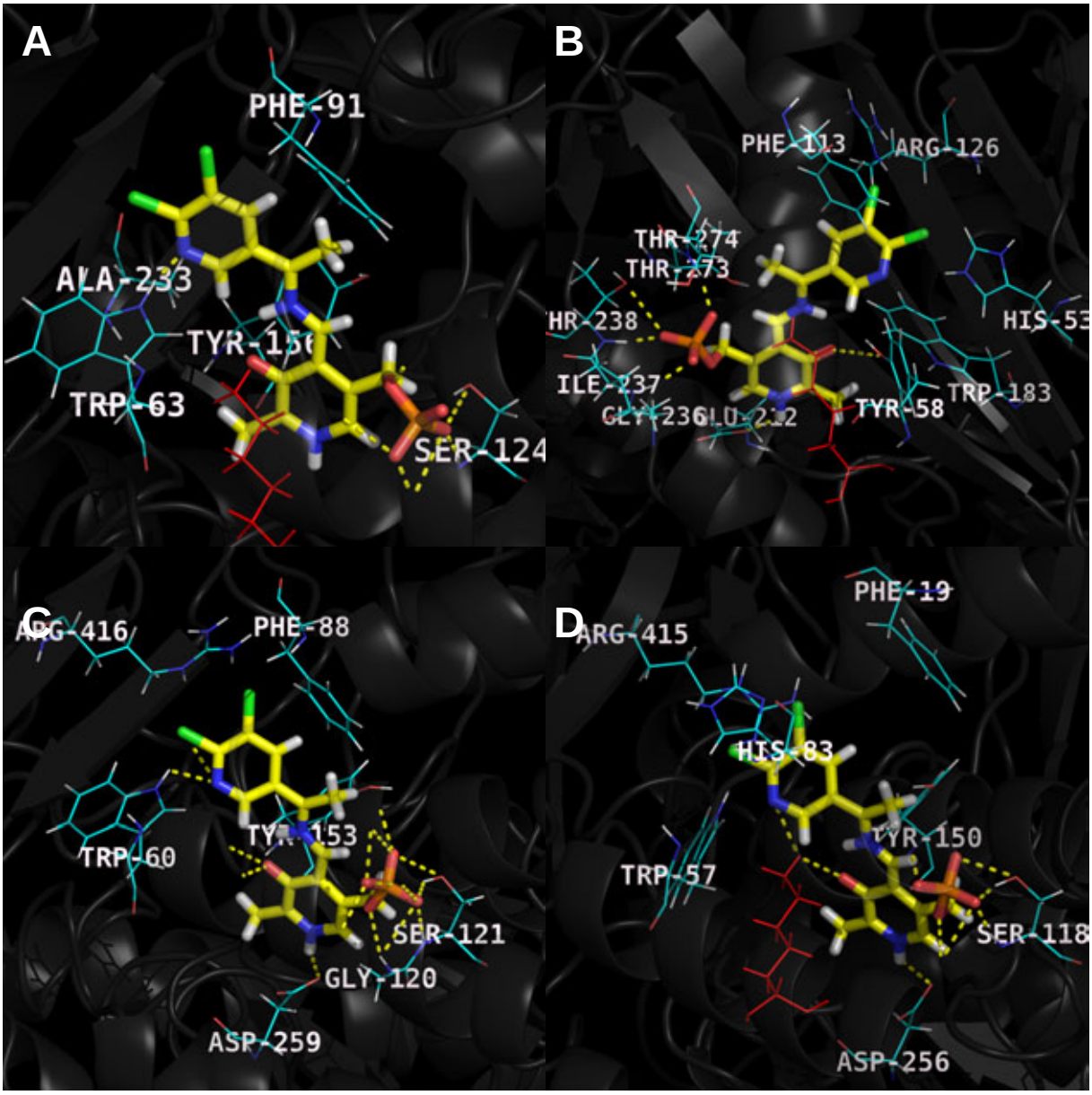

Figure S3. *Pymol* illustration of the docking experiments with Spo-TA (A), Afu-TA (B), Cvi-TA (C) and Vfl-TA (D). The PDB IDs for all ATAs were 3HMU, 4CHI, 4A6T and 4E3Q, respectively. The catalytic lysine is indicated in red, hydrogen bonds are indicated with yellow dash lines. The quinoid intermediate of **12b** was docked into the active site of all four ATAs according to the procedure described in the Experimental Section. For details see caption of Figure S1.

Investigation of amine donor acceptance

In order to find a suitable reaction setup using the transaminases from *Silicibacter pomeroyi* (Spo-TA), *Chromobacterium violaceum* (Cvi-TA), *Vibrio fluvialis* (Vfl-TA) and *Aspergillus fumigatus* (Afu-TA) three amine donors were initially focused on: beside isopropylamine (IPA, which was finally used), 1-phenylethylamine (1-PEA) and D- or L-alanine. Table S1 shows the results of the experiments testing the latter two amine donors. 1-(4-bromophenyl)propan-2-one **1a** was used as model substrate. 1-PEA was applied in slight excess (5-fold) to drive the reaction to the product side. D- or L-alanine was used in combination with the co-product removal system using lactate dehydrogenase (LDH) and glucose dehydrogenase (GDH). The amine transaminase of *Silicibacter pomeroyi* was used here with isopropylamine and 1-PEA only due to the results of previous investigations.

Table S1. Summary of preliminary tests applying 1-PEA or alanine for the amination of 1-(4-bromophenyl)propan-2-one **1a** (5 mM). 1-PEA was used in a 5-fold excess (25 mM) compared to the substrate and D- or L-alanine (depends on the ATA) in combination with the LDH/GDH system according to literature[4]: 250 mM alanine, 150 mM Glucose, 1 mM NADH, 90 U/mL LDH and 15 U/mL GDH. The reaction was carried at 30 °C for 18 h and analyzed as described in the Experimental Section. *n.d. = not detectable.

Transaminase	**Conversion [%]**	
	Alanine/LDH/GDH system	**1-PEA**
Cvi-TA	99	n.d.*
Vfl-TA	n.d.*	n.d.*
Spo-TA	-	95
Afu-TA	86	89

Aliphatic diamines were also tested to check the possibility and the potential of those amines for the desired reaction (Figure S4). As an example the transaminase Afu-TA was tested with 1,4-di-aminobutane and 1,5-di-aminopentane[5] in the asymmetric synthesis of 1-(4-bromophenyl)-2-propanamine **1b**. Preliminary experiments eliminated 1,5-di-aminopentane as there was no conversion (not shown). The conversion level with 1,4-di-amino-butane as amine donor was checked in the pH range from 9–11, since high pH values are addressed to be crucial for the necessary and spontaneous oligomerisation step in co-product removal.[5] An overall conversion of only ~35–40 % was reached.

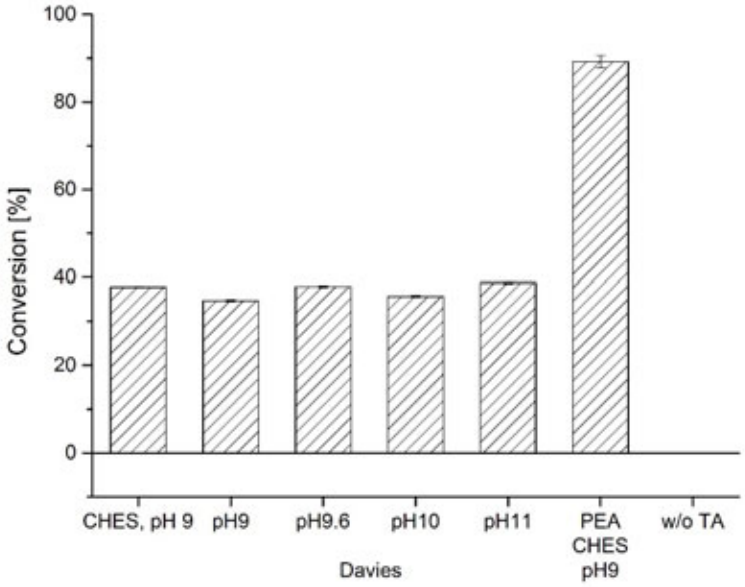

Figure S4. Asymmetric synthesis of 1-(4-bromophenyl)-2-propanamine **1b** in dependence of the pH. Davies buffer[6] was used to adjust the range of pH as indicated. 1,4-di-amino-butane (1,4-DAB) was applied in a 10-fold excess to drive the reaction equilibrium to the favored site. CHES buffer pH 9 containing 1,4-DAB or 1-PEA (25 mM) were used as control experiments. General procedure of the batch reaction: 5 mM 1-(4-bromophenyl)propan-2-one **1a**, 50 mM 1,4-DAB, 10 % DMF, 50 mM buffer reagent.

Investigation of the right donor-acceptor ratio

Since a large excess of IPA is critical for the shifting of the reaction equilibrium, investigations were performed to find the best ratio of donor and acceptor. Again 1-(4-bromophenyl)propan-2-one **1a** was used as model substrate. The conversion to 1-(4-bromophenyl)-2-propanamine **1b** in dependence of the IPA concentration is shown in Figure S5. This investigation was performed for both of the ATAs, which were finally used for biocatalysis. In all reactions a pH value of 7–7.5 was set. In case of Spo-TA 200 mM IPA were already sufficient to drive the reaction almost to completeness. For Afu-TA significantly higher IPA concentrations were necessary. It has to be mentioned that the drop of activity in case of Afu-TA at 500 mM IPA was due to reproducible enzyme precipitation certainly at this concentration.

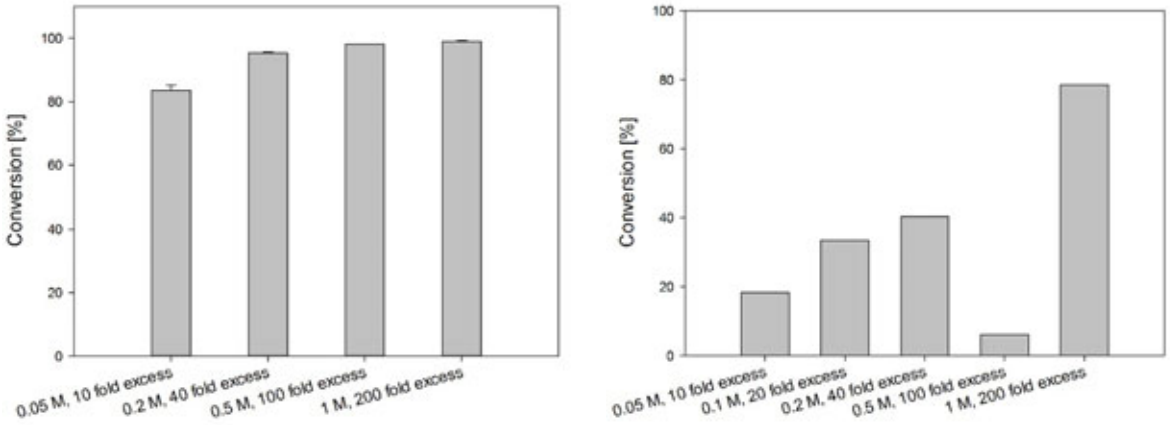

Figure S5. Conversion of 1-(4-bromophenyl)propan-2-one **1a** in dependence of the excess of isopropylamine using Spo-TA (left) and Afu-TA (right). General procedure: 5 mM of **1a**, 10 % DMF, IPA as indicated, HEPES buffer (50 mM, pH 7–7.5), 30 °C for 18 h. Each reaction was extracted and analyzed via GC.

Control experiment with ATA-free crude cell lysate

In order to ensure the enzyme activity we expected to have, ATA-free crude cell lysate was produced by cultivation of *E. coli* BL21 (DE3) containing an empty vector (pET22b). For details about cultivation and crude cell lysate preparation see Experimental Section. A biocatalysis was performed with this ATA-free lysate as descried in the Experimental Section. Table S2 shows the results.

Table S2. Results of the control experiment with ATA-free crude cell lysate. The biocatalysis was performed and analyzed as described for the ATA-containing reactions. *n.d. = not detectable.

Substrate	Apparent substrate consumption [%]
1a	0.98
2a	n.d.*
3a	-
4a	1.6
5a	n.d.*
6a	2.9
7a	7.66
8a	5.6
9a	9.95
10a	4.53
11a	1
12a	1

Chiral analysis

Sample extraction and analysis was performed as described (see Experimental Section). The amine products were identified via GCMS yielding the expected fragmentation pattern (Table S3). The retention times for the substrate and products are shown in Table S4. The respective mass spectra for each amine product and the spectra of the chiral analysis are shown below. The GC methods which were used are given in the description of Table S4.

Table S3. Expected mass peaks of the amine products **1b**–**12b** after derivatization with *N*-Methyl-bis-trifluoroacetamide (MBTFA) and GCMS analysis.

Derivatized amine product	**Expected *m/z***
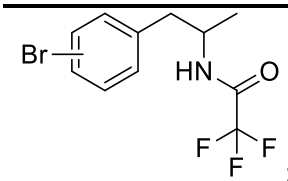 **1b**, **3b**	140 168 197 230
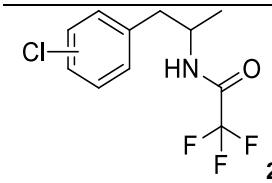 **2b**, **4b**	125 140 153 168 196
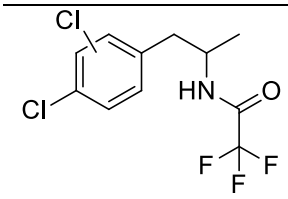 5**b**, 6**b**	140 159 187 200
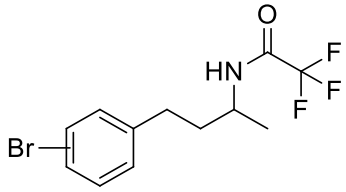 **7b, 8b**	133 140 155 168 183 211 255 323
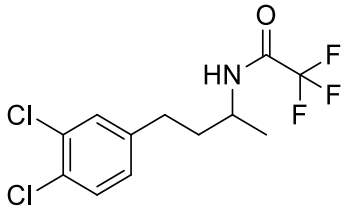 **9b**	140 168 173 201 244 313

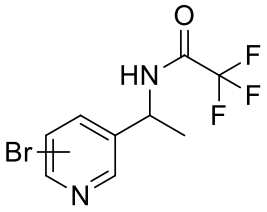 **10b**, **11b**	140 156 184 199 217 296
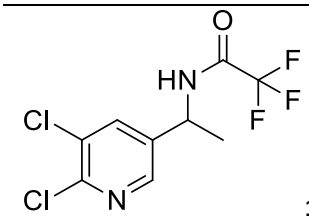 **12b**	174 217 270 286

Table S4. Overview of retention times for all investigated compounds revealed by GC analysis. The chiral GC column Hydrodex-ß-TBDAc (25 m) from Macherey & Nagel was used. The retention times for the ketones refer to the following temperature profile: 80 °C, kept for 10 min, linear gradient of 4 °C min^{-1} to 175 °C, kept for 13 min, linear gradient of 20 °C min^{-1} to 220 °C, kept for 10 min. The same method was used for the chiral separation of **10b** and **12b** (marked with *). The separation of all the other chiral amine products was performed with the following GC method: 60 °C, kept for 35 min, linear gradient of 2°C min^{-1} to 165 °C, kept for 20 min, linear gradient of 5 °C min^{-1} to 220 °C, kept for 10 min.

Compound	**Retention time [min]**		
	Ketone	**(*S*)-product**	**(*R*)-product**
1	32.3	114.8	115.5
2	29.4	110.2	111.5
3	30.1	112.4	113.5
4	27.8	105	108
5	34.5	118.5	119.25
6	29.9	111.45	113.5
7	34.3	119.7	120.15
8	33.2	117.8	119.05
9	38.1	112.6	123.8
10*	34.5	121.64	121.23
11	28.2	118.6	120.05
12*	33.4	120.13	120.5

GC-MS Chromatograms

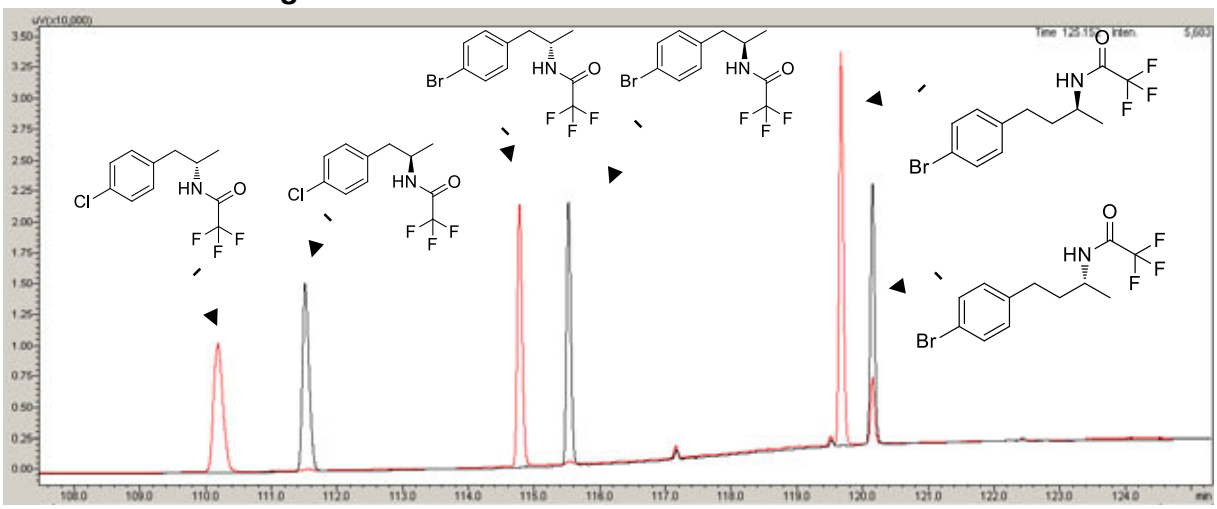

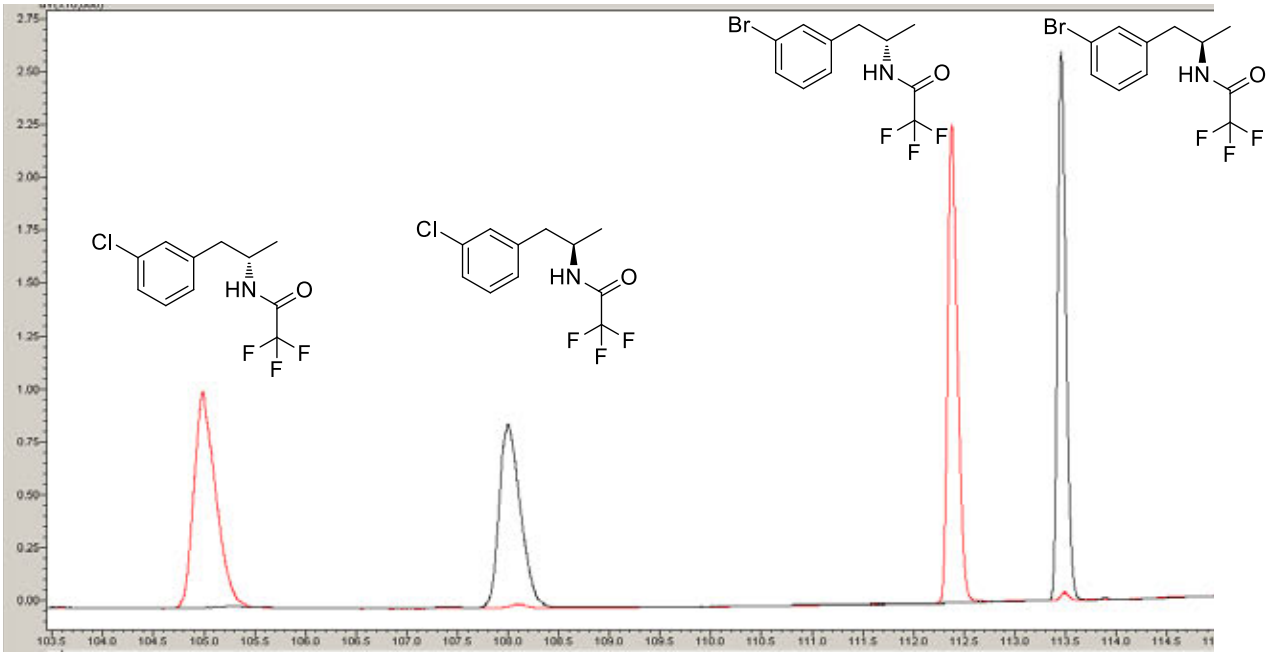

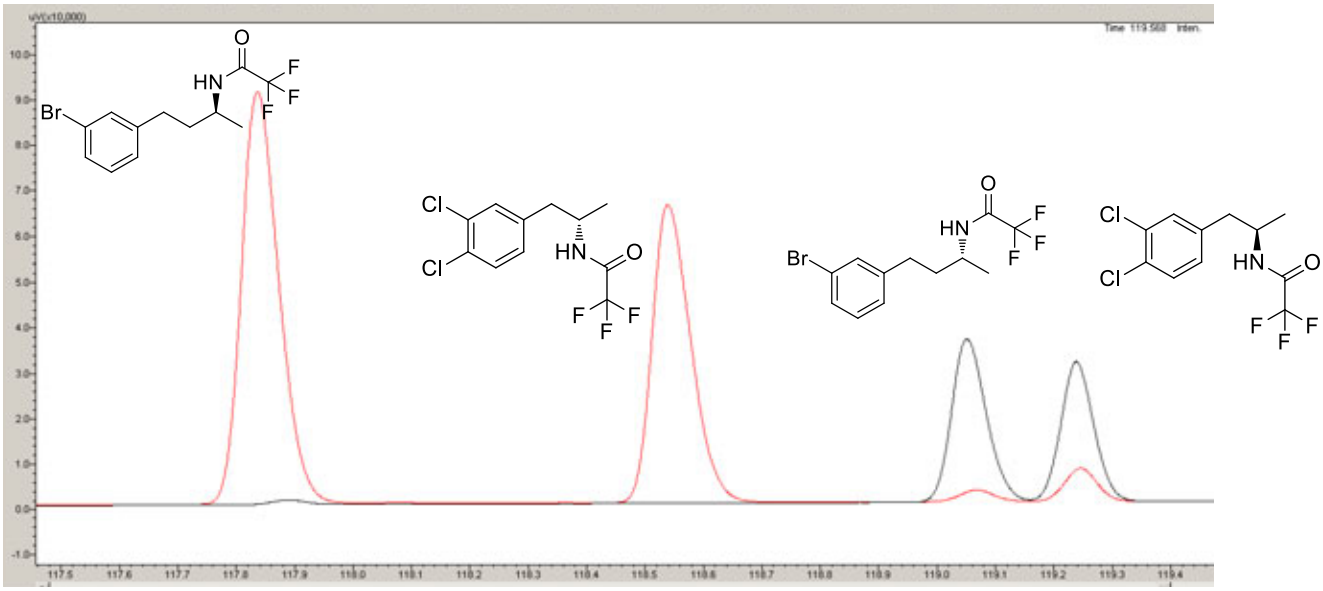

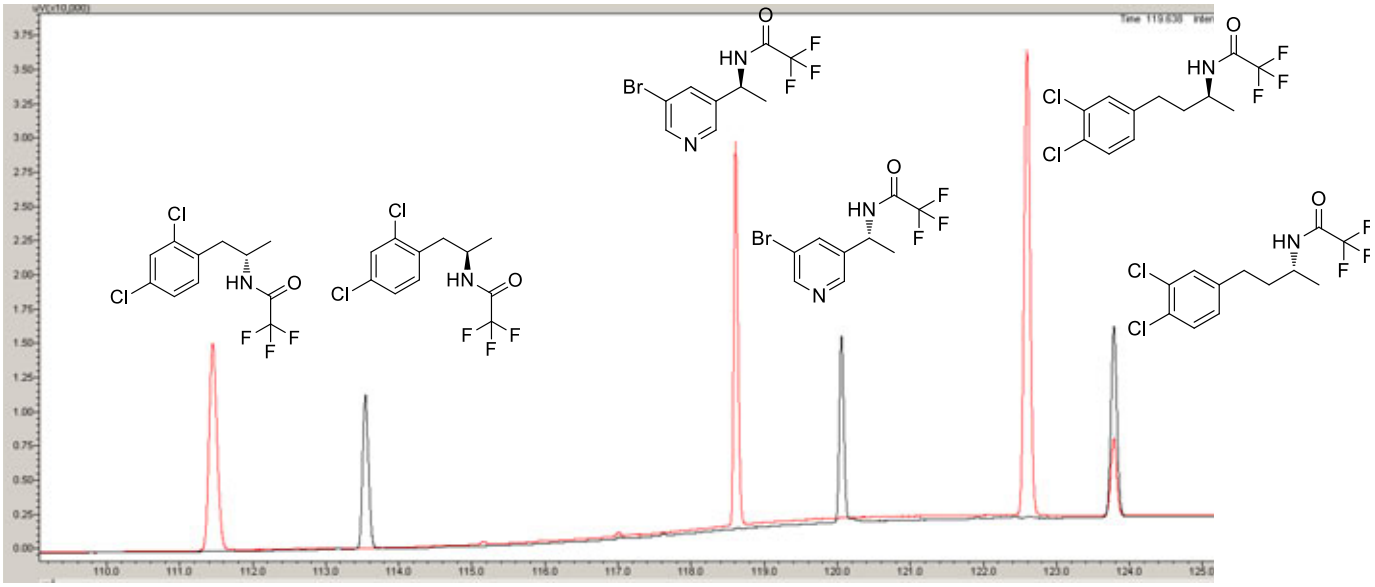
Cl
Cl
HN
O
F
F
F
Br
N

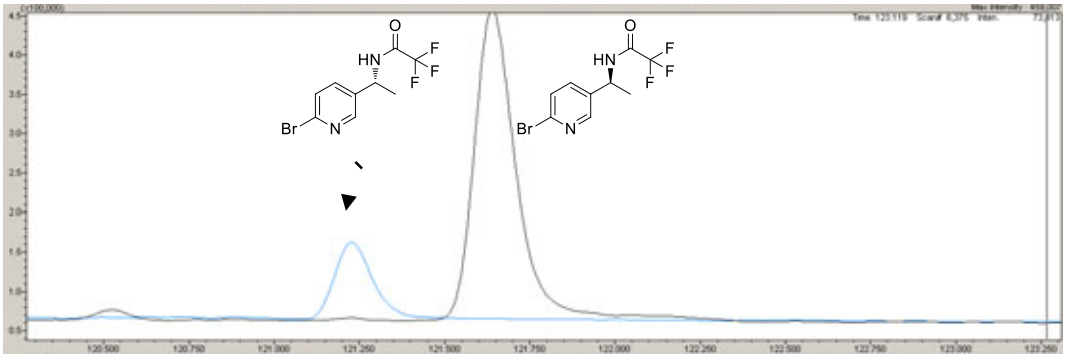
HN
O
F
F
F
Br
N

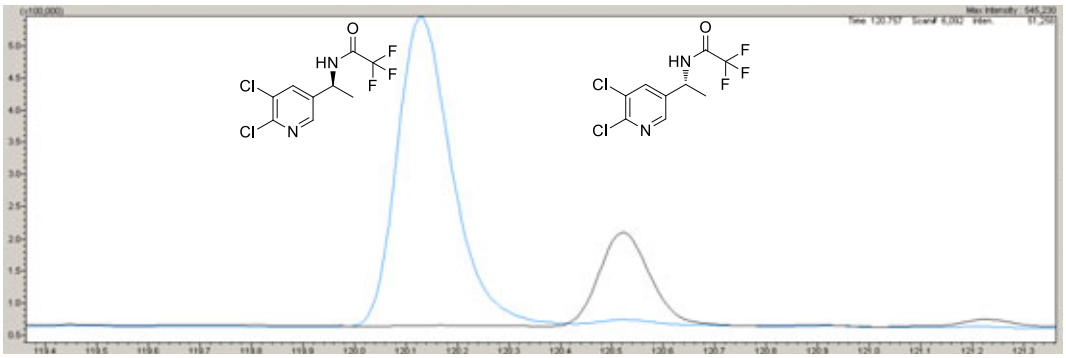
HN
O
F
F
F
Cl
Cl
N

Mass spectra of each amine product after GCMS analysis

1b

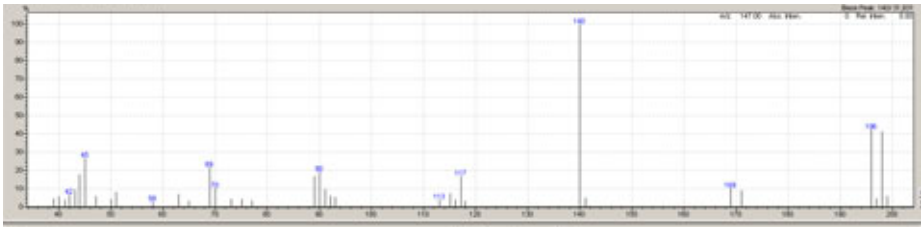

2b

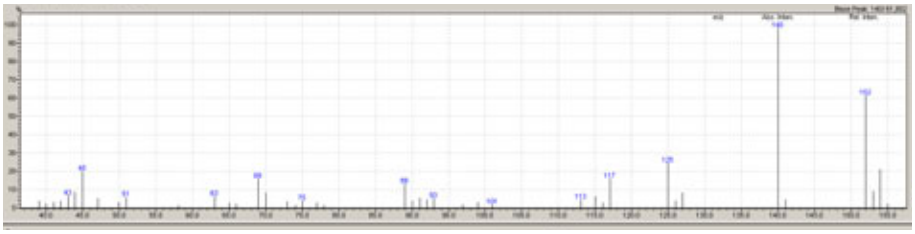

3b

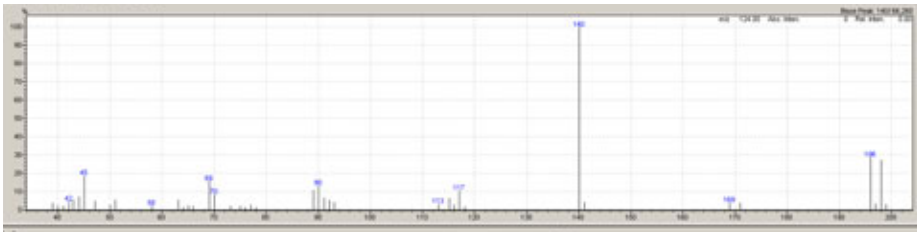

4b

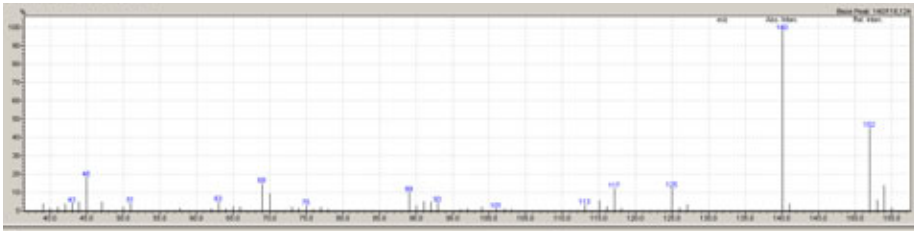

5b

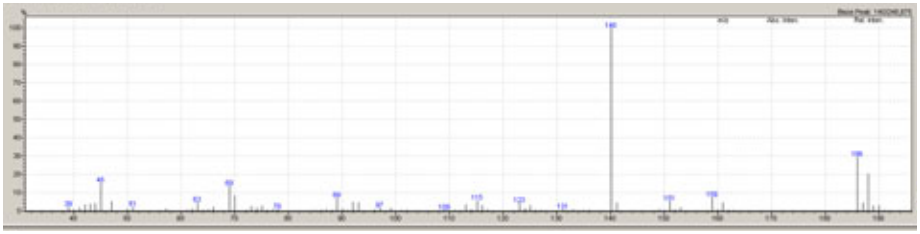

6b

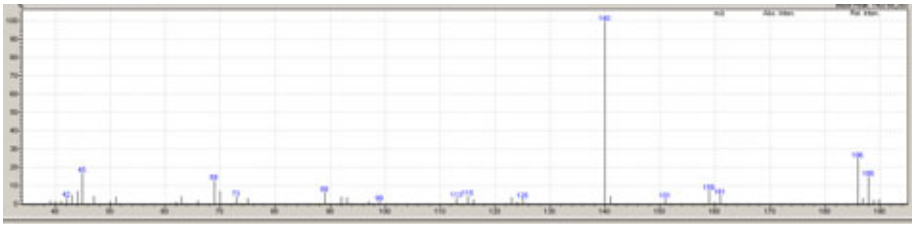

7b

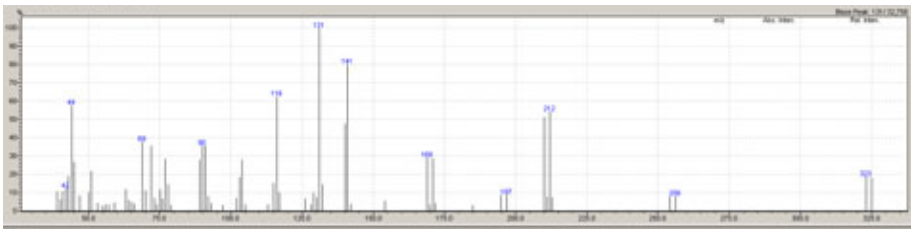

8b

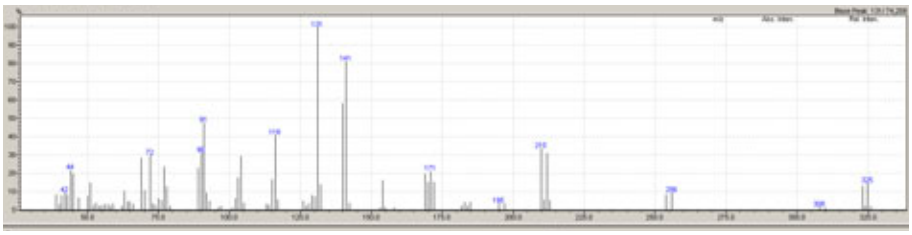

9b

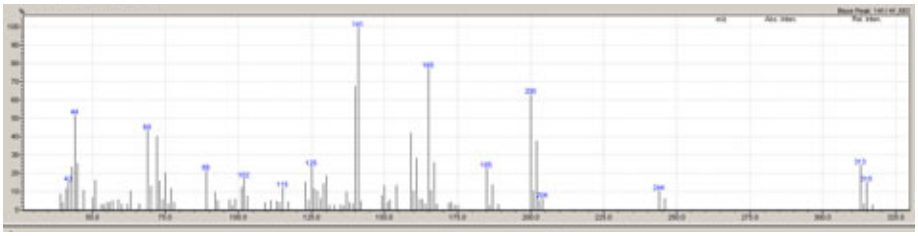

10b

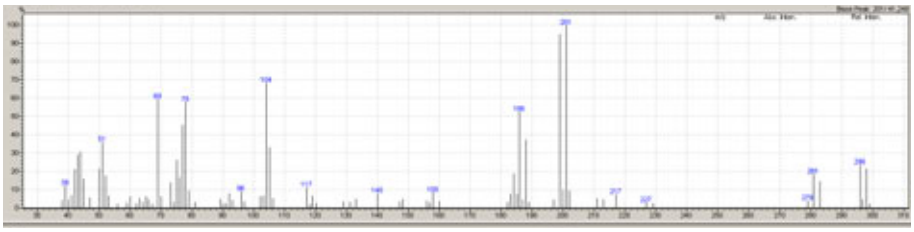

11b

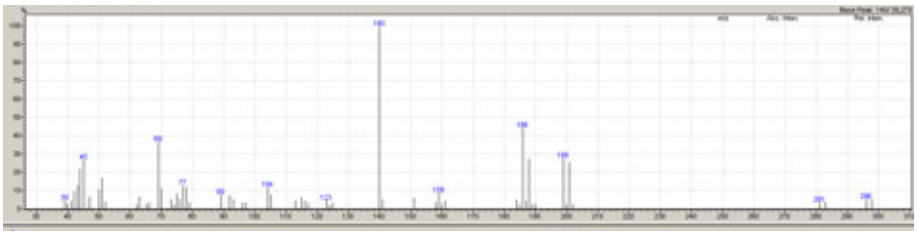

12b

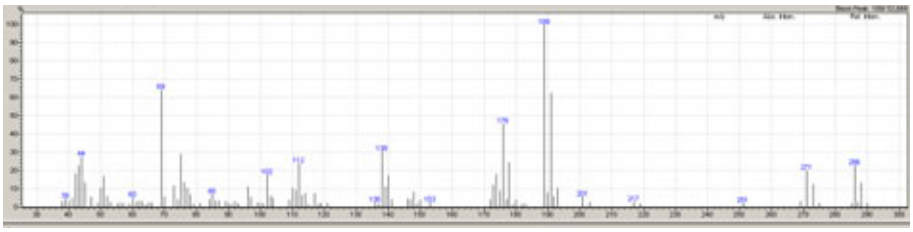

Preparative scale synthesis of 1b

GC analysis of (*S*)-**1b** (Spo-TA) after reaction workup (see Experimental Section)

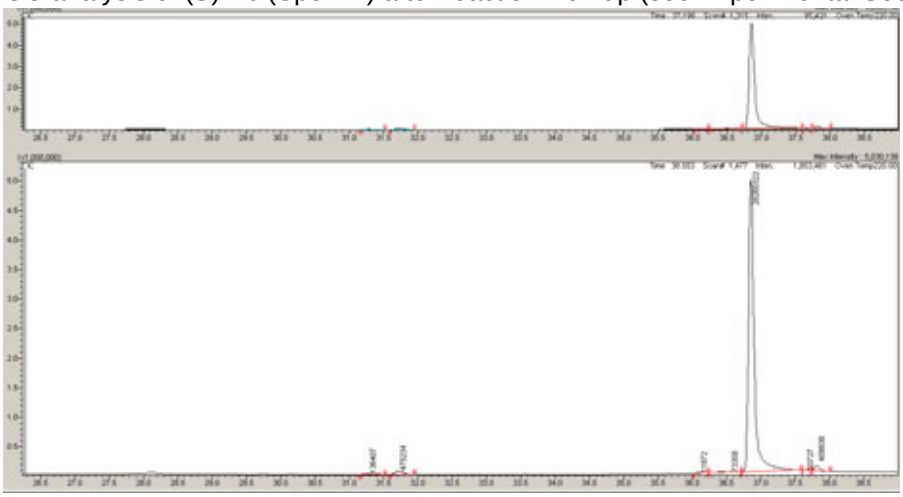

GC analysis of (*R*)-**1b** (Afu-TA) after reaction workup

Comparison of (*S*)-**1b** (blue) and (*R*)-**1b** (red) with the racemic standard (black)

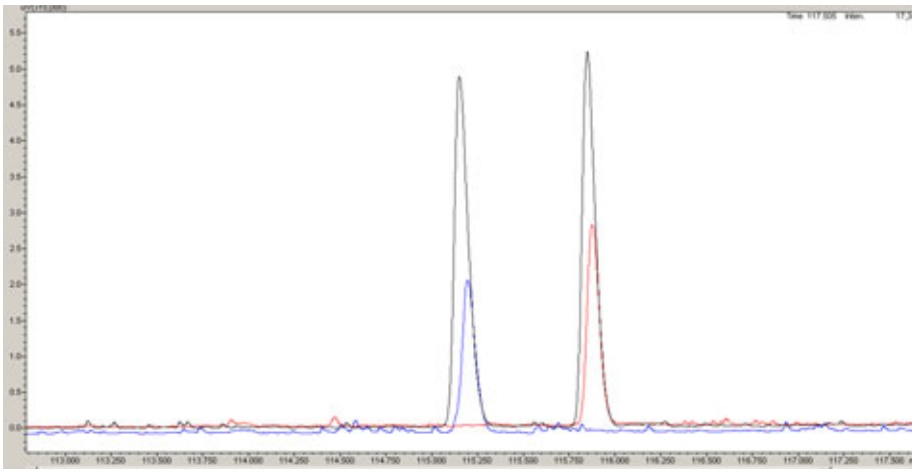

NMR spectra

rac-1-(4-bromophenyl)propan-2-amine

^{1}H-NMR (300 MHz, $CDCl_3$, TMS): δ(ppm) 1.16 (d, *J*=6.54, 3H, -CH_3), 2.52-2.73 (m, 2H, -CH_2-), 3.16 (m, 1H), 5.3 (s, NH_2), 7.07 (d, *J*=8.3, 2H, Ph), 7.43 (d, *J*=8.3, 2H, Ph)

^{13}C-NMR (300 MHz, $CDCl_3$, TMS): δ(ppm) 21.78 (s), 44.1 (s), 48.7 (s), 120.47 (s), 130.98 (s), 131.65 (s), 137.24 (s)

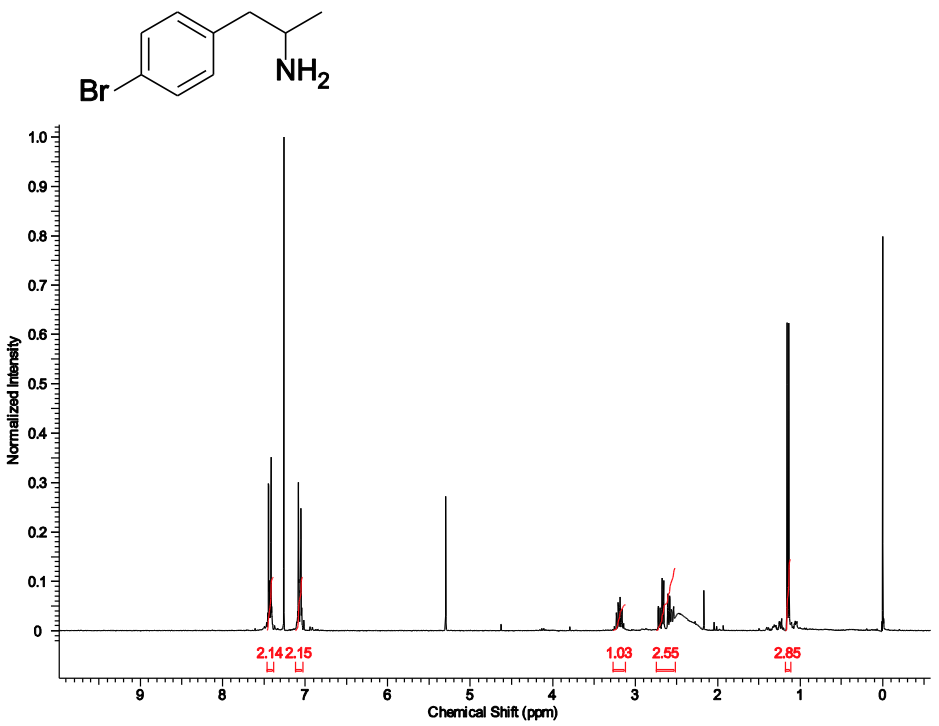

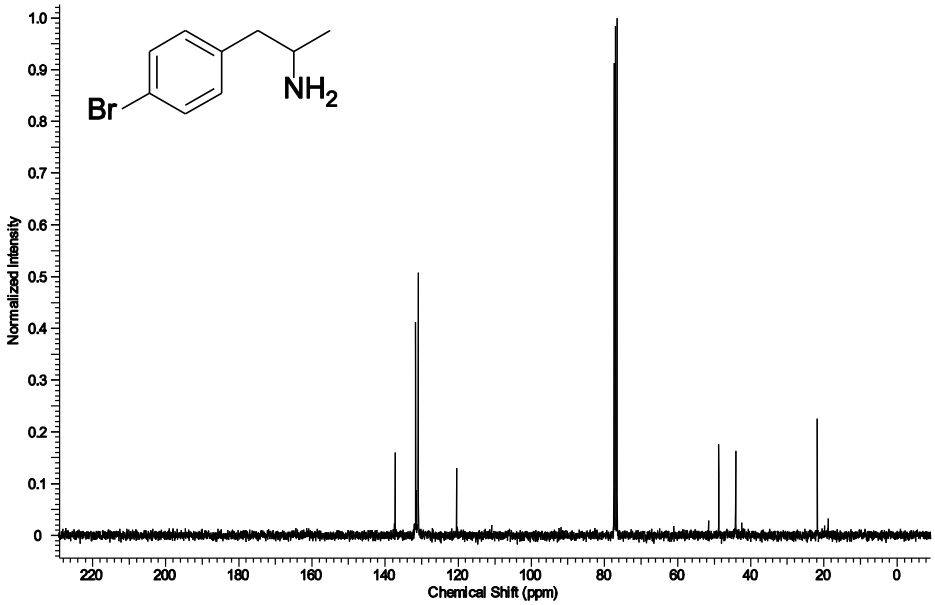

(R)-1-(4-bromophenyl)propan-2-amine

^{1}H-NMR (300 MHz, $CDCl_3$, TMS): δ(ppm) 1.11 (d, *J*=6.3, 3H, -CH_3), 2.43-2.71 (m, 2H, -CH_2-), 3.16 (m, 1H), 7.02-7.1 (dd, *J*=8.3, 1.8, 2H, Ph), 7.38-7.46 (dd, *J*=8.3, 1.89, 2H, Ph)

^{13}C-NMR (300 MHz, $CDCl_3$, TMS): δ(ppm) 23.37 (s), 45.8 (s), 48.3 (s), 120.04 (s), 130.95 (s), 131.44 (s), 138.5 (s)

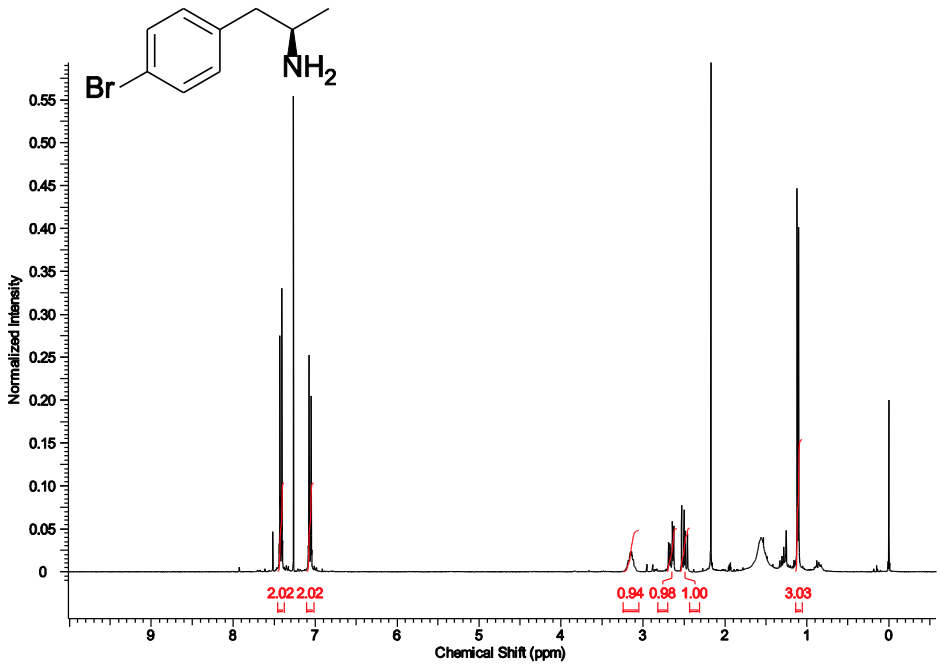

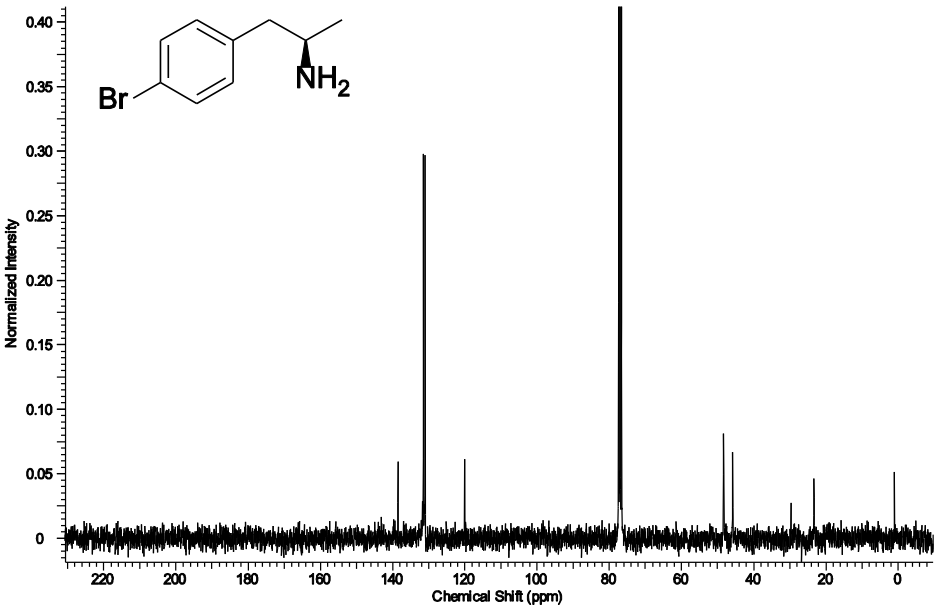

(S)-1-(4-bromophenyl)propan-2-amine

^{1}H-NMR (300 MHz, $CDCl_3$, TMS): δ(ppm) 1.11 (d, *J*=6.2, 3H, -CH_3), 2.44-2.72 (m, 2H, -CH_2-), 3.15 (m, 1H), 7.06 (d, *J*=8.3, 2H, Ph), 7.42 (d, *J*=8.3, 2H, Ph)

^{13}C-NMR (300 MHz, $CDCl_3$, TMS): δ(ppm) 23.24 (s), 45.68 (s), 48.35 (s), 120.07 (s), 130.95 (s), 131.46 (s), 138.42 (s)

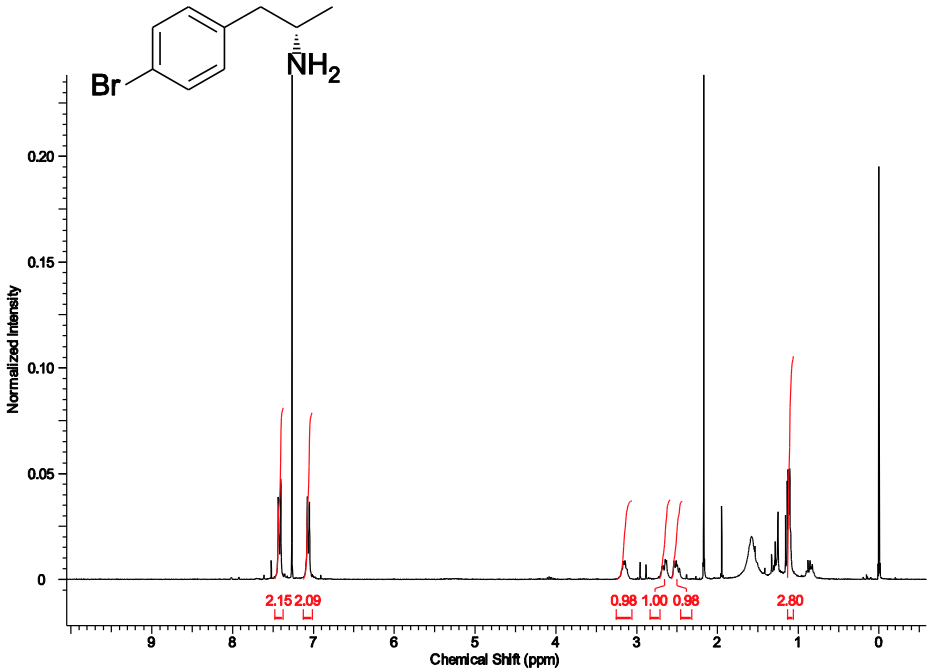

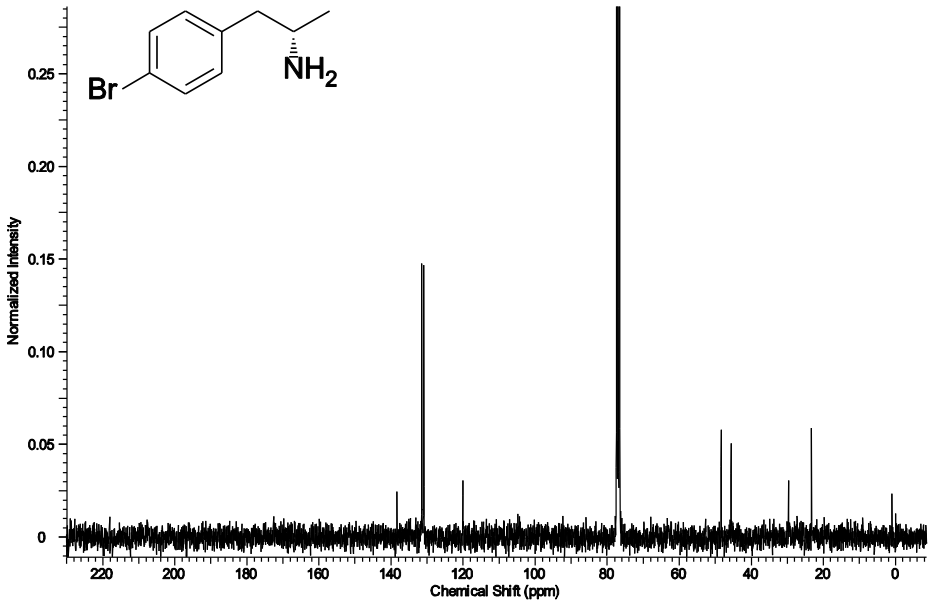

1-(4-bromophenyl)propan-2-one

^{13}C-NMR (300 MHz, $CDCl_3$, TMS): δ(ppm) 29.38 (s), 50.1 (s), 121.1 (s), 131.1 (s), 131.78 (s), 133.04 (s), 205.53 (s)

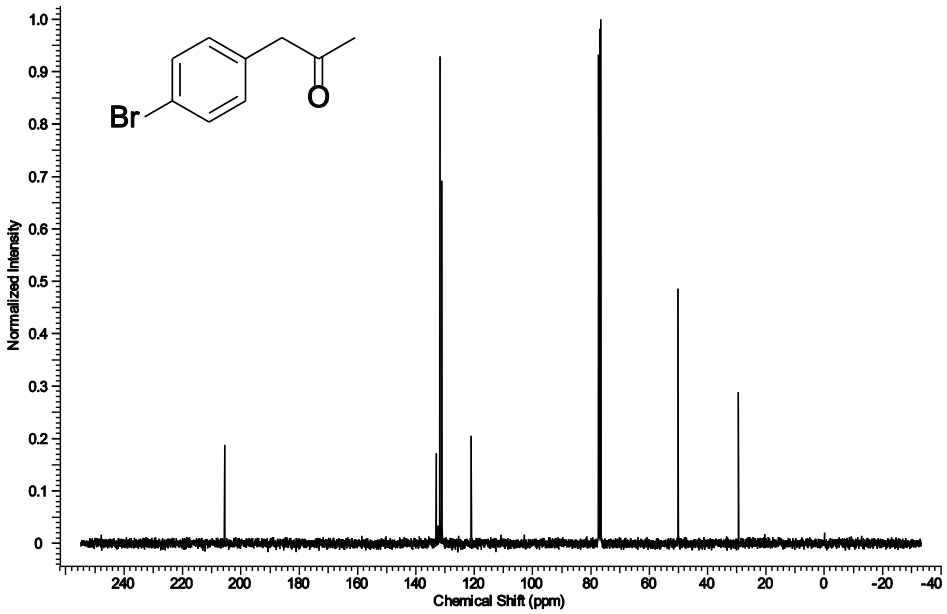

BLAST® » blastp suite » RID-T5AMD1ZW014

BLAST Results

Job title: 2 sequences (3HMU:A|PDBID|CHAIN|SEQUENCE)

RID T5AMD1ZW014 (Expires on 08-16 16:02 pm)

Query ID lcl|Query_290752 **Database Name** pdb

Description 3HMU:A|PDBID|CHAIN|SEQUENCE **Description** PDB protein database

Molecule type amino acid **Program** BLASTP 2.6.1+

Query Length 472

New Analyze your query with SmartBLAST

Graphic Summary

Distribution of the top 93 Blast Hits on 93 subject sequences

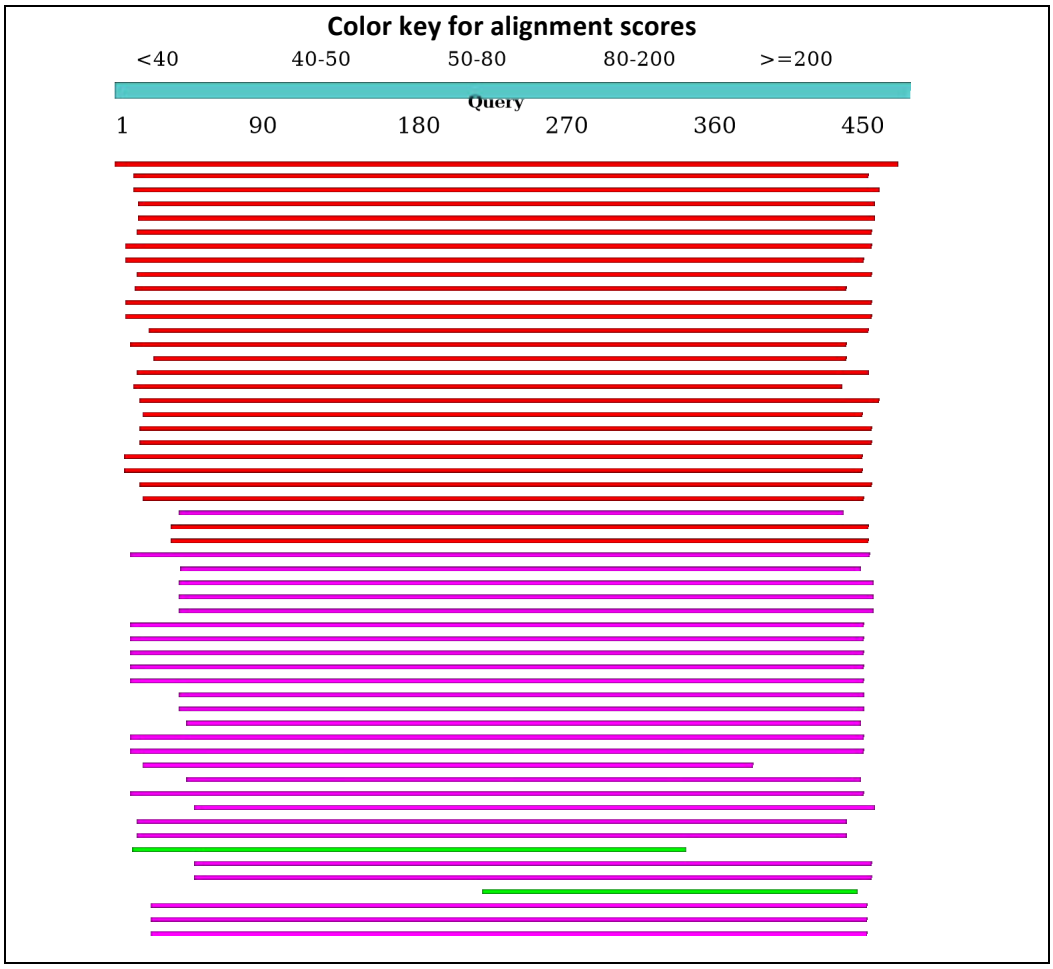

Description	Max score	Total score	Query cover	E value	Ident	Accession
Chain A, Crystal Structure Of A Class Iii Aminotransferase From Silicibacter Pomeroyi	976	976	100%	0.0	100%	3 HMU_A
Chain A, Crystal Structure Of An Aspartate Aminotransferase From Pseudomonas	556	556	93%	0.0	60%	5 TI8_A
Chain A, Crystal Structure Of The Omega Transaminase From Chromobacterium Violaceum In The Apo Form, Crystallised From Polyacrylic Acid	489	489	95%	8e-171	53%	**4 A6R_A**
Chain A, Transaminase With L-ala	356	356	94%	7e-119	42%	5 GHF_A
Chain A, Transaminase W58l With Smba	353	353	94%	2e-117	42%	5 GHG_A
Chain A, Directed Evolution Of Transaminases By Ancestral Reconstruction. Using Old Proteins For New Chemistries	335	335	93%	2e-110	41%	5 KQW_A
Chain A, Directed Evolution Of Transaminases By Ancestral Reconstruction. Using Old Proteins For New Chemistries	350	350	95%	2e-116	41%	5 KR6_A
Chain A, Directed Evolution Of Transaminases By Ancestral Reconstruction. Using Old Proteins For New Chemistries	329	329	94%	4e-108	41%	5 KR5_A
Chain A, Directed Evolution Of Transaminases By Ancestral Reconstruction. Using Old Proteins For New Chemistries	331	331	93%	1e-108	41%	5 KQU_A
Chain A, Directed Evolution Of Transaminases By Ancestral Reconstruction. Using Old Proteins For New Chemistries	315	315	90%	1e-102	41%	5 KQT_A
Chain A, Directed Evolution Of Transaminases By Ancestral Reconstruction. Using Old Proteins For New Chemistries	325	325	95%	1e-106	41%	5 KR3_A
Chain A, Directed Evolution Of Transaminases By Ancestral Reconstruction. Using Old Proteins For New Chemistries	321	321	95%	7e-105	40%	5 KR4_A
Chain A, Crystal Structure Of Aminotransferase Prk07036 From Rhodobacter Sphaeroides Kd131	306	306	91%	5e-99	39%	3 I5T_A
Chain A, Crystal Structure Of Putative Aminotransferase (Yp_614685.1) From Silicibacter Sp. Tm1040 At 1.80 A Resolution	297	297	91%	7e-96	39%	3 FCR_A
Chain A, Amine Transaminase Crystal Structure From An Uncultivated Pseudomonas Species In The Plp-bound (internal Aldimine) Form	282	282	88%	6e-90	37%	5 LH9_A
Chain A, Crystal Structure Of A Putative Aminotransferase (Mll7127) From Mesorhizobium Loti Maff303099 At 1.55 A Resolution	274	274	93%	7e-87	37%	3 GJU_A
Chain A, Crystals Structure Of A Bacillus Anthracis Aminotransferase	254	254	90%	4e-79	36%	3 N5M_A
Chain A, Crystal Structure Of OmegaTransferase From Vibrio Fluvialis Js17	284	284	94%	1e-90	36%	3 NUI_A
Chain A, The Structure Of The Omega						

Description	Max score	Total score	Query cover	E value	Ident	Accession
Aminotransferase From Pseudomonas Aeruginosa	267	267	91%	2e-84	35%	4 B98_A
Chain A, Pmp-Bound Form Of Aminotransferase Crystal Structure From Vibrio Fluvialis	273	273	93%	2e-86	35%	4 E3Q_A
Chain A, Structure Of An Omega-aminotransferase From Paracoccus Denitrificans	274	274	93%	6e-87	35%	4 GRX_A
Chain A, Characterization Of A Novel Transaminase From Pseudomonas Sp. Strain Aac	257	257	94%	2e-80	35%	4 UHM_A
Chain A, Characterization Of A Novel Transaminase From Pseudomonas Sp. Strain Aac	257	257	94%	3e-80	35%	4 UHN_A
Chain A, Plp-Bound Aminotransferase Mutant Crystal Structure From Vibrio Fluvialis	270	270	93%	4e-85	34%	4 E3R_A
Chain X, Crystal Structure Of OmegaAmino Acid:pyruvate Aminotransferase	242	242	91%	8e-75	34%	3 A8U_X
Chain A, Crystal Structure Of Aminotransferase, Class Iii From Deinococcus Radiodurans	174	174	84%	4e-49	32%	3 I4J_A
Chain A, Crystal Structure Of 7-Keto-8Aminopelargonic Acid Bound 7,8Diaminopelargonic Acid Synthase In Bacillus Subtilis	224	224	88%	6e-68	31%	3 DU4_A
Chain A, Crystal Structure Of Plp Bound 7,8-diaminopelargonic Acid Synthase In Bacillus Subtilis	223	223	88%	1e-67	31%	3 DOD_A
Chain A, Crystal Structure Of Bioa / 7,8-diaminopelargonic Acid Aminotransferase / Dapa Synthase From Citrobacter Rodentium, Plp Complex	168	168	94%	6e-47	31%	5 UC7_A
Chain A, Crystal Structure Of Acetylornithine Aminotransferase From Aquifex Aeolicus Vf5	157	157	86%	4e-43	30%	2 EH6_A
Chain A, Structure Of Amino Acid Racemase, 2.65 A	168	168	88%	1e-46	30%	5 WYA_A
Chain A, Structure Of Amino Acid Racemase, 2.12 A	168	168	88%	1e-46	30%	5 WYF_A
Chain A, Structure Of Isoleucine 2-epimerase From Lactobacillus Buchneri (apo Form)	168	168	88%	2e-46	30%	5 LL2_A
Chain A, Crystal Structure Of 7,8-diaminopelargonic Acid Synthase In Complex With 7-keto-8-aminopelargonic Acid	167	167	93%	9e-47	30%	1 QJ3_A
Chain A, Crystal Structure Of The Y17f Mutant Of 7,8- Diaminopelargonic Acid Synthase	167	167	93%	2e-46	30%	1 S0A_A
Chain A, Crystal Structure Of The D147n Mutant Of 7,8- Diaminopelargonic Acid Synthase	166	166	93%	5e-46	29%	1 S08_A
Chain A, Crystal Structure Of The R391a Mutant Of 7,8-Diaminopelargonic Acid Synthase	165	165	93%	1e-45	29%	1 MGV_A
Chain A, Crystal Structure Of The R253a						

Mutant Of 7,8-Diaminopelargonic Acid Synthase	165	165	93%	1e-45	29%	1 S07_A
Chain A, Structure Of Plasmodium Falciparum Ornithine Deltaaminotransferase	171	171	87%	4e-48	29%	3 LG0_A
Chain A, Ornithine Aminotransferase Py00104 From Plasmodium Yoelii	162	162	87%	8e-45	29%	1 Z7D_A
Chain A, Crystal Structure Of Acetylornithine Aminotransferase From Thermotoga Maritima	154	154	86%	6e-42	29%	2 E54_A

Description	Max score	Total score	Query cover	E value	Ident	Accession
Chain A, Crystal Structure Of The R253k Mutant Of 7,8- Diaminopelargonic Acid Synthase	164	164	93%	2e-45	29%	1 S06_A
Chain A, Crystal Structure Of The Y144f Mutant Of 7,8- Diaminopelargonic Acid Synthase	164	164	93%	2e-45	29%	1 S09_A
Chain A, Crystal Structure Of Pige: A Transaminase Involved In The Biosynthesis Of 2-methyl-3-n-amylpyrrole (map) From Serratia Sp. Fs14	139	139	77%	9e-35	29%	4 PPM_A
Chain A, Crystal Structure Of Acetylornithine Aminotransferase (Ec 2.6.1.11) (Acoat) (Tm1785) From Thermotoga Maritima At 1.40 A Resolution	147	147	86%	2e-39	29%	2 ORD_A
Chain A, Crystal Structure Of Adenosylmethionine-8-Amino7- Oxonanoate Aminotransferase With Pyridoxal Phosphate Cofactor	163	163	93%	5e-45	29%	1 DTY_A
Chain A, Crystal Structure Of Ygjg In Complex With Pyridoxal-5'-phosphate And Putrescine	166	166	86%	1e-45	29%	4 UOX_A
Chain A, Crystal Structure Of 7,8-diaminopelargonic Acid Synthase (bioa) From Mycobacterium Tuberculosis, Complexed With A Thiazole Inhibitor	160	160	90%	4e-44	29%	4 W1V_A
Chain A, Crystal Structure Of 7,8diaminopelargonic Acid Synthase (bioa) From Mycobacterium Tuberculosis, Complexed With 7-(diethylamino)-3(thiophene-2-carbonyl)-2h-chromen-2one	160	160	90%	4e-44	29%	4 W1W_A
Chain A, Crystal Structure Of Glutamate-1-Semialdehyde 2,1-Aminomutase From Thermus Thermophilus Hb8	76.3	76.3	70%	1e-14	29%	2 E7U_A
Chain A, Crystal Structure Of The Ygjgprotein A-zpa963-calmodulin Complex	164	164	86%	7e-45	28%	5 H7D_A
Chain A, Crystal Structure Of The Ygjgprotein A-zpa963-pka Catalytic Domain	164	164	86%	8e-45	28%	5 X3F_A
Chain A, Crystal Structure Of Aminotransferase Crmg From Actinoalloteichus Sp. Wh1-2216-6 In Complex With Plp	74.7	74.7	47%	6e-14	28%	5 DDS_A
Chain A, The Structure Of Gamma-Aminobutyrate Aminotransferase Mutant: E211s	141	141	91%	5e-37	28%	1 SZK_A
Chain A, Structure Of E. Coli GammaAminobutyrate Aminotransferase	140	140	91%	1e-36	28%	1 SF2_A
Chain A, The Structure Of Gamma-						

aminobutyrate Aminotransferase Mutant: I50q	139	139	91%	4e-36	28%	1 SZS_A
Chain A, Crystal Structure Of 7,8Diaminopelargonic Acid Synthase (Bioa) From Mycobacterium Tuberculosis, Pre-Reaction Complex With A 3,6-Dihydropyrid-2-One Heterocycle Inhibitor	162	162	93%	2e-44	28%	3 TFT_A
Chain A, The Structure Of Gamma-Aminobutyrate Aminotransferase Mutant: V241a	138	138	91%	5e-36	28%	1 SZU_A
Chain A, Crystal Structure Of Plp Bound 7,8-Diaminopelargonic Acid Synthase In Mycobacterium Tuberculosis	159	159	93%	1e-43	28%	3 BV0_A
Chain A, Crystal Structure Of 4-aminobutyrate Transaminase From Mycobacterium Smegmatis	119	119	66%	5e-29	28%	3 OKS_A

Description	Max score	Total score	Query cover	E value	Ident	Accession
Chain A, Crystal Structure Of Mycobacterium Tuberculosis 7,8-Diaminopelargonic Acid Synthase In Complex With Substrate Analog Sinefungin	159	159	93%	3e-43	28%	3 LV2_A
Chain A, Crystal Structure Of 4-Aminobutyrate Aminotransferase From Sulfolobus Tokodaii Strain7	145	145	86%	1e-38	28%	2 EO5_A
Chain A, Structure Of Gaba-Transaminase A1r958 From Arthrobacter Aurescens In Complex With Plp	92.8	92.8	54%	6e-20	28%	4 ATP_A
Chain A, The Crystal Structure Of A S-selective Transaminase From Bacillus Megaterium Bound With R-alphamethylbenzylamine	147	147	94%	9e-39	28%	5 G09_A
Chain A, Crystal Structure Of Acetylornithine Aminotransferase (Argd) From Campylobacter Jejuni	136	136	86%	2e-35	27%	3 NX3_A
Chain A, The Crystal Structure Of A S-selective Transaminase From Arthrobacter Sp	144	144	94%	1e-37	27%	5 G2P_A
Chain A, Acetylornithine Aminotransferase From Thermus Thermophilus Hb8	124	124	86%	3e-31	27%	1 VEF_A
Chain A, Structural And Functional Study Of Succinyl-ornithine Transaminase From E. Coli	145	145	84%	1e-38	27%	4 ADB_A
Chain A, Crystal Structure Of A Putative Ornithine Aminotransferase From Toxoplasma Gondii Me49 In Complex With Pyrodoxal-5'-phosphate	115	115	88%	1e-27	27%	4 NOG_A
Chain A, Crystal Structure Of The Ornithine Aminotransferase From Toxoplasma Gondii Me49 In A Complex With The Schiff Base Between Plp And Lys286	115	115	88%	2e-27	27%	4 ZLV_A
Chain A, Crystal Structure Of A 4-aminobutyrate Aminotransferase (gabt) From Mycobacterium Abscessus	96.3	96.3	84%	4e-21	27%	4 FFC_A
Chain A, Alpha-amino Epsilon-						

caprolactam Racemase D210a Mutant In Complex With Plp And Geminal Diamine Intermediate	114	114	87%	2e-27	27%	5 M4B_A
Chain A, E198a Mutant Of N-acetylornithine Aminotransferase From Salmonella Typhimurium	145	145	87%	1e-38	26%	4 JEY_A
Chain A, Y21k Mutant Of N-acetylornithine Aminotransferase Complexed With L- Canaline Chain A, N-acetylornithine	143	143	87%	7e-38	26%	4 JEX_A
Aminotransferase From S. Typhimurium Complexed With Gabaculine	144	144	87%	4e-38	26%	4 JEV_A
Chain A, R144q Mutant Of N-acetylornithine Aminotransferase	144	144	87%	5e-38	26%	4 JF1_A
Chain A, N-acetylornithine Aminotransferase From S. Typhimurium Complexed With L-canaline	144	144	87%	6e-38	26%	4 JEW_A
Chain A, N79r Mutant Of N-acetylornithine Aminotransferase Complexed With L- Canaline	143	143	87%	9e-38	26%	4 JEZ_A
Chain A, Structure Of Biosynthetic N-Acetylornithine Aminotransferase From Salmonella Typhimurium: Studies On Substrate Specificity And Inhibitor Binding	143	143	87%	1e-37	26%	2 PB0_A
Chain A, N79r Mutant Of N-acetylornithine Aminotransferase	141	141	87%	6e-37	26%	4 JF0_A

Description	Max score	Total score	Query cover	E value	Ident	Accession
Chain A, Ornithine Aminotransferase Mutant Y85i	123	123	90%	1e-30	26%	2 BYJ_A
Chain A, Human Ornithine Aminotransferase Complexed With L-Canaline	122	122	90%	2e-30	26%	2 CAN_A
Chain A, Ornithine Aminotransferase	122	122	90%	3e-30	26%	1 OAT_A
Chain A, Crystal Structure Of 4- aminobutyrate Aminotransferase Gabt From Mycobacterium Marinum Covalently Bound To Pyridoxal Phosphate	117	117	84%	2e-28	26%	3 R4T_A
Chain A, Structure Of Ornithine Aminotransferase Triple Mutant Y85i Y55a G320f	119	119	90%	3e-29	26%	2 BYL_A
Chain A, Crystal Structure Of 4-aminobutyrate Transaminase From Mycobacterium Smegmatis	94.4	94.4	73%	2e-20	25%	3 Q8N_A
Chain A, Crystal Structure Of The Ornithine-Oxo Acid Transaminase Rocd From Bacillus Anthracis	122	122	92%	2e-30	25%	3 RUY_A
Chain A, Crystal Structure Of Acetylornithine Aminotransferase From Elizabethkingia Anophelis	126	126	92%	9e-32	25%	5 VIU_A
Chain A, E243 Mutant Of M. Tuberculosis Rv3290c	77.8	77.8	86%	4e-15	24%	2 JJH_A
Chain A, N328a Mutant Of M. Tuberculosis Rv3290c	76.3	76.3	86%	1e-14	24%	2 JJF_A
Chain A, Lysine Aminotransferase From M. Tuberculosis In The Internal Aldimine Form	76.3	76.3	86%	2e-14	24%	2 CIN_A
Chain A, Crystal Structure Of D-Phenylglycine Aminotransferase (DPhgat) From Pseudomonas Strutzeri St-201	57.0	57.0	53%	2e-08	24%	2 CY8_A

Chain A, Crystal Structure Of T330s Mutant Of Rv3290c From M. Tuberculosis	74.7	74.7	86%	4e-14	24%	2 JJE_A

References

[1] F. Steffen-Munsberg, C. Vickers, A. Thontowi, S. Schätzle, T. Tumlirsch, M. Svedendahl Humble, H. Land, P. Berglund, U. T. Bornscheuer, M. Höhne, *ChemCatChem* **2013**, *5*, 150–153.

[2] M. Thomsen, L. Skalden, G. J. Palm, M. Höhne, U. T. Bornscheuer, W. Hinrichs, *Acta Crystallogr. D Biol. Crystallogr.* **2014**, *70*, 1086–1093.

[3] M. S. Humble, K. E. Cassimjee, M. Haakansson, Y. R. Kimbung, B. Walse, V. Abedi, H.-J. Federsel, P. Berglund, D. T. Logan, *FEBS J.* **2012**, *279*, 779–792.

[4] A. Nobili, F. Steffen-Munsberg, H. Kohls, I. Trentin, C. Schulzke, M. Höhne, U. T. Bornscheuer, *ChemCatChem* **2015**, *7*, 757–760.

[5] A. Gomm, W. Lewis, A. P. Green, E. O'Reilly, *Chem.- Eur. J.* **2016**, *22*, 12692–12695.

[6] M. Davies, *Analyst* **1959**, *84*, 248–251.

Article II

ChemPubSoc Europe

DOI: 10.1002/cctc.201800936

CHEMCATCHEM Communications

Isopropylamine as Amine Donor in Transaminase-Catalyzed Reactions: Better Acceptance through Reaction and Enzyme Engineering

Ayad W. H. Dawood,[a] Martin S. Weiß,[a] Christian Schulz,[a] Ioannis V. Pavlidis,[a, b] Hans Iding,[c] Rodrigo O. M. A. de Souza,[d] and Uwe T. Bornscheuer*[a]

Amine transaminases (ATA) have now become frequently used biocatalysts in chemo-enzymatic syntheses including industrial applications. They catalyze the transfer of an amine group from a donor to an acceptor leading to an amine product with high enantiopurity. Hence, they represent an environmentally benign alternative for waste intensive chemical amine synthesis. Isopropylamine (IPA) is probably one of the most favored amine donors since it is cheap and achiral, but nevertheless there is no consistency in literature concerning reaction conditions when IPA is best to be used. At the same time there is still a poor understanding which structural properties in ATA are responsible for IPA acceptance. Herein, we demonstrate, on the basis of the 3FCR enzyme scaffold, a substantial improvement in catalytic activity towards IPA as the amine donor. The asymmetric synthesis of industrial relevant amines was used as model reaction. A systematic investigation of the pH-value as well as concentration effects using common benchmark substrates and several ATA indicates the necessity of a substrate- and ATA-dependent reaction engineering.

Transaminases are versatile and widely used biocatalysts for the production of chiral amines. They catalyze the transfer of an amine group from an amine donor to a ketone or aldehyde acceptor, following a Ping-Pong Bi-Bi-reaction mechanism utilizing pyridoxal-5′-phosphate (PLP) as cofactor, revealing the amine product in a high enantiopurity. Transaminases belong to the fold types I and IV of PLP-dependent enzymes and are additionally divided into six subclasses, depending on the natural substrate and especially the position of the transferred amine group and/or carboxyl moiety.[1,2] Amine transaminases (ATA), a subgroup of ω-transaminases (ω-TA, class III transaminase family), are of special interest for the chemo-enzymatic application. In contrast to ω-TA, which accept carbonylic substrates with a distal carboxylate group, ATA tolerate substrates without a carboxyl moiety and therefore a wide range of ketones and aldehydes. Hence, in the last decade ATA became very attractive targets for enzyme engineering[3–13] representing an environmentally benign alternative for the chemical transition metal-catalyzed amine synthesis in pharmaceutical and agrochemical industries.[14] For instance, the production of imagabaline,[10] (*S*)-rivastigmine[15,16] or (*S*)-ivabradine[17] has been realized on larger scale using ATA. Certainly, one of the most notable examples is the manufacturing of (*R*)-sitagliptin in >200 g/L scale after several rounds of protein engineering of the selected ATA.[3] In this specific example, enzyme engineering resulted not only in a better substrate acceptance or higher temperature and solvent stability, but also in an enhanced isopropylamine (IPA) acceptance. The best variant contained 27 mutations. To have the enzyme accepting the bulky prositagliptin ketone, the most mutations were around the active site region. However, to ensure acceptance/tolerance of IPA many mutations were globally distributed over the entire protein since the majority of wild-type ATA do not accept it well as the amine donor. More recently, we could also design (*S*)-selective ATA for the asymmetric synthesis of chiral amines from sterically demanding bulky ketones.[6,13,18]

The asymmetric synthesis is the most convenient and economically favored route to a target chiral amine. In contrast to the kinetic resolution mode, the asymmetric synthesis starts from the prochiral ketone and results in the desired chiral product with a theoretical yield of 100%.[19–21] The downside of this strategy is a very often unfavorable reaction equilibrium, which makes strategies for equilibrium shifting necessary. Therefore several equilibrium displacement techniques were established, for instance involving enzymatic cascades in order to remove co-products,[19,22–26] utilization of 'smart-donors' which are converted into sacrificial co-substrates after transamination[27–32] or application of the amine donor in large excess.[33] In fact, IPA is the industrially favored amine donor for asymmetric syntheses since it is cheap, achiral – so the enantioselectivity of the ATA has not to be considered – and the by-product acetone is supposed to have a drastic lower reactivity in the back reaction.[33] Additionally, in terms of shifting the equilibrium, acetone can be easily removed from the reaction solution.[3] In general, it was reported in many cases that an excess of IPA needs to be applied to drive the

[a] *A. W. H. Dawood, M. S. Weiß, C. Schulz, I. V. Pavlidis, U. T. Bornscheuer*
Department of Biotechnology & Enzyme Catalysis, Institute of Biochemistry, Greifswald University, Felix-Hausdorff-Str. 4, Greifswald 17487 (Germany)
E-mail: uwe.bornscheuer@uni-greifswald.de
Homepage: http://biotech.uni-greifswald.de
[b] *I. V. Pavlidis*
Department of Chemistry, University of Crete, Voutes University Campus, Heraklion 70013 (Greece)
[c] *H. Iding*
Process Chemistry and Catalysis, Biocatalysis, F. Hoffmann–La Roche Ltd., Grenzacher Strasse 124, Basel 4070 (Switzerland)
[d] *R. O. M. A. de Souza*
Biocatalysis and Organic Synthesis Group, Institute of Chemistry, Federal University of Rio de Janeiro (Brazil)

Supporting information for this article is available on the WWW under https://doi.org/10.1002/cctc.201800936

transamination of various substrates to the desired product side[8,13,18,23,34–44] when enzyme engineering did not lead to a better IPA acceptance, as mentioned above. In particular, different reaction conditions were reported such as varying donor-acceptor-ratios from 1.5-fold[39] over 40-fold[38] to 200-fold[8] and a pH range from 7.3[41] to 9.5.[45]

So far, there has been no study, in which the influence of IPA on transaminase activity has been explored to cover both aspects, the acceptance of IPA as amine donor (requiring identification of optimal pH values, concentration dependency as well as mutations in the active site region) and the influence of IPA to the overall protein stability as this amine donor also has solvent effects on the enzyme. In this work, crucial amino acid residues around the active site were identified for IPA acceptance and also a systematic investigation was performed for a range of ATA, different ketone substrates and different reaction conditions with the aim of providing a more generic solution for ATA-catalyzed asymmetric synthesis using IPA.

Recently, we reported the engineering of the ATA from *Ruegeria* sp. TM1040 (PDB-ID: 3FCR) for the acceptance of bulky ketones where the corresponding amines have pharmaceutical relevance.[6,13,18] The best variants from this approach (e.g. one quadruple mutant, 3FCR-Y59W-Y87F-Y152F-T231A, 3FCR-QM) did not accept IPA well as the amine donor.[13,18] We already identified position 59 in 3FCR (according to Protein Data Bank numbering) as very crucial for the activity towards aromatic and bulky substrates.[6,46] Interestingly, the homolog position in the ω-TA from *Ochrobactrum anthropoi* (OATA, W58) was reported to play a comparable role in which the mutation OATA-W58L led to a better acceptance of aromatic ketones and amines.[12] However, at the same time this mutation was obviously responsible for a higher affinity towards IPA, which was proven by lower K_M values and explained by steric interference of W58 with one of the methyl groups of IPA. Because of the notable sequence identity between OATA (PDB-ID 5GHG) and 3FCR of approx. 43% we decided to focus again on position 59 in the 3FCR scaffold. Starting from the variant 3FCR-QM as template we saturated position 59 and screened the NNK library against IPA using the glycine oxidase (GO) assay, as described previously.[47] It turned out that the only variant with significant higher activity towards IPA as amine donor contained the mutation 3FCR-QM-W59L which led to a 4.6-fold higher activity compared to the template (see Table S1, Supporting Information, SI). Moreover, transaminases are remarkable for their dual substrate recognition facilitated by a flexible arginine residue, which is forming a salt bridge to the carboxylate function of the respective substrate. It is highly conserved in e.g. amino acid transaminases, ornithine transaminases and amine transaminases.[1,46] Notably, the ω-amino acid transaminase from *Bacillus anthracis* (Ban-TA) represents an exception as the 'flipping arginine' is naturally replaced by a glycine, which means that no movement of an amino acid residue is required for substrate recognition. Ban-TA showed provable activity towards propylamines (e.g. IPA) as amine donors.[48] However, when the choice of substrates make the coordination of acidic moieties obsolete, the role of the 'flipping arginine' (position 420 in 3FCR) is questionable and in addition a strong positive charge at the entrance of the active site tunnel was considered to be detrimental for the accessibility of IPA on the PLP molecule. We used 3FCR-QM as template and introduced at position 420 several amino acids with different characteristics (hydrophobic, basic and acidic). The variants were interrogated in our chosen asymmetric synthesis model reactions (Scheme 1), because the GO-assay demands coordination of glyoxylate and therefore was not suitable for the purpose of a screening. The best-performing variant was the mutation R420W (Table S2, SI), which we later introduced into the 3FCR-QM-W59L variant. Additionally, we produced the variant 3FCR-QM-W59L-R420A in order to provide an amino acid residue at this position, which causes more space and low interference at the entrance of the active site tunnel. Both variants were compared in the mentioned model reactions with IPA revealing a drastic improvement in conversion of **1a** and **2a** compared to 3FCR-QM and 3FCR-QM-W59L (Table 1), especially in case of 3FCR-QM-W59L-R420W. Remarkably, the mutation at position 59 in 3FCR-QM – which showed a significant improvement in the GO-assay with IPA – did not lead to a better conversion of **1a** to **1b** but at the same time a detectable product formation of **2b**. These results (especially for 3FCR-QM-W59L-R420W) are more meaningful when the activities in kinetic resolution mode using *rac*-**1b** and *rac*-**2b** are considered.

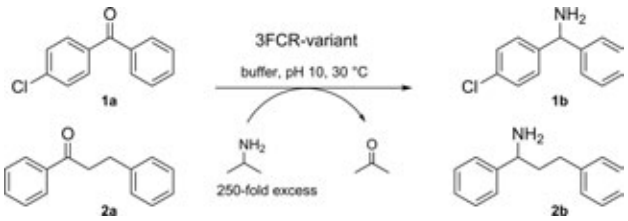

Scheme 1. Model reactions and preparative scale reactions with IPA as amine donor using substrates as reported in literature.[6]

All three variants of 3FCR-QM showed lower activities for both racemic amines (Table 1). For comparison, pentanal was used as amine acceptor for all four enzymes because pyruvate was not a suitable amine acceptor anymore mainly due to the lack of the 'flipping arginine' (details in Figure S1 in the Supporting Information).[49] These results are demonstrating that the introduced mutations in 3FCR-QM were not responsible for a better substrate acceptance of **1a** and **2a** – since mutations at position 59 have a great impact on the reactivity towards bulky substrates in 3FCR – but rather they did lead to a higher catalytic activity in asymmetric synthesis mode with IPA as the amine donor. The best two variants 3FCR-QM-W59L-R420A/W were subjected to the preparative scale production of amines **1b** and **2b** in a 80 mg scale applying 0.5 M IPA (see experimental section). The identity of the products was confirmed via GC-MS, ^{1}H- and ^{13}C-NMR spectroscopy (see SI).

Next, we investigated the influence of reaction conditions on the transaminase reactivity with IPA as amine donor. For that we included our presented variants of 3FCR-QM and additionally several commonly known wild-type ATA, which in pre-tests showed significant conversion with IPA. Those wild-

Table 1. Comparison of the presented variants of 3FCR regarding initial activity measurements with racemic **1b** or **2b** and asymmetric synthesis of **1b** or **2b** using IPA as the amine donor. * n.d.: not detectable.

ATA variant	Specific activity [mU mg^{-1}][a]		Substrate conversion [%][b]			
	rac-1b	*rac*-2b	1a	ee_P [%][c]	2a	ee_P [%][c]
3FCR-QM	218.6 ± 16.8	104.9 ± 1.6	12.8 ± 1.2	> 99 (*R*)	n.d.*	–
3FCR-QM-W59L	88.1 ± 4.2	70.3 ± 1.5	6.8 ± 1.5	86 (*R*)	8.9 ± 1.8	> 99 (*S*)
3FCR-QM-W59L-R420A	141.2 ± 1.6	63.5 ± 0.6	50.6 ± 3.6	91 (*R*)	23.8 ± 2.5	> 99 (*S*)
3FCR-QM-W59L-R420W	70.9 ± 0.7	90.9 ± 4.3	83.5 ± 4.0	80 (*R*)	85.8 ± 3.5	> 99 (*S*)

[a] Assay conditions for the kinetic resolution: 0.5 mM *rac*-**1b** or 0.25 mM *rac*-**2b**, pentanal in equimolar ratio, 10% (v/v) DMSO, CHES pH 10 (50 mM), 0.045–0.07 mg mL^{-1} purified enzyme, 30 °C. [b] Assay conditions for the asymmetric synthesis: 2 mM ketone (**1a** or **2a**), 0.5 M IPA, 30% (v/v) DMSO, CHES buffer pH 10 (50 mM), 0.1 mM PLP, 0.89–1.2 mg mL^{-1} purified enzyme (substrate to enzyme ratio, s/e ~ 0.35–0.47 w/w), 30 °C. Conversion was determined after 20 h via gas chromatography (GC) with 2-iodoacetophenone as internal standard for the quantification of amine product formation. Samples were taken in triplicate from three parallel reactions. [c] The enantiomeric excess was determined via chiral GC analysis using a Hydrodex-ß-TBDAc column (Macherey & Nagel).

type ATA were utilized in engineering and asymmetric synthesis approaches before.[4–6,21,26,46,49–53] For instance, Afu-TA (ATA from *Aspergillus fumigatus*) and Spo-TA (ATA from *Silicibacter pomeroyi*) were recently used for the production of halogenated chiral amines[54] and Arth-TA (ATA from *Arthrobacter* sp.) for the synthesis of e.g. (*R*)-3,4-dimethoxy-amphetamine.[20,21] 3FCR wild-type and 3FCR-QM were excluded from these experiments due to their low reactivity in pre-tests. We selected commonly used aromatic benchmark substrates for the evaluation of amine donors[26,31,32,38] (**3a** and **4a**, Scheme 2) and tested different pH values as well as donor-acceptor ratio (Figure 1). The amination of acetophenone **3a** to 1-phenylethylamine **3b** is challenging due to the unfavorable equilibrium,[14,55] so significant effects were expected after reaction engineering. Additionally, we investigated one halogenated derivative of acetophenone (**4a**), since Cassimjee *et al.*[26] show-cased significant differences in conversion with substituted acetophenones and IPA using the ATA from *Chromobacterium violaceum* (Cvi-TA). The donor-acceptor ratio varied in a range of 5 – 100-fold excess of IPA at the respective pH optimum of the ATA (see Figure S2 (SI) for all ATA).

In case of acetophenone **3a** the gradual increase of the IPA concentration resulted in an increased conversion of **3a**. The only exception out of all investigated ATA was Cvi-TA showing a decreased conversion level of **3a** at high IPA concentrations. For 2′-bromoacetophenone **4a** no general statement in terms of IPA excess effect could be made. While the results for Arth-TA showed an increased activity at higher IPA concentrations, Spo-TA and Cvi-TA were apparently less active the more IPA was applied. But for the rest of the investigated ATA there was no

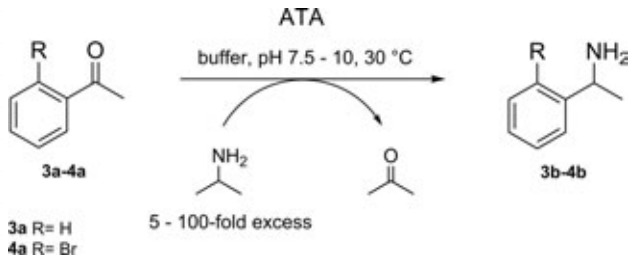

Scheme 2. Reactions studied for the investigation of conditions using IPA as amine donor. Various donor-acceptor ratio and pH values were compared.

significant difference in conversion over the whole range of applied IPA concentrations indicating a more favored equilibrium situation. This was in line with previous results from literature mentioned above.[38] All three 3FCR-QM variants showed indeed the highest conversion of **4a**, in case of 3FCR-QM-R420A and 3FCR-QM-R420W even with quantitative conversion. The effect of the pH on the conversion level of **3a** and **4a** was investigated over a range of pH 7.5–10, which was considered as the common pH range for the most ATA reactions in literature. For these experiments the IPA concentration was fixed to 0.5 M to ensure no limitations here. Beside two significant exceptions (Afu-TA and Arth-TA) the pH value did not influence the catalytic activity of the ATA in both of the shown model reactions with IPA. The two mentioned exceptions showed the trend that a more basic pH is more beneficial for transamination reactions with IPA since the concentration of unprotonated IPA is certainly higher (Figure 1C, 1D). Especially Arth-TA is interesting in this manner since the best conversion of both **3a** and **4a** was reached at pH 10 and in contrast the pH optimum of this enzyme is at pH 8 (see SI). But the majority of the ATA showed a similar activity in both reactions regardless of pH optima and protonation state of IPA. To further support the results from Figure 1 we looked at enzyme stability in presence of IPA. Beside the three presented variants of 3FCR-QM we chose exemplary Cvi-TA and Spo-TA to cover all variations of catalytic activity from Figure 1. 3FCR wild-type and 3FCR-QM were included for comparison. After incubation with IPA (final concentration of 0.05 and 0.5 M) over 8 h at 30 °C the residual activity of the ATA were quantified via the initial activity assay (acetophenone assay,[57] Figure 2). Interestingly, the majority of the 3FCR variants were apparently affected by IPA incubation and not any wild-type enzyme. But a considerable detrimental effect due to IPA incubation was not obvious for any investigated ATA. Additionally, protein melting points were determined in the presence of IPA (see Table S5, SI) giving a similar result. This experiment on ATA stability demonstrated that a higher tolerance towards IPA was not the reason for the better conversion in the investigated reactions by 3FCR-QM variants.

Conclusively, the results from the pH and donor-acceptor-ratio experiments revealed that both aspects should be considered as enzyme as well as substrate dependent (or a

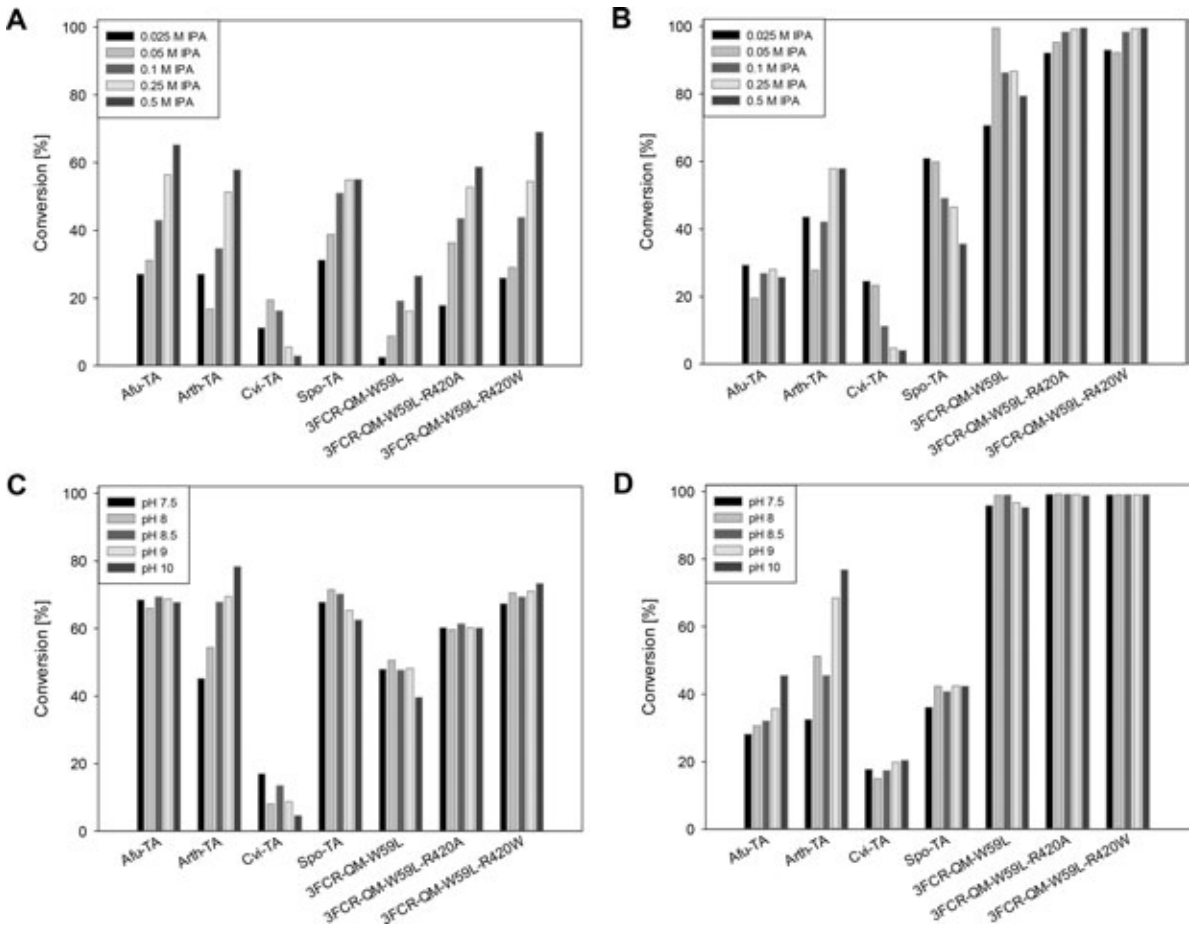

Figure 1. Asymmetric synthesis of **3b** (A, C) and **4b** (B, D) using IPA as amine donor. The influence of different donor-acceptor-ratio (A, B) and pH values (C, D) was investigated. Wild type ATA from *Aspergillus fumigatus* (Afu-TA), *Arthrobacter* sp. (Arth-TA), *Chromobacterium violaceum* (Cvi-TA), *Silicibacter pomeroyi* (Spo-TA) and the presented variants of 3FCR (ATA from *Ruegeria* sp. TM1040) were used. **A**, **B** IPA was applied in the following excess related to the amine acceptor: from left to right 5-fold, 10-fold, 25-fold, 50-fold and 100-fold (in a range of 0.025–0.5 M). The concentration of the ketone substrates was fixed at 5 mM. **C, D** Different pH values were set using Davies buffer[56]: from left to right pH 7.5, pH 8, pH 8.5, pH 9 and pH 10. The shown conversion levels are mean values out of duplicates. For single values see Supporting Information. General reaction conditions: 1 mg mL^{-1} purified enzyme, 5 mM **3a** (substrate to enzyme ratio, s/e ~0.6 w/w) or **4a** (s/e ~0.9 w/w), 5% (v/v) DMSO, 0.1 mM PLP, 50 mM HEPES/CHES buffer pH 7.5 or 9 (according to each pH optimum, see Supporting Information), 30 °C. Samples were taken after 20 h and analyzed via gas chromatography with 2-iodoacetophenone as internal standard.

combination of both). Therefore no general guideline for an optimal reaction setup can be derived. It appears that every ATA reaction using IPA needs to be optimized relating to the mentioned aspects since they likely have overlapping effects, e.g. pH optima of the enzyme, pH/solvent stability and protonation state of IPA. Through this reaction engineering even wild-type enzymes could reach moderate to good activities with IPA as shown here and also in previous works.[54] Thus, we demonstrated a remarkable increase in catalytic activity towards IPA as amine donor mutating amino acid residues around the active site in the 3FCR-QM scaffold, namely positions 59 and 420. It has to be highlighted that the presented 3FCR-QM variants exhibit a good to excellent performance in all shown reactions, e.g. over a broad range of pH values and donor-acceptor ratio. The mutation 59 L is an important key mutation for the catalytic activity towards IPA since the conversion in reactions with **2a**–**4a** was already substantially increased. It should be noted however that in terms of better IPA acceptance the role of both positions (59 and 420) is definitely substrate dependent. With the variant 3FCR-QM-W59L-R420W a general approach for an improved IPA acceptance for the investigated reactions was identified.

Experimental Section

All chemicals and kits were purchased either from Sigma Aldrich (Darmstadt, Germany), Roth (Karlsruhe, Germany), or Acros/Thermo Fisher Scientific (Waltham, USA) in analytical grade. The ketones **1a** and **2a** as well as the corresponding racemic amines (Scheme 1) were kindly provided by F. Hoffmann-La Roche.

Enzyme Expression, Cell Lysis and Protein Purification

Information about the plasmids containing genes of ATAs from *Chromobacterium violaceum*, *Silicibacter pomeroyi*, *Arthobacter* sp., *Aspergillus fumigatus* and *Ruegeria* sp. TM1040 are given in Table S3 (Supporting Information). The protein expression was done in Terrific Broth (TB) media with 100 μg mL^{-1} ampicillin or 50 μg mL^{-1} kanamycin at 160 rpm and 20 °C. After the optical density at

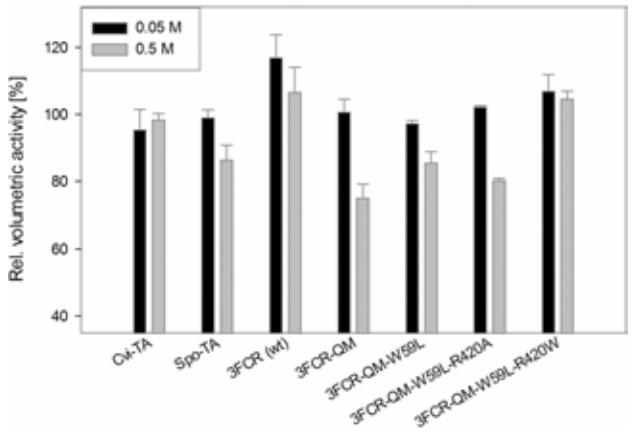

Figure 2. Volumetric activities (U/mL) determined via the initial activity assay after incubation with IPA over 8 h (two final concentrations were used as indicated). Relative activities were normalized to an IPA free control experiment. Reaction conditions: 0.05–0.1 mg mL^{-1} purified protein, 1.25 mM (*S*)-PEA (1-phenylethylamine), pyruvate or pentanal in equimolar ratio, 0.5–5% (v/v) DMSO in CHES pH 9 (50 mM). The formation of acetophenone was quantified at 245 nm at 30 °C. All measurements were performed in triplicate. The compatibility of this assay under these conditions was ensured by previous solvent exchange (Figures S5 and S6, Supporting Information).

600 nm (OD_{600}) reached 0.5–0.7, expression was induced by adding 0.2 mM isopropyl β-D-1-thiogalactopyranoside (final concentration). After 18 h the cultures were centrifuged (4,000×*g*, 15 min, 4 °C) and washed with lysis buffer (HEPES (50 mM pH 7.5), 0.1 mM PLP, 300 mM NaCl). Cell disruption was performed via sonication using the Bandelin Sonoplus HD 2070 (8 min, 50% pulsed cycle, 50% power) on ice followed by centrifugation in order to remove cell debris (12,000×*g*, 45 min, 4 °C, Sorvall centrifuge). The supernatant containing the crude ATA was stored at 4 °C until use. Metal affinity chromatography was used to purify all enzymes with an Äkta purifier and a 5-mL HiTrap Fast Flow column (GE Healthcare, Freiburg, Germany). Elution was mediated by the lysis buffer additionally containing 300 mM imidazole. The desalting step was performed using three HiTrap desalting columns in line (each 5 mL; GE Healthcare, Freiburg, Germany) and lysis buffer without NaCl. The protein concentration was determined via the Pierce BCA Protein Assay Kit according to the manual.

Point Mutations via *QuikChange* Mutagenesis

Variants of 3FCR-QM were produced using a modified version of the *QuikChange* PCR method. Primers were designed with the desired mismatches to provide the desired mutations. For each PCR, Pfu buffer, 0.2 mM dNTPs, 0.2 ng μL^{-1} parental plasmid, 0.2 μM of each primer and 0.2 μL of Pfu Plus! DNA polymerase were applied. A DMSO concentration of 3% (v/v) was set. The amplification was performed as follows: (a) 94 °C, 2 min; (b) 25 cycles: 94 °C, 30 s; 55 °C or 60 °C, 30 s; 72 °C, 7:05 min (c) 72 °C, 14 min. The PCR product was digested with DpnI (20 μL mL^{-1}) for 2 h at 37 °C and the restriction enzyme was inactivated by incubation at 80 °C for 20 min. Chemo-competent Top10 *E. coli* cells were transformed with the PCR product. After confirmation of the correct sequence, the plasmids were isolated from Top10 and chemo-competent *E. coli* BL21 (DE3) cells were transformed for protein expression as described above.

Determination of Transaminase Activity

The characterization of the ATA was done via the initial activity assay (acetophenone assay) according to Schätzle *et al.*[57] with slight modifications. In the reaction solution the concentrations of the amine donor ((*R*)-/(*S*)-1-PEA **3b**, *rac*-**1b** or *rac*-**2b**) and the acceptor pyruvate or pentanal was set to 1.25 mM or as indicated in 0.5%–10% (v/v) DMSO. Briefly, 10 μL of a pre-diluted ATA solution was mixed with the respective buffer (according to the pH optimum of each ATA, HEPES or CHES buffer) and the reaction was initiated by the addition of the 4-fold concentrated stock of reaction solution. The formation of the corresponding ketone was quantified at 245 nm (**2a** and **3a**) or 265 nm (**1a**), respectively using the Tecan Infinite M200 Pro (Crailsheim, Germany) at 30 °C. One unit (U) of ATA activity was defined as the formation of 1 μmol of **1a**–**3a** per minute (**1a** ε = 16.56 M^{-1} cm^{-1}, **2a** ε = 9.65 M^{-1} cm^{-1}, **3a** ε = 12 M^{-1} cm^{-1}). All measurements were performed in triplicate. The pH optimum of each ATA was determined by using Davies[56] buffer with a pH value as indicated.

Asymmetric Synthesis of the Chiral Amines 1 b–4 b

Biotransformations were performed in 0.25 mL scale using 1.5 mL glass vials at 30 °C and 950 rpm shaking. The reaction mixtures contained 1 mg mL^{-1} purified ATA, 5 mM ketone, 30% DMSO as co-solvent, the respective concentration of IPA (from a 4 M IPA-HCl stock solution, pH 7) in HEPES, CHES (50 mM) or Davies buffer as indicated. The final pH was checked. Additionally, control experiments with desalting buffer instead of enzyme were performed. After 20 h incubation, the reaction was quenched by adding 3 M NaOH (resulting in pH ≥ 12). Samples for gas chromatography (GC) analysis were taken immediately after quenching.

GC Analysis

Samples of 100 μL were withdrawn for chiral GC analysis and extracted with 300 μL of ethyl acetate containing 1 mM 2′-iodoacetophenone as internal standard for quantification. The organic layers were dried over anhydrous $MgSO_4$ and derivatized (when necessary) with *N*-Methyl-bis-trifluoroacetamide (MBTFA) by adding 7.5 μL of the commercial stock solution to 100 μL of the organic layer and incubation at 60 °C for 30 min. Afterwards, the samples were analyzed immediately using the Hydrodex-ß-TBDAc column (Macherey & Nagel). For the analysis of substances **1** and **2** the following temperature gradient program was established: initial temperature 140 °C, kept for 15 min, linear gradient to 180 °C with a slope of 15 °C min^{-1}, kept for 35 min, linear gradient to 220 °C with a slope of 15 °C min^{-1}, kept for 10 min. For **3**: initial temperature 120 °C, kept for 5 min, linear gradient to 220 °C with a slope of 10 °C min^{-1}, kept for 5 min. For **4**: initial temperature 100 °C, kept for 7.5 min, linear gradient to 220 °C with a slope of 5 °C min^{-1}, kept for 5 min. For retention times see Supporting Information. The conversion of **1a** and **2a** was determined by quantification of amine product formation via calculation of the response factor. In case of **3a** and **4a** the same principle was followed regarding substrate consumption. Each sample included the mentioned internal standard and was set in relation to ATA-free control experiments.

Preparative Scale Synthesis of 1 b and 2 b

The conversion of **1a** and **2a** to the corresponding amines was performed in preparative scale. 87 mg **1a** (using 3FCR_QM_W59L_R420A) and 84 mg **2a** (using 3FCR_QM_W59L_R420W) were applied respectively in an Erlenmeyer flask and dissolved in DMSO

(5% final concentration). CHES buffer (50 mM final, pH 9) and isopropylamine (0.5 M final concentration) were added under stirring. The pH was adjusted with aqueous HCl. The reaction was started by addition of 1 mg mL^{-1} enzyme which led to a final working volume of 0.2 L and a final substrate concentration of 2 mM (**1a** s/e ~ 0.43, **2a** s/e ~ 0.42). The reaction mixture was incubated for 48 h at 30 °C under agitation. For the quantification of the conversion samples were taken, extracted as described above and analyzed via GCMS. The reaction was stopped when no further conversion was observed during reaction monitoring (for **1a** 53%, for **2a** 27%). The following reaction workup was done: After reaction quenching with 10 mL 3 M NaOH to a pH of > 12, an extraction with 1 × 0.2 L and 1 × 0.1 L hexane was performed in a separation funnel. The combined organic layers were dried over anhydrous $MgSO_4$ and evaporated under vacuum to a volume of 0.5 mL. The crude reaction product was applied to a silica column with ethyl acetate as mobile phase. The fractionation monitoring was done via TLC. Fractions containing the respective amine product were pooled and evaporated under vacuum until dryness. The consistency of the amine products was a yellow oil. Each product was confirmed via GCMS and 10–12 mg each were subjected to ^{1}H- and ^{13}C-NMR spectroscopy (see Supporting Information). **1b**, 53% conv., 35% isolated yield (not optimized), 55.5% *ee*. **2b**, 27% conv., 33% isolated yield (not optimized), 98% *ee*.

ATA Stability in the Presence of IPA

Enzyme stability was investigated by incubation samples of ATA with IPA (0, 0.05 and 0.5 M final concentration) for 8 h at 30 °C at 950 rpm shaking. Afterwards a solvent change was performed via PD columns® (GE Healthcare, Freiburg, Germany) according to the manual. Fractions of 0.5 mL were taken and the most active one was subjected to further investigations. The residual enzyme activity was measured via the initial activity assay. For reaction conditions see figure caption of Figure 1. Additionally, melting points T_M of each subjected ATA in presence of 0, 0.05 and 0.5 M IPA (final concentration) were determined using the Prometheus NT.48 device from nanotemper® (see Supporting Information). The protein concentration was set to 1 mg mL^{-1} in HEPES buffer pH 7.5 (50 mM) including 50 μM of PLP. The heating rate was set to 0.5 °C min^{-1} from 20–95 °C. Inflection points (or melting points, respectively) were determined by the first derivative of the measured fluorescence at a 330/350 nm ratio.

Acknowledgements

We thank the Bundesministerium für Bildung und Forschung (Grant 01DN14016) for financial support. Prof. Dr. de Souza thanks the Alexander-von-Humboldt foundation for a Capes-Humboldt research fellowship.

Conflict of Interest

The authors declare no conflict of interest.

Keywords: Amine transaminases · biocatalysis · chiral amines · enzyme engineering · isopropylamine

[1] F. Steffen-Munsberg, C. Vickers, H. Kohls, H. Land, H. Mallin, A. Nobili, L. Skalden, T. van den Bergh, H.-J. Joosten, P. Berglund, *Biotechnol. Adv.* **2015**, *33*, 566–604.
[2] N. V. Grishin, M. A. Phillips, E. J. Goldsmith, *Protein Sci.* **1995**, *4*, 1291–1304.
[3] C. K. Savile, J. M. Janey, E. C. Mundorff, J. C. Moore, S. Tam, W. R. Jarvis, J. C. Colbeck, A. Krebber, F. J. Fleitz, J. Brands, *Science* **2010**, *329*, 305–309.
[4] A. Nobili, F. Steffen-Munsberg, H. Kohls, I. Trentin, C. Schulzke, M. Höhne, U. T. Bornscheuer, *ChemCatChem* **2015**, *7*, 757–760.
[5] M. Genz, O. Melse, S. Schmidt, C. Vickers, M. Dörr, T. van den Bergh, H.-J. Joosten, U. T. Bornscheuer, *ChemCatChem* **2016**, *8*, 3199–3202.
[6] I. V. Pavlidis, M. S. Weiß, M. Genz, P. Spurr, S. P. Hanlon, B. Wirz, H. Iding, U. T. Bornscheuer, *Nat. Chem.* **2016**, *8*, 1076–1082.
[7] B.-K. Cho, H.-Y. Park, J.-H. Seo, J. Kim, T.-J. Kang, B.-S. Lee, B.-G. Kim, *Biotechnol. Bioeng.* **2008**, *99*, 275–84.
[8] D. F. Dourado, S. Pohle, A. T. Carvalho, D. S. Dheeman, J. M. Caswell, T. Skvortsov, I. Miskelly, R. T. Brown, D. J. Quinn, C. C. Allen, *ACS Catal.* **2016**, *6*, 7749–7759.
[9] K. Deepankumar, S. P. Nadarajan, S. Mathew, S.-G. Lee, T. H. Yoo, E. Y. Hong, B.-G. Kim, H. Yun, *ChemCatChem* **2015**, *7*, 417–421.
[10] K. S. Midelfort, R. Kumar, S. Han, M. J. Karmilowicz, K. McConnell, D. K. Gehlhaar, A. Mistry, J. S. Chang, M. Anderson, A. Villalobos, *Protein Eng. Des. Sel.* **2013**, *26*, 25–33.
[11] S.-W. Han, E.-S. Park, J.-Y. Dong, J.-S. Shin, *Adv. Synth. Catal.* **2015**, *357*, 2712–2720.
[12] S.-W. Han, E.-S. Park, J.-Y. Dong, J.-S. Shin, *Adv. Synth. Catal.* **2015**, *357*, 1732–1740.
[13] M. S. Weiß, I. V. Pavlidis, P. Spurr, S. P. Hanlon, B. Wirz, H. Iding, U. T. Bornscheuer, *ChemBioChem* **2017**, *18*, 1022–1026.
[14] M. Höhne, U. T. Bornscheuer, *ChemCatChem* **2009**, *1*, 42–51.
[15] M. Fuchs, D. Koszelewski, K. Tauber, W. Kroutil, K. Faber, *Chem. Commun.* **2010**, *46*, 5500–5502.
[16] M. Fuchs, D. Koszelewski, K. Tauber, J. Sattler, W. Banko, A. K. Holzer, M. Pickl, W. Kroutil, K. Faber, *Tetrahedron* **2012**, *68*, 7691–7694.
[17] S. Pedragosa-Moreau, A. Le Flohic, V. Thienpondt, F. Lefoulon, A.-M. Petit, N. Ríos-Lombardía, F. Morís, J. González-Sabín, *Adv. Synth. Catal.* **2017**, *359*, 485–493.
[18] M. S. Weiß, I. V. Pavlidis, P. Spurr, S. P. Hanlon, B. Wirz, H. Iding, U. T. Bornscheuer, *Org. Biomol. Chem.* **2016**, *14*, 10249–10254.
[19] M. Höhne, S. Kühl, K. Robins, U. T. Bornscheuer, *ChemBioChem* **2008**, *9*, 363–365.
[20] A. Iwasaki, Y. Yamada, Y. Ikenaka, J. Hasegawa, *Biotechnol. Lett.* **2003**, *25*, 1843–1846.
[21] A. Iwasaki, Y. Yamada, N. Kizaki, Y. Ikenaka, J. Hasegawa, *Appl. Microbiol. Biotechnol.* **2006**, *69*, 499–505.
[22] D. Koszelewski, I. Lavandera, D. Clay, G. M. Guebitz, D. Rozzell, W. Kroutil, *Angew. Chem.* **2008**, *120*, 9477–9480; *Angew. Chem. Int. Ed.* **2008**, *47*, 9337–9340.
[23] M. D. Truppo, J. D. Rozzell, J. C. Moore, N. J. Turner, *Org. Biomol. Chem.* **2009**, *7*, 395–8.
[24] D. Koszelewski, I. Lavandera, D. Clay, D. Rozzell, W. Kroutil, *Adv. Synth. Catal.* **2008**, *350*, 2761–2766.
[25] P. Tufvesson, J. Lima-Ramos, J. S. Jensen, N. Al-Haque, W. Neto, J. M. Woodley, *Biotechnol. Bioeng.* **2011**, *108*, 1479–1493.
[26] K. E. Cassimjee, C. Branneby, V. Abedi, A. Wells, P. Berglund, *Chem. Commun.* **2010**, *46*, 5569–5571.
[27] A. Gomm, W. Lewis, A. P. Green, E. O'Reilly, *Chem. Eur. J.* **2016**, *22*, 12692–12695.
[28] A. P. Green, N. J. Turner, E. O'Reilly, *Angew. Chem. Int. Ed.* **2014**, *53*, 10714–10717; *Angew. Chem.* **2014**, *126*, 10890–10893.
[29] L. Martınez-Montero, V. Gotor, V. Gotor-Fernández, I. Lavandera, *Adv. Synth. Catal.* **2016**, *358*, 1618–1624.
[30] S. E. Payer, J. H. Schrittwieser, W. Kroutil, *Eur. J. Org. Chem.* **2017**, *2017*, 2553–2559.
[31] I. Slabu, J. L. Galman, C. Iglesias, N. J. Weise, R. C. Lloyd, N. J. Turner, *Catal. Today* **2017**, doi.org/10.1016/j.cattod.2017.01.025.
[32] J. L. Galman, I. Slabu, N. J. Weise, C. Iglesias, F. Parmeggiani, R. C. Lloyd, N. J. Turner, *Green Chem.* **2017**, *19*, 361–366.
[33] I. Slabu, J. L. Galman, R. C. Lloyd, N. J. Turner, *ACS Catal.* **2017**, *7*, 8263–8284.
[34] F. G. Mutti, C. S. Fuchs, D. Pressnitz, J. H. Sattler, W. Kroutil, *Adv. Synth. Catal.* **2011**, *353*, 3227–3233.
[35] W. Neto, M. Schürmann, L. Panella, A. Vogel, J. M. Woodley, *J. Mol. Catal. B* **2015**, *117*, 54–61.

[36] A. Cuetos, M. Garcıa-Ramos, E.-M. Fischereder, A. Dıaz-Rodrıguez, G. Grogan, V. Gotor, W. Kroutil, I. Lavandera, *Angew. Chem.* **2016**, *128*, 3196–3199; *Angew. Chem. Int. Ed.* **2016**, *55*, 3144–3147.
[37] U. Kaulmann, K. Smithies, M. E. Smith, H. C. Hailes, J. M. Ward, *Enzyme Microb. Technol.* **2007**, *41*, 628–637.
[38] C. E. Paul, M. Rodrıguez-Mata, E. Busto, I. Lavandera, V. Gotor-Fernández, V. Gotor, S. Garcıa-Cerrada, J. Mendiola, Ó. de Frutos, I. Collado, *Org. Process Res. Dev.* **2014**, *18*, 788–792.
[39] E.-S. Park, J.-Y. Dong, J.-S. Shin, *Org. Biomol. Chem.* **2013**, *11*, 6929–6933.
[40] M. Truppo, J. M. Janey, B. Grau, K. Morley, S. Pollack, G. Hughes, I. Davies, *Catal. Sci. Technol.* **2012**, *2*, 1556–1559.
[41] M. Svedendahl, C. Branneby, L. Lindberg, P. Berglund, *ChemCatChem* **2010**, *2*, 976–980.
[42] D. Koszelewski, K. Tauber, K. Faber, W. Kroutil, *Trends Biotechnol.* **2010**, *28*, 324–32.
[43] L. H. Andrade, W. Kroutil, T. F. Jamison, *Org. Lett.* **2014**, *16*, 6092–6095.
[44] T. Börner, S. Rämisch, E. R. Reddem, S. Bartsch, A. Vogel, A.-M. W. H. Thunnissen, P. Adlercreutz, C. Grey, *ACS Catal.* **2017**, *7*, 1259–1269.
[45] H. Mallin, M. Höhne, U. T. Bornscheuer, *J. Biotechnol.* **2014**, *191*, 32–7.
[46] F. Steffen-Munsberg, C. Vickers, A. Thontowi, S. Schätzle, T. Meinhardt, M. Svedendahl Humble, H. Land, P. Berglund, U. T. Bornscheuer, M. Höhne, *ChemCatChem* **2013**, *5*, 154–157.
[47] M. S. Weiß, I. V. Pavlidis, C. Vickers, M. Höhne, U. T. Bornscheuer, *Anal. Chem.* **2014**, *86*, 11847–53.
[48] F. Steffen-Munsberg, P. Matzel, M. A. Sowa, P. Berglund, U. T. Bornscheuer, M. Höhne, *Appl. Microbiol. Biotechnol.* **2016**, *100*, 4511–4521.
[49] M. Genz, C. Vickers, T. van den Bergh, H.-J. Joosten, M. Dörr, M. Höhne, U. T. Bornscheuer, *Int. J. Mol. Sci.* **2015**, *16*, 26953–26963.
[50] A. Iwasaki, K. Matsumoto, J. Hasegawa, Y. Yasohara, *Appl. Microbiol. Biotechnol.* **2012**, *93*, 1563–1573.
[51] M. Höhne, S. Schätzle, H. Jochens, K. Robins, U. T. Bornscheuer, *Nat. Chem. Biol.* **2010**, *6*, 807–813.
[52] K. E. Cassimjee, M. S. Humble, H. Land, V. Abedi, P. Berglund, *Org. Biomol. Chem.* **2012**, *10*, 5466–5470.
[53] F. Steffen-Munsberg, C. Vickers, A. Thontowi, S. Schätzle, T. Tumlirsch, M. Svedendahl Humble, H. Land, P. Berglund, U. T. Bornscheuer, M. Höhne, *ChemCatChem* **2013**, *5*, 150–153.
[54] A. W. H. Dawood, R. O. M. A. de Souza, U. T. Bornscheuer, *ChemCatChem* **2018**, *10*, 951–955.
[55] J. S. Shin, B. G. Kim, *Biotechnol. Bioeng.* **1999**, *65*, 206–11.
[56] M. Davies, *Analyst* **1959**, *84*, 248–251.
[57] S. Schätzle, M. Höhne, E. Redestad, K. Robins, U. T. Bornscheuer, *Anal. Chem.* **2009**, *81*, 8244–8248.

Manuscript received: June 11, 2018
Accepted Article published: June 29, 2018
Version of record online: July 19, 2018

Supporting Information

Isopropylamine as Amine Donor in Transaminase-Catalyzed Reactions: Better Acceptance through Reaction and Enzyme Engineering

Ayad W. H. Dawood, Martin S. Weiß, Christian Schulz, Ioannis V. Pavlidis, Hans Iding, Rodrigo O. M. A. de Souza, and Uwe T. Bornscheuer*

Supporting Information

Isopropylamine as Amine Donor in Transaminase-Catalyzed Reactions: Better Acceptance through Reaction and Enzyme Engineering

Ayad W.H. Dawood,[a] Martin S. Weiß[a], Christian Schulz[a], Ioannis V. Pavlidis[a,b], Hans Iding[c], Rodrigo O.M.A. de Souza,[d] Uwe T. Bornscheuer*[a]

Table of content

1. Glycine oxidase assay of 3FCR-QM variant

Table S1. Initial activity of purified 3FCR variants determined via the glycine oxidase assay[1] towards two concentrations of IPA as the amine donor. Measurements were performed in triplicate.

Transaminase / variant	**Activity [mU/mg]**		**Fold increase in activity**
	IPA 0.05 M	**IPA 0.2 M**	
3FCR-QM	3.64 ± 0.15	8.55 ± 1.28	2.3
3FCR-QM-W59L	16.8 ± 1.13	39.04 ± 0.17	2.3
Fold increase in activity	4.6	4.5	

Reaction conditions: CHES buffer (2-(Cyclohexylamino)ethanesulfonic acid), pH 9.5 (50 mM), 2 mM glyoxylate, IPA concentration as indicated, 37 °C.

2. Mutagenesis of position 420 in 3FCR-QM

Table S2. Conversion of **1a** and **2a** obtained by asymmetric synthesis using IPA as amine donor and purified variants of 3FCR. Protein concentration was normalized to 0.5 mg mL^{-1}.

TA / variant	**Conversion [%] of substrate**	
	1a	2a
3FCR-QM	1.3 ± 0.18	6.6 ± 0.35
3FCR-QM-R420L	2.5 ± 0.94	10.8 ± 0.21
3FCR-QM-R420M	1.9 ± 0.13	9.9 ± 0.11
3FCR-QM-R420H	5.0 ± 0.08	12.7 ± 0.05
3FCR-QM-R420W	6.8 ± 0.09	14.4 ± 0.03
3FCR-QM-R420E	4.9 ± 0.56	12.9 ± 0.25
3FCR-QM-R420D	3.3 ± 0.27	9.5 ± 0.19

Reaction conditions: HEPES buffer ((4-(2-hydroxyethyl)-1-piperazineethanesulfonic acid), pH 8 (50 mM), 1 mM PLP, 2 mM ketone (**1a** or **2a**), 0.5 M IPA, 30% (v/v) DMSO, 30 °C. Conversion was determined after 48 h via HLPC (C8 column) and after measuring duplicates.

3. The amine acceptor in the initial activity assay for 3FCR-QM variants

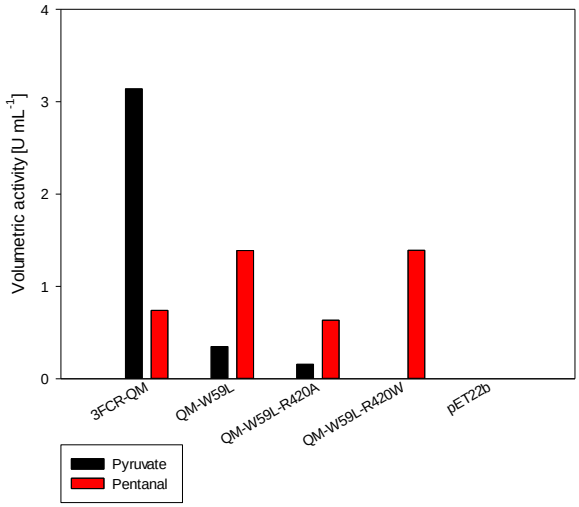

Fig. S1. Comparison of the presented variants of 3FCR-QM in terms of pyruvate and pentanal acceptance. Crude cell lysate with overexpressed ATA-variant (and empty vector expression as negative control) were subjected to the initial activity assay (Acetophenone assay). (*S*)-PEA was used as the amine donor. Both, amine donor and acceptor were applied in equimolar ratio of 1.25 mM in CHES buffer pH 9 (50 mM) and 5% (v/v) DMSO. The formation of acetophenone was quantified at 245 nm at 30 °C. One unit (U) of ATA activity was defined as the formation of 1 µmol of acetophenone per minute (ε= 12 $mM^{-1}cm^{-1}$). All measurements were performed in triplicate.

4. Investigated ATA

Table S3. Overview of all investigated wild type ATA, including the basis of the presented variants of 3FCR(-QM). *E. coli* BL21 (DE3) was used as expression strain. See method section for the expression protocol.

Abbreviation	PDB ID	Origin (species)	Vector
Afu-TA	4CHI	*Aspergillus fumigatus* Af293	pET22b
Arth-TA	3WWH	*Arthrobacter* sp.	pET28a
Cvi-TA	4A6T	*Chromobaterium violaceum*	pET28a
Spo-TA	3HMU	*Silicibacter pomeroyi*	pET22b
3FCR-TA	3FCR	*Ruegeria* sp. TM1040	pET22b

5. pH optima of investigated Amine Transaminases

pH optima were determined via the initial activity assay (Acetophenone assay) according to Schätzle *et al.*[2] with slight modifications. Davies buffer[3] was used instead of HEPES or CHES to cover a broad pH range with the same buffer reagent.

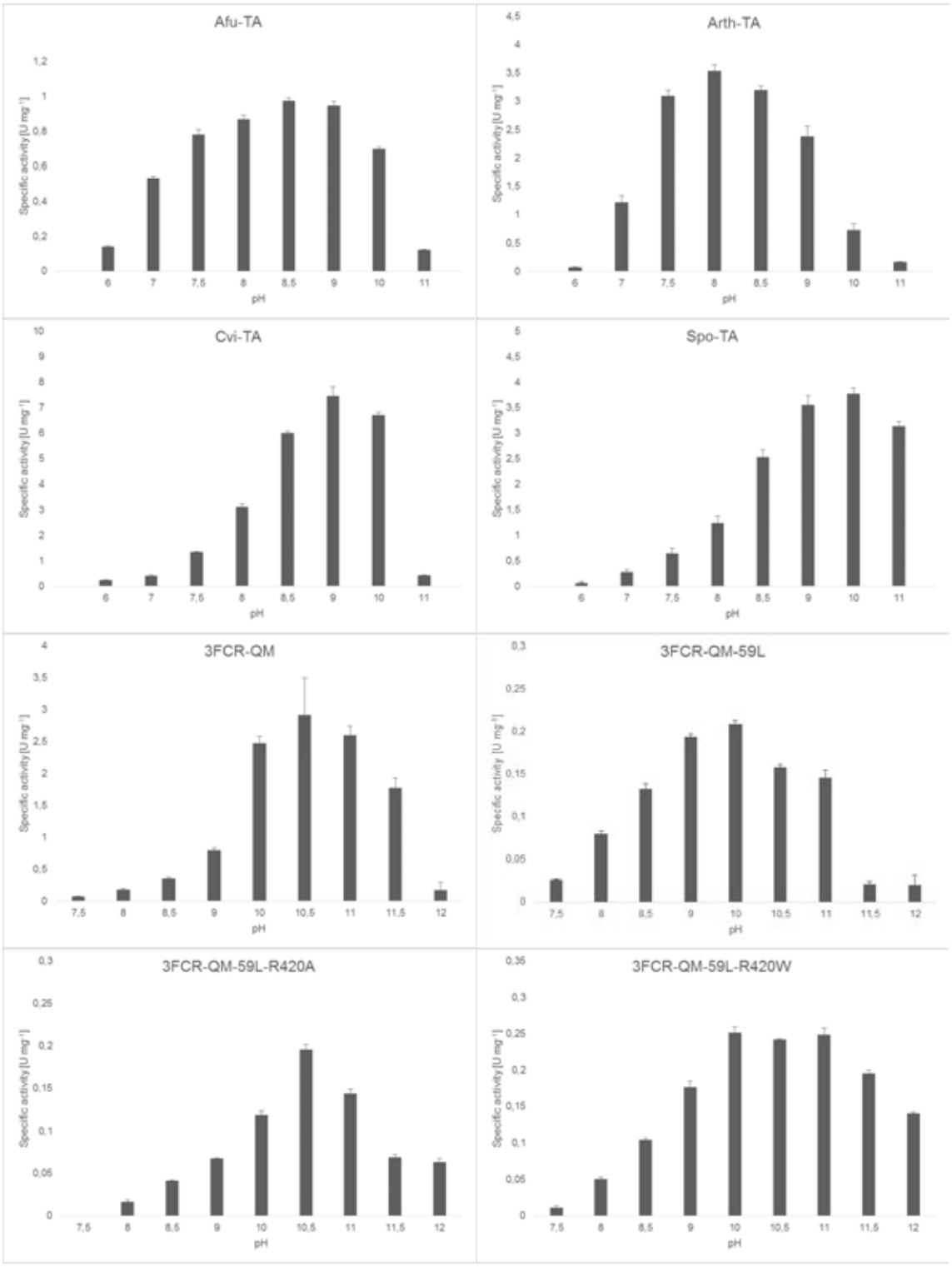

Fig. S2. Determination of the pH optima of investigated ATA via the initial activity assay (Acetophenone Assay according to[2] with modifications). The final concentration of (*R*/*S*)-PEA (depended on the respective enantioselectivity) and pyruvate/pentanal was 1.25 mM, 5% (v/v) DMSO in Davies buffer[3] in a range from pH 6 – 12 at 30 °C. Pentanal had to be applied for the 3FCR-QM variants (see Fig. S2). The formation of acetophenone was quantified at 245 nm. One unit (U) of ATA activity was defined as the formation of 1 µmol of acetophenone per minute (ε= 12 $mM^{-1}cm^{-1}$). All measurements were performed in triplicate.

6. Investigations on effects of pH and donor-acceptor-ratio

3a, 25 mM IPA

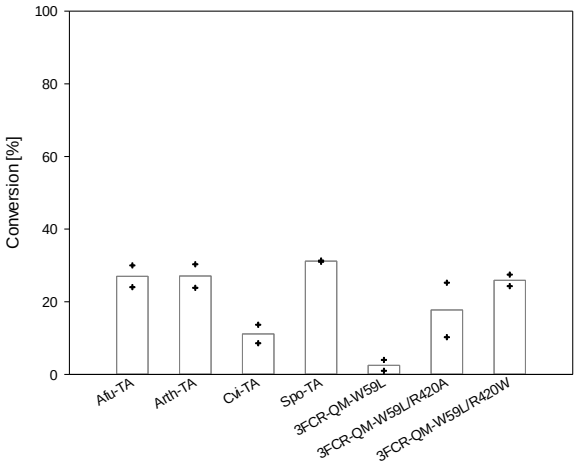

3a, 50 mM IPA

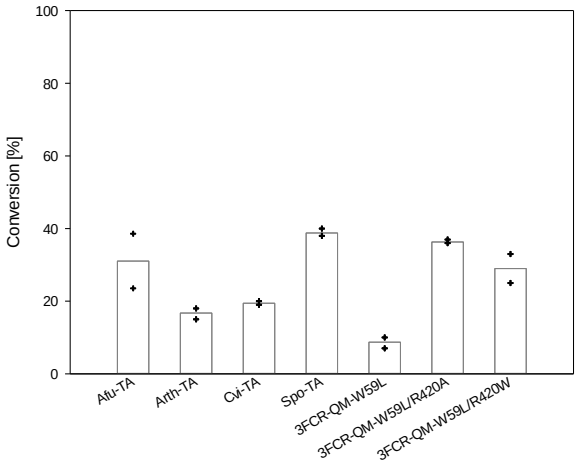

3a, 100 mM IPA

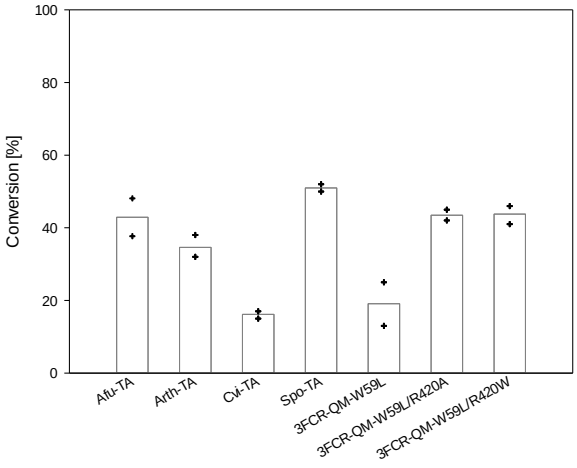

3a, 250 mM IPA

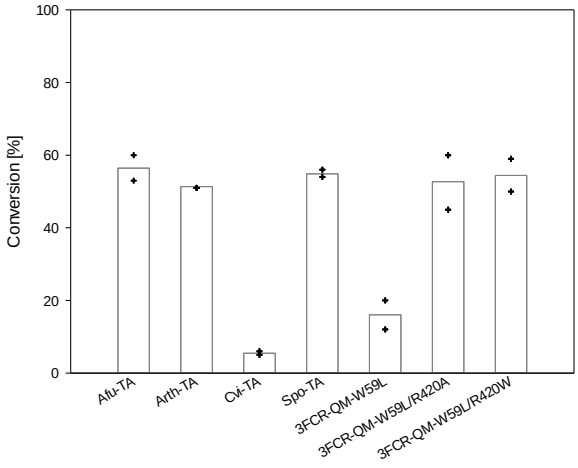

3a, 500 mM IPA

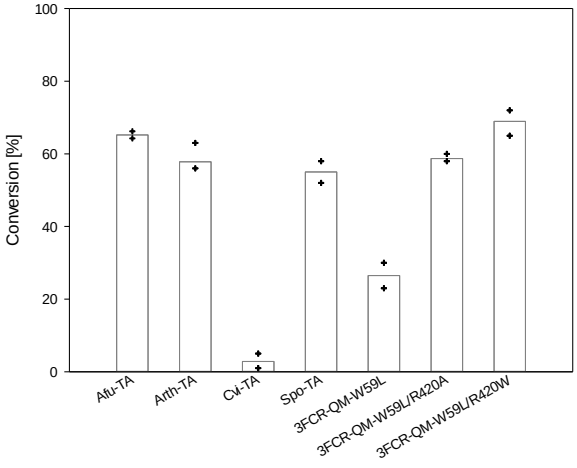

4a, 25 mM IPA

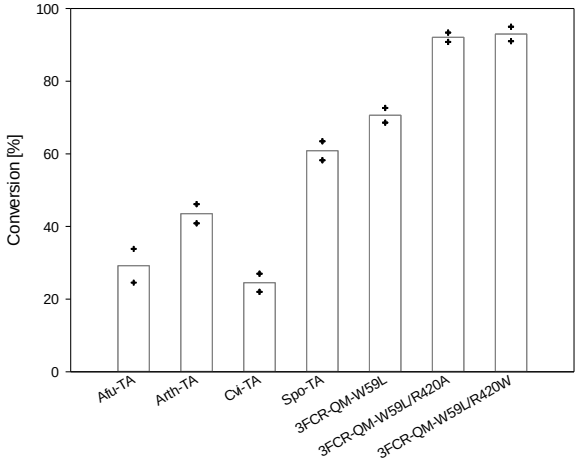

4a, 50 mM IPA

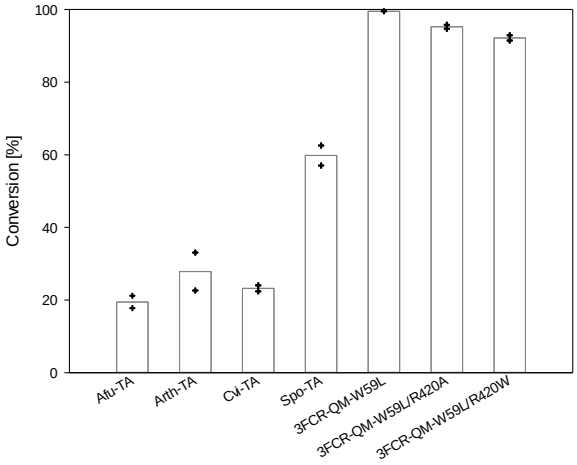

4a, 100 mM IPA

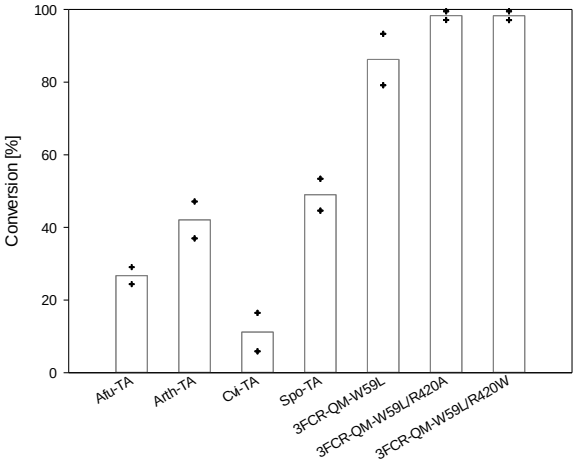

4a, 250 mM IPA

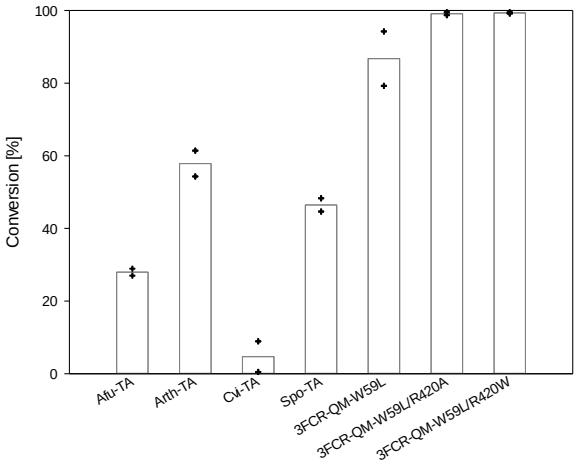

4a, 500 mM IPA

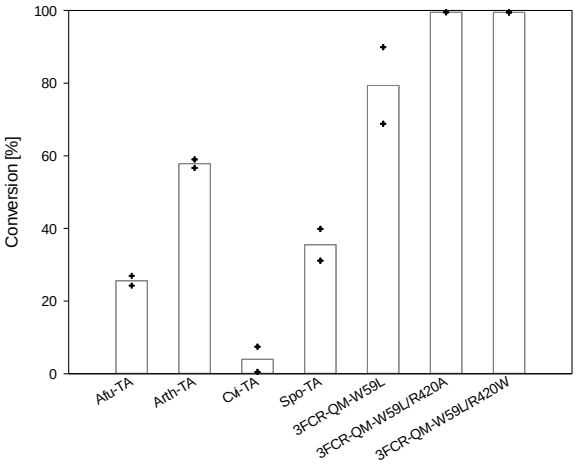

3a, Davies buffer pH 7.5

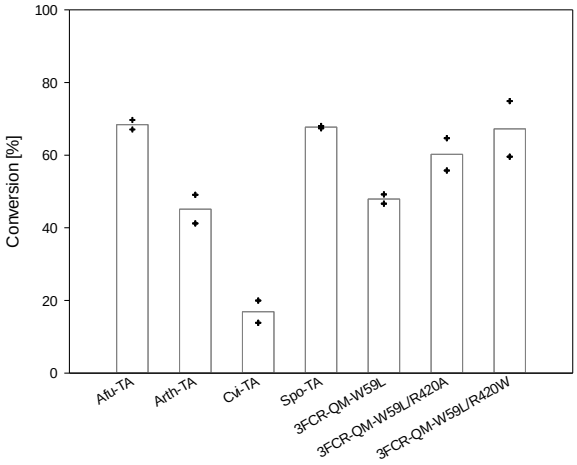

3a, Davies buffer pH 8

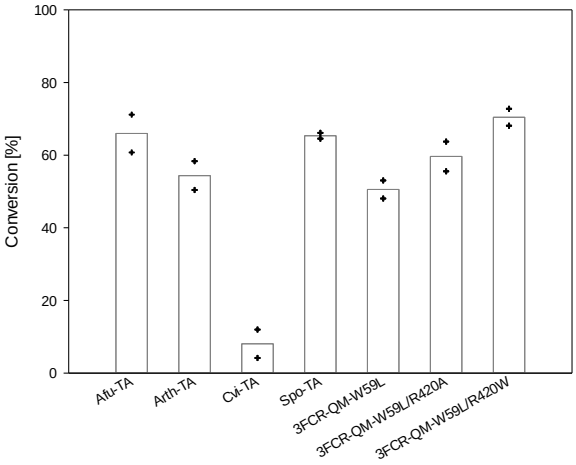

3a, Davies buffer pH 8.5

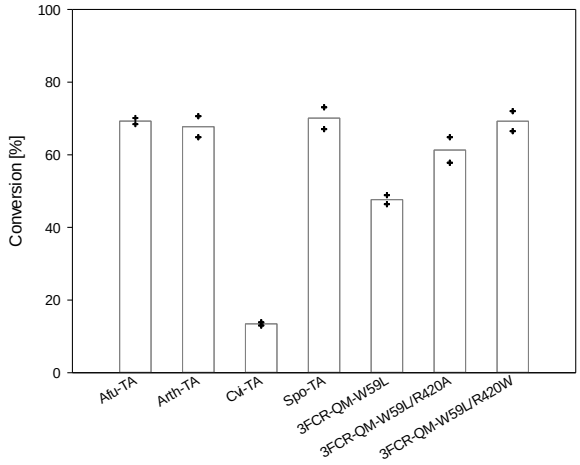

3a, Davies buffer pH 9

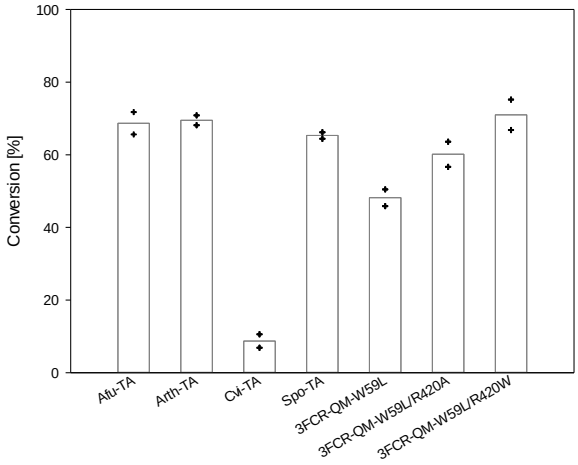

3a, Davies buffer pH 10

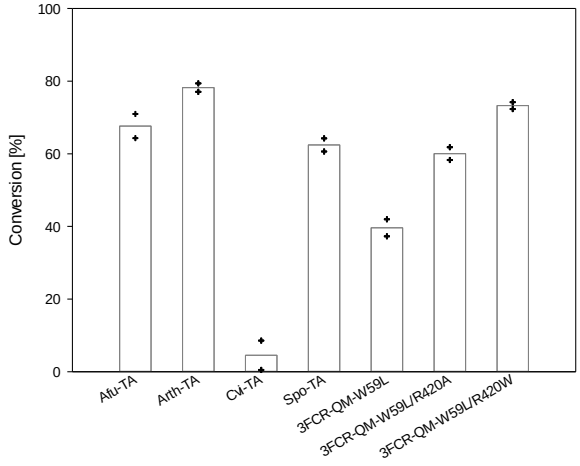

4a, Davies buffer pH 7.5

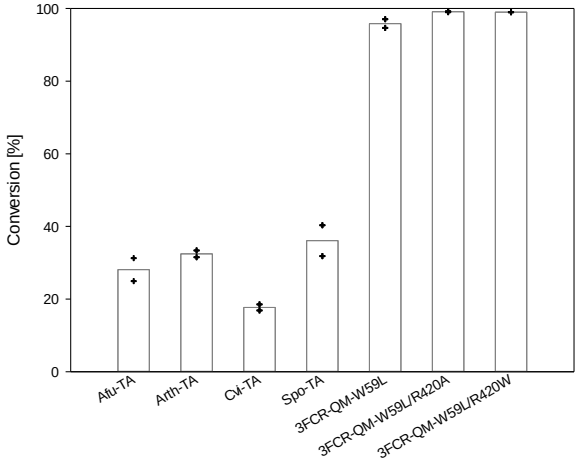

4a, Davies buffer pH 8

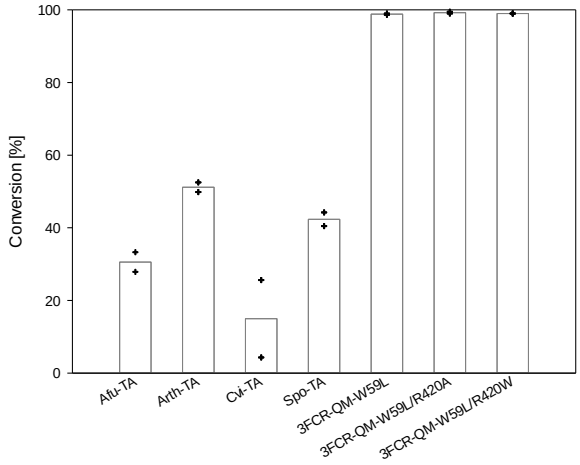

4a, Davies buffer pH 8.5

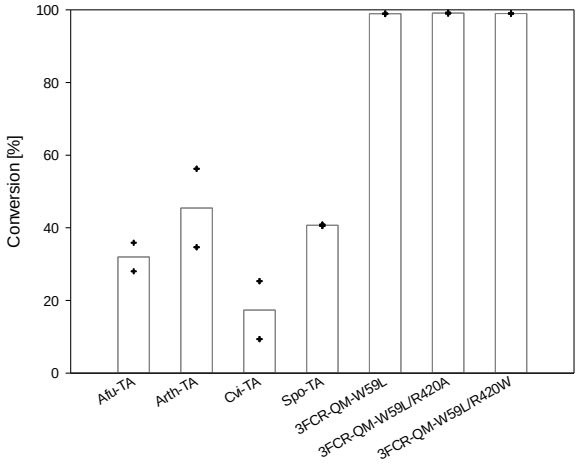

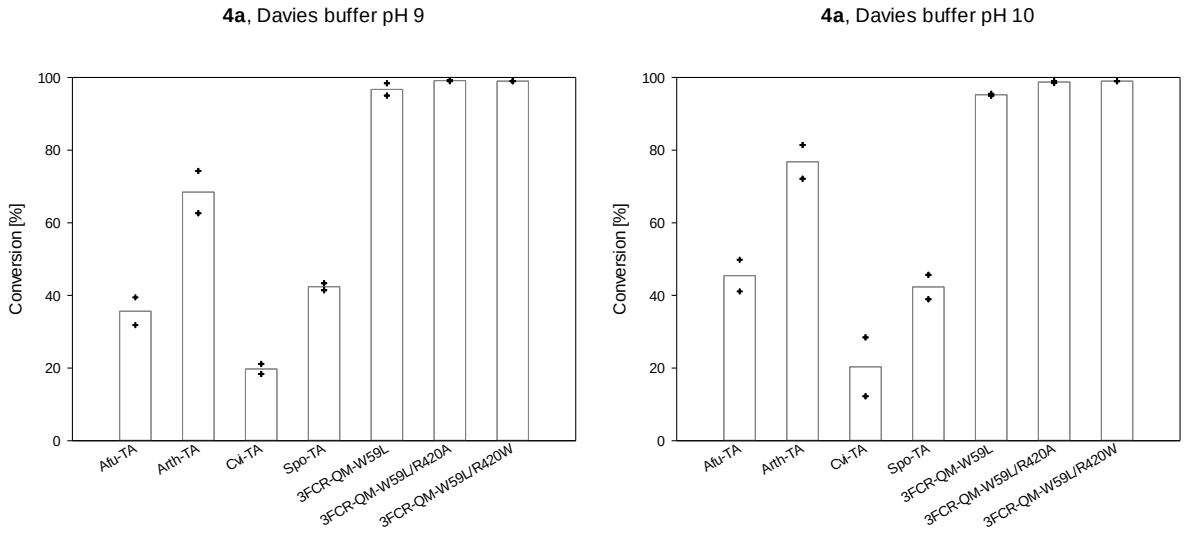

Fig. S3. Conversion levels of the asymmetric synthesis of **3b** and **4b** using the indicated pH or concentration of IPA. Single values for each reaction are given as crosses and mean values were the basis for bar plot. Wild type ATA from *Aspergillus fumigatus* (Afu-TA), *Arthrobacter* sp. (Arth-TA), *Chromobacterium violaceum* (Cvi-TA), *Silicibacter pomeroyi* (Spo-TA), *Ruegeria* sp. TM1040 (3FCR) and variants of 3FCR were investigated. The substrate concentration was set to 5 mM. IPA was applied in the following excess related to the substrate concentration: 5-fold, 10-fold, 25-fold, 50-fold and 100-fold (in a range of 0.025 – 0.5 M, see plot titles). The pH experiments were performed in a range of pH 7.5 – 10 using Davies buffer at 0.5 M IPA. General reaction conditions: 1 mg mL^{-1} purified enzyme, 5 mM **3a** (s/e ~ 0.6 w/w) or **4a** (s/e ~0.9 w/w), 5% (v/v) DMSO, 0.1 mM PLP, 50 mM HEPES/CHES buffer pH 7.5 or 9 (according to each pH optimum), 30 °C. Samples were withdrawn after 20 h and analyzed via gas chromatography with 2-iodoacetophenone as internal standard.

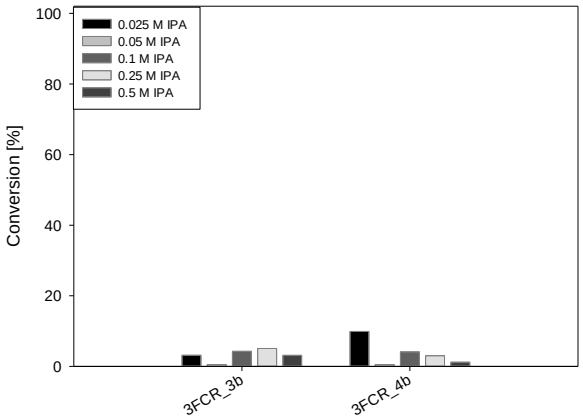

Fig. S4. Conversion values of the asymmetric synthesis of **3b** (left) and **4b** (right) with 3FCR wild-type for comparison reasons. Different IPA concentrations were applied (from 0.025 M – 0.5M). The substrate concentration was fixed to 5 mM. For further reaction conditions see figure caption above (Fig. S3).

7. Retention times and chromatograms

Table S4. Overview of retention times for all investigated compounds revealed by GC analysis. The GC column Hydrodex-ß-TBDAc (25 m) from Macherey & Nagel was used. The retention times for all compounds (ketones and corresponding amines) refer to the following temperature profiles. For compound **1**/**2**: initial temperature 140 °C, kept for 15 min, linear gradient to 180 °C with a slope of 15 °C min^{-1}, kept for 35 min, linear gradient to 220 °C with a slope of 15 °C min^{-1}, kept for 10 min. For **3**: initial temperature 120 °C, kept for 5 min, linear gradient to 220 °C with a slope of 10 °C min^{-1}, kept for 5 min. For **4**: initial temperature 100 °C, kept for 7.5 min, linear gradient to 220 °C with a slope of 5 °C min^{-1}, kept for 5 min.

Compound	Retention time [min]	
	Ketone	Amine product
1	27.8	46.9 / 47.6
2	30.2	45.3 / 46.9
3	5.5	5.1
4	14.1	17.5

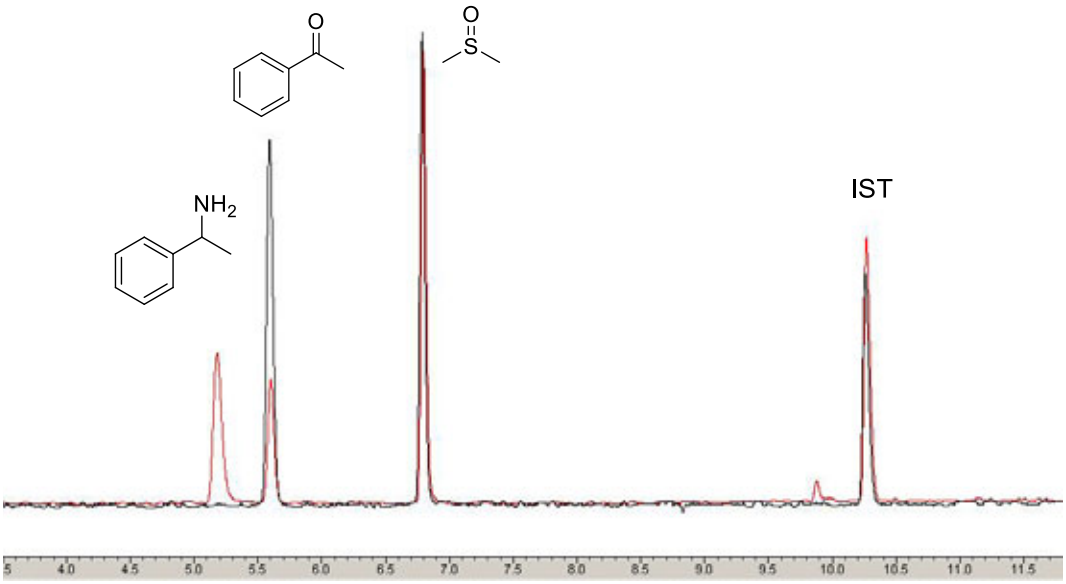

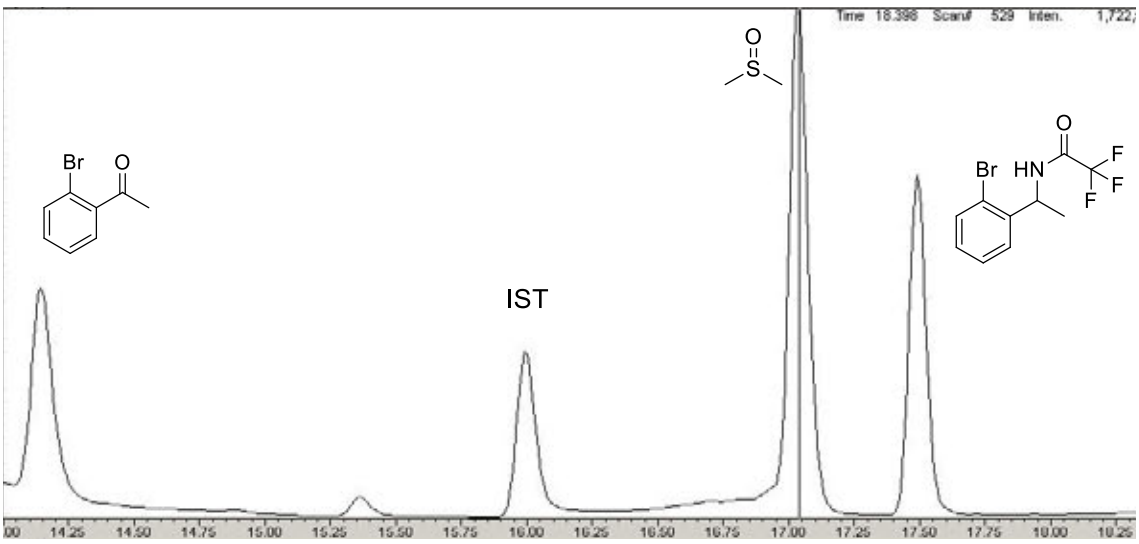
Time 16.398 Scan# 529 Inten. 1,722,
O
S
Br
O
IST
Br
HN
O
F
F
F

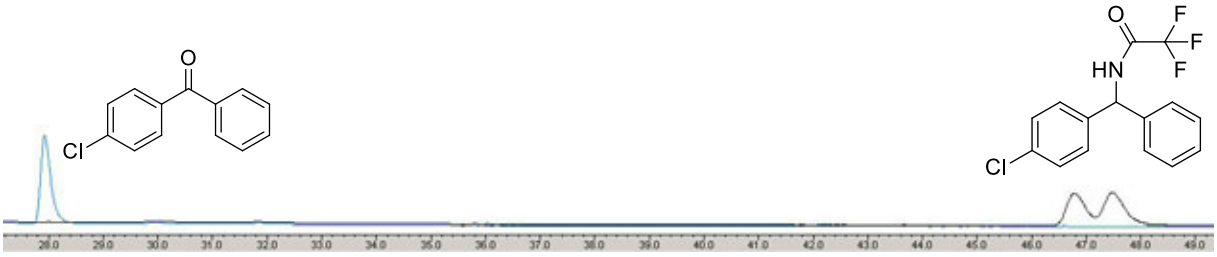
O
Cl
O
F
F
HN
F
Cl

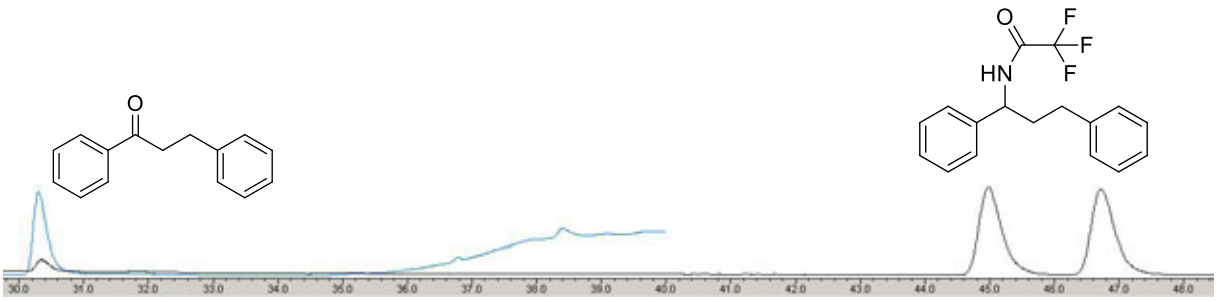
O
O
F
F
HN
F

8. NMR spectra

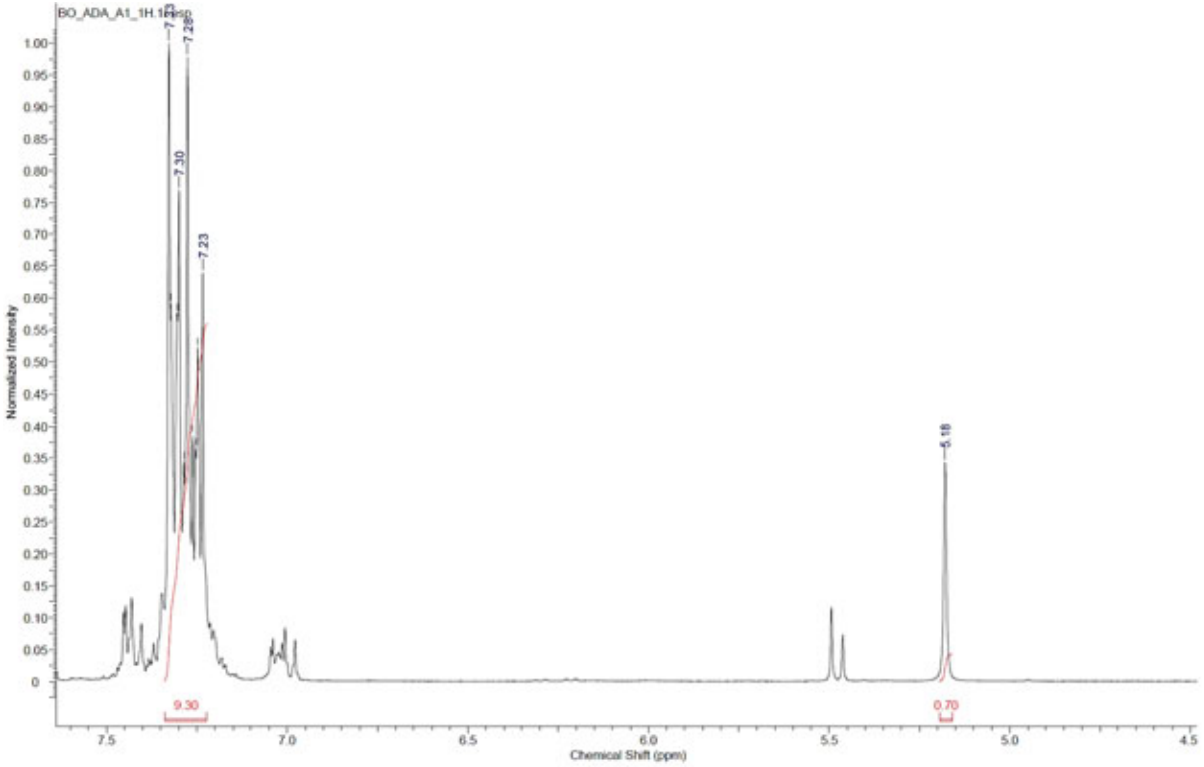

Amine **1b** ^{1}H-NMR (300 Mhz, $CDCl_3$) δ (ppm): 5.18 (s, 1H), 7.23 – 7.33 (m, 9 H)

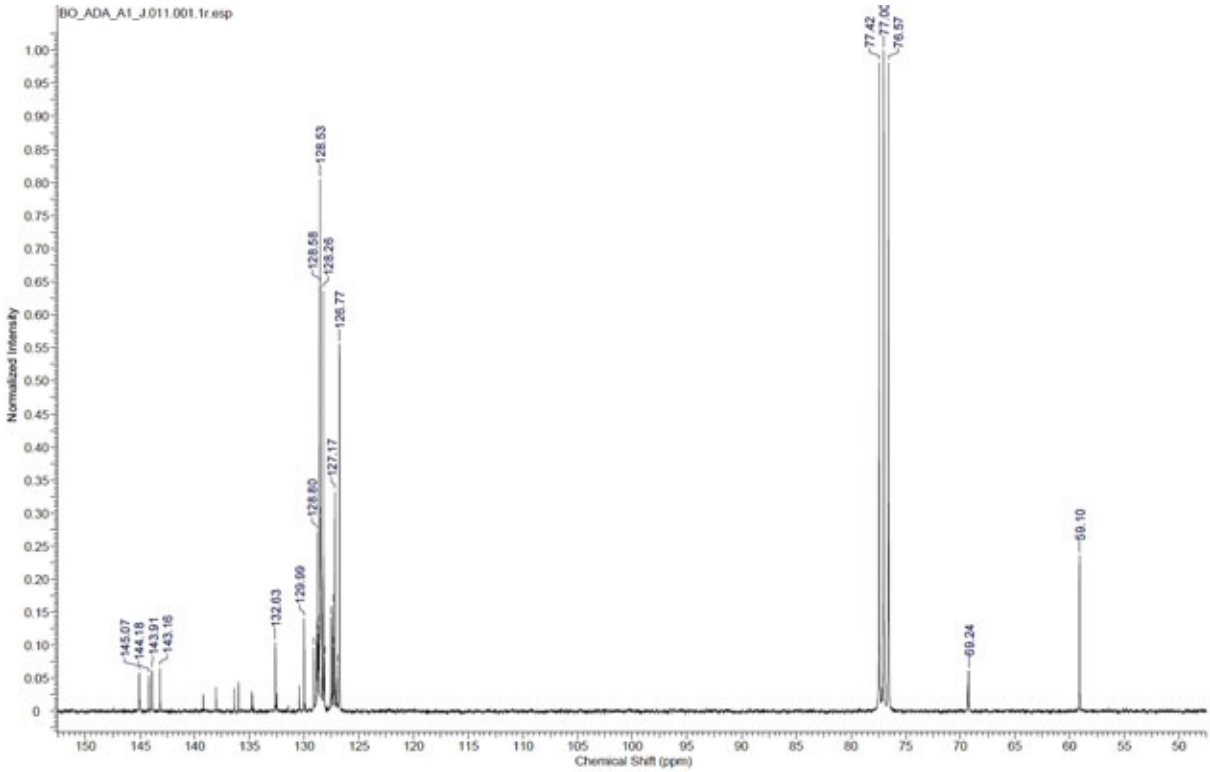

Amine **1b** ^{13}C-NMR (300 Mhz, $CDCl_3$) δ (ppm): 59.1 (s), 126.77 (s), 128.26 (s), 128.53 (s), 128.6 (s), 132.63 (s), 143.16 (s), 145.07 (s)

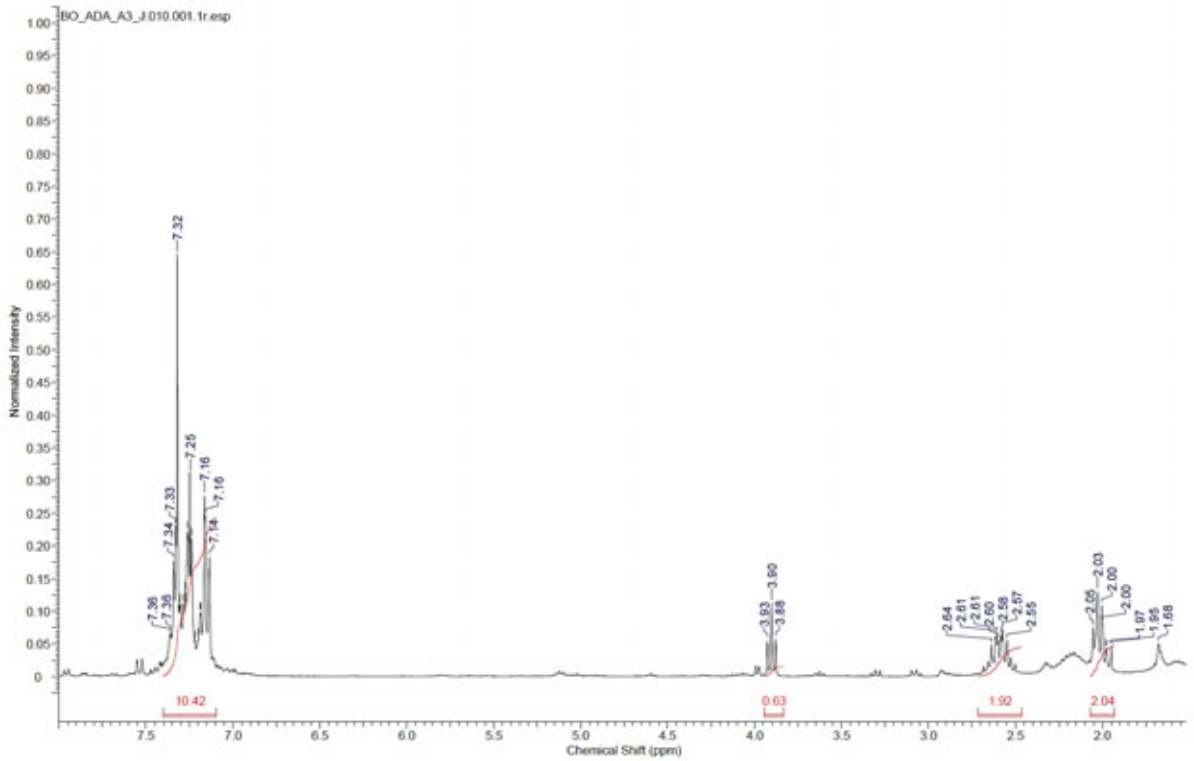

Amine **2b** ^{1}H-NMR (300 Mhz, $CDCl_3$) δ (ppm): 1.93 – 2.07 (m, 2H), 2.46 – 2.71 (m, 2H), 3.9 (t, J=6.9, 1H), 7.14 – 7.36 (m, 10H)

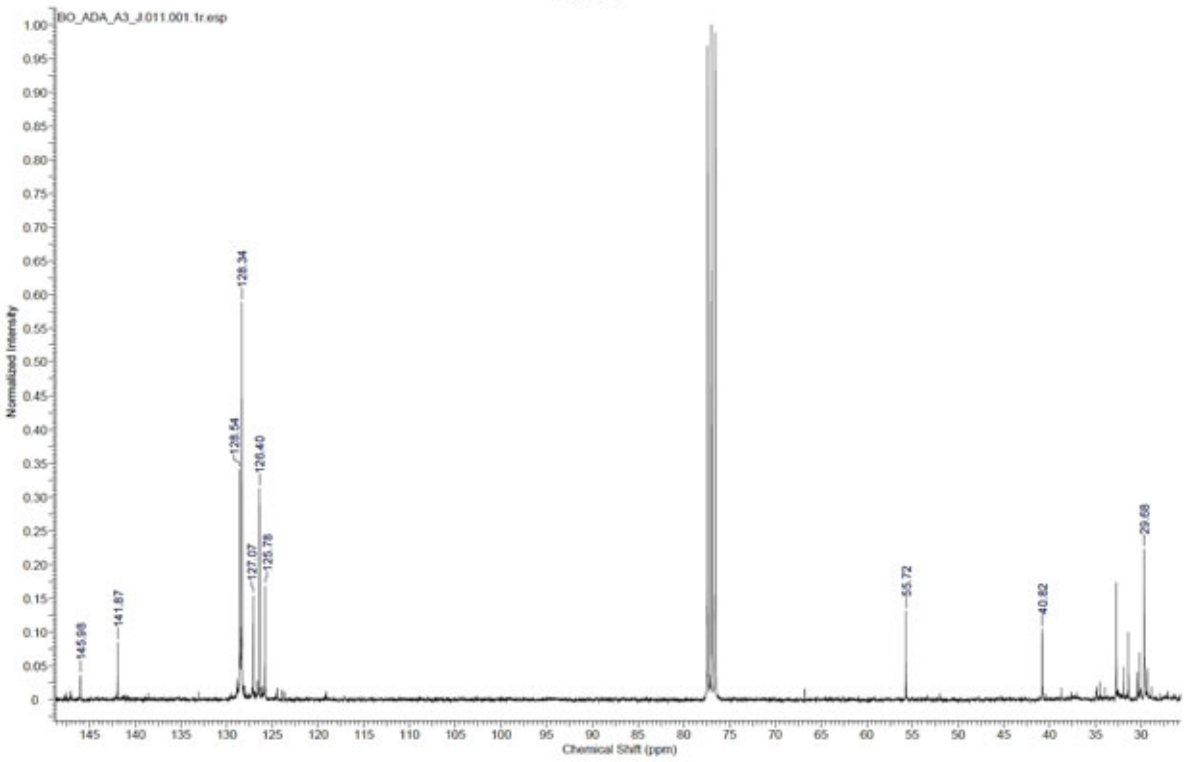

Amine **2b** ^{13}C-NMR (300 Mhz, $CDCl_3$) δ (ppm): 29.68 (s), 40.82 (s), 55.76 (s), 125.78 (s), 126.4 (s), 127.07 (s), 128.34 (s), 128.54 (s), 141.87 (s), 145.98 (s)

9. Enzyme stability in presence of IPA

Determination of melting points

Table S5. Stability experiments in the presence of IPA (concentration is given in M). The protein concentration was normalized at 1 mg mL^{-1}. Melting points were determined via the Prometheus NT.48 (nanotemper®) with a heating rate of 0.5 °C min^{-1} from 20 – 95 °C and a device specific excitation power of 20-30%. The experiment was performed in triplicate. *No melting point was definable.

ATA / variant	**Melting Point (T_M) [°C]**		
IPA concentration [M]	0	0.05	0.5
Cvi-TA	76.2 ± 0.05	76.6 ± 0.04	77.0 ± 0.02
Spo-TA	66.9 ± 0.03	61.0 ± 0.02	56.3 ± 0.13
3FCR-wt	56.6 ± 0.07	55.7 ± 0.06	53.6 ± 0.14
3FCR-QM	61.5 ± 0.3	56.9 ± 0.1	51.8 ± 0.1
3FCR-QM-W59L	65.0 ± 0.2	54.4 ± 0.1	52.6 ± 0.1
3FCR-QM-R420A	68.6 ± 0.3	53.0 ± 0.2	50.3 ± 0.2
3FCR-QM-R420W	70.2 ± 0.1	-*	46.8 ± 0.2

Initial activity assay after incubation with IPA

Stability experiments should performed by incubating chosen ATA with IPA and quantifying the residual activity by the Acetophenone assay. Pre-tests revealed a drastic influence of IPA on the apparent activity of the tested ATA, indicating a competitive effect of the two amine donors (PEA and IPA, Fig. S4). To ensure the usability of the Acetophenone assay in this experiment a solvent change was done after incubation with IPA and prior activity measuring via PD-10 columns® (Fig. S5).

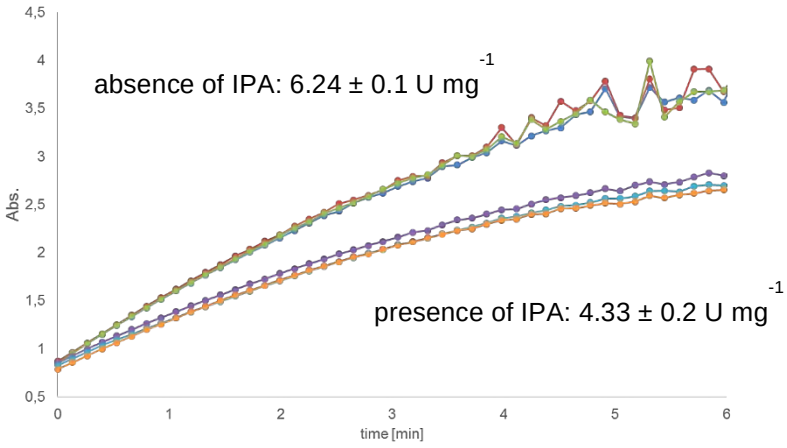

Fig. S5. Initial activity measurement via the Acetophenone assay in presence or absence of IPA (~10-fold excess related to (*S*)-PEA). Exemplary Spo-TA was used. The formation of acetophenone was monitored at 245 nm. Reaction conditions: 0.05 mg mL^{-1} purified enzyme, 1.25 mM (*S*)-PEA/pyruvate, 0.5% (v/v) DMSO, CHES pH 9 (50 mM), 10 mM IPA, 30 °C. Measurement were performed in triplicate.

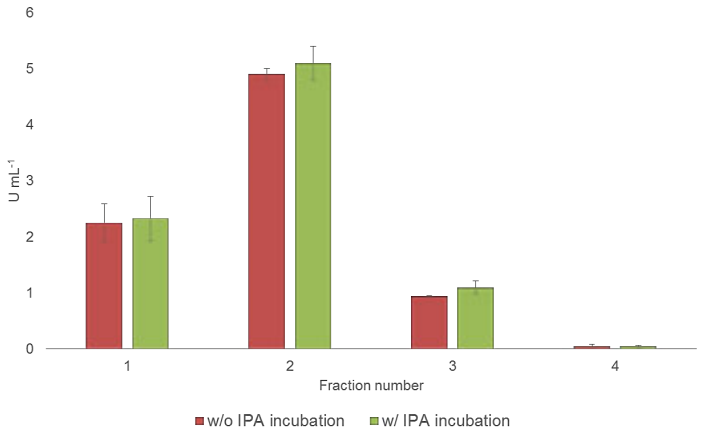

Fig. S6. Samples of Spo-TA with and without IPA (0.5 M final concentration) were subjected to a solvent change via the PD-columns® (according to the manual) and fractions of 0.5 mL were taken. Initial activity of each fraction was measured via the Acetophenone assay as described above and are given in volumetric activities. Incubation conditions: 1 mg mL^{-1} purified enzyme in CHES pH 9 (50 mM), IPA concentration as indicated.

Literature

[1] M. S. Weiß, I. V. Pavlidis, C. Vickers, M. Höhne, U. T. Bornscheuer, *Anal. Chem.* **2014**, *86*, 11847–53.
[2] S. Schätzle, M. Höhne, E. Redestad, K. Robins, U. T. Bornscheuer, *Anal. Chem.* **2009**, *81*, 8244–8248.
[3] M. Davies, *Analyst* **1959**, *84*, 248–251.

Article III

ChemPubSoc Europe

DOI: 10.1002/chem.201804366

CHEMISTRY A European Journal Communication

Cross-Coupling

Combination of the Suzuki–Miyaura Cross-Coupling Reaction with Engineered Transaminases

Ayad W. H. Dawood,[a] Jonathan Bassut,[b] Rodrigo O. M. A. de Souza,[b] and Uwe T. Bornscheuer*[a]

Abstract: The combination of enzymatic and chemical reaction steps is one important area of research in organic synthesis, preferentially as cascade reactions in one-pot to improve total conversion and achieve high operational stability. Here, the combination of the Suzuki–Miyaura reaction is described to synthesize biaryl compounds followed by a transamination reaction. Careful optimization of the reaction conditions required for the chemo- and biocatalysis reaction enabled an efficient two-step-one-pot reaction yielding the final chiral amines with excellent optical purity (>99% *ee*) in up to 84% total conversion. Key to the success was the protein engineering of the amine transaminases from *Asperguillus fumigatus* (4CHI-TA) where single alanine mutations increased the conversion up to 2.3-fold. Finally, the transfer to a continuous flow system after immobilization of the best 4CHI-TA variant is demonstrated.

In the last few decades enzymes played an increasing role as catalysts in organic chemistry. The access to a large number of compounds or intermediates in pharmaceutical and chemical industries has been realized by the utilization of for example, reductases, hydrolases, oxygenases, dehalogenases or transaminases.[1] Enzymatic routes are an environmentally benign alternative to classical chemical synthesis strategies because of their mild and less waste intensive operation conditions.[2] Nevertheless, the application of enzymes in synthetic chemistry suffers very often from limitations for example, in operational stability, substrate scope and stereo- or regioselectivity which of course hampers the industrial relevance of a biocatalyst.[3] To address these limitations enzyme engineering became a highly relevant field of organic chemistry and more recently to combine also chemo- and biocatalysis in the form of cascades, preferentially in one-pot-reactions.[4]

Transaminases (TA) are certainly one of the most versatile and widely used biocatalysts for the production of chiral amines which are important compounds or building blocks for the pharmaceutical and agrochemical industry.[5] TAs catalyze the transfer of an amine group from an amine donor to a ketone or aldehyde acceptor, following a Ping–Pong Bi–Bi reaction mechanism utilizing pyridoxal-5′-phosphate (PLP) as cofactor. TAs are grouped into the fold types I and IV of PLP-dependent enzymes which is at the same time the basis for the classification of their stereoselectivity. The substrate recognition is ensured by two binding pockets: a small one, naturally only able to accommodate a methyl or ethyl group and a large one, with space for, for example, a phenyl or a carboxyl moiety. Additionally they are divided into six subclasses, depending on the natural substrate and the position of the transferred amine group and/or carboxyl moiety.[6] Amine transaminases (ATAs), a subgroup of ω-TAs (class III transaminase family), are of special interest for the chemo-enzymatic application. ATAs tolerate substrates without a carboxyl moiety and therefore a wide range of ketones and aldehydes. Hence, in the last decade ATAs became very attractive targets for enzyme engineering mainly with the aim to enlarge the small binding pocket in order to allow the acceptance of sterically more demanding substrates.[5,7]

The Suzuki–Miyaura cross-coupling reaction has received increasing attention over the last two decades mainly because of the access to biaryl compounds and the introduction of functional groups.[8–10] This type of transition-metal-dependent reaction catalyzes the C–C-bond formation between halides and boronic acids under transmetalation as key reaction step. Originally the Suzuki–Miyaura reaction was performed in organic solvents and employed phosphine ligands to reduce the metal catalyst to the active Pd^0 species which often meant that the Pd catalyst was water and air sensitive.[8,11] Very intensive research in this field generated a great number of reports where the Suzuki–Miyaura reaction took place in phosphine-free and water-solvent systems in order to address the demands of green chemistry.[8,10,12–16] Especially the compatibility of the Suzuki–Miyaura reaction with water was meaningful because water is one of the most attractive solvents in terms of costs, availability, toxicity, safety and environmental protection.[8,10,13] One beneficial aspect for the field of biocatalysis is certainly the "enzyme-compatibility" of water as "natural solvent". First successful one-pot-chemo-enzymatic approaches

[a] A. W. H. Dawood, Prof. Dr. U. T. Bornscheuer
Dept. of Biotechnology & Enzyme Catalysis
Institute of Biochemistry, Greifswald University
Felix-Hausdorff-Str. 4, 17487 Greifswald (Germany)
E-mail: uwe.bornscheuer@uni-greifswald.de
Homepage: http://biotech.uni-greifswald.de

[b] Dr. J. Bassut, Prof. Dr. R. O. M. A. de Souza
Biocatalysis and Organic Synthesis Group, Institute of Chemistry
Federal University of Rio de Janeiro (Brazil)

Supporting information and the ORCID identification number(s) for the author(s) of this article can be found under:
https://doi.org/10.1002/chem.201804366.

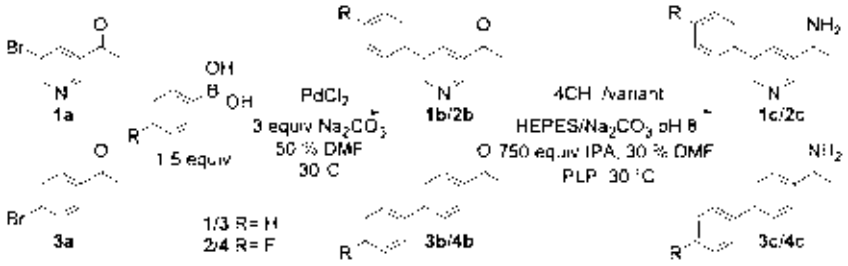

Scheme 1. Starting from aryl halides chiral biaryl amines could be obtained by the sequential order of Suzuki–Miyaura and ATA reaction. The crude Suzuki–Miyaura reaction product was diluted with an ATA/IPA/PLP-containing solution achieving the final conditions for the ATA reaction. Molar equivalents were given in relation to **1a** and **3a**.

combining Suzuki–Miyaura reaction and enzymes included the activity of an alcohol dehydrogenase,[17–19] whereby Burda et al. and Borchert et al. gained the chiral biaryl-alcohol through asymmetric synthesis with very good conversion and enantiomeric excess values (91–97%, >99% *ee*).[18,19] Furthermore, Ahmad et al. produced bi-phenylalanine via the involvement of a phenylalanine ammonia lyase prior to the cross-coupling reaction.[20] Interestingly, France et al. included both, enzymatic transamination via ATA013 and Suzuki–Miyaura reaction, to facilitate their route to dibenzazepines.[21] However, the latter work contained intermediate purification steps and solvent changes and therefore did not met our targeted reaction compatibility and the envisaged benefits of a one-pot reaction setup.

Inspired from those works we considered the approach of a compatible combination of a cross-coupling reaction with a transamination reaction as evident.

Thus, we present a successful two-step-one-pot-reaction including a ligand-free, palladium-catalyzed Suzuki–Miyaura cross-coupling combined with an engineered ATA activity to obtain chiral biaryl amines.

Reports of phosphine-free palladium-catalyzed Suzuki–Miyaura reactions usually contained the replacement of the original ligand with other stabilizing additives or activating supports, such as palladium on carbon (Pd/C)[22] or mesoporous silica,[23] ethylene glycol or EDTA.[14,15,24] Also water-soluble ligands on phosphine basis were presented (see ref. [18,25]). Interestingly, we found several works which showed a simplified ligand-free application of the Suzuki–Miyaura reaction in *N*,*N*-dimethylformamide (DMF)/water mixtures and/or in the presence of an inorganic base.[12,16,22,26] Liu et al. underlined the robustness of their method for the fast reaction of aryl bromides with arylboronic acids at ambient temperature and in the presence of water and air.[16] DMF/water mixtures were a good starting point for our claim of ATAs compatibility. Recently, we reported the successful production of chiral halogenated amines in DMF/water mixtures using the ATA from *Aspergillus fumigatus* (4CHI-TA) and *Silicibacter pomeroyi*.[27] We chose four biphenyl model compounds which cover several aspects regarding position and substitution of the biphenyl moiety as well as the presence of heterocycles (Scheme 1). Starting with the aryl bromides 5-bromo-3-acetyl-pyridine (**1a**) as well as 4′-bromoacetophenone (**3a**) and (fluoro-substituted) arylboronic acids we were able to synthesize the desired biphenyl ketones **1b**–**4b** with very good conversion according to the mentioned method from Liu et al. using sodium carbonate[14,19,28] as activating base and using free $PdCl_2$ as catalyst (Table S1, Figure S2, Supporting Information). However, after attempts to convert **3a** to **3b** failed in the presence of buffer traces and PLP, we considered the part of the cross-coupling reaction as a determining factor in our setup (Table S2). Simultaneously, we examined the ATA reaction part in terms of reaction conditions (presence or absence of reactants or reagents of the Suzuki–Miyaura reaction) and acceptance of sterically demanding biphenyl ketones. We tested the ATAs mentioned above with 4-acetyl-biphenyl (**3b**) and 1-(1,1′-biphen-4-yl)-ethanamine (**3c**) and indeed 4CHI-TA turned out as interesting candidate with good starting activity (Table 1). Moreover, the activity of 4CHI-TA revealed as quite robust in the presence of DMF, sodium carbonate, $PdCl_2$ and even in the absence of buffer reagents (Figure S5 and S6, Supporting Information). So, we decided to

Table 1. Comparison of 4CHI-TA variants in the synthesis of biphenyl amines **1c**–**4c** with isopropylamine (IPA) as amine donor. The ATA reaction was initiated after the Suzuki–Miyaura cross-coupling reaction by adding of ATA crude lysate and IPA/PLP-containing reaction solution (Scheme 1).

ATA/ variant	Substrate conversion [%][a]			
	1b	2b	3b	4b
4CHI-wt	38.5±3.8	39.7±4.2	38.9±1.6	27.2±2.4
4CHI-H53A	45.6±3.2	48.6±3.1	21.6±2.7	27.1±2.5
4CHI-F113A	72.5±1.0	75.0±2.6	19.2±2.9	18.4±2.5
4CHI-R126A	37.6±2.7	18.2±2.8	46.8±3.1	35.7±2.8
4CHI-I146A	87.5±1.4	79.1±3.7	23.6±3.4	14.8±2.0
4CHI-F113A-I146A	83.8±4.2	79.8±3.5	17.4±3.2	17.4±4.2

[a] Assay conditions for the asymmetric synthesis (final concentrations): 1 mM ketone (**1b**–**4b**), 0.75 M IPA, 30% (v/v) DMF, HEPES/Na_2CO_3 buffer (27 mM) pH 10, 0.1 mM PLP, 30 °C, 0.37–6.79 U mL^{-1} of ATA (crude cell lysate with overexpressed ATA, given activities refer to (*R*)-PEA as amine donor and pentanal as amine acceptor). Because of fluctuations in activity in the acetophenone assay obtained after mutagenesis, the expression level was also checked via SDS-PAGE (Figure S1, Supporting Information). Samples were taken in triplicate from three parallel reactions. Conversion was determined after 20 h via gas chromatography (GC) with 2-iodoacetophenone as internal standard for the quantification of ATA-substrate consumption (**1b**–**4b**). Corresponding amines were identified via GC/MS. Retention times for all compounds are given in Table S3 and enantiomeric excess values for **3c** in Table S5.

design our reaction setup accordingly, namely to start with the Suzuki–Miyaura cross-coupling reaction to produce the biphenyl ketones **1b**–**4b** and perform the transamination reaction subsequently by addition of a solution containing the amine donor, PLP and 4CHI-TA (Scheme 1, Table 1). We used isopropylamine (IPA) as amine donor, because it is certainly one of the most favored amine donors for asymmetric syntheses since it is cheap, achiral (the enantioselectivity of the used ATA has not to be considered) and a co-product removal is not critical in contrast to the usage of alanine. 4CHI-TA wild type showed indeed quite well starting activity for all investigated biphenyl ketones **1b**–**4b** but conversion did not exceed 40% in any case.

We performed in silico studies to identify possible amino acid residues around the active site of 4CHI-TA which might hamper the acceptance of bulky biphenyls. Molecular docking studies indicated in total four amino acid residues in the large binding pocket (or at the interface between the large and the small one) of 4CHI-TA which possibly cause interferences with the substrates: H53, F113, R126 and I146 (according to the PDB numbering, see Figure S7). Alanine variants were produced via the *QuikChange* protocol to generate more space at the respective position in the active site. The application of the 4CHI variants in the asymmetric synthesis of amines **1c**–**4c** showed in fact a remarkable effect of mutations F113A and I146A for the conversion of compounds **1b** and **2b**. For both substrates high conversion values of 72–75% with 4CHI-F113A as well as 79–87.5% with 4CHI-I146A could be reached keeping in mind that a single alanine mutation was sufficient in both cases to double total conversion. The "flipping arginine" in 4CHI, R126[29] obviously plays a slight detrimental role for the acceptance of **3b** and **4b** but the exchange to alanine did not achieve the desired impact.

In fact, this highly conserved residue is supposed to be very flexible because it is known to facilitate the dual substrate recognition of transaminases by salt bridge formation to the carboxylate function of respective substrates. On the other hand it has to "flip out" when hydrophobic substrates need to be coordinated.[6,30] So, by a simple replacement of this residue sustainable effects on the activity towards bulky substrates are probably not expectable. In contrast to the in silico indication the mutation of H53 had a rather detrimental effect on the synthesis of **3c** and **4c** and only a slight improving effect on substrates **1b** and **2b**. In response to the results shown in Table 1 a double mutant of 4CHI-TA containing the mutations F113A and I146A was produced in the hope to further increase the conversion, but no significant difference in conversion could be detected in comparison to each single mutant (Table 1). The excellent stereoselectivity of 4CHI-TA wild type and the variants was confirmed for amine **3c**, whereby in any case an enantiomeric excess of $>99\%$ *ee* was reached (Table S5, Supporting Information). This was indeed not unexpected because the small binding pocket was not changed and additionally the demand on the large binding pocket was even increased by substrates **1b**–**4b**. Therefore, changes in enantioselectivity were indeed considered unlikely.

Having improved biocatalysts and a compatible reaction system for the combination of the Suzuki–Miyaura coupling and the ATA reaction established, we next transferred this to a continuous flow system as exemplified for the production of **1c**. A large variety of flow systems were already reported in the field of biocatalysis in general, but also for the production of biaryl compounds via the Suzuki–Miyaura reaction since continuous reaction systems have several advantages in terms of economic aspects for example, the increase of the space–time–yield, lowering of reaction times and decreased waste production.[31] Another aspect is the possible compartmentalization of several sub-reactions. For such processes, efficient immobilization of the enzyme becomes significant. Several reports dealt with the successful immobilization of ATAs using different supports (e.g., chitosan,[32] functionalized cellulose,[33] polystyrene[34] or methacrylate beads[35] as well as concepts for the co-immobilization of the cofactor PLP.[35,36] For our example here, the immobilization via metal affinity resins[37] was choosen because this is a convenient method for the immobilization of recombinant proteins without pre-treatment or activating of supports with for example, cross-linking agents. At the same time, it allows a more specific loading with the recombinant target protein. We decided to use EziG™ carriers[38] and ran initial experiments regarding efficiency, selectivity and stability of the 4CHI-TA-immobilisates: 10 U g^{-1} support were reached and no enzyme leaching was found in the presence of 30% DMF (Figure S8 and S9, Supporting Information). The reaction setup for the continuous flow experiment is shown in Scheme 2. The two reaction solutions—first, the crude Suzuki–Miyaura reaction mixture producing **1b** and second an IPA/PLP-containing solution—were pumped synchronically through a column with the immobilized variant 4CHI-I146 resulting in a total conversion of 43% from **1a** to **1c** representing a proof-of principle study.

Herein, we presented the access to chiral biaryl amines via the combination of the Suzuki–Miyaura cross-coupling with a transaminase-catalyzed reaction under ligand-free and mild conditions. Major achievements were the excellent compatibility of chemo- and biocatalysis to achieve the cross-coupling reaction in the presence of oxygen and DMF-water mixtures while maintaining high robustness of the 4CHI-TA in the presence of reagents required for the Suzuki–Miyaura reaction. Furthermore, the starting activity of the (*R*)-selective 4CHI-TA towards biaryl ketones could be increased up to 2.3-fold (substrate **1b** and 4CHI-I146A) by simple alanine mutations of four amino acid residues around the active site as derived from in silico studies. This complements a recent example for the engineering of the (*S*)-selective ATA from *Vibrio fluvialis* to accept biphenyl ketone substrates.[39] Our concept to use the biaryl cross-coupling products directly for the transamination reaction represents certainly a great advantage as amine group protection strategies could be avoided (free amines are known as Pd-chelating functional groups). Additionally, a Suzuki–Miyaura reaction with *N*-protected educts is known to be less effective.[13] In addition, we provided a proof-of-concept for a transfer of the system to continuous flow conditions.

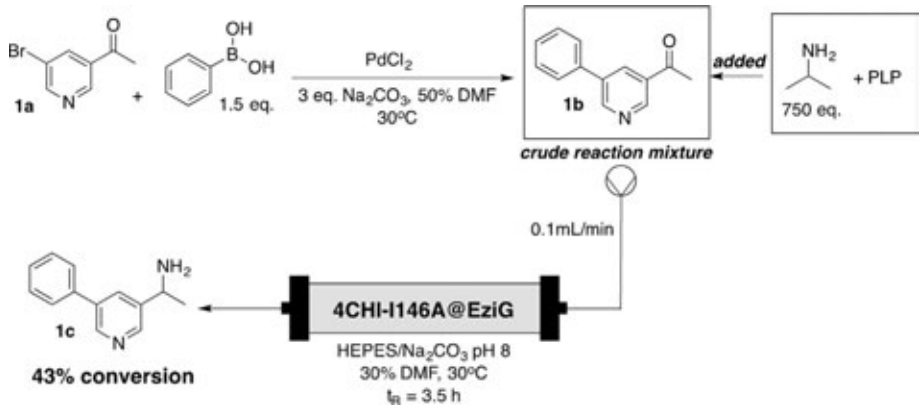

Scheme 2. Setup of the continuous flow synthesis of 1-(5-phenylpyridin-3-yl)ethanamine **1 c**. Molar equivalents are given in relation to **1 a**. The crude Suzuki–Miyaura reaction product was added in flow to an IPA and PLP containing solution and subsequently pumped through a column containing the immobilized variant 4CHI-I146A at a flow rate of 0.1 mL h^{-1}. After pumping 0.45 mL, samples for GC analysis were withdrawn. The conversion was calculated on the basis of ATA substrate conversion (1-(5-phenylpyridin-3-yl)ethanone **1 b**) and set in relation to a blank experiment with empty carrier instead of immobilisate.

Acknowledgements

We thank the Bundesministerium für Bildung und Forschung (Grant 01DN14016) for financial support. Prof. Dr. de Souza thanks the Alexander-von-Humboldt foundation for a CAPES-Humboldt research fellowship.

Conflict of interest

The authors declare no conflict of interest.

Keywords: amine transaminases · cross-coupling · enzyme engineering · enzyme immobilization · Suzuki–Miyura

[1] a) B. M. Nestl, S. C. Hammer, B. A. Nebel, B. Hauer, *Angew. Chem. Int. Ed.* **2014**, *53*, 3070 – 3095; *Angew. Chem.* **2014**, *126*, 3132 – 3158; b) O. Pàmies, J.-E. Bäckvall, *Chem. Rev.* **2003**, *103*, 3247 – 3262.

[2] a) U. T. Bornscheuer, G. W. Huisman, R. J. Kazlauskas, S. Lutz, J. C. Moore, K. Robins, *Nature* **2012**, *485*, 185 – 194; b) M. Höhne, U. T. Bornscheuer, *ChemCatChem* **2009**, *1*, 42 – 51.

[3] M. T. Reetz, *J. Am. Chem. Soc.* **2013**, *135*, 12480 – 12496.

[4] F. Rudroff, M. D. Mihovilovic, H. Gröger, R. Snajdrova, H. Iding, U. T. Bornscheuer, *Nat. Catal.* **2018**, *1*, 12 – 22.

[5] a) K. S. Midelfort, R. Kumar, S. Han, M. J. Karmilowicz, K. McConnell, D. K. Gehlhaar, A. Mistry, J. S. Chang, M. Anderson, A. Villalobos, *Protein Eng. Des. Sel.* **2013**, *26*, 25 – 33; b) M. Fuchs, D. Koszelewski, K. Tauber, W. Kroutil, K. Faber, *Chem. Commun.* **2010**, *46*, 5500 – 5502; c) M. Fuchs, D. Koszelewski, K. Tauber, J. Sattler, W. Banko, A. K. Holzer, M. Pickl, W. Kroutil, K. Faber, *Tetrahedron Lett.* **2012**, *68*, 7691 – 7694; d) S. Pedragosa-Moreau, A. Le Flohic, V. Thienpondt, F. Lefoulon, A.-M. Petit, N. Ríos-Lombardía, F. Morís, J. González-Sabín, *Adv. Synth. Catal.* **2017**, *359*, 485 – 493.

[6] a) F. Steffen-Munsberg, C. Vickers, H. Kohls, H. Land, H. Mallin, A. Nobili, L. Skalden, T. van den Bergh, H.-J. Joosten, P. Berglund, *Biotechnol. Adv.* **2015**, *33*, 566 – 604; b) N. V. Grishin, M. A. Phillips, E. J. Goldsmith, *Protein Sci.* **1995**, *4*, 1291 – 1304.

[7] a) C. K. Savile, J. M. Janey, E. C. Mundorff, J. C. Moore, S. Tam, W. R. Jarvis, J. C. Colbeck, A. Krebber, F. J. Fleitz, J. Brands, *Science* **2010**, *329*, 305 – 309; b) A. Nobili, F. Steffen-Munsberg, H. Kohls, I. Trentin, C. Schulzke, M. Höhne, U. T. Bornscheuer, *ChemCatChem* **2015**, *7*, 757 – 760; c) M. Genz, O. Melse, S. Schmidt, C. Vickers, M. Dörr, T. van den Bergh, H.-J. Joosten, U. T. Bornscheuer, *ChemCatChem* **2016**, *8*, 3199 – 3202; d) I. V. Pavlidis, M. S. Weiß, M. Genz, P. Spurr, S. P. Hanlon, B. Wirz, H. Iding, U. T. Bornscheuer, *Nat. Chem.* **2016**, *8*, 1076 – 1082; e) B.-K. Cho, H.-Y. Park, J.-H. Seo, J. Kim, T.-J. Kang, B.-S. Lee, B.-G. Kim, *Biotechnol. Bioeng.* **2008**, *99*, 275 – 284; f) K. Deepankumar, S. P. Nadarajan, S. Mathew, S.-G. Lee, T. H. Yoo, E. Y. Hong, B.-G. Kim, H. Yun, *ChemCatChem* **2015**, *7*, 417 – 421; g) S.-W. Han, E.-S. Park, J.-Y. Dong, J.-S. Shin, *Adv. Synth. Catal.* **2015**, *357*, 2712 – 2720; h) S.-W. Han, E.-S. Park, J.-Y. Dong, J.-S. Shin, *Adv. Synth. Catal.* **2015**, *357*, 1732 – 1740; i) M. S. Weiß, I. V. Pavlidis, P. Spurr, S. P. Hanlon, B. Wirz, H. Iding, U. T. Bornscheuer, *Org. Biomol. Chem.* **2016**, *14*, 10249 – 10254; j) M. S. Weiß, I. V. Pavlidis, P. Spurr, S. P. Hanlon, B. Wirz, H. Iding, U. T. Bornscheuer, *ChemBioChem* **2017**, *18*, 1022 – 1026.

[8] R. Franzén, Y. Xu, *Can. J. Chem.* **2005**, *83*, 266 – 272.

[9] a) N. Miyaura, A. Suzuki, *Chem. Rev.* **1995**, *95*, 2457 – 2483; b) N. Miyaura, T. Yanagi, A. Suzuki, *Synth. Commun.* **1981**, *11*, 513 – 519; c) F. Bellina, A. Carpita, R. Rossi, *Synthesis* **2004**, 2419 – 2440; d) C. Bolm, *Org. Lett.* **2012**, *14*, 2925 – 2928.

[10] C.-J. Li, *Chem. Rev.* **2005**, *105*, 3095 – 3166.

[11] a) J. P. Wolfe, R. A. Singer, B. H. Yang, S. L. Buchwald, *J. Am. Chem. Soc.* **1999**, *121*, 9550 – 9561; b) L. Wu, Z.-W. Li, F. Zhang, Y.-M. He, Q.-H. Fan, *Adv. Synth. Catal.* **2008**, *350*, 846 – 862.

[12] a) G. A. Grasa, A. C. Hillier, S. P. Nolan, *Org. Lett.* **2001**, *3*, 1077 – 1080; b) C. W. K. Gstöttmayr, V. P. W. Böhm, E. Herdtweck, M. Grosche, W. A. Herrmann, *Angew. Chem. Int. Ed.* **2002**, *41*, 1363 – 1365; *Angew. Chem.* **2002**, *114*, 1421 – 1423; c) N. Shahnaz, B. Banik, P. Das, *Tetrahedron Lett.* **2013**, *54*, 2886 – 2889; d) D. Badone, M. Baroni, R. Cardamone, A. Ielmini, U. Guzzi, *J. Org. Chem.* **1997**, *62*, 7170 – 7173; e) N. A. Bumagin, D. N. Korolev, *Tetrahedron Lett.* **1999**, *40*, 3057 – 3060; f) N. A. Bumagin, *Catal. Commun.* **2016**, *79*, 17 – 20; g) T. I. Wallow, B. M. Novak, *J. Org. Chem.* **1994**, *59*, 5034 – 5037; h) T. Huang, C.-J. Li, *Tetrahedron Lett.* **2002**, *43*, 403 – 405; i) S. Venkatraman, T. Huang, C.-J. Li, *Adv. Synth. Catal.* **2002**, *344*, 399 – 405; j) C.-J. Li, *Acc. Chem. Res.* **2002**, *35*, 533 – 538; k) P. Sharma, A. Singh, *Catal. Sci. Technol.* **2014**, *4*, 2978 – 2989; l) S. Jindabot, K. Teerachanan, P. Thongkam, S. Kiatisevi, T. Khamnaen, P. Phiriyawirut, S. Charoenchaidet, T. Sooksimuang, P. Kongsaeree, P. Sangtrirutnugul, *J. Organomet. Chem.* **2014**, *750*, 35 – 40.

[13] C. A. Fleckenstein, H. Plenio, *Chem. Eur. J.* **2008**, *14*, 4267 – 4279.

[14] D. N. Korolev, N. A. Bumagin, *Tetrahedron Lett.* **2005**, *46*, 5751 – 5754.

[15] J. Zhang, W. Zhang, Y. Wang, M. Zhang, *Adv. Synth. Catal.* **2008**, *350*, 2065 – 2076.

[16] C. Liu, Q. Ni, F. Bao, J. Qiu, *Green Chem.* **2011**, *13*, 1260 – 1266.

[17] a) A. Prastaro, P. Ceci, E. Chiancone, A. Boffi, R. Cirilli, M. Colone, G. Fabrizi, A. Stringaro, S. Cacchi, *Green Chem.* **2009**, *11*, 1929; b) V. Gauchot, W. Kroutil, A. R. Schmitzer, *Chem. Eur. J.* **2010**, *16*, 6748 – 6751.

[18] E. Burda, W. Hummel, H. Gröger, *Angew. Chem. Int. Ed.* **2008**, *47*, 9551 – 9554; *Angew. Chem.* **2008**, *120*, 9693 – 9696.

[19] S. Borchert, E. Burda, J. Schatz, W. Hummel, H. Gröger, *J. Mol. Catal. B* **2012**, *84*, 89 – 93.

[20] S. T. Ahmed, F. Parmeggiani, N. J. Weise, S. L. Flitsch, N. J. Turner, *ACS Catal.* **2015**, *5*, 5410 – 5413.
[21] S. P. France, G. A. Aleku, M. Sharma, J. Mangas-Sanchez, R. M. Howard, J. Steflik, R. Kumar, R. W. Adams, I. Slabu, R. Crook, *Angew. Chem. Int. Ed.* **2017**, *56*, 15589 – 15593; *Angew. Chem.* **2017**, *129*, 15795 – 15799.
[22] G. Zhang, *Synthesis* **2005**, 537 – 542.
[23] Q. Yang, S. Ma, J. Li, F. Xiao, H. Xiong, *Chem. Commun.* **2006**, 2495 – 2497.
[24] T. Maegawa, Y. Kitamura, S. Sako, T. Udzu, A. Sakurai, A. Tanaka, Y. Kobayashi, K. Endo, U. Bora, T. Kurita, *Chem. Eur. J.* **2007**, *13*, 5937 – 5943.
[25] V. Polshettiwar, A. Decottignies, C. Len, A. Fihri, *ChemSusChem* **2010**, *3*, 502 – 522.
[26] a) J. Qiu, L. Wang, M. Liu, Q. Shen, J. Tang, *Tetrahedron Lett.* **2011**, *52*, 6489 – 6491; b) Z. Li, C. Gelbaum, W. L. Heaner, J. Fisk, A. Jaganathan, B. Holden, P. Pollet, C. L. Liotta, *Org. Process Res. Dev.* **2016**, *20*, 1489 – 1499; c) Z. Li, C. Gelbaum, J. S. Fisk, B. Holden, A. Jaganathan, G. T. Whiteker, P. Pollet, C. L. Liotta, *J. Org. Chem.* **2016**, *81*, 8520 – 8529; d) N. A. Bumagin, V. V. Bykov, *Tetrahedron Lett.* **1997**, *53*, 14437 – 14450.
[27] A. W. H. Dawood, R. O. M. A. de Souza, U. T. Bornscheuer, *ChemCatChem* **2018**, *10*, 951 – 955.
[28] a) L. Liu, Y. Dong, N. Tang, *Green Chem.* **2014**, *16*, 2185 – 2189; b) A. N. Marziale, D. Jantke, S. H. Faul, T. Reiner, E. Herdtweck, J. Eppinger, *Green Chem.* **2011**, *13*, 169 – 177.
[29] L. Skalden, M. Thomsen, M. Höhne, U. T. Bornscheuer, W. Hinrichs, *FEBS J.* **2015**, *282*, 407 – 415.
[30] F. Steffen-Munsberg, C. Vickers, A. Thontowi, S. Schätzle, T. Meinhardt, M. Svedendahl Humble, H. Land, P. Berglund, U. T. Bornscheuer, M. Höhne, *ChemCatChem* **2013**, *5*, 154 – 157.
[31] a) N. G. Anderson, *Org. Process Res. Dev.* **2012**, *16*, 852 – 869; b) J. Britton, S. Majumdar, G. A. Weiss, *Chem. Soc. Rev.* **2018**, *47*, 5891 – 5918; c) L. van den Biggelaar, P. Soumillion, D. P. Debecker, *Catalysts* **2017**, *7*, 54; d) C. Len, S. Bruniaux, F. Delbecq, V. Parmar, *Catalysts* **2017**, *7*, 146; e) T. Razzaq, C. O. Kappe, *Chem. Asian J.* **2010**, *5*, 1274 – 1289; f) G. Jas, A. Kirschning, *Chem. Eur. J.* **2003**, *9*, 5708 – 5723.
[32] a) H. Mallin, M. Höhne, U. T. Bornscheuer, *J. Biotechnol.* **2014**, *191*, 32 – 37; b) H. Mallin, U. Menyes, T. Vorhaben, M. Höhne, U. T. Bornscheuer, *ChemCatChem* **2013**, *5*, 588 – 593.
[33] S. P. de Souza, I. I. Junior, G. M. Silva, L. S. Miranda, M. F. Santiago, F. L.-Y. Lam, A. Dawood, U. T. Bornscheuer, R. O. de Souza, *RSC Adv.* **2016**, *6*, 6665 – 6671.
[34] W. Neto, M. Schürmann, L. Panella, A. Vogel, J. M. Woodley, *J. Mol. Catal. B* **2015**, *117*, 54 – 61.
[35] L. H. Andrade, W. Kroutil, T. F. Jamison, *Org. Lett.* **2014**, *16*, 6092 – 6095.
[36] S. Velasco-Lozano, A. I. Benıtez-Mateos, F. López-Gallego, *Angew. Chem. Int. Ed.* **2017**, *56*, 771 – 775; *Angew. Chem.* **2017**, *129*, 789 – 793.
[37] J. Britton, R. P. Dyer, S. Majumdar, C. L. Raston, G. A. Weiss, *Angew. Chem. Int. Ed.* **2017**, *56*, 2296 – 2301; *Angew. Chem.* **2017**, *129*, 2336 – 2341.
[38] K. Engelmark Cassimjee, M. Kadow, Y. Wikmark, M. Svedendahl Humble, M. L. Rothstein, D. M. Rothstein, J.-E. Bäckvall, *Chem. Commun.* **2014**, *50*, 9134 – 9137.
[39] D. F. Dourado, S. Pohle, A. T. Carvalho, D. S. Dheeman, J. M. Caswell, T. Skvortsov, I. Miskelly, R. T. Brown, D. J. Quinn, C. C. Allen, *ACS Catal.* **2016**, *6*, 7749 – 7759.

Manuscript received: August 27, 2018
Accepted manuscript online: August 29, 2018
Version of record online: October 4, 2018

CHEMISTRY
A European Journal

Supporting Information

Combination of the Suzuki–Miyaura Cross-Coupling Reaction with Engineered Transaminases

Ayad W. H. Dawood,[a] Jonathan Bassut,[b] Rodrigo O. M. A. de Souza,[b] and Uwe T. Bornscheuer*[a]

chem_201804366_sm_miscellaneous_information.pdf

Table of content

Experimental Section

All chemicals and kits were purchased either from Sigma Aldrich (Darmstadt, Germany) or Acros/Thermo Fisher Scientific (Waltham, USA) in analytical grade unless stated otherwise.

Suzuki-Miyaura-cross coupling reaction

2 mM (final concentration) of starting material **1a** and **3a** as well as 1.5 eq. of phenyl boronic acid or the fluorinated derivative, respectively were dissolved in DMF. Distilled water containing 3 eq. of Na_2CO_3 were added leading to a final DMF concentration of 50%. The reaction was started by adding of 0.1 eq. $PdCl_2$ stored in DMF. Negative controls were performed by adding DMF instead of $PdCl_2$. The reaction vessels were incubated at 30 °C for 2 h under agitation. The reaction monitoring was done via gas chromatography (GC). The crude reaction mixture was immediately used for biotransformation reactions after incubation.

Enzyme expression, cell lysis and protein purification

The gene encoding the ATA from *Aspergillus fumigatus* Af293 was cloned in a pET22b vector. The protein expression was done in Terrific Broth (TB) media with 100 µg mL^{-1} ampicillin at 160 rpm and 20°C. After the optical density at 600 nm (OD_{600}) reached 0.5–0.7, expression was induced by adding 0.2 mM isopropyl β -D-1-thiogalactopyranoside (final concentration). After 18 h the cultures were centrifuged (4,000 x *g*, 15 min, 4 °C) and washed with lysis buffer (HEPES (50 mM pH 7.5), 0.1 mM PLP, 300 mM sodium chloride). Cell disruption was performed via sonication using the Bandelin Sonoplus HD 2070 (8 min, 50% pulsed cycle, 50% power) on ice followed by centrifugation in order to remove cell debris (12,000 x *g*, 45 min, 4 °C, Sorvall centrifuge). The supernatant containing the crude ATA was stored at 4 °C until use.

Determination of transaminase activity

The characterization of the ATA was done via the initial activity assay (acetophenone assay) according to Schätzle *et al.*[1] with slight modifications. In the reaction solution the concentrations of the amine donor ((*R*)-1-PEA) and the acceptor pyruvate or pentanal was set to 2 mM in 2–7% (v/v) DMSO. Briefly, 10 µL of a pre-diluted ATA solution was mixed with the respective buffer (CHES buffer or the respective reaction medium as indicated) and the reaction was initiated by the addition of the 4-fold concentrated stock of the reaction solution. The formation of acetophenone was quantified at 245 nm using the Tecan Infinite M200 Pro (Crailsheim, Germany) at 30 °C. One unit (U) of ATA activity was defined as the formation of 1 µ mol of acetophenone per minute (ε= 12 $M^{-1}cm^{-1}$). All measurements were performed in triplicate.

Asymmetric synthesis of amines 1c – 4c

Biotransformations were performed in 0.25 mL scale using 1.5 mL glass vials at 30 °C and 950 rpm shaking. The reaction mixtures contained 100 µL of the crude Suzuki-Miyaura reaction product (1 mM final concentration of the biphenyl ketone), 30% DMF (final concentration) as co-solvent, 0.75 M IPA (from a 4 M IPA-HCl stock solution, pH 7 in HEPES) and Na_2CO_3 solution. The residual concentration of $PdCl_2$ was approx. 70 µM. The final pH was checked (pH 8). Additionally, control experiments with the crude lysate of an empty vector expression instead of enzyme were performed. After 20 h incubation, the reaction was quenched by adding 3 M NaOH (resulting in pH ≥12). Samples for GC analysis were taken immediately after quenching.

GC analysis

Samples of the Suzuki-Miyaura cross-coupling reaction (50 µL) were quenched with 5 µL HCl solution (6 M) and saturated with sodium chloride. Samples were considered as saturated when a pellet was formed. Extraction was performed with 200 µ L methyl *tert*-butyl ether containing 0.5 mM 2'-iodoacetophenone as internal standard for quantification. The organic layers were dried over anhydrous $MgSO_4$ and analyzed immediately using the Hydrodex-ß-TBDAc column (Macherey & Nagel). Biotransformation samples of 100 µ L were quenched with 25 µ L of NaOH solution (3 M) and saturated with sodium chloride. Extraction was performed with 200 µL of methyl *tert*-butyl ether containing the mentioned internal standard. The organic layers were dried over anhydrous $MgSO_4$ and derivatized with *N*-methyl-bis-trifluoroacetamide (MBTFA) by adding 10 µL of the commercial stock solution to 100 µL of organic layer and incubation at 60 °C for 30 min. Afterwards, the samples were analyzed immediately using the mentioned column. For the analysis of the Suzuki-Miyaura cross-coupling reaction the following temperature profile was used: initial temperature 80 °C, kept for 10 min, linear gradient to 160 °C with a slope of 4 °C min^{-1}, linear gradient to 220 °C with a slope of 20 °C min^{-1}, kept for 5 min. For the analysis of biotransformation samples the following temperature profile was established: initial temperature 150 °C, kept for 5 min, linear gradient to 220 °C with a slope of 10 °C min^{-1}, kept for 18 min. For retention times see Table S3. Conversion values were determined by quantification of ketone educt / substrate consumption via calculation of the response factor. Each sample included the mentioned internal standard and was set in relation to ATA-free or catalyst-free control experiments. The chiral GC analysis of amine **3c** was performed with the same column with the following temperature profile: initial temperature 150 °C, kept for 5 min, linear gradient to 190 °C with a slope of 5 °C min^{-1}, kept for 25 min, linear gradient to 195 °C with a slope of 1 °C min^{-1}, linear gradient to 220 °C with a slope of 20 °C min^{-1}, kept for 5 min.

Bioinformatic analyses

Molecular docking studies were performed using *YASARA Structure* (v.17.1.28).[2] The quinoid intermediate (the reactive intermediate in the ATA reaction) consisting of PLP and **1b**/**3b** was modelled by a combination of *ChemDraw*® (v.11) and *YASARA* followed by energy minimization. Prior to the docking experiments a refinement of the lowest energy ligand conformation and the crystal structure 4CHI from the PDB database was performed with the built in macro (YAMBER3 force field at 298 K for 500 ps, standard settings). The applied docking method was the implemented *AutoDock VINA* algorithm with standard settings, which means 100 runs in total and subsequent clustering to give distinct complex conformations. The output was evaluated visually by superposing the docked ligand-receptor complex with the refined, PLP containing crystal structure and checking the coverage of the pyridine ring of the PLP. Usually the best conformation revealed by this way was one of those with the highest binding energy and lowest dissociation constant according to the docking experiment log file. All illustrations were made with *Pymol* (v.1.7)

Production of 4CHI variants via *QuikChange* mutagenesis

Variants of 4CHI-TA were produced using a modified version of the *QuikChange* PCR method. Primers were designed with the desired mismatches to provide the desired mutations. For each PCR, *Pfu* buffer, 0.2 mM dNTPs, 0.2 ng μL^{-1} parental plasmid, 0.5 µM of each primer and 0.4 µL of *Pfu* Plus! DNA polymerase were applied. The amplification was performed as follows: (a) 94 °C, 2 min; (b) 19 cycles: 95 °C, 30 s; 63 °C, 30 s; 72 °C, 7 min (c) 72 °C, 10 min. The PCR product was digested with DpnI (40 µL mL^{-1}) for 2 h at 37 °C and the restriction enzyme was inactivated by incubation at 80 °C for 20 min. Chemo-competent Top10 *E. coli* cells were transformed with the PCR product after verification of an amplification product via agarose gel electrophoresis. The plasmids were isolated from Top10 and the correct sequence was confirmed. Afterwards chemo-competent *E. coli* BL21 (DE3) cells were transformed for protein expression as described above.

ATA immobilization procedure

Commercially available EziG™ carriers were pre-treated with HEPES buffer (50 mM, pH 7.5) containing 0.1 mM PLP and 300 mM sodium chloride at room temperature for 1 h. After careful removal of buffer the crude lysate containing the overexpressed 4CHI-TA variant was added and incubated for 1 h at 4 °C under agitation. After enzyme immobilization the supernatant was discarded. To remove unspecific bounded protein the immobilisate was washed via sequential adding and removal of HEPES buffer containing PLP and sodium chloride. Finally the immobilisate was centrifuged in order to reduce the residual amount of buffer.

Continuous flow reaction

The continuous flow reaction setup was designed as follows: The Suzuki-Miyaura cross-coupling reaction was performed initially as described above. The crude reaction product (the biphenyl ketone **1b**) was pumped simultaneously with an IPA (from a 4 M IPA-HCL-HEPES stock solution) and PLP containing solution into a packed bed reactor (column volume 0.3 mL) filled with immobilized 4CHI-I146A. The flow rate was set to 0.1 mL h^{-1} resulting in a residence time of 3.5 h. Samples were withdrawn after 1.5 column volumes (0.45 mL) and extracted as well as analyzed as described.

SDS-PAGE analysis

Analysis of protein samples was carried out by sodium dodecyl sulfate polyacrylamide gel electrophoresis (SDS-PAGE) with 4% stacking gel and 12.5% resolving gel containing 2,2,2-tri-chloro-ethanol as staining agent. Samples were mixed with 4-fold stock of SDS sample buffer and were denaturated by incubation at 95 °C for 10 min. Unstained protein molecular weight marker (Thermo Scientific, Waltham, MA, USA) was used as reference. Protein staining was done via irradiation with UV light to trigger the fluorescence detection of proteins.

Suzuki-Miyaura-cross coupling reaction of model compounds

Table S1. Synthesis of biphenyl ketones **1b** – **4b** (see Scheme 1, main article) via Suzuki-Miyaura cross-coupling reaction. Reaction conditions: 2 mM (final concentration) of starting material **1a** or **3a**, 1.5 eq. of (fluoro-) phenyl boronic acid, 3 eq. of Na_2CO_3, 50% DMF, 30 °C, 2h. The reaction was started by adding of 0.1 eq. $PdCl_2$. The conversion was determined via gas chromatography (GC) analysis.

Product	Ar-Br	R-Ar-B(OH)$_2$	Conversion [%]
1b	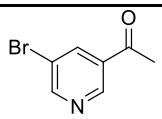	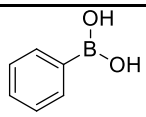	99
2b	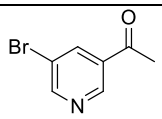	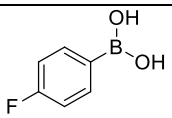	80
3b	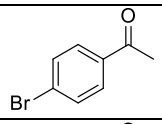	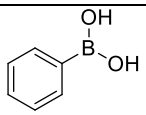	99
4b	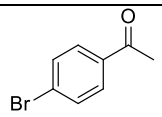	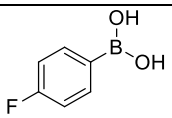	99

Table S2. Investigation of disturbing effects of HEPES/CHES buffer and pyridoxal-5'-phosphate (PLP) in the Suzuki-Miyaura reaction to 4-Acetyl-biphenyl **3b**. For reaction conditions see Table S1. * n.d.: not detectable.

Disturbing factor / concentration [mM]	**Conversion of** 3a **to** 3b **[%]**
HEPES / 50	n.d.*
HEPES / 25	n.d.
HEPES / 12.5	n.d.
CHES / 25	n.d.
CHES / 12.5	n.d.
PLP / 0.05	25

SDS-PAGE of 4CHI-TA variants

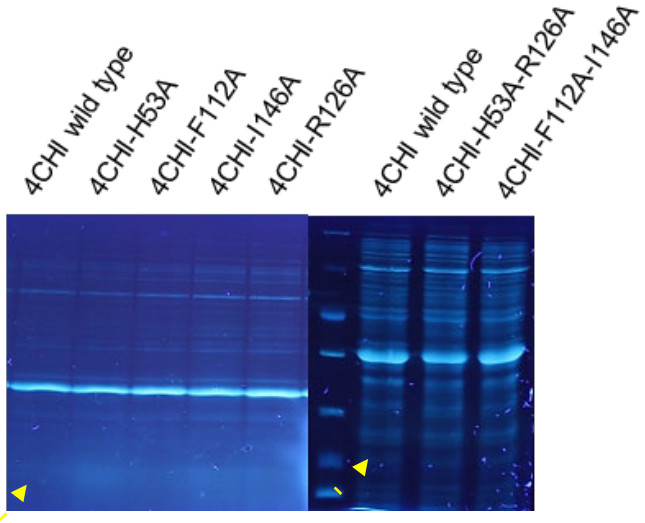

Fig. S1. Samples of overexpressed 4CHI-TA wild type and variants were normalized on the basis of OD_{600}. The soluble fractions after cell lysis were analyzed via SDS-PAGE. The expression level was compared with the wild type expression. The line without annotation contained the molecular weight marker.

Retention times and chromatograms

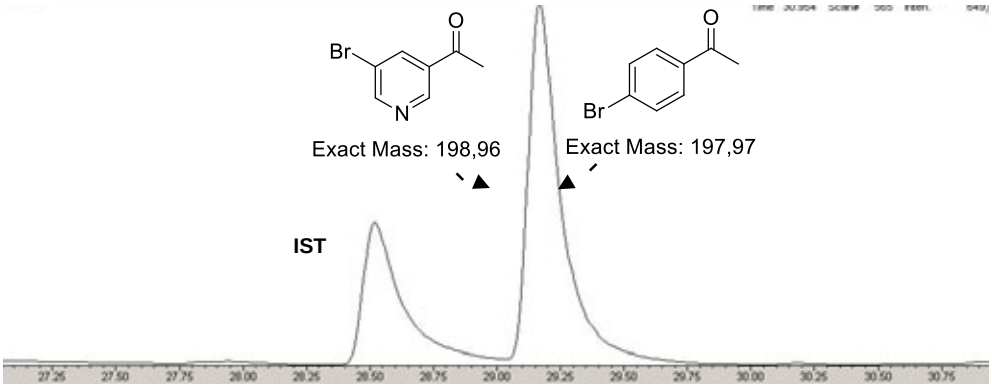

Fig. S2. The determination of conversion in the Suzuki-Miyaura reaction was done via GCMS analysis by calculation of educt consumption. The retention time of both educts **1a** and **2a** (29.2 min) refer to the following temperature profile: initial temperature 80 °C, kept for 10 min, linear gradient to 160 °C with a slope of 4 °C min^{-1}, linear gradient to 220 °C with a slope of 20 °C min^{-1}, kept for 5 min. The GC column Hydrodex-ß-TBDAc (25 m) from Macherey & Nagel was used.

Table S3. Overview of retention times for the biphenyl compounds (ketones and corresponding amines) of the transaminase reaction. Retention times were revealed by GC analysis (for the amines after MBTFA derivatization) and refer to the following temperature profile: initial temperature 150 °C, kept for 5 min, linear gradient to 220 °C with a slope of 10 °C min^{-1}, kept for 18 min. The GC column Hydrodex-ß-TBDAc (25 m) from Macherey & Nagel was used.

Compound / Entry	Retention time [min]	
	Biphenyl ketone (b)	**Amine product (c)**
1b/c	14.3	23.1
2b/c	14.8	23.6
3b/c	13.5	17.1
4b/c	13.8	17.5

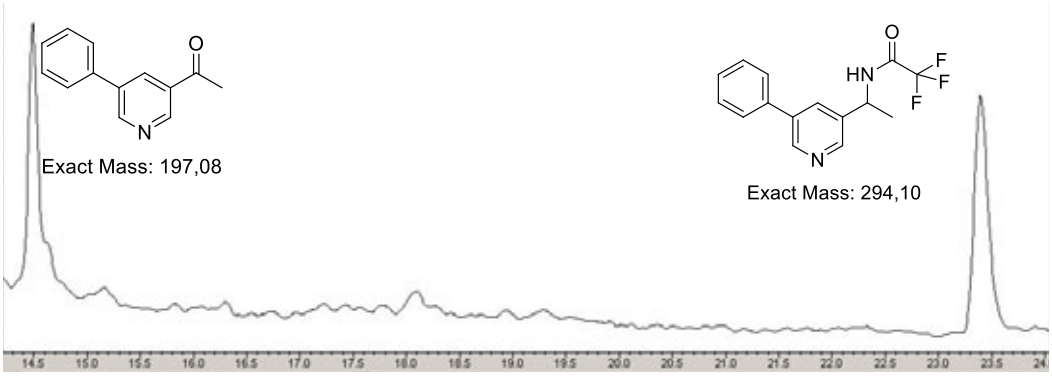

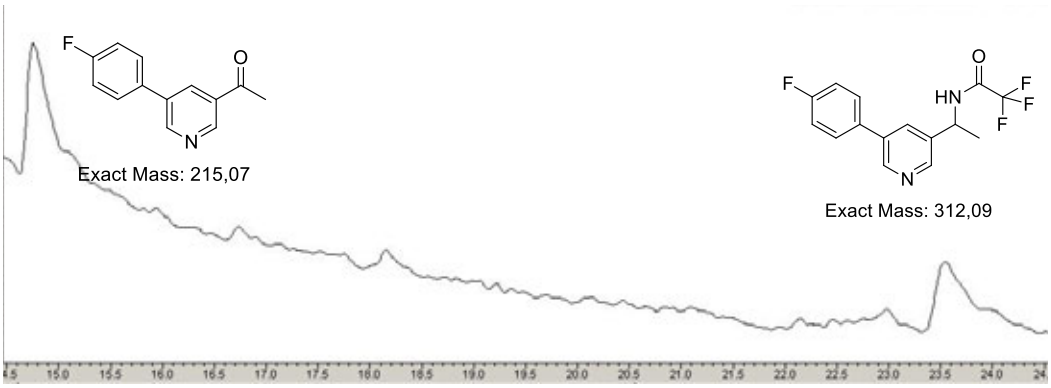

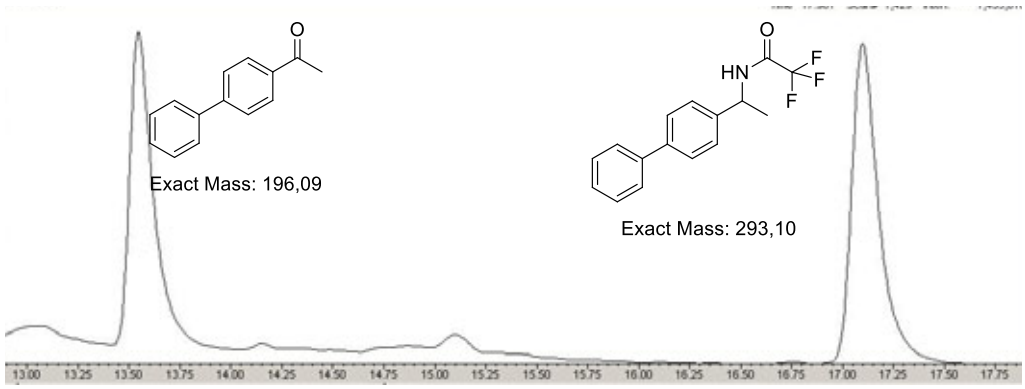

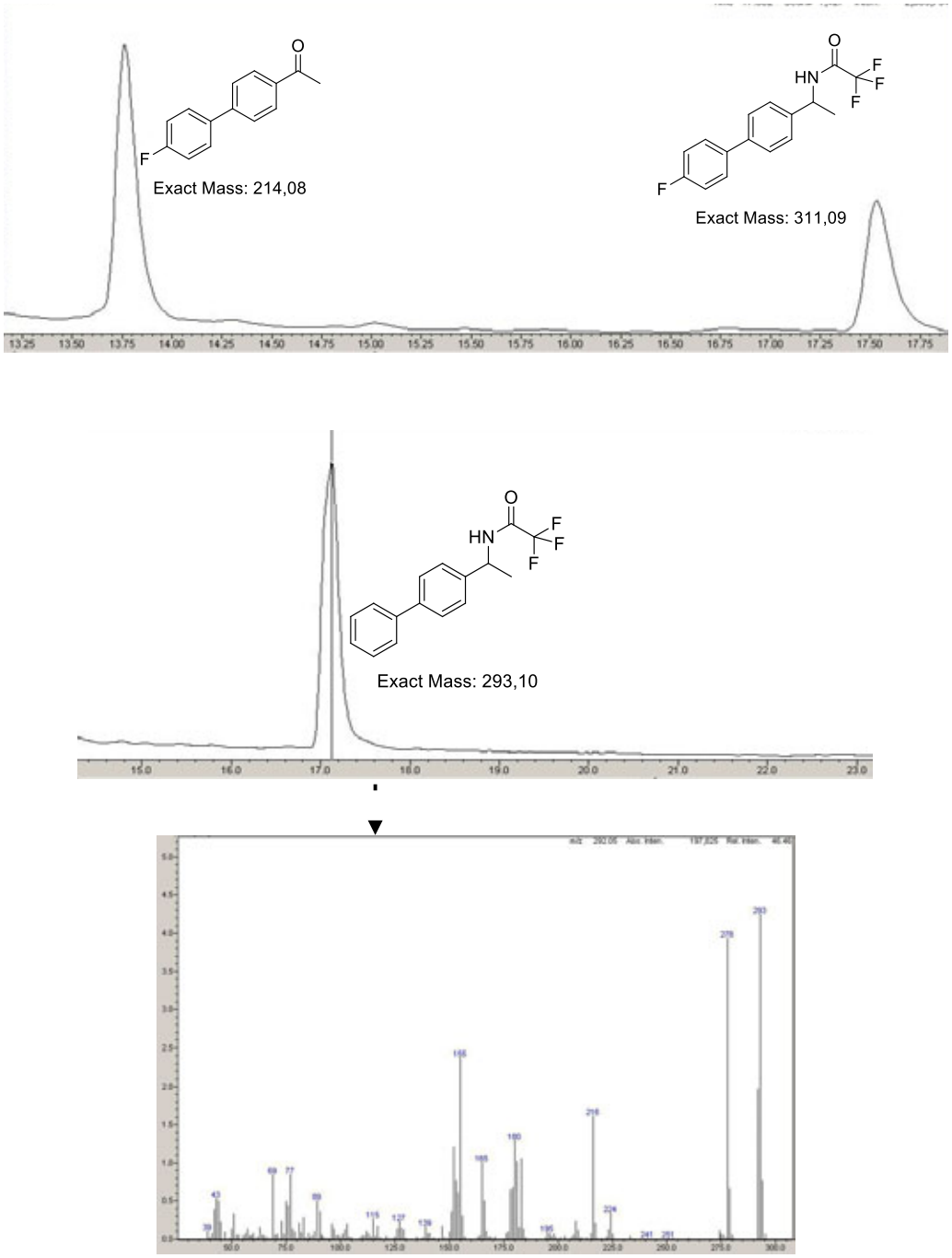

Fig. S3. GC chromatograms and MS spectra of the commercial product standard of **3c** after derivatization with MBTFA. Table S4 shows the expected and given *m/z*.

Table S4. MS analysis of product standard **3c**.

Calculated *m/z*	Measured *m/z*
140	139
155	155
181	180
216	216
224	224
278	278
293	293

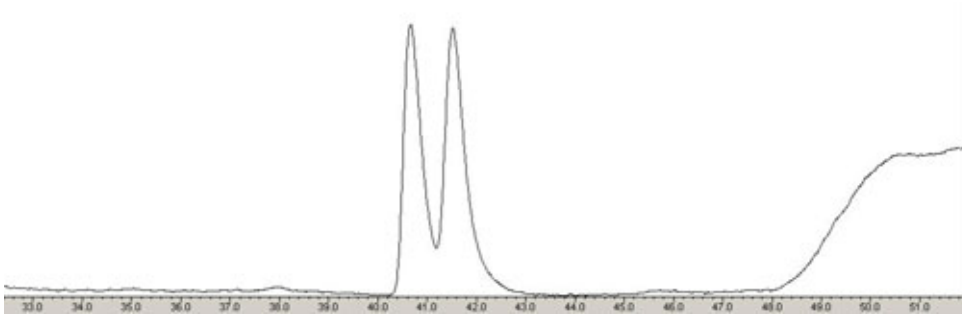

Fig. S4. Chiral GC analysis of the commercial product standard of **3c** after derivatization with MBTFA. The following temperature profile was used: initial temperature 150 °C, kept for 5 min, linear gradient to 190 °C with a slope of 5 °C min^{-1}, kept for 25 min, linear gradient to 195 °C with a slope of 1 °C min^{-1}, linear gradient to 220 °C with a slope of 20 °C min^{-1}, kept for 5 min.

Chiral GC analysis

Table S5. Chiral GC analysis of amine product **3c** after biotransformation reaction with 4CHI-TA wild type and 4CHI variants. For the GC temperature profile see Fig. S4.

4CHI-TA (variant)	ee_P [%]
4CHI wild type	>99
4CHI-H53	>99
4CHI-F112	>99
4CHI-R126A	>99
4CHI-I146A	>99
4CHI-H53A-R126A	>99
4CHI-F112A-I146A	>99

Activity of 4CHI-TA under Suzuki-Miyaura reaction conditions

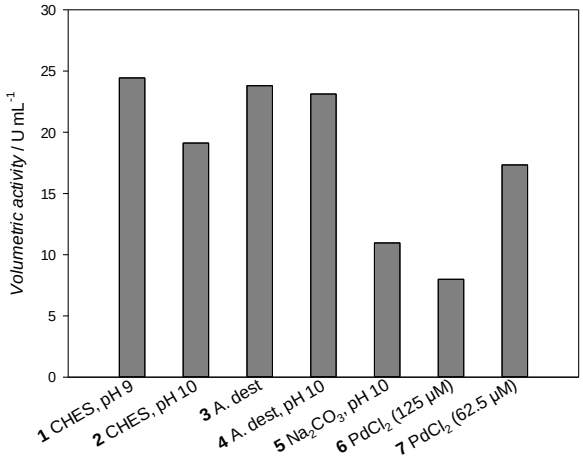

Fig. S5. Crude lysate with overexpressed 4CHI-TA wild type was tested under different reaction conditions or in presence of $PdCl_2$, respectively. Volumetric activity (U mL^{-1}) values were determined via the initial activity assay (acetophenone assay).[1] Reaction conditions were: 2 mM (*R*)-1-phenylethylamine, 2 mM pyruvate, 2% DMSO dissolved in **1** distilled water (A. dest.) and CHES (50 mM pH 9), **2** A. dest. and CHES (50 mM pH 10), **3** pure A. dest. (pH 7.4), **4** A. dest.-NaOH (pH 10), **5** 6 mM Na_2CO_3 in A. dest. (pH 10), **6** CHES (50 mM pH 9) and 125 µM $PdCl_2$, **7** CHES (50 mM pH 9) and 62.5 µM $PdCl_2$. Measurements were performed in triplicate.

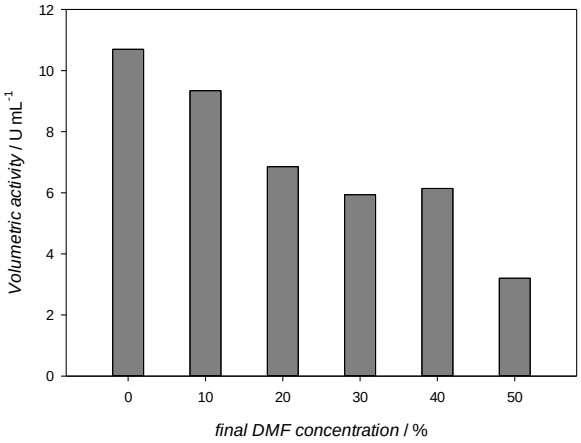

Fig. S6. Samples of crude lysate with overexpressed 4CHI-TA wild type (initial activity 6.5 U mL^{-1}) were incubated with different concentrations of DMF at 30 °C for 20 h. Samples were withdrawn, centrifuged and pre-diluted 1:20. Volumetric activity after incubation was determined via the initial activity assay (acetophenone assay). Reaction conditions were: 2 mM (*R*)-1-phenylethylamine, 2 mM pyruvate, 2% DMSO, CHES (50 mM pH 9). Controls with untreated crude lysate were performed in presence of 0.125% DMF – the highest possible residual concentration from the 50% DMF-incubation – revealing no drastic negative effect on ATA activity (95% residual activity in presence of 0.125% DMF). All measurements were performed in triplicate.

Molecular docking experiments

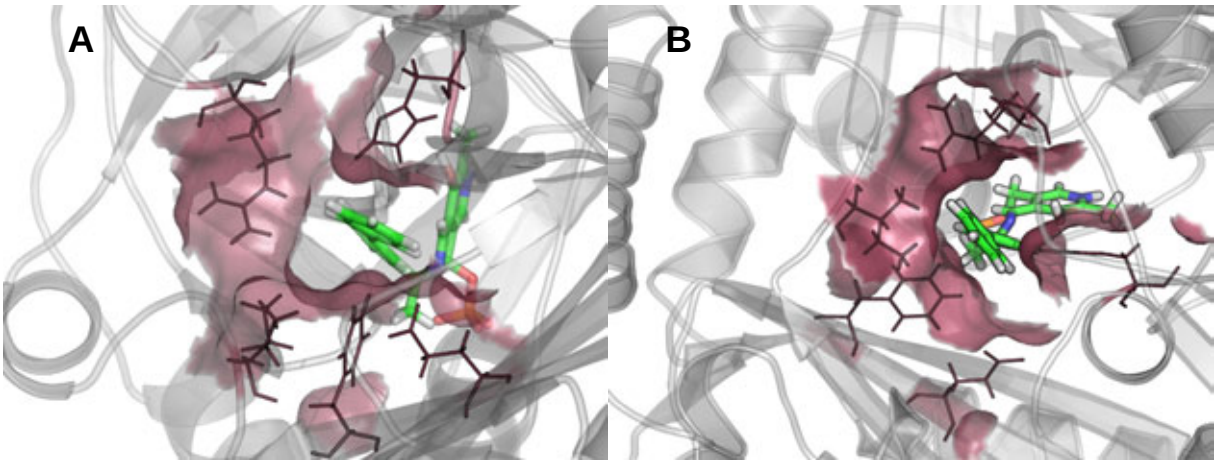

Fig. S7. Output of the molecular docking experiments using the Software *Yasara Structure*[2] and the crystal structure of the ATA from *Asperguillus fumigatus* (4CHI-TA, PDB-ID: 4CHI).[3] The quinoid intermediate (the key intermediate of the transamination reaction) of substrate **1b** (**A**) and **3b** (**B**) were built and docked via the built-in macro of *Yasara Structure*. The best and most plausible ligand-receptor complex was evaluated via an alignment with the crystal structure 4CHI and coverage of the containing PMP/PLP molecule. The Van-der-Waals surfaces of those amino acid residues with a distance of < 5 Å around the ligand (especially around the biphenyl moiety) were visualized and considered as possible interfering: H53, F113, R126 and I146 (according to the PDB numbering, given in red).

Immobilization of 4CHI-TA

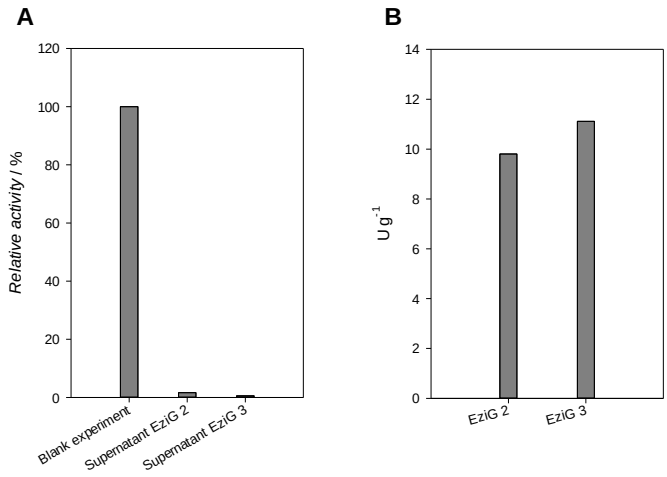

Fig. S8. Evaluation of the immobilization of 4CHI-TA on EziG™ carrier 2 and 3 (each number refers to respective carrier in the commercially available kit). **A** The residual activity in the supernatant after immobilization was determined via the initial activity assay (acetophenone assay) with pyruvate as amine acceptor (see method section for reaction conditions). The blank experiment contained crude lysate with overexpressed 4CHI-TA incubated under immobilization conditions but w/o carrier. **B** Amounts of U g^{-1} (wet) carrier determined via the modified acetophenone assay according to Ref [4].

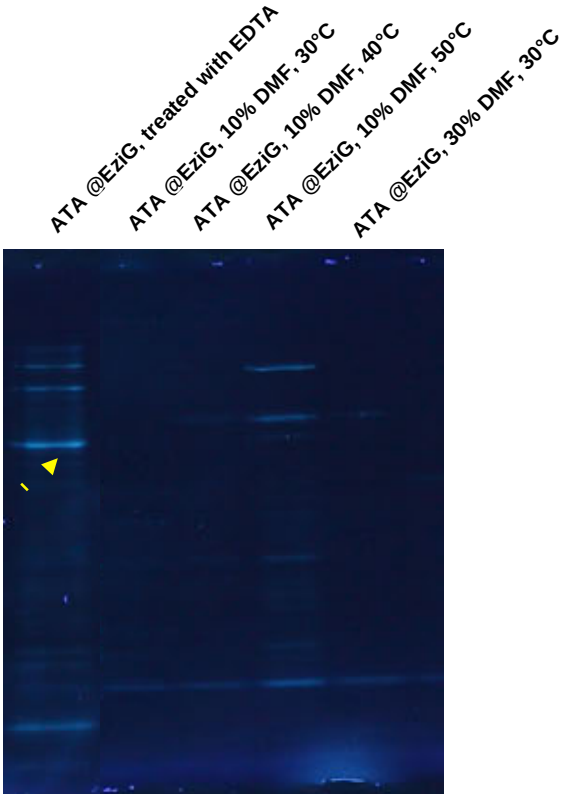

Fig. S9. Enzyme leaching test with immobilisates of 4CHI-TA on EziG™ carrier. 50 mg of freshly prepared immobilisates were incubated at different temperatures and final concentrations of DMF/HEPES buffer in a volume of 0.5 mL. After incubation the supernatant was analyzed via SDS-PAGE. A sample was treated with EDTA (50 mM final concentration in HEPES buffer, 50 mM, pH 7.5) to visualize the specificity of the immobilization. 4CHI-TA is indicated with an arrow.

References

[1] S. Schätzle, M. Höhne, E. Redestad, K. Robins, U. T. Bornscheuer, *Anal. Chem.* **2009**, *81*, 8244–8248.
[2] E. Krieger, G. Koraimann, G. Vriend, *Proteins Struct. Funct. Bioinforma.* **2002**, *47*, 393–402.
[3] a) M. Thomsen, L. Skalden, G. J. Palm, M. Höhne, U. T. Bornscheuer, W. Hinrichs, *Acta Crystallograph. Sect. F Struct. Biol. Cryst. Commun.* **2013**, *69*, 1415–1417; b) M. Thomsen, L. Skalden, G. J. Palm, M. Höhne, U. T. Bornscheuer, W. Hinrichs, *Acta Crystallogr. D Biol. Crystallogr.* **2014**, *70*, 1086–1093.
[4] H. Mallin, U. Menyes, T. Vorhaben, M. Höhne, U. T. Bornscheuer, *ChemCatChem* **2013**, *5*, 588–593.

Article IV

RSC Advances

PAPER

View Article Online
View Journal | View Issue

Cite this: *RSC Adv.*, 2016, **6**, 6665

Cellulose as an efficient matrix for lipase and transaminase immobilization†

Stefânia P. de Souza,[a] Ivaldo I. Junior,[b] Guilherme M. A. Silva,[a] Leandro S. M. Miranda,[a] Marcelo F. Santiago,[c] Frank Leung-Yuk Lam,[d] Ayad Dawood,[e] Uwe T. Bornscheuer*[e] and Rodrigo O. M. A. de Souza*[a]

Received 24th November 2015
Accepted 14th December 2015

DOI: 10.1039/c5ra24976g

www.rsc.org/advances

Immobilization of enzymes is important to improve their stability and to facilitate their recyclability, aiming to make biocatalytic processes more efficient. One of the important aspects is the utilization of cheap, abundant, and environmentally friendly carriers for enzyme immobilization. Here we report the use of functionalized cellulose for lipase and transaminase immobilization. High immobilization efficiencies (up to 90%) could be achieved for the transaminase from *Vibrio fluvialis*. For immobilized lipase CAL-B as well as the transaminase, good conversions and recyclability could be demonstrated in kinetic resolutions to afford chiral alcohols or amines. Moreover, such application of the immobilized transaminase enabled very high conversions in a continuous-flow process in the asymmetric synthesis of (*S*)-phenylethylamine (80% conversion, >99% ee).

Introduction

As already pointed out by Sheldon & van Pelt,[1] enzymes are Nature's sustainable catalysts. This statement is based on the mild conditions required for performing the requested transformation in addition to biocompatibility and biodegradability characteristics.[2] Producing large quantities of an efficient and stable biocatalyst is still an important challenge even with advances in the 90s in biotechnology and protein engineering which have provided researchers with better tools for the discovery and improvement of enzymes by means of genetic manipulations.[3]

The commercial large scale application of enzymes is not hampered by a lack of immobilization protocols, since it is easy to find different methods for enzyme immobilization in the literature,[4–11] but rather because most of them use expensive carrier materials with prices being prohibitive for large-scale operations. Hence, finding a cheap and readily available support for enzyme immobilizations is crucial for the development of new immobilized biocatalysts. Cellulose is the most abundant biopolymer consisting of a linear polysaccharide chain composed of D-glucose units linked by β(1 → 4) glycosidic bonds, fully decorated with hydroxyl groups. Since the discovery of cellulose in 1839 by Anselme Payen, this natural biopolymer has been used for many different applications ranging from thermoplastic polymers to cellulose nanofibers.[12–15]

The use of cellulose as a matrix for enzyme immobilization dates from the beginning of the seventies when Kennedy and co-workers have modified cellulose for chymotrypsin A immobilization.[16–18] A few years later lipases were also immobilized on cellulose by different methods and successfully used for hydrolytic and esterification reaction.[19] As a cheap and abundant biopolymer, cellulose occurs as a very interesting matrix for enzyme immobilization representing an affordable immobilized biocatalyst for large-scale operations.

In continuation of our efforts on the development of carriers and protocols for enzyme immobilization,[20–26] herein we report the functionalization of cellulose followed by enzyme immobilization (exemplified for lipase and transaminase) *via* covalent bonds and its application in the production of chiral alcohols and amines.

Materials and methods

Materials

Cellulose, 3-aminopropyltriethoxysilane (APTES), (3-glycidyloxypropyl)trimethoxysilane (GLYMO) and glutaraldehyde were purchased from Sigma-Aldrich. Immobilized *Candida antarctica* lipase B (Novozyme 435, NZ435 – 30 mg g^{-1} of support) was purchased from Novozymes as well as free *Candida antarctica* lipase B on phosphate buffer (Cal-B, 5.7 mg mL^{-1}). GDH-105

[a]*Biocatalysis and Organic Synthesis Group, Chemistry Institute, Federal University of Rio de Janeiro, Rio de Janeiro, Brazil. E-mail: rodrigosouza@iq.ufrj.br*
[b]*School of Chemistry, University of Rio de Janeiro, Rio de Janeiro, Brazil*
[c]*Institute of Biophysics Carlos Chagas Filho (IBCCF), Federal University of Rio de Janeiro (UFRJ), Rio de Janeiro, Brazil*
[d]*Department of Chemical and Biomolecular Engineering, The Hong Kong University of Science and Technology, Hong Kong SAR, China*
[e]*Institute of Biochemistry, Dept. of Biotechnology & Enzyme Catalysis, Greifswald University, Greifswald, Germany*

† Electronic supplementary information (ESI) available. See DOI: 10.1039/c5ra24976g

(Lot# D12010) and LDH-101 (Lot# A10036) was purchased from Codexis Inc (Redwood City, CA). All other materials were at least reagent-grade.

Preparation of APTES functionalized cellulose

(3-Aminopropyl)trimethoxysilane, APTES (5 mL) and tetrahydrofuran (50 mL) were mixed and 500 mg of cellulose were added. This mixture was stirred at room temperature for 3 h. Then the solvent was evaporated and 10 mL phosphate buffer pH 7 (50 mM) was added to the product, followed by 2 mL glutaraldehyde. This mixture was stirred at room temperature for 24 h. The product was filtered and washed repeatedly with distilled water to eliminate unreacted residues.

Preparation of Glymo functionalized cellulose

(3-Glycidyloxypropyl)trimethoxysilane, GLYMO (5 mL) and tetrahydrofuran (50 mL) were mixed and 500 mg cellulose were added. This mixture was stirred at room temperature for 5 h. Then the solvent was evaporated and the product was filtered and washed repeatedly with distilled water to eliminate unreacted residues.

Vibrius fluvialis transaminase production

Overnight cultures of Vfl-TA-WT (in pET24b vector with kanamycin resistance) were used for inoculation of 150 mL TB media containing 50 μg mL^{-1} kanamycin. When OD_{600} of 0.6 was reached IPTG was added for induction in a final concentration of 0.2 mM. The expression occurs at 20 °C for 18–20 h. The harvesting of cells was performed at 4000 × *g* for 15 min and 4 °C. French Press at 1700 psi was used for cell disruption after resuspension in 50 mM NaPP pH 7.5, 0.1 mM PLP and 300 mM NaCl. The subsequent centrifugation step was done at 37 000 × *g* for 1 h and 4 °C. The crude lysate was filtered with a 0.2 μm filter and stored at 4 °C.

Immobilization conditions

The support (functionalized cellulose) was subjected to the following immobilization process:

Lipase immobilization protocol: 2 mL lipase B from *Candida antarctica* enzyme solution (5.7 mg mL^{-1}) was dissolved in 10 mL 0.025 mM phosphate buffer pH 7.0 and added to support (2 g). The mixture was stirred for 24 h at 40 °C using a flask shaker or thermomixer, before being filtered and dried under vacuum followed by drying over night at ambient temperature. Immobilization efficiency was evaluated by the difference between initial amount of units added and that in the supernatant after filtration of the immobilized enzyme.

Transaminase immobilization protocol: 5 mL *Vibrius fluvialis* transaminase solution (8.8 mg mL^{-1}) was dissolved in 30 mL 50 mM phosphate buffer pH 7.5 and added to the support (1 g). The mixture was stirred for 24 h at 30 °C using a flask shaker or thermomixer, before being filtered and dried under vacuum followed by drying over night at ambient temperature. Immobilization efficiency was evaluated by the difference between the initial amount of units added and that in the supernatant after filtration of the immobilized enzyme.

Esterification reactions

The immobilized lipase (10 mg of support in 1 mL reaction media) was evaluated in an esterification reaction between oleic acid and ethanol (1 : 1, 100 mM in *n*-heptane) at different temperatures. The reactions were performed in cryotubes at 200 rpm agitation on a shaker. Samples (10 μL) were collected after 1 h. For calculation of the initial reaction velocity, the reaction times were varied from 5, 10, 15, 20, and 30 min. For thermal stability, the reaction was investigated at 50–70 °C. Quantification of esters formed was performed by GC-MS analysis.

Kinetic resolution using immobilized lipase

Rac-1-Phenylethanol (1 mmol, 122 mg), vinyl acetate (1 mol per eq.) as acyl donor, and 18 mg (15% w/w) of the corresponding immobilized enzyme were reacted in cyclohexane (3 mL) for 2, 4 and 5 h at 60 °C. Enantiomeric excess values (ee) were determined by chiral GC analysis (chiral column Betadex-325, for details as shown in the section of "GC analysis").

Discontinuous acetophenone assay

For immobilized transaminases a 24 deep-well plate was heated in a thermomixer to 30 °C. A total of 50 mg wet immobilized transaminase was used for each measurement. The reaction was started by adding 5 mL of pre-warmed reaction solution (HEPES buffer 50 mM, pH 7.5, 2.5 mM (±)-α-phenylethylamine ((±)-α-PEA), 5 mM pyruvate, and 0.5% DMSO). Then, 200 μL samples were taken and the absorbance was measured at 245 nm. The slope was determined and conversions calculated.[27]

Asymmetric synthesis using immobilized transaminase

Asymmetric synthesis of (*S*)-phenylethylamine was performed using the GDH/LDH system for shifting the equilibrium and cofactor recycling.[28,29] Reactions were performed in a 5 mL mixture using 50 mM HEPES buffer (pH 7.5), 10 mM acetophenone, 250 mM alanine, 10% DMSO, LDH-GDH (88 U mL^{-1} and 15 U mL^{-1}, respectively), 1 mM NADH and 150 mM glucose, at 30 °C. For batch experiments, 100 mg immobilized enzyme was used in a total reaction volume of 5 mL on a thermomixer at 800 rpm. The starting mixture was stirred for 5 min while the instrument Asia Flow Reactor was equipped with Omnifit (6.6 mm × 10 mm with 0.3421 cm^2 base and height 10 cm column) containing 2 g of the immobilized catalysts. The reaction solution was pumped using an Asia syringe pump at different flow rates in order to achieve the desired residence time. Samples were collected and analysed by HPLC.[32]

GC analysis

All GC-MS measurements were carried out in duplicate using a DB 5 (Agilent, J&W Scientific®, USA) capillary column (30 m × 0.25 mm × 0.25 μm). The GC-MS samples were prepared by dissolving 10 μL of the sample in 98 mL of heptane and 10 μL of MSTFA (*N*-methyl-*N*-(trimethylsilyl) trifluoroacetamide). 1 μL of

this sample was then injected into the Shimadzu CG2010 GC. The injector and detector temperatures were 250 °C and the oven temperature was constant at 60 °C for 1 min, and then increased by 10 °C min^{-1} to 250 °C, where it was held constant for 3 min. The conversion and the selectivity were analyzed from the peak areas in the chromatograms. GC-FID: chiral column Betadex-325 capillary column; 1 μL samples were injected at 100 °C. The oven was heated at 15 °C min^{-1} to 150 °C, at 8 °C min^{-1} to 200 °C, at 2 °C min^{-1} to 240 °C and then maintained for 4 min. After this, the oven was heated at 15 °C min^{-1} to 300 °C. Chiral GC analysis was performed on a Shimadzu GC-2010 chromatograph equipped with a FID, an AOC-20i autosampler and a chiral CP-Chirasil-Dex CB (25 m × 0.25 mm ID) or a chiral β-Dex325 (30 m × 0.24 mm ID) column using hydrogen as carrier gas. Injector and detector temperatures were set at 220 °C. GC-FID temperature program for 1-phenylethylamine (PEA) using β-Dex325 column: 90 °C|30 min → 180 °C, 40 °C min^{-1}|10 min.

HPLC analysis

For quantitative analysis 150 μL samples of the reaction mixture were derivatized with 15 μL trifluoroacetic acid (TFA), centrifuged (13 000 g, 5 min) and 15 μL of the supernatant were directly analyzed by HPLC (Hitachi LaChrom) using a reversed-phase C18 column (LiChrospher®). Detection took place with a UV detector set at 245 nm.

Thermogravimetric (TG) analysis

The TG curves were obtained in a thermogravimetric module, coupled to a thermal analyzer, both manufactured by Netzsch®. Thermogravimetric measurements were performed using a platinum sample holder containing about 10 mg of each immobilized enzyme. Each sample was heated from 35 to 600 °C at 10 °C min^{-1}, under atmosphere of synthetic air and N_2, both at a flow rate of 60 mL min^{-1}.

X-Ray photoelectron spectroscopy (XPS)

The XPS was conducted using a Kratos Axis Ultra DLD spectrometer. A monochromatic Al source was used as X-ray source. The soft X-rays emitted from excitation of Al source generate photoelectrons from the surface layers of atoms in a solid sample. The electrons thus emitted are analyzed according to their kinetic energy and the spectrum produced is used to identify the elements present and their chemical states.

Infrared analysis

Analysis by infrared spectroscopy used a Shimadzu 8300 FTIR spectrophotometer. The spectrum was obtained with 32 scans and with 4 cm^{-1} resolution. For the analysis, 10 mg of a sample was placed in the sample collector to form tablets of approximately 2 mm thickness and 5 mm diameter without KBr addition.

Scanning electron microscopy (SEM) analysis

Cellulose, functionalized cellulose and supported enzyme had their structure analyzed by scanning electron microscopy (SEM) using a Zeiss EVO® 50H microscope. All micrographs were obtained using a Shimadzu® sputter equipment. For this, each sample was placed in a sample holder on carbon tape and then they were metallized under vacuum. After preparation, the samples were placed under the microscope and bombarded by an electron beam interacting with the sample's atoms. From the interaction between the electron beam and the sample, the radiation was possible to form a magnified image of the sample.

Laser confocal microscopy analysis (LCMS)

Prior to being analyzed, the immobilized enzyme samples were mixed with fluorescamine solution (50 mg mL^{-1}, in acetone) for 3 min to form a highly fluorescent product through the reaction between the primary amines in proteins and the fluorescamine. Fluorescence intensity quantification of both biocatalyst containing fluorescent lipase (GCel-CalB) and transaminase (ECel-VF) were analyzed by confocal microscopy (Zeiss, LSM 510 META). For this purpose, slides were mounted with VectaShield (Vector Laboratories) and covered with a glass lamina. Stack images were analyzed using Image J software (NIH).

Results and discussion

First, cellulose was modified in order to introduce the epoxy (GLYMO) and amino (APTES) groups for covalent bond immobilization protocols. Cellulose was successively mixed with APTES and glutaraldehyde in order to deliver the glutaraldehyde-functionalized cellulose (GCel), after 24 h. The epoxy-functionalized cellulose (ECel), was also produced by the reaction between GLYMO and cellulose for 5 h, using THF as solvent (Scheme 1).

After drying the functionalized cellulose (GCel and ECel) at ambient temperature for 48 h, the enzyme immobilization was performed. For the lipase immobilization, 2 mL lipase B from *Candida antarctica* solution was dissolved in 10 mL 0.025 mM phosphate buffer pH 7.0. The functionalized cellulose (GCel and ECel) was added (2 g) and allowed to react for 24 hours at 40 °C. Immobilization efficiency was evaluated by the difference

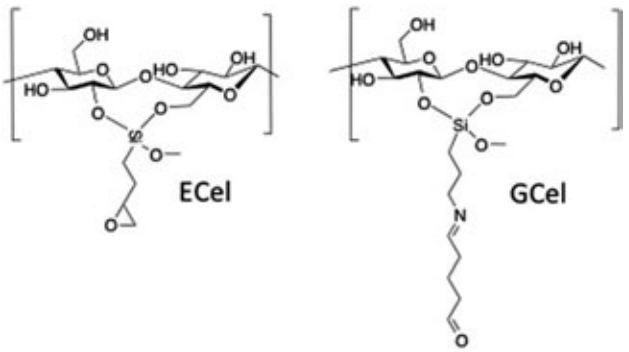

Scheme 1 GLYMO- and APTES-functionalized cellulose.

between initial amount of enzyme added and that in the supernatant after filtration of the immobilized enzyme (Table 1). For the transaminase immobilization procedure, 5 mL *Vibrius fluviaris* transaminase solution was dissolved in 30 mL 50 mM HEPES buffer pH 7.5. The functionalized cellulose (GCel and ECel) was added (1 g) and underwent the reaction for 24 hours at 30 °C. No optimization was done in order to first verify the feasibility of using the functionalized cellulose as a matrix for enzyme immobilization. All supports were characterized by infrared (IR), thermogravimetry analysis (TG), scanning electron microscopy (SEM) and X-ray Photoelectron Spectroscopy (XPS) (see ESI† for further details).

The immobilization efficiency obtained for Cal-B on epoxy-cellulose (ECel-CalB), Cal-B on glutaraldehyde–cellulose (GCel-CalB), VF transaminase on epoxy–cellulose (ECel-VF) and VF transaminase on glutaraldehyde–cellulose (GCel-VF) are shown on Table 1.

As shown on Table 1, the immobilization protocol developed did not present efficient results for the immobilization of lipase B from *Candida antarctica*, leading to very low protein incorporation. The VF transaminase leads to good to excellent immobilization efficiencies on both epoxy (up to 90.1%, Table 1) and glutaraldehyde functionalized cellulose. In order to prove the concept of using functionalized cellulose as a renewable support for enzyme immobilization, the two supports were attempted where the immobilization efficiency was higher, C–B on glutaraldehyde–cellulose (GCel-CalB) and VF transaminase on epoxy–cellulose (ECel-VF).

The solid state ^{13}C NMR spectroscopy of the functionalized cellulose clearly demonstrates the incorporation of the APTES and glutaraldehyde in the cellulosic material. The presence of the imino as well as the silyl propyl groups can be inferred by the presence of the signals in 163–164 ppm and the signals at higher field 10–50 ppm, respectively. When the same analysis was performed after the incorporation of the enzyme into the cellulosic support, an increase in the number of signals in the range of 164–180 ppm can be observed, which correlates to the presence of imino and amide functions (see ESI† for further details). This result corroborates the XPS analysis where a peak at the binding energy of 400 eV is observed for the glutaraldehyde-functionalized cellulose (GCel) being an indicator of nitrogen atoms in the sample. For the sample GCel-CalB there is a shoulder peak shown at the binding energy of 402 eV. This shoulder peak is the main difference compared to the GCel sample, meaning that the nitrogen atom is in a higher oxidation state, which can be related to the protein binding to the support (see ESI† for further details). In order to verify the presence of protein on the functionalized cellulose, we decided to perform a confocal laser scanning microscopy (CLSM) experiment to visualize the dispersion of protein into the

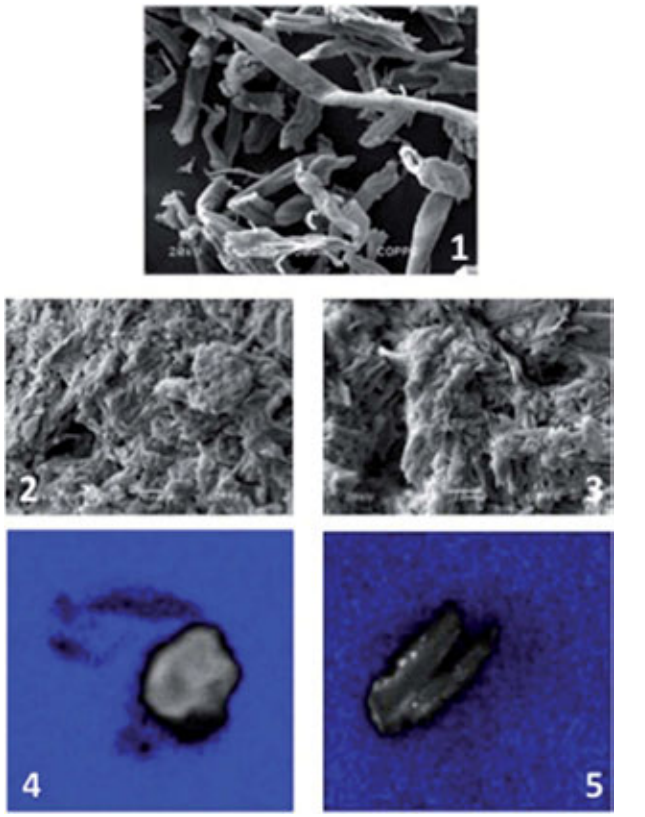

Fig. 1 Confocal Laser Scanning Microscopy (CLSM) and Scanning Electron Microscopy (SEM) analysis of ECel-VF and GCel-VF. (1) SEM analysis of cellulose before functionalization; (2) SEM analysis of ECel-VF; (3) SEM analysis of GCel-VF; (4) CLMS analysis of ECel-VF; (5) CLMS analysis of GCel-VF.

Table 1 Immobilization efficiency of lipase B from *Candida Antarctica* and *Vibrius fluviaris* transaminase into glutaraldehyde–cellulose and epoxy-cellulose

Immob. biocatalyst	Immob. efficiency[a] (%)	Amount of protein (mg g^{-1} of support)
ECel-CalB	3.5	0.2
GCel-CalB	10.5	0.6
ECel-VF	90.1	40.5
GCel-VF	27.7	12.4

[a] Immobilization efficiency was evaluated by the difference between initial amount of units added and that in the supernatant after filtration of the immobilized enzyme.

Table 2 Temperature profile for the esterification reaction catalyzed by GCel-CalB and comparison with the results obtained for Novozyme 435[a]

Entry	Immob. enzyme	Temperature (°C)	Conversion (%)
1	GCel-CalB	50	85
2		60	97
3		70	84
4	Novozyme 435	50	84
5		60	80
6		70	81

[a] Reaction conditions: GCel-CalB or Novozyme 435 (10 mg immobilized enzyme in 1 mL reaction media) was evaluated in the esterification reaction between oleic acid and ethanol (1 : 1 – 100 mM in *n*-heptane) at different temperatures.

support (Fig. 1).[29,30] As displayed in Fig. 1a (ECel-VF) the white color reveals the presence of well dispersed protein on the surface of cellulose granules. In addition, the CLSM analysis of GCel-VF (Fig. 1b) shows a punctual localization of protein, which reflects the low immobilization efficiency compared to the epoxy-functionalized pattern (Table 1).

With the characterized results, catalytic performances of the immobilized enzymes at different reaction temperatures were evaluated in the designed reactions. The immobilized lipase GCel-CalB was evaluated by the esterification reaction between oleic acid and ethanol (1 : 1, 100 mM in heptane and 200 rpm), at different temperatures (50–70 °C) for 1 h. The behavior presented by GCel-CalB was compared to the commercial immobilized lipase Novozyme 435 and the results are presented, as shown in Table 2. A similar evaluation was made for ECel-VF immobilized enzyme, in this case the kinetic resolution of (+/-)-phenylethylamine (PEA) was used as standard reaction at temperatures ranging from 30 to 60 °C. Unfortunately, there is no commercial transaminase that can be used as a positive control for comparison purpose.

A first look at the results presented on Table 2, can take the reader to the wrong assumption that GCel-CalB and Novozyme 435 have the same behavior at different temperatures, but it is worthy to note that Novozyme 435 has 50× more protein attached to the support compared to GCel-CalB, making this one much more efficient than the commercial immobilized enzyme. GCel-CalB was also evaluated at higher temperatures (80 °C) and the results obtained show a similar behavior, leading to the desired product on 75% of conversion (see ESI† for further details). The results for temperature profile of ECel-VF (Table 3) show good results at temperatures ranging from 30 to 50 °C and a slight decrease is observed at 60 °C. Especially for the transaminase, the pH profile was also evaluated in the range between 7.5 and 9.5, where the case at pH 7.5 offered the best result.

At this stage we also evaluated the recyclability of the immobilized biocatalysts GCel-CalB and ECel-VF. After each reaction the immobilized biocatalyst was washed three times with buffer and dried at ambient temperature for 24 h and this was repeated five times (Table 4).

The findings of the recyclability study show that using the GCel-CalB immobilized lipase a decrease of the conversion was observed in the second cycle compared to the commercial enzyme while Novozyme 435 continues to lose its activity for four consecutive cycles to only 20% conversion. The immobilized transaminase ECel-VF presented a better stability affording the same conversion in fours cycles and only a slight decrease in the last one.

Table 3 Temperature profile of the ATA as determined by the acetophenone assay for ECel-VF[a,31]

Entry	Immob. enzyme	Temp. (°C)	Conv. (%)
1	ECel-VF	30	38
2		40	42
3		50	43
4		60	35

[a] Reaction conditions: ECel-VF (50 mg immobilized enzyme in 5 mL reaction media) was evaluated using the discontinuous acetophenone assay (5 mL 50 mM HEPES buffer, (±)-PEA 2.5 mM, 5 mM pyruvate, 0.5% DMSO and 800 rpm) at different temperatures.

Table 4 Recyclability of the immobilized enzymes under standard conditions

		Conversion (%)				
Entry	Immob. enzyme	Cycle 1	Cycle 2	Cycle 3	Cycle 4	Cycle 5
1	Novozyme 435[a]	84	71	56	26	20
2	GCel-CalB[a]	85	60	54	51	43
3	ECel-VF[b]	43	39	39	40	35

[a] Reaction conditions: GCel-CalB or Novozyme 435 (10 mg immobilized enzyme in 1 mL reaction media) was evaluated in the esterification reaction between oleic acid and ethanol (1 : 1 – 100 mM in *n*-heptane) at 50 °C. [b] Reaction conditions: ECel-VF (50 mg immobilized enzyme in 5 mL reaction media) was evaluated using the discontinuous acetophenone assay (5 mL 50 mM HEPES buffer, (±)-PEA 2.5 mM, 5 mM pyruvate, 0.5% DMSO and 800 rpm) at 30 °C.

Table 5 Kinetic resolution of (*R*,*S*)-α-phenylethanol catalyzed by GCel-CalB[a]

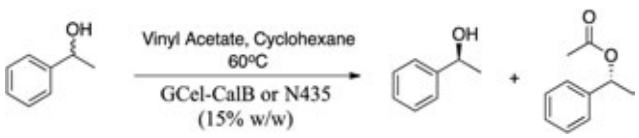

Entry	Immob. enzyme	Reaction time	Conv.(%)	*E*	Productivity (g of product per h per mg protein)
1	Novozyme 435	2 hours	49	>200	0.053
2	GCel-CalB	2 hours	35	>200	1.80
3		4 hours	40	>200	1.08
4		5 hours	42	>200	0.91

[a] Reaction conditions: (*R*,*S*)-α-phenylethanol (1 mmol), vinyl acetate (1 mol per eq.) as acyl donor, and 18 mg (15% w/w) immobilized enzyme were reacted in cyclohexane (3 mL) for 2, 4, and 5 h at 60 °C. Enantiomeric excess values (ee) were determined by chiral GC analysis.

Table 6 Asymmetric synthesis catalyzed by ECel-VF in batch and under continuous-flow conditions[a]

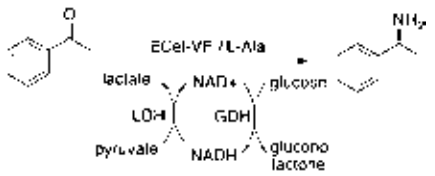

Entry	Reaction/residence time	Conv. (%)	ee (%)
1	48 h (batch)	31	>99
2	96 h (batch)	33	>99
3	15 min (cont. flow)	14	>99
4	30 min (cont. flow)	37	>99
5	60 min (cont. flow)	72	>99
6	90 min (cont. flow)	80	>99

[a] Reaction conditions: 50 mM HEPES buffer (pH 7.5), 10 mM acetophenone, 250 mM alanine, 10% DMSO, LDH-GDH, 1 mM NADH and 150 mM glucose. For the batch experiments, 100 mg immobilized enzyme was used in a total reaction volume of 5 mL on a shaker at 800 rpm at 30 °C. For continuous-flow experiments, 2 g immobilized enzyme were packed arriving on a packed bed with a total volume of 10 mL.

Finally, the newly developed immobilized biocatalysts GCel-CalB and ECel-VF were used for the synthesis of chiral products. The immobilized biocatalysts GCel-CalB was applied in the kinetic resolution of (*R*,*S*)-α-phenylethanol using vinyl acetate as acyl donor at 60 °C for 5 h (Table 5).

Comparatively, GCel-CalB immobilized enzyme could not mimic the efficiency shown by Novozyme 435, arriving to 49% of conversion after 2 h. However a promising result could be obtained by the use of GCel-CalB with conversions reaching 40% after 4 h. The most important feature of this immobilized biocatalyst is the fact that even a low protein loading can lead to very high productivities (up to 1.8 g of product per h per mg immob. enzyme), which could never be reached by the commercial immobilized enzyme.

The immobilized transaminase ECel-VF was subject to an asymmetric synthesis protocol using acetophenone as starting material. At this stage – since the development of immobilized transaminases is an emerging area – the performance of ECel-VF was evaluated in both, batch and continuous-flow reactors (Table 6).

As observed in Table 6, the asymmetric synthesis protocol under continuous-flow conditions is better than in batch mode since lower reaction/residence times are needed and higher conversions could be obtained without compromising the enantiomeric excess. Probably, the continuous-flow system enables to enhance mass transfer and consequently leads to better conversions. The packed bed, after washing for 3 h with HEPES buffer, was stored and re-used with the same behaviour presented before.

Conclusion

In conclusion, we have developed one lipase (GCel-CalB) and one transaminase (ECel-VF) immobilized onto functionalized cellulose for different applications. Effects of temperature, pH and recyclability profiles were evaluated and satisfactory results were presented. The GCel-CalB immobilized enzyme has shown very good results in the kinetic resolution of (*R*,*S*)-α-phenylethanol enabling high productivities. ECel-VF immobilized enzyme demonstrates its excellent catalytic activity in the kinetic resolution as well as in asymmetric synthesis where batch and continuous flow protocols have been applied, reducing the reaction time from 48 h to 90 min and increasing the conversion from 30% to 80%.

Acknowledgements

The authors thank CAPES, CNPq, FAPERJ and DLR (Grant No: 01DN14016) and the Alexander von Humboldt Foundation (Germany) for financial support.

References

1 R. A. Sheldon and S. van Pelt, *Chem. Soc. Rev.*, 2013, **42**, 6223–6235.
2 U. T. Bornscheuer, *Angew. Chem., Int. Ed.*, 2003, **42**, 3336–3337.
3 U. T. Bornscheuer, G. W. Huisman, R. J. Kazlauskas, S. Lutz, J. C. Moore and K. Robins, *Nature*, 2012, **485**, 185–194.
4 L. Bayne, R. V. Ulijn and P. J. Halling, *Chem. Soc. Rev.*, 2013, **42**, 9000–9010.
5 S. Cantone, V. Ferrario, L. Corici, C. Ebert, D. Fattor, P. Spizzo and L. Gardossi, *Chem. Soc. Rev.*, 2013, **42**, 6262–6276.
6 U. Hanefeld, L. Cao and E. Magner, *Chem. Soc. Rev.*, 2013, **42**, 6211–6212.
7 M. Hartmann and X. Kostrov, *Chem. Soc. Rev.*, 2013, **42**, 6277–6289.
8 A. Liese and L. Hilterhaus, *Chem. Soc. Rev.*, 2013, **42**, 6236–6249.
9 E. Magner, *Chem. Soc. Rev.*, 2013, **42**, 6213–6222.
10 R. C. Rodrigues, C. Ortiz, A. Berenguer-Murcia, R. Torres and R. Fernandez-Lafuente, *Chem. Soc. Rev.*, 2013, **42**, 6290–6307.
11 F. Secundo, *Chem. Soc. Rev.*, 2013, **42**, 6250–6261.
12 S. Alila, A. M. Ferraria, A. M. Botelho do Rego and S. Boufi, *Carbohydr. Polym.*, 2009, **77**, 553–562.
13 S. J. Eichhorn, A. Dufresne, M. Aranguren, N. E. Marcovich, J. R. Capadona, S. J. Rowan, C. Weder, W. Thielemans, M. Roman, S. Renneckar, W. Gindl, S. Veigel, J. Keckes, H. Yano, K. Abe, M. Nogi, A. N. Nakagaito, A. Mangalam, J. Simonsen, A. S. Benight, A. Bismarck, L. A. Berglund and T. Peijs, *J. Mater. Sci.*, 2010, **45**, 1–33.
14 Y. Habibi, L. A. Lucia and O. J. Rojas, *Chem. Rev.*, 2010, **110**, 3479–3500.
15 N. Lavoine, I. Desloges, A. Dufresne and J. Bras, *Carbohydr. Polym.*, 2012, **90**, 735–764.

16 A. S. Karsakevich, R. A. Zhagat and V. Y. Son, *Khim. Prir. Soedin.*, 1976, 639–643.
17 J. F. Kennedy and A. Rosevear, *J. Chem. Soc., Perkin Trans. 1*, 1974, 757–762.
18 J. Kucera, *Collect. Czech. Chem. Commun.*, 1979, **44**, 804–807.
19 M. Rucka, B. Turkiewicz and J. S. Zuk, *J. Am. Oil Chem. Soc.*, 1990, **67**, 887–889.
20 A. S. de Miranda, L. S. M. Miranda and R. O. M. A. de Souza, *Biotechnol. Adv.*, 2015, **33**, 372–393.
21 A. S. de Miranda, R. C. Simon, B. Grischek, G. C. de Paula, B. A. C. Horta, L. S. M. de Miranda, W. Kroutil, C. O. Kappe and R. O. M. A. de Souza, *ChemCatChem*, 2015, **7**, 984–992.
22 C. Garcia, I. I. Junior, R. O. M. A. de Souza and R. Luque, *Catal. Sci. Technol.*, 2015, **5**, 1840–1846.
23 R. O. Lopes, S. Grimm, J. B. Ribeiro, I. C. R. Leal, L. S. M. Miranda and R. O. M. A. de Souza, *J. Braz. Chem. Soc.*, 2015, **26**, 550–554.
24 S. P. de Souza, J. Bassut, H. V. Marquez, I. I. Junior, L. S. M. Miranda, Y. Huang, G. Mackenzie, A. N. Boa and R. O. M. A. de Souza, *Catal. Sci. Technol.*, 2015, **5**, 3130–3136.
25 I. Itabaiana Jr, K. M. Goncalves, M. Zoumpanioti, I. C. R. Leal, L. S. M. E. Miranda, A. Xenakis and R. O. M. A. de Souza, *Org. Process Res. Dev.*, 2014, **18**, 1372–1376.
26 F. K. Sutili, D. d. O. Nogueira, S. G. F. Leite, L. S. M. Miranda and R. O. M. A. de Souza, *RSC Adv.*, 2015, **5**, 37287–37291.
27 H. Mallin, U. Menyes, T. Vorhaben, M. Höhne and U. T. Bornscheuer, *ChemCatChem*, 2013, **5**, 588–593.
28 N. J. Turner, M. D. Truppo, D. Rozzell and J. C. Moore, *Org. Biomol. Chem.*, 2009, **7**, 395–398.
29 W. Kroutil, D. Rozzell, D. Clay, I. Lavandera and D. Koszelewski, *Adv. Synth. Catal.*, 2008, **350**, 2761–2766.
30 D. J. Cui, L. L. Li and M. Y. Zhao, *Ind. Eng. Chem. Res.*, 2014, **53**, 16176–16182.
31 Y. Li, G. Fei, W. Wei, B. Jian, H. M. Guang and Q. Z. Wei, *J. Mol. Catal. B: Enzym.*, 2010, **66**, 182.
32 S. Schätzle, M. Höhne, E. Redestad, K. Robins and U. T. Bornscheuer, *Anal. Chem.*, 2009, **81**, 8244–8248.

Electronic Supplementary Material (ESI) for RSC Advances.

Cellulose as an Efficient Matrix

for Lipase and Transaminase Immobilization

Stefânia P. de Souza, [a] Ivaldo I. Junior, [b] Leandro S. M. Miranda, [a] Marcelo F. Santiago, [c] Frank Leung-Yuk Lam, [d] Ayad Dawood, [e] Uwe T. Bornscheuer, [e*] Rodrigo O. M. A. de Souza, [a*]

a- Biocatalysis and Organic Synthesis Group, Chemistry Institute, Federal University of Rio de Janeiro, Rio de Janeiro, Brazil;

b- School of Chemistry, University of Rio de Janeiro, Rio de Janeiro, Brazil;

c- Institute of Biophysics Carlos Chagas Filho (IBCCF), Federal University of Rio de Janeiro (UFRJ), Rio de Janeiro, Brazil

d- Department of Chemical and Biomolecular Engineering, The Hong Kong University of Science and Technology, Hong Kong SAR, China

e- Institute of Biochemistry, Dept. of Biotechnology & Enzyme Catalysis, Greifswald University, Greifswald, Germany

Supporting Information

1. **Laser Confocal Microscopy Analysis (LCMS)**.

The immobilized enzyme samples were mixed with fluorescamine solution (50 mg/mL, in acetone) for 3 min to form a highly fluorescent product through the reaction between the primary amines in proteins and the fluorescamine. Fluorescence intensity quantification of both biocatalyst containing fluorescent lipase (GCel-CalB) and transaminase (ECel-VF) was analyzed by confocal microscopy (Zeiss, LSM 510 META). For this purpose, slides were mounted with VectaShield (Vector Laboratories) and covered with a glass lamina. Stack images were analyzed using Image J software (NIH).

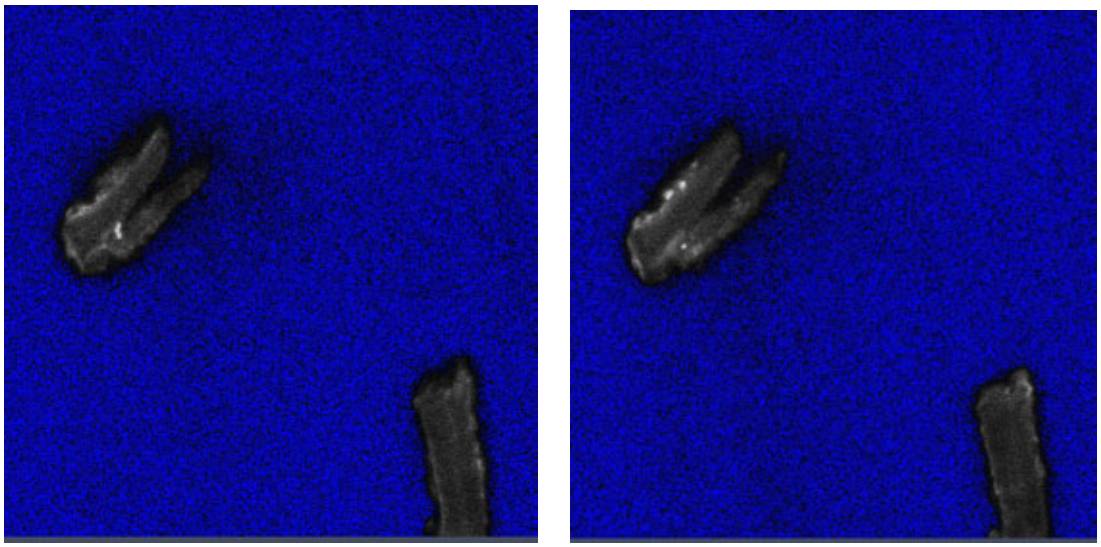

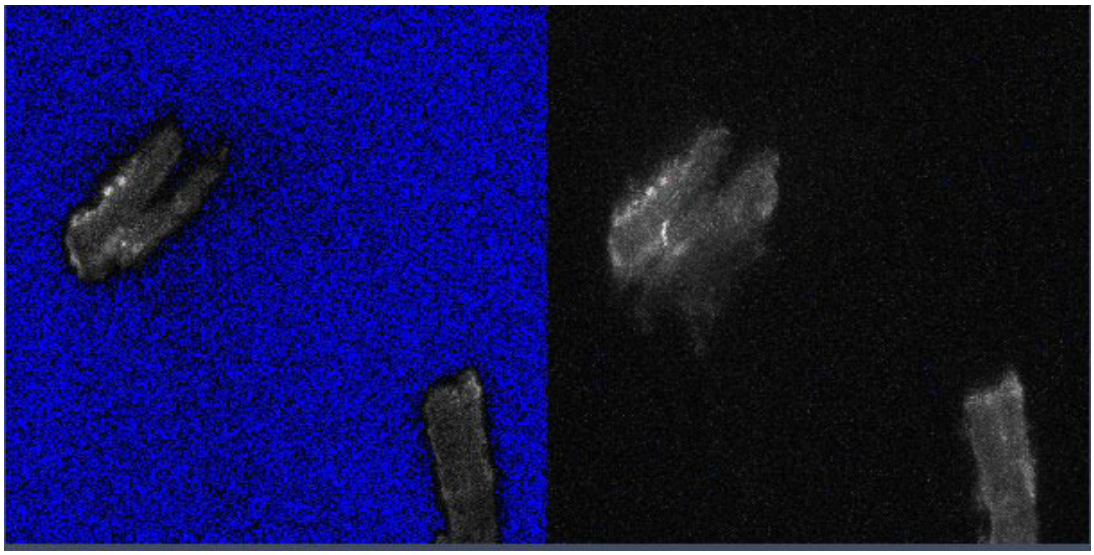

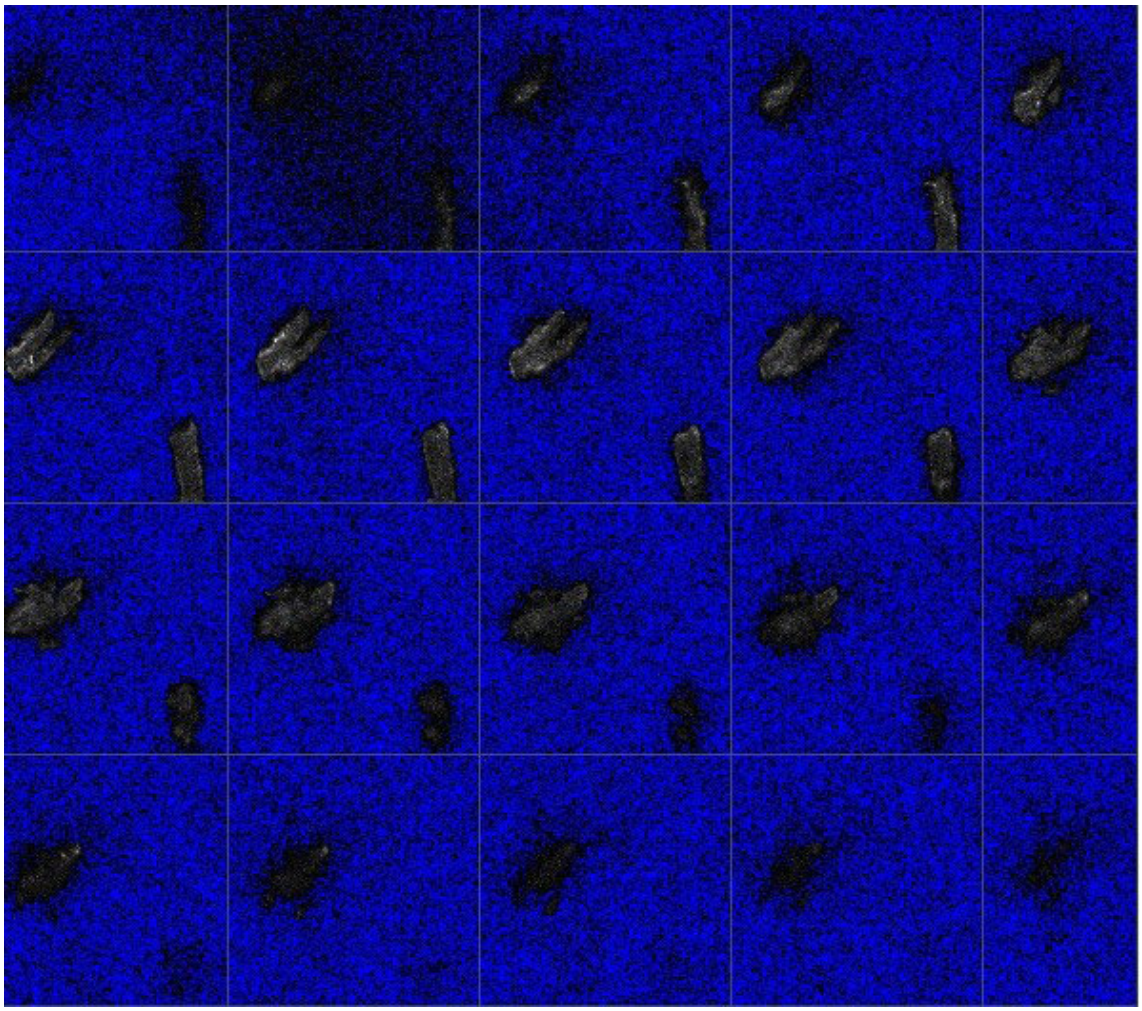

Figure S1: CLMS analysis of glutaraldehyde-functionalized cellulose (GCel_VF).

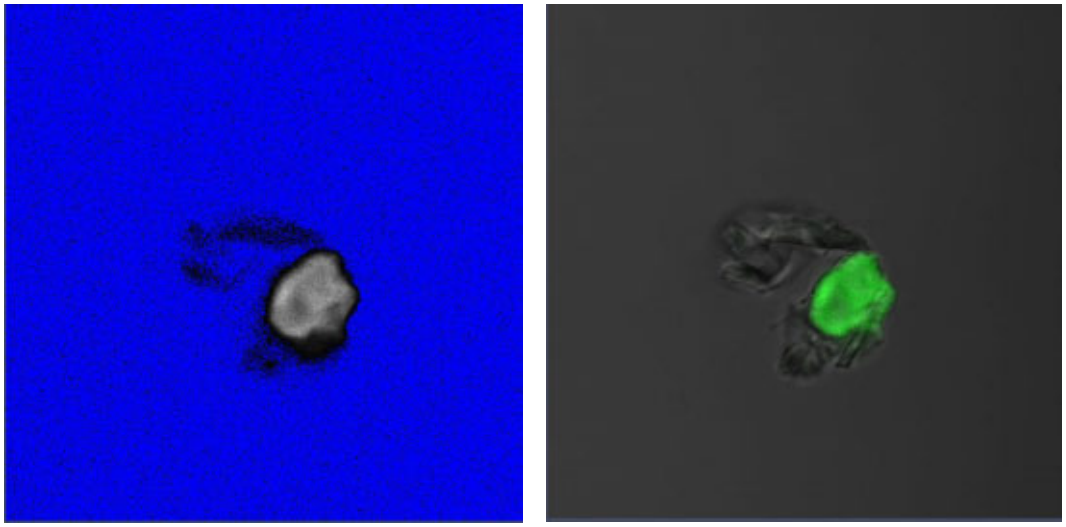

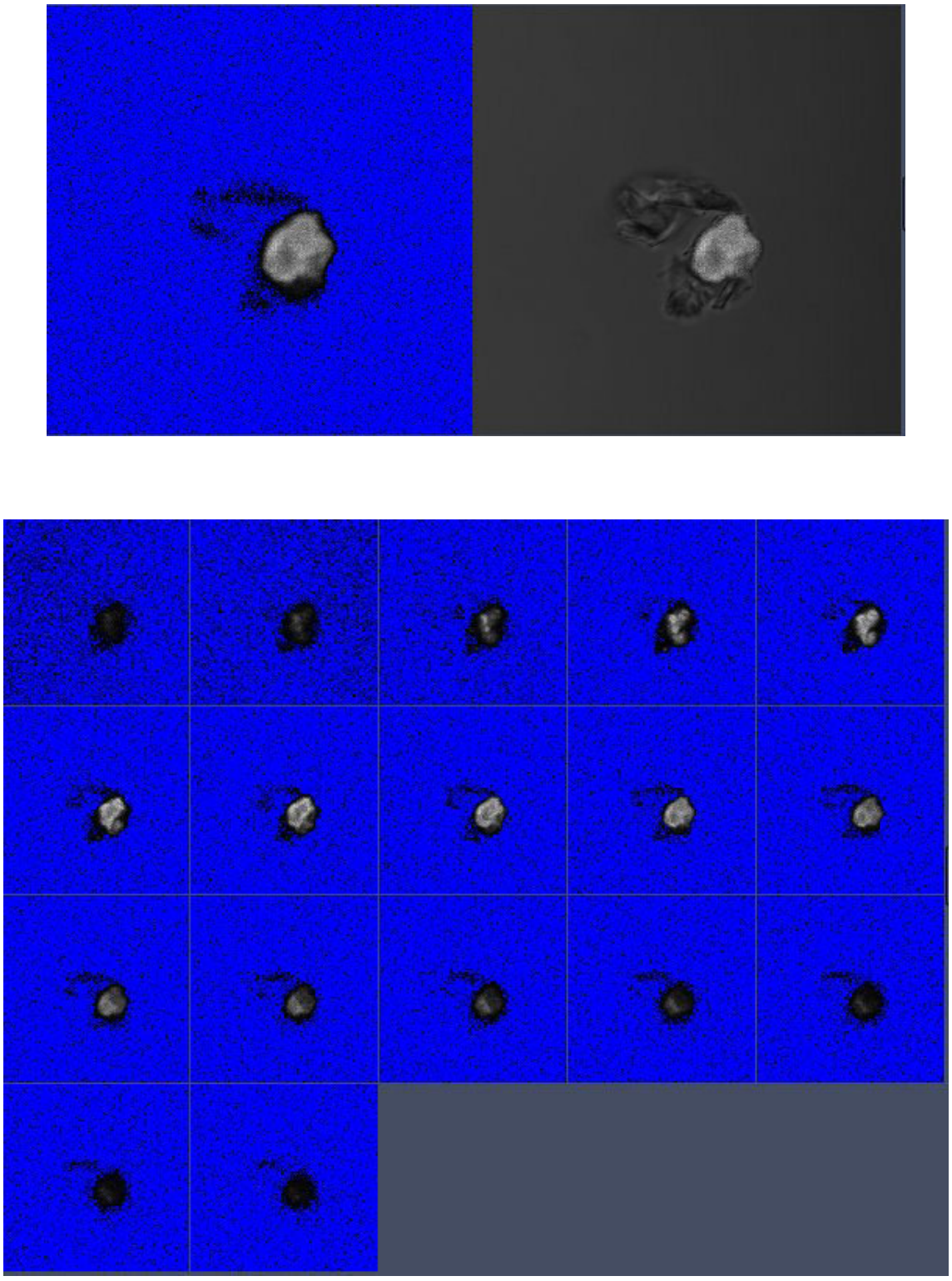

Figure S2: CLMS analysis of epoxy-functionalized cellulose (ECel_VF).

2. **Scanning electron microscopy (SEM) analysis**.

Cellulose, functionalized cellulose and supported enzyme had their structure analysed by scanning electron microscopy (SEM) using a Zeiss EVO® 50H microscope. All micrographs were obtained from the fractured surfaces of SECs coated with gold, prepared using a Shimadzu® sputter equipment. For this, each sample was placed in a sample holder on carbon tape and was metallized under vacuum. After preparation, the samples were placed under the microscope and bombarded by an electron beam interacting with the sample's atoms.

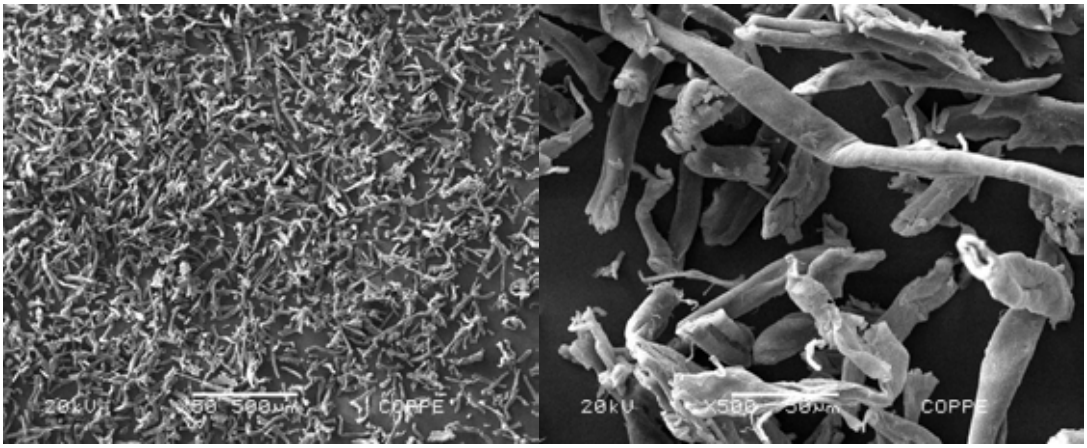

Figure S3: SEM analysis of celullose. Experimental Conditions: 1 mg sample metallized by gold under vacuum, analysed in a Zeiss EVO® 50H microscopy.

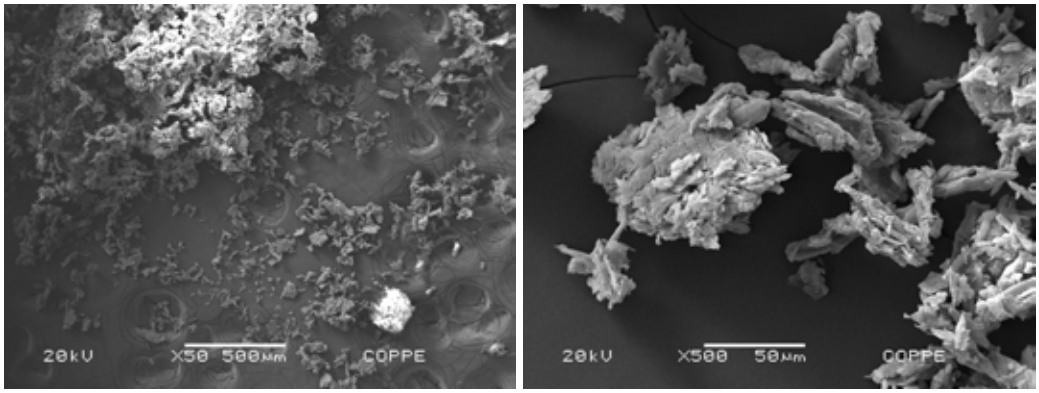

Figure S4: SEM analysis of APTES functionalized celullose. Experimental Conditions: 1 mg sample metallized by gold under vacuum, analysed in a Zeiss EVO® 50H microscopy.

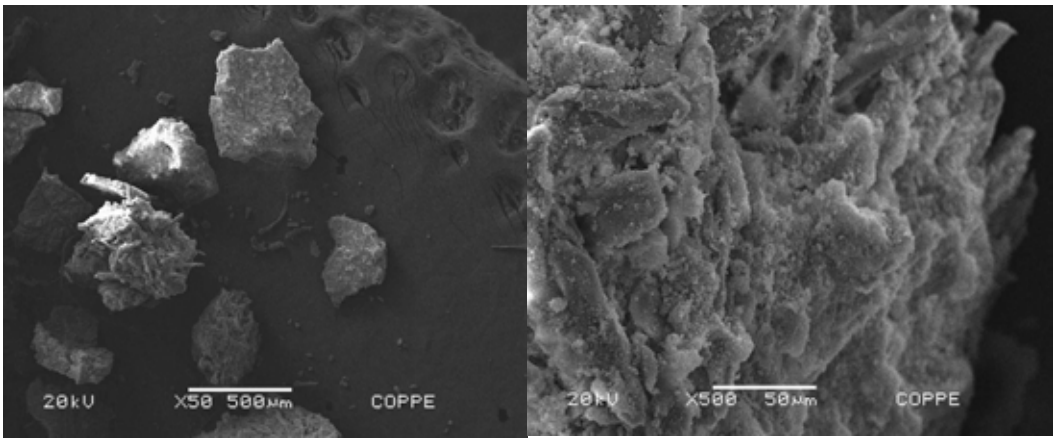

Figure S5: SEM analysis of APTES + glutaraldehyde functionalized celullose. Experimental Conditions: 1 mg sample metallized by gold under vacuum, analysed in a Zeiss EVO® 50H microscopy.

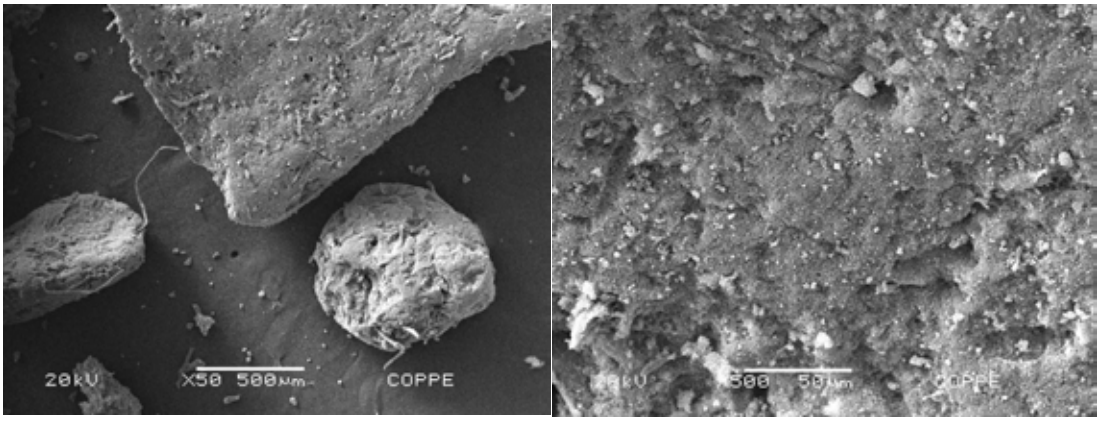

Figure S6: SEM analysis of Cal-B immobilized on glutaraldehyde functionalized cellulose. Experimental Conditions: 1 mg sample metallized by gold under vacuum, analysed in a Zeiss EVO® 50H microscopy.

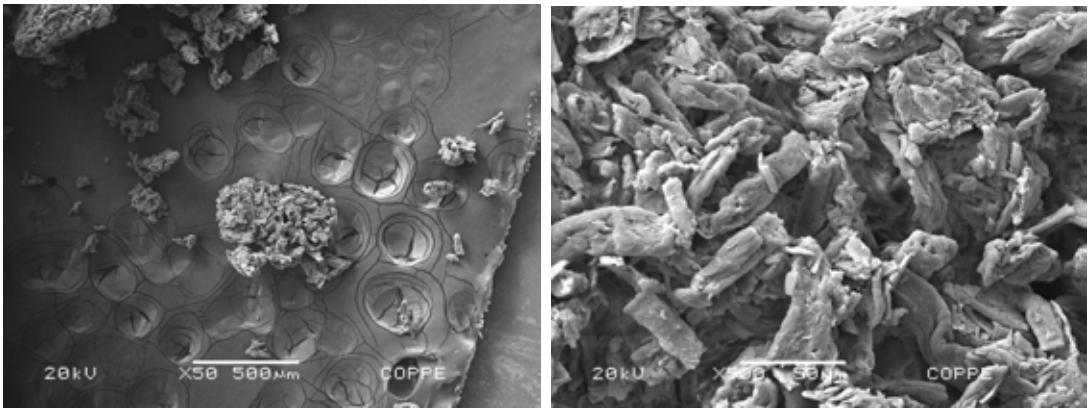

Figure S7: SEM analysis of cellulose functionalized with Glymo. Experimental Conditions: 1 mg sample metallized by gold under vacuum, analysed in a Zeiss EVO® 50H microscopy.

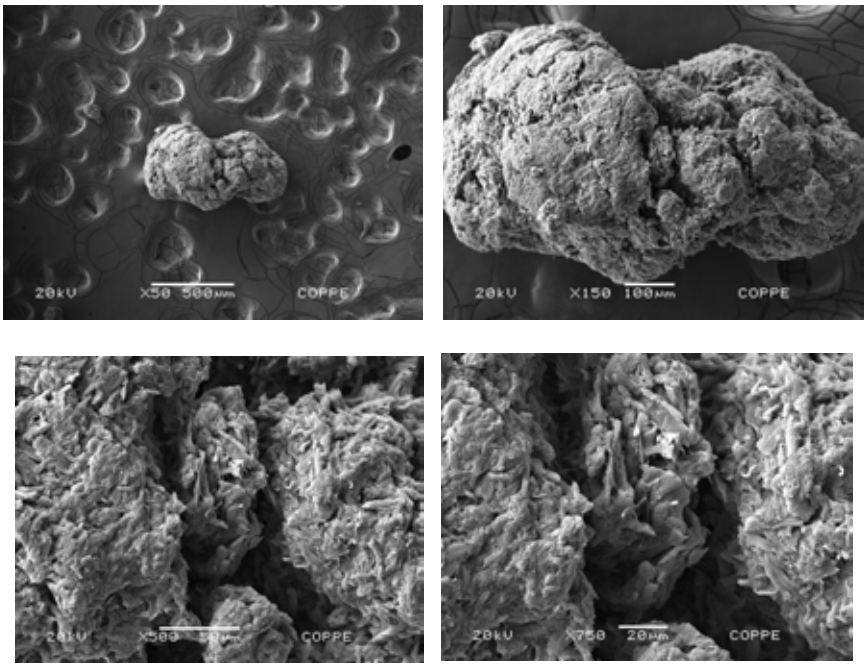

Figure S8: SEM analysis of Glymo functionalized cellulose with Cal-B. Experimental Conditions: 1 mg sample metallized by gold under vacuum, analysed in a Zeiss EVO® 50H microscopy.

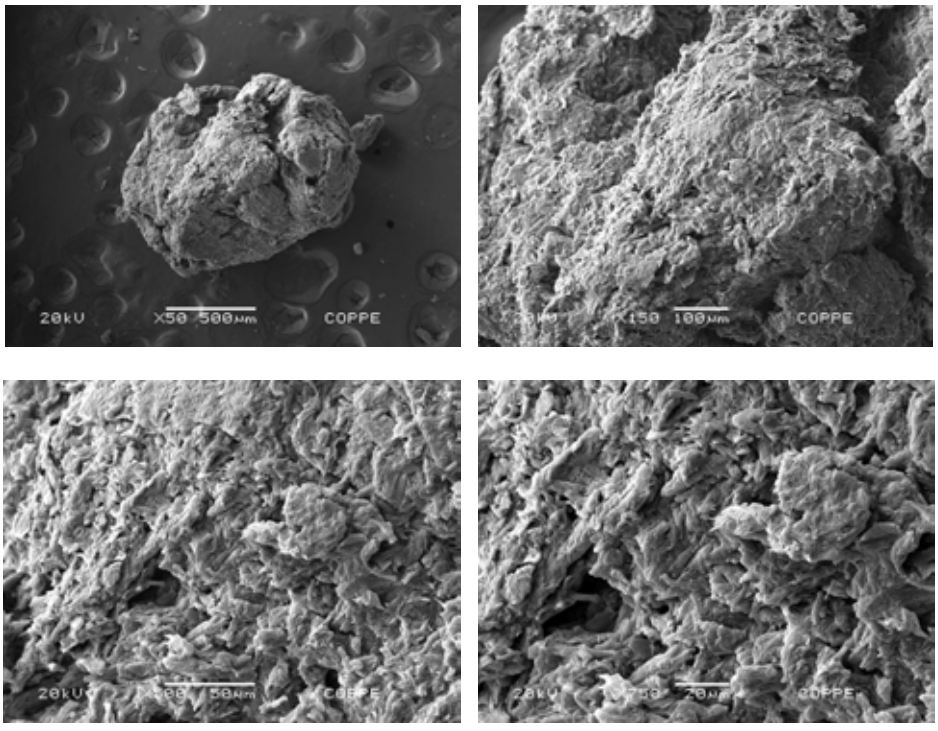

Figure S9: SEM analysis of Glymo functionalized cellulose with transaminase. Experimental Conditions: 1 mg sample metallized by gold under vacuum, analysed in a Zeiss EVO® 50H microscopy.

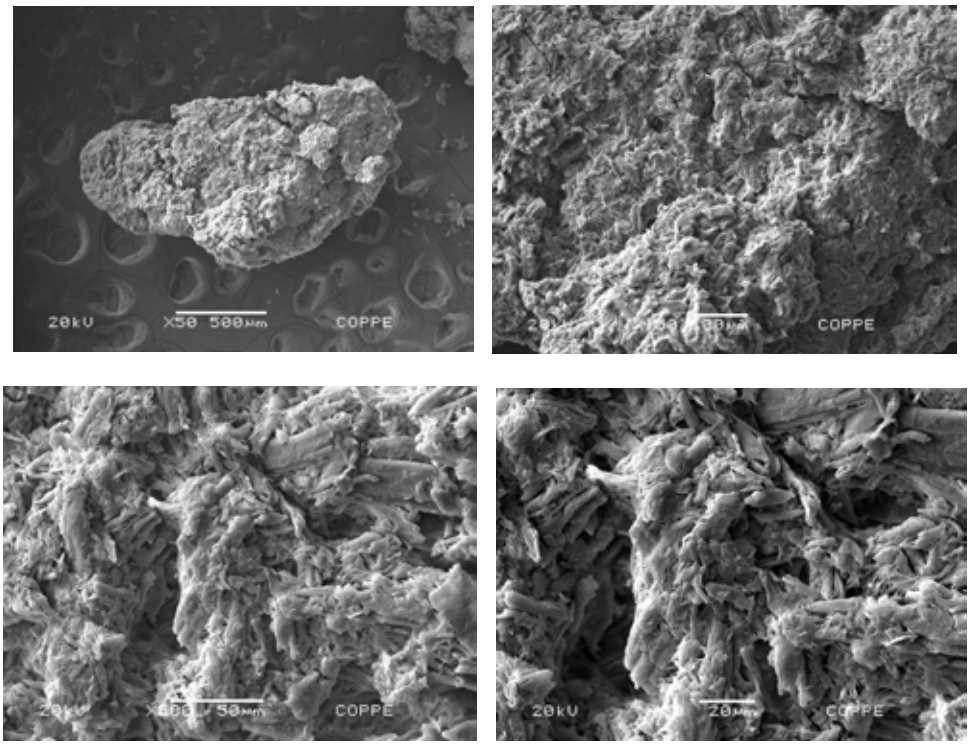

Figure S10: SEM analysis of glutaraldehyde-functionalized cellulose with transaminase. Experimental Conditions: 1 mg sample metallized by gold under vacuum, analysed in a Zeiss EVO® 50H microscopy.

3. **Infrared analysis**.

Analysis by infrared spectroscopy used a Shimadzu 8300 FTIRspectrophotometer. The spectrum was obtained with 32 scans and with 4 cm^{-1} of resolution. For the analysis, 10 mg sample was placed in sample collector to form tablets of approximately 2 mm of thick and 5 mm in diameter, without KBr addition.

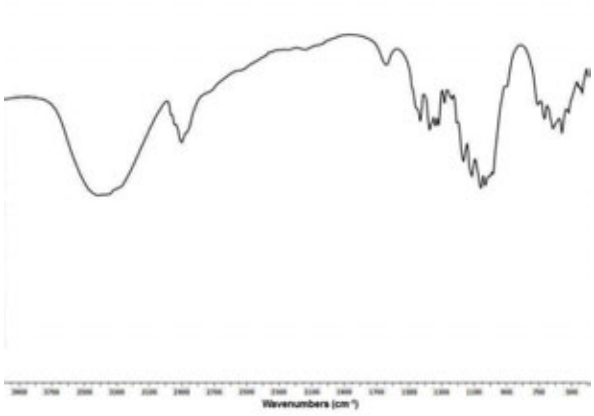

Figure S11: IR-RT spectra of cellulose.

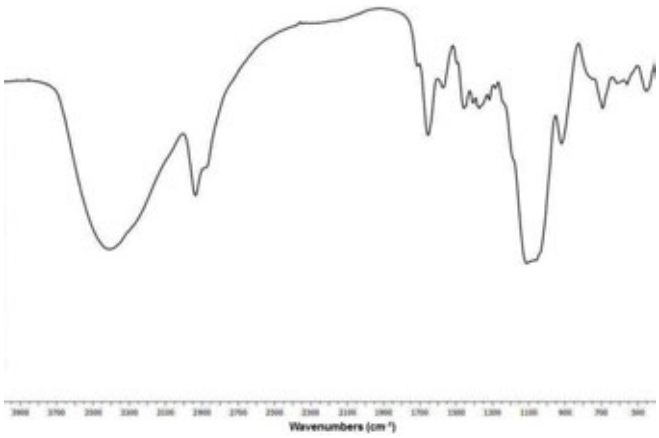

Figure S12: IR-RT spectra of cellulose functionalized with Aptes.

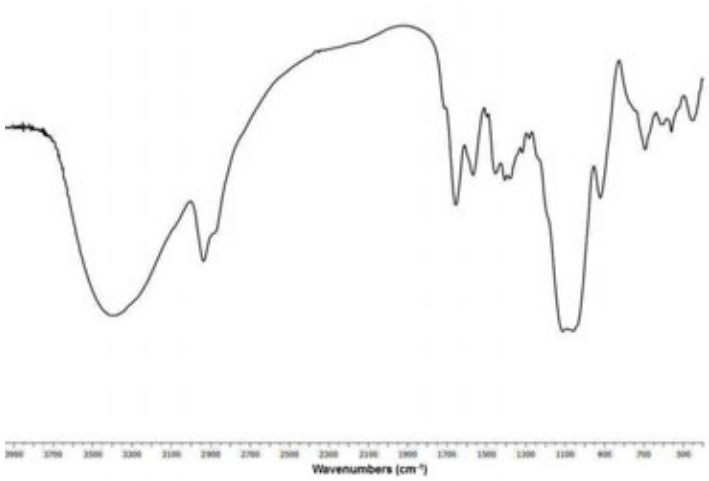

Figure S13: IR-RT spectra of Cal-B immobilized on glutaraldehyde functionalized cellulose.

4. **X-Ray Photoelectron Spectroscopy (XPS).**

The XPS was conducted using a Kratos Axis Ultra DLD spectrometer. Monochromatic Al source was used as X-ray source. Depending upon the sample the spectrum mode may vary from 10 mA to 15 KV. X-ray Photoelectron Spectroscopy (XPS) used soft X-rays emitted from excitation of Al source to produce photoelectrons from the surface layers of atoms in a solid

sample. The electrons thus emitted are analyzed according to their kinetic energy and the spectrum produced is used to identify the elements present and their chemical states.

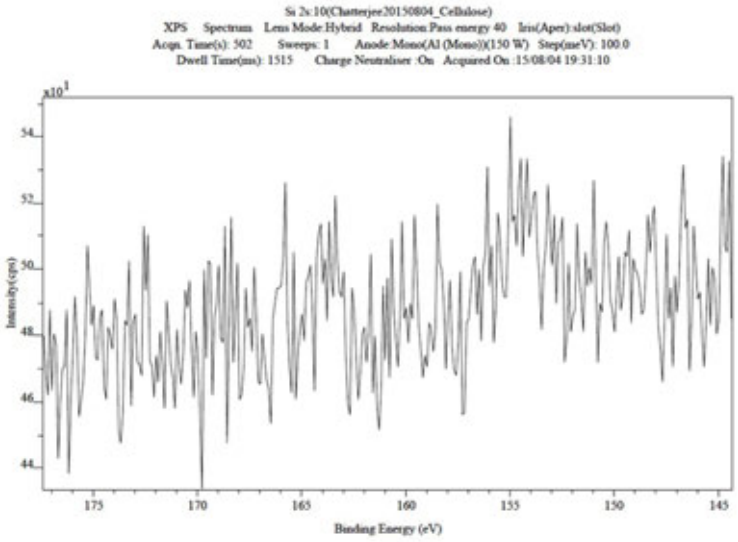

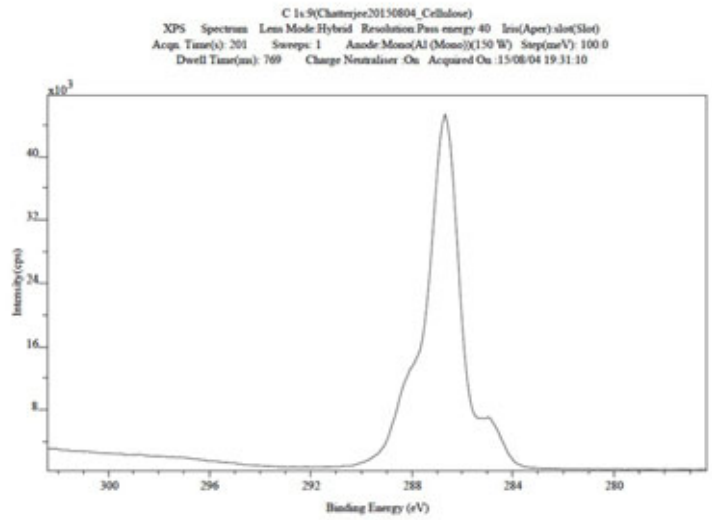

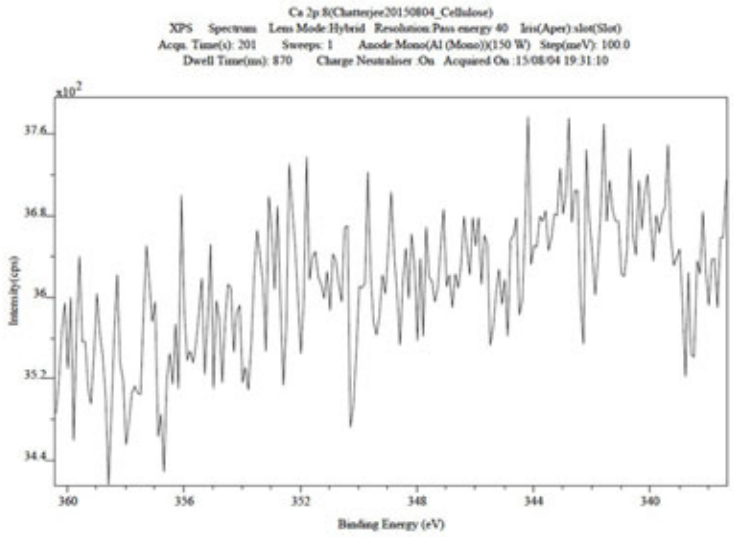
C₆ 2p 8(Chatterjee20150804_Cellulose)
XPS Spectrum Lens Mode:Hybrid Resolution:Pass energy 40 Iris(Aper):slot(Slot)
Acqn. Time(s): 201 Sweeps: 1 Anode:Mono(Al (Mono))(150 W) Step(meV): 100.0
Dwell Time(ms): 870 Charge Neutraliser :On Acquired On :15/08/04 19:31:10
x10^2
37.6
36.8
36
35.2
34.4
Intensity(cps)
360
356
352
348
344
340
Binding Energy (eV)

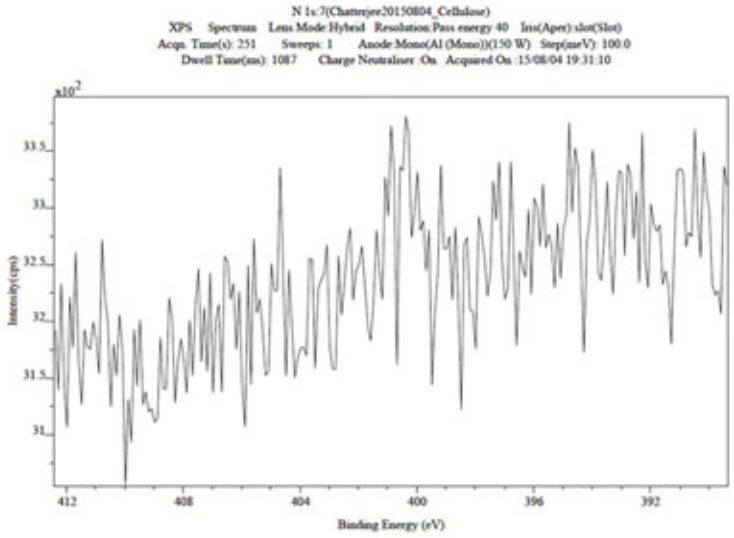
N 1s 7(Chatterjee20150804_Cellulose)
XPS Spectrum Lens Mode:Hybrid Resolution:Pass energy 40 Iris(Aper):slot(Slot)
Acqn. Time(s): 251 Sweeps: 1 Anode:Mono(Al (Mono))(150 W) Step(meV): 100.0
Dwell Time(ms): 1087 Charge Neutraliser :On Acquired On :15/08/04 19:31:10
x10^2
33.5
33
32.5
32
31.5
31
Intensity(cps)
412
408
404
400
396
392
Binding Energy (eV)

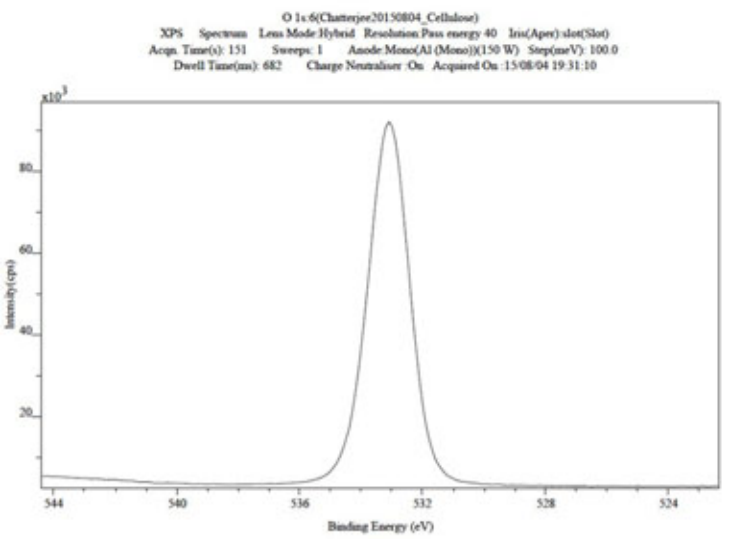
O 1s 6(Chatterjee20150804_Cellulose)
XPS Spectrum Lens Mode:Hybrid Resolution:Pass energy 40 Iris(Aper):slot(Slot)
Acqn. Time(s): 151 Sweeps: 1 Anode:Mono(Al (Mono))(150 W) Step(meV): 100.0
Dwell Time(ms): 682 Charge Neutraliser :On Acquired On :15/08/04 19:31:10
x10^3
80
60
40
20
Intensity(cps)
544
540
536
532
528
524
Binding Energy (eV)

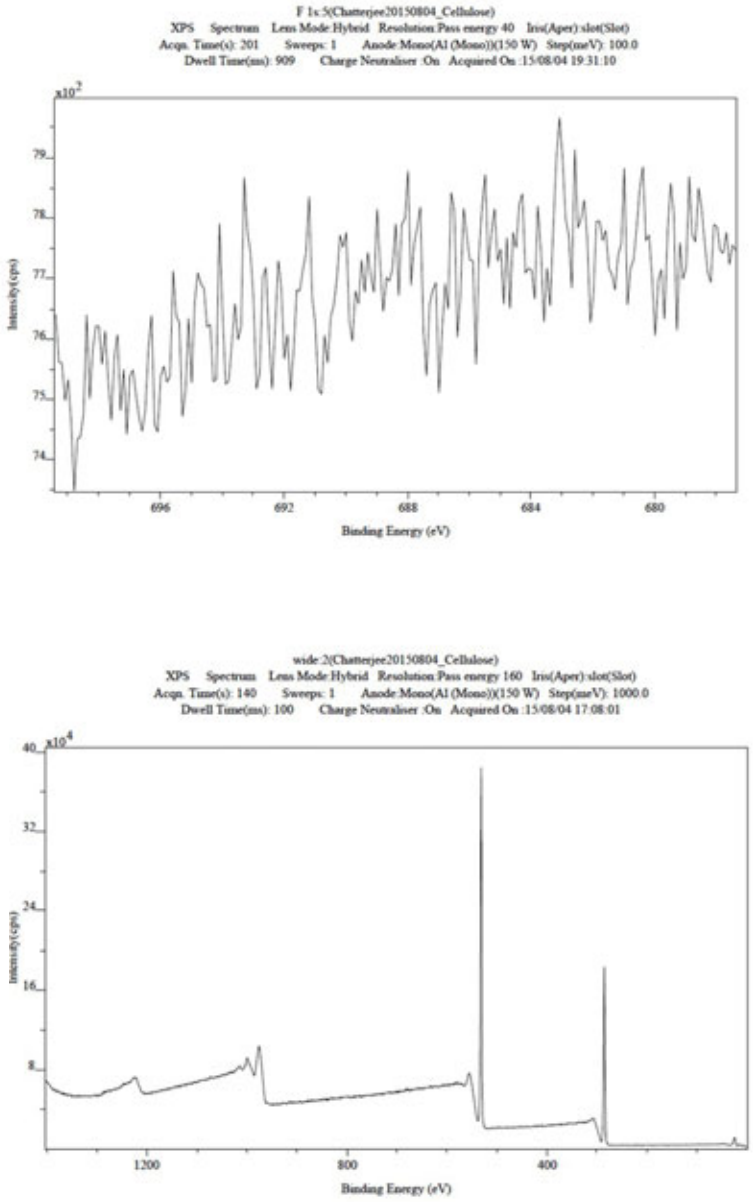

Figure S14: XPS analysis of cellulose.

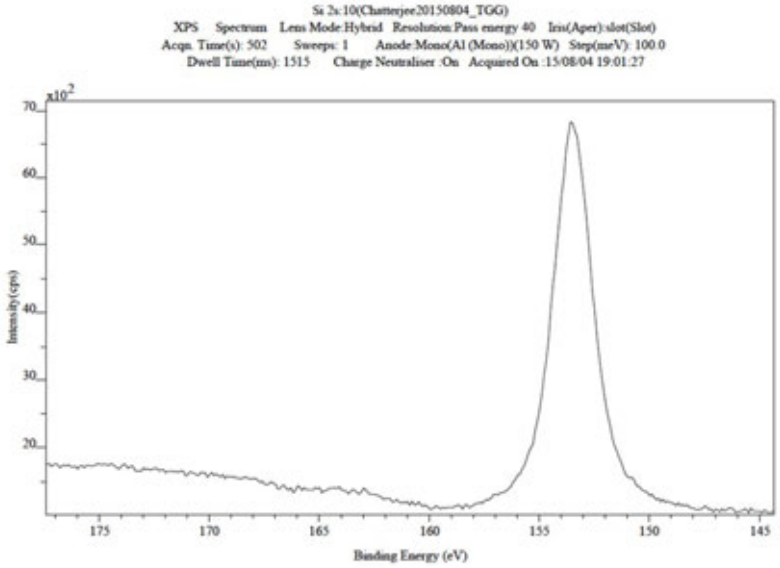
Si 2s:10(Chatterjee20150804_TGG)
XPS Spectrum Lens Mode:Hybrid Resolution:Pass energy 40 Iris(Aper):slot(Slot)
Acqn. Time(s): 502 Sweeps: 1 Anode:Mono(Al (Mono))(150 W) Step(meV): 100.0
Dwell Time(ms): 1515 Charge Neutraliser :On Acquired On :15/08/04 19:01:27
x10^2
Intensity(cps)
Binding Energy (eV)

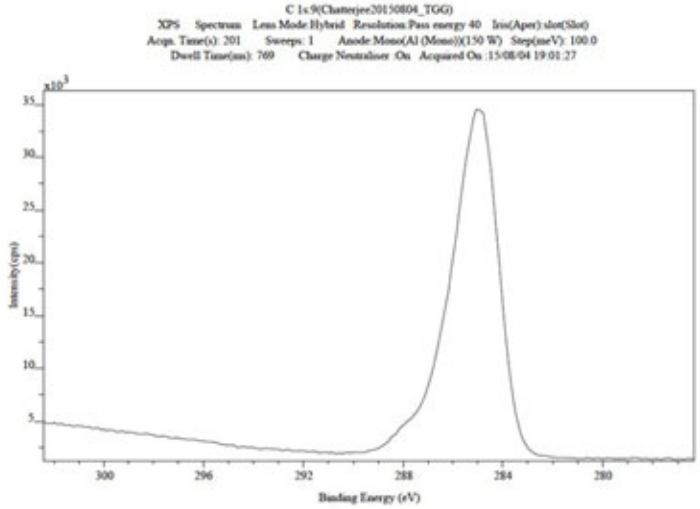
C 1s:9(Chatterjee20150804_TGG)
XPS Spectrum Lens Mode:Hybrid Resolution:Pass energy 40 Iris(Aper):slot(Slot)
Acqn. Time(s): 201 Sweeps: 1 Anode:Mono(Al (Mono))(150 W) Step(meV): 100.0
Dwell Time(ms): 769 Charge Neutraliser :On Acquired On :15/08/04 19:01:27
x10^3
Intensity(cps)
Binding Energy (eV)

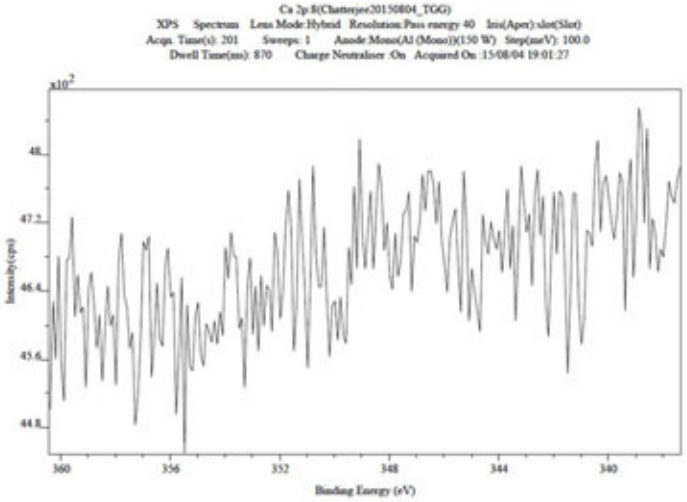
Ca 2p:8(Chatterjee20150804_TGG)
XPS Spectrum Lens Mode:Hybrid Resolution:Pass energy 40 Iris(Aper):slot(Slot)
Acqn. Time(s): 201 Sweeps: 1 Anode:Mono(Al (Mono))(150 W) Step(meV): 100.0
Dwell Time(ms): 870 Charge Neutraliser :On Acquired On :15/08/04 19:01:27
x10^2
Intensity(cps)
Binding Energy (eV)

N 1s:7(Chatterjee20150804_TGG)
XPS Spectrum Lens Mode:Hybrid Resolution:Pass energy 40 Iris(Aper):slot(Slot)
Acqn. Time(s): 251 Sweeps: 1 Anode:Mono(Al (Mono))(150 W) Step(meV): 100.0
Dwell Time(ms): 1087 Charge Neutraliser :On Acquired On :15/08/04 19:01:27

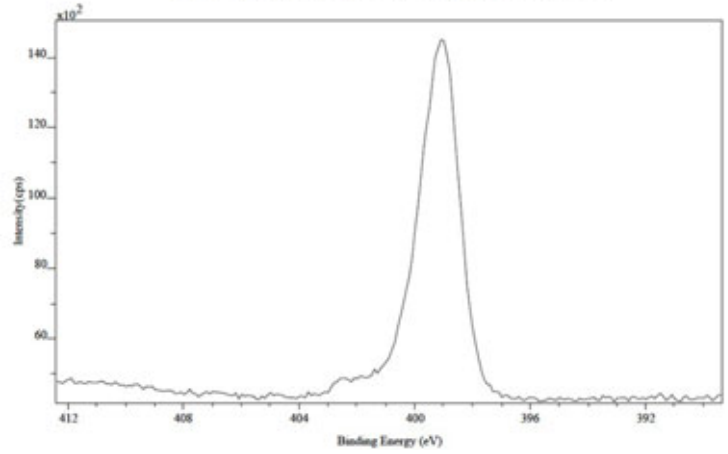

O 1s:6(Chatterjee20150804_TGG)
XPS Spectrum Lens Mode:Hybrid Resolution:Pass energy 40 Iris(Aper):slot(Slot)
Acqn. Time(s): 151 Sweeps: 1 Anode:Mono(Al (Mono))(150 W) Step(meV): 100.0
Dwell Time(ms): 682 Charge Neutraliser :On Acquired On :15/08/04 19:01:27

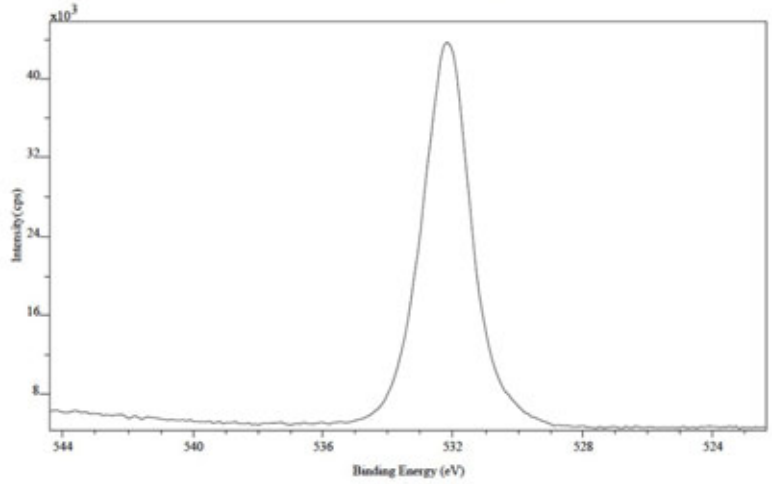

F 1s:5(Chatterjee20150804_TGG)
XPS Spectrum Lens Mode:Hybrid Resolution:Pass energy 40 Iris(Aper):slot(Slot)
Acqn. Time(s): 201 Sweeps: 1 Anode:Mono(Al (Mono))(150 W) Step(meV): 100.0
Dwell Time(ms): 909 Charge Neutraliser :On Acquired On :15/08/04 19:01:27

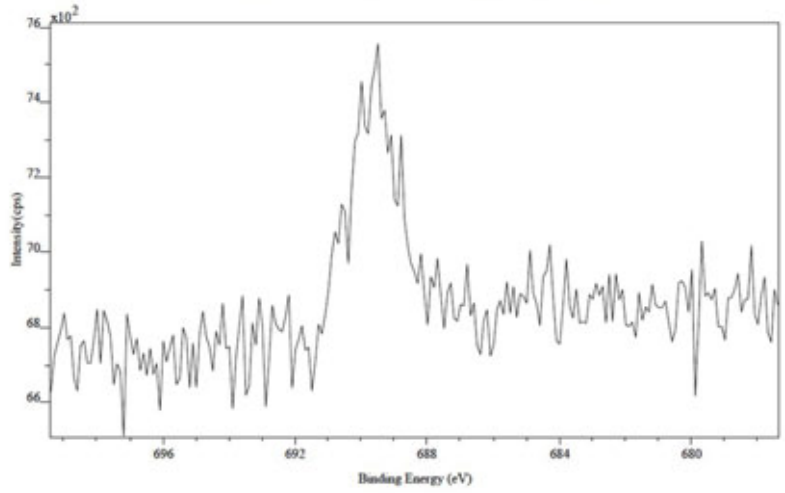

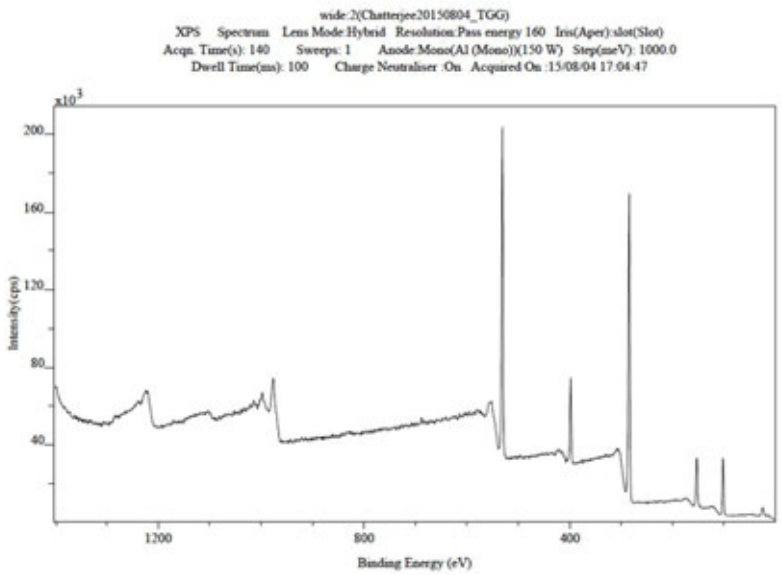

Figure S15: XPS analysis of glutaraldehyde functionalized cellulose.

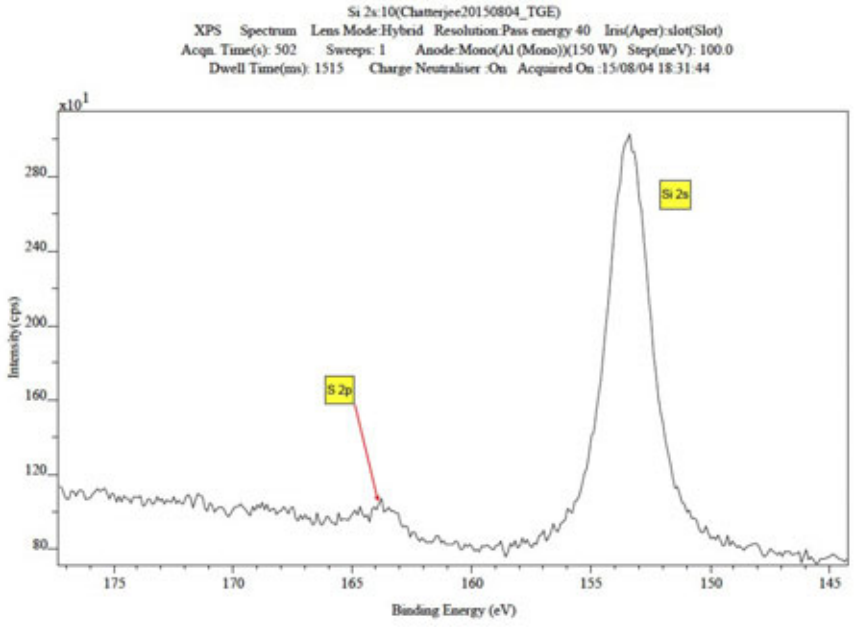

C 1s:9(Chatterjee20150804_TGE)
XPS Spectrum Lens Mode:Hybrid Resolution:Pass energy 40 Iris(Aper):slot(Slot)
Acqn. Time(s): 201 Sweeps: 1 Anode:Mono(Al (Mono))(150 W) Step(meV): 100.0
Dwell Time(ms): 769 Charge Neutraliser :On Acquired On :15/08/04 18:31:44

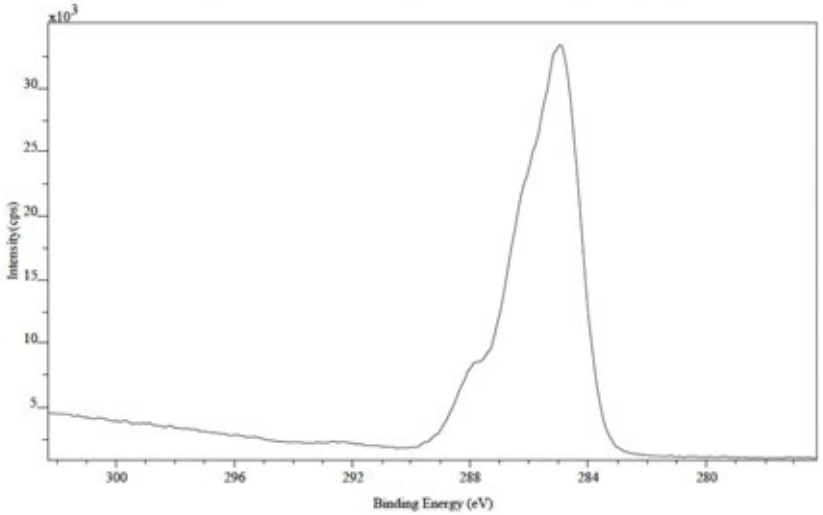

Ca 2p:8(Chatterjee20150804_TGE)
XPS Spectrum Lens Mode:Hybrid Resolution:Pass energy 40 Iris(Aper):slot(Slot)
Acqn. Time(s): 201 Sweeps: 1 Anode:Mono(Al (Mono))(150 W) Step(meV): 100.0
Dwell Time(ms): 870 Charge Neutraliser :On Acquired On :15/08/04 18:31:44

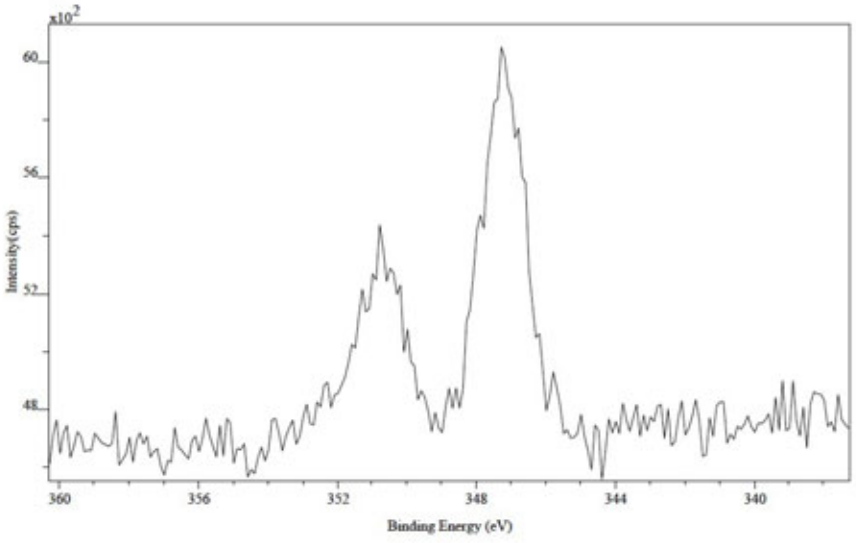

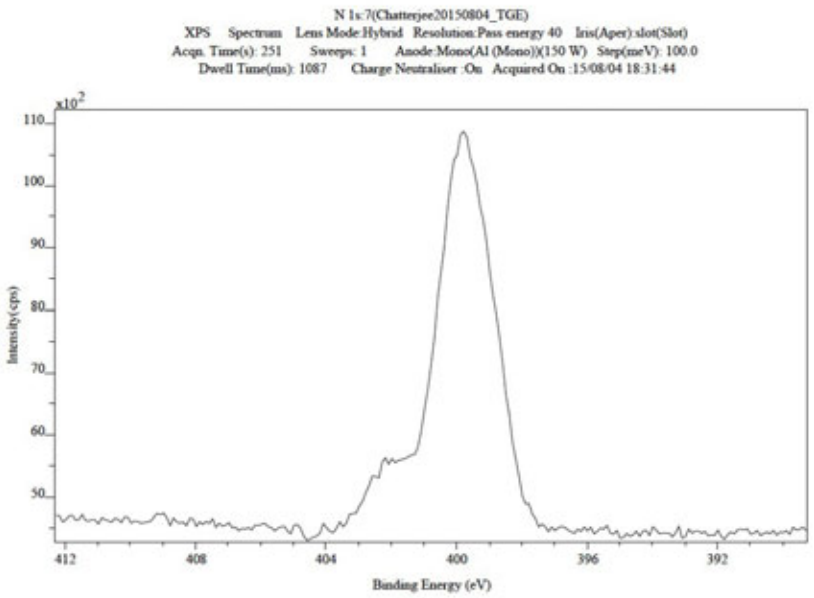
N 1s:7(Chatterjee20150804_TGE)
XPS Spectrum Lens Mode:Hybrid Resolution:Pass energy 40 Iris(Aper):slot(Slot)
Acqn. Time(s): 251 Sweeps: 1 Anode:Mono(Al (Mono))(150 W) Step(meV): 100.0
Dwell Time(ms): 1087 Charge Neutraliser :On Acquired On :15/08/04 18:31:44
x10^2
110
100
90
80
70
60
50
Intensity(cps)
412
408
404
400
396
392
Binding Energy (eV)

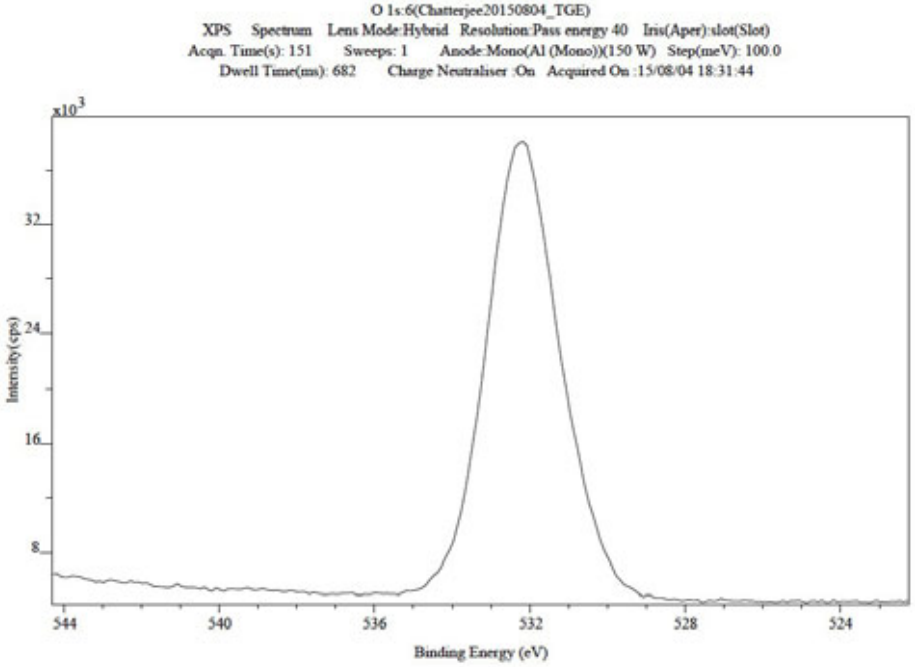
O 1s:6(Chatterjee20150804_TGE)
XPS Spectrum Lens Mode:Hybrid Resolution:Pass energy 40 Iris(Aper):slot(Slot)
Acqn. Time(s): 151 Sweeps: 1 Anode:Mono(Al (Mono))(150 W) Step(meV): 100.0
Dwell Time(ms): 682 Charge Neutraliser :On Acquired On :15/08/04 18:31:44
x10^3
32
24
16
8
Intensity(cps)
544
540
536
532
528
524
Binding Energy (eV)

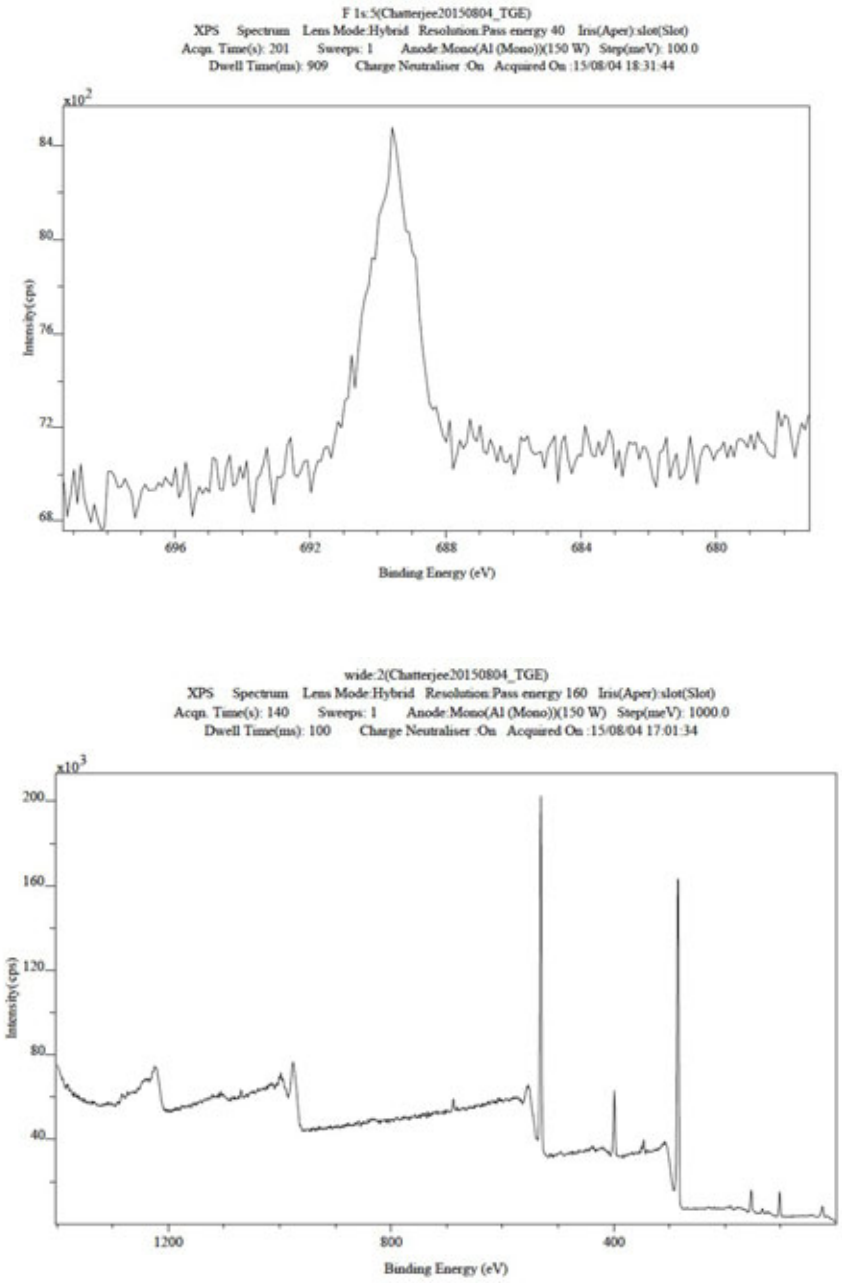

Figure S16: XPS analysis of Cal-B immobilized on functionalized cellulose.

5. **Thermogravimetric analysis**.

The TG curves were obtained in a thermogravimetric module, coupled in a thermal analyzer, both manufactured by Netzsch®. Thermogravimetric measurements were performed using a platinum sample holder containing about 10 mg of each immobilized enzyme. Each sample was heated from 35 to 600 °C at 10 °C min^{-1}, under atmosphere of synthetic air and N_2, both with a flow rate of 60 mL min^{-1}.

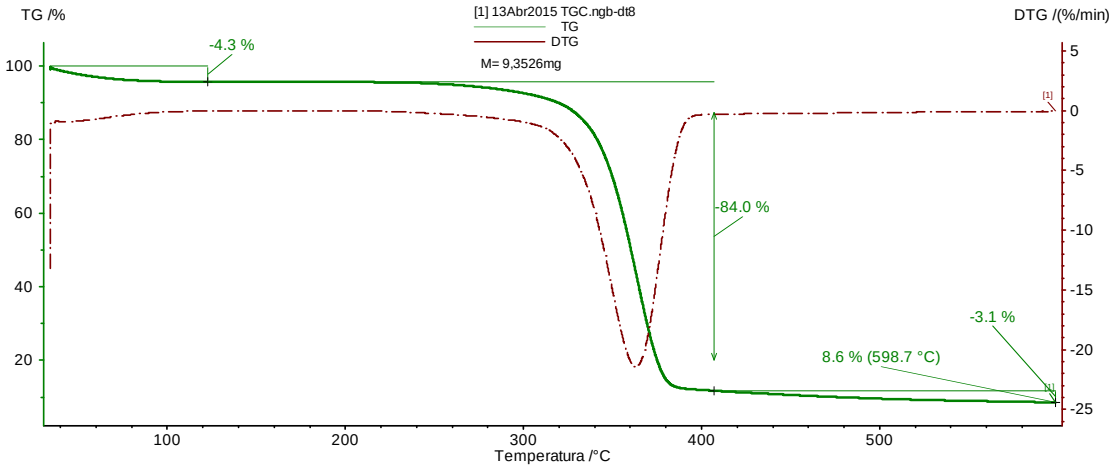

Figure S17: TG spectra of celullose.

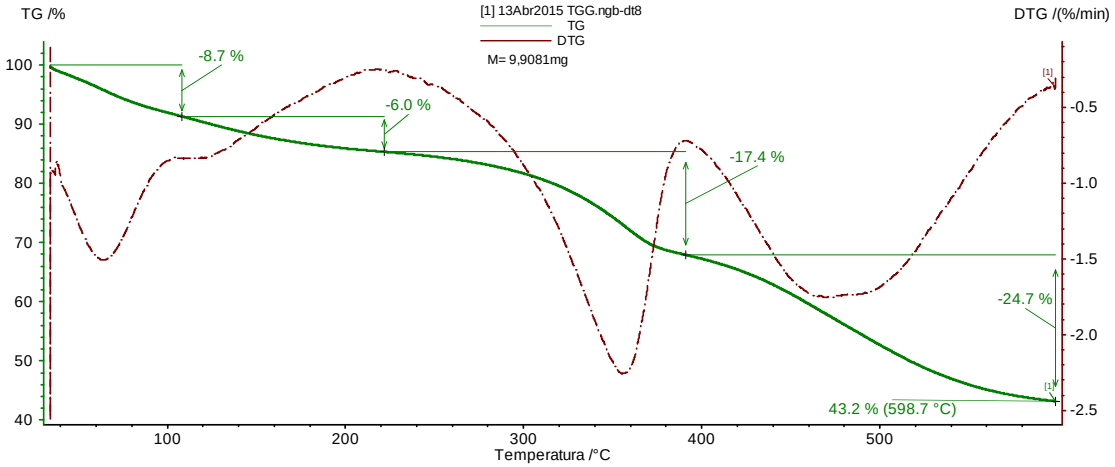

Figure S18: TG spectra of glutaraldehyde functionalized celullose.

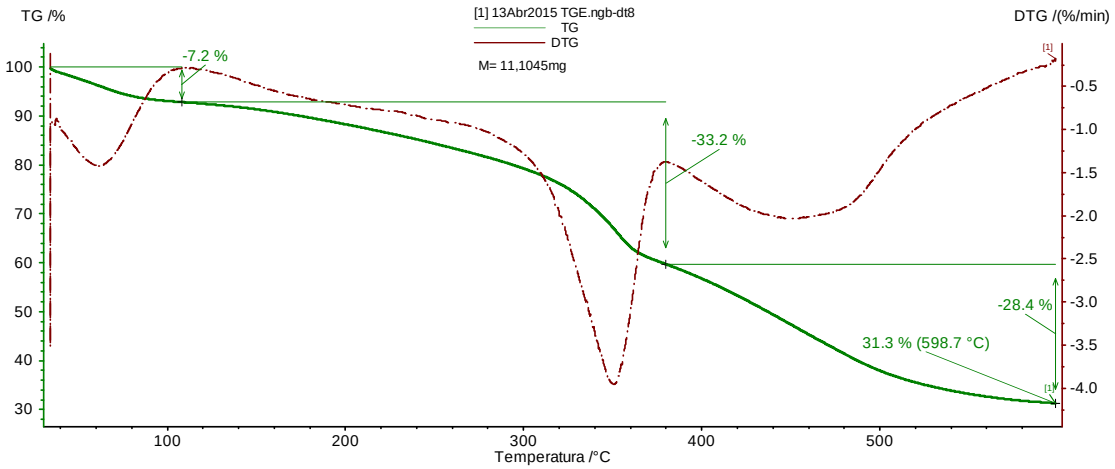

Figure S19: TG spectra of Cal-B immobilized on glutaraldehyde-functionalized cellulose.

6. **Esterification reactions**.

The immobilized lipase (10 mg support in 1 mL reaction media) was evaluated in an esterification reaction between oleic acid and ethanol (1 : 1 – 100 mM in *n*-heptane) at different temperatures. The reactions were performed in cryotubes under 200 rpm of agitation on a shaker. Samples (10 μL) were collected after 1 h. For calculation of the initial reaction velocity, reaction times were varied from 5, 10, 15, 20, and 30 min. For thermal stability, reaction were investigated at 50–70 °C. All quantifications were done by GC-MS analysis.

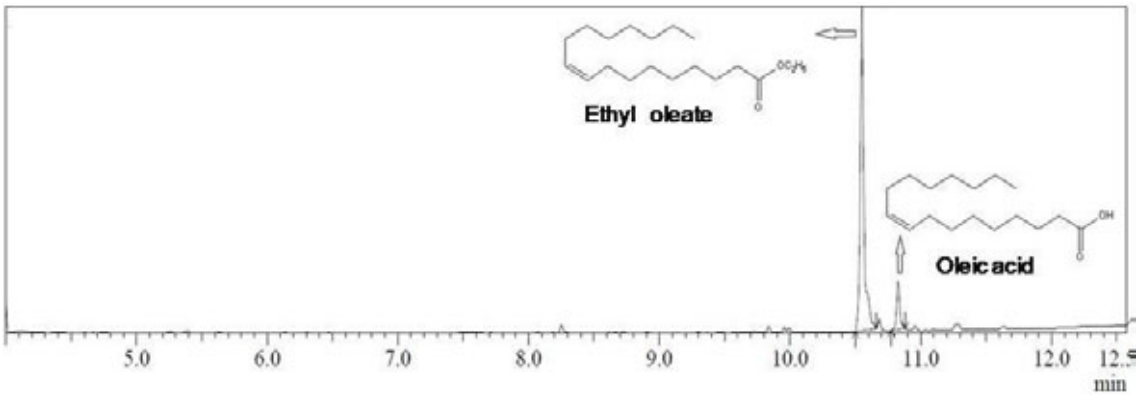

Figure S20: Esterification actitivty of immobilized Cal-B. Experimental conditions: 10 mg support in 1 mL oleic acid and ethanol (1:1 – 100mM in *n*-heptane) at 60 °C.

7. Kinetic resolution using immobilized lipase.

rac-1-Phenylethanol (1 mmol, 122 mg), vinyl acetate (1 mol. eq.) as acyl donor, and 18 mg (15% w/w) of the corresponding immobilized enzyme were reacted in cyclohexane (3 mL) for 2 h, 4 h, and 5 h at 60 °C. Enantiomeric excess values (ee) were determined by chiral GC analysis (chiral column Betadex-325).

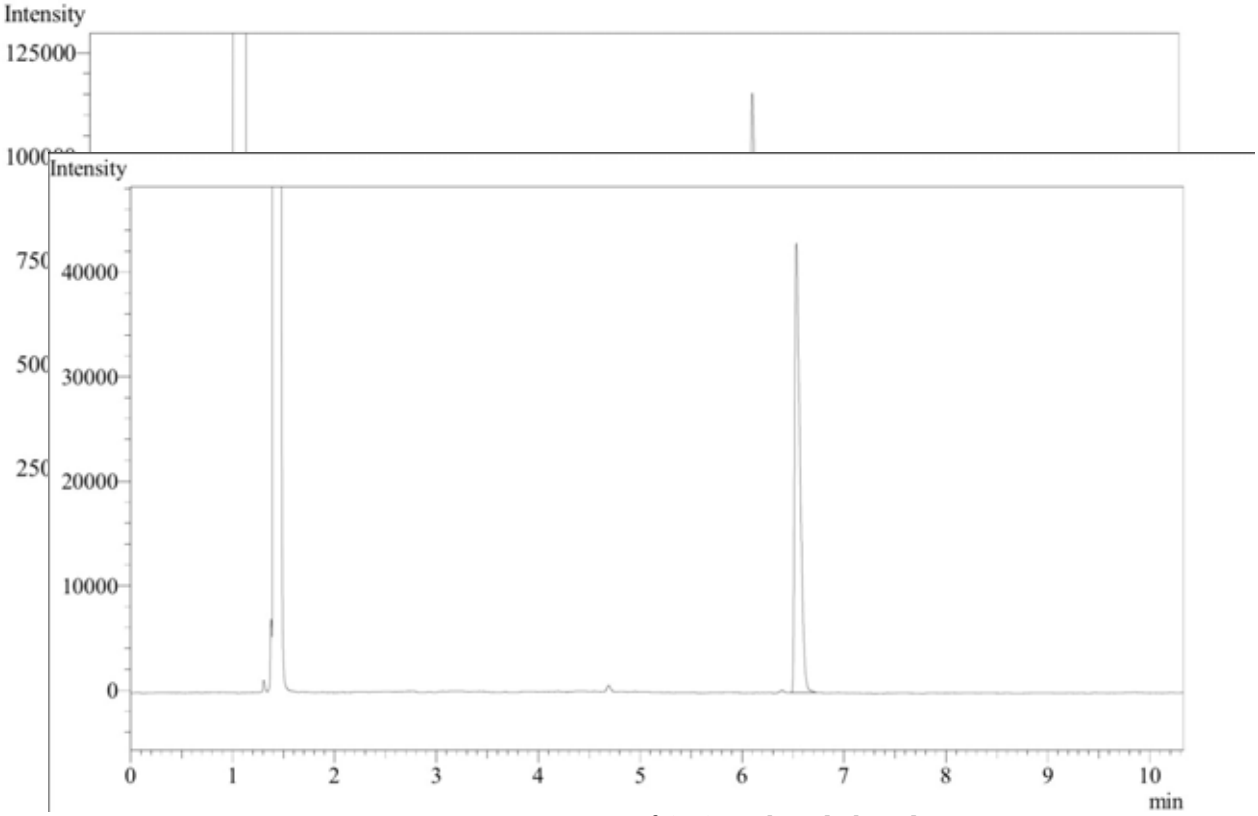

Figure S21. GC-FID of (*RS*)-1-Phenylethanol.

Figure S22: (*S*)-1-Phenylethanol.

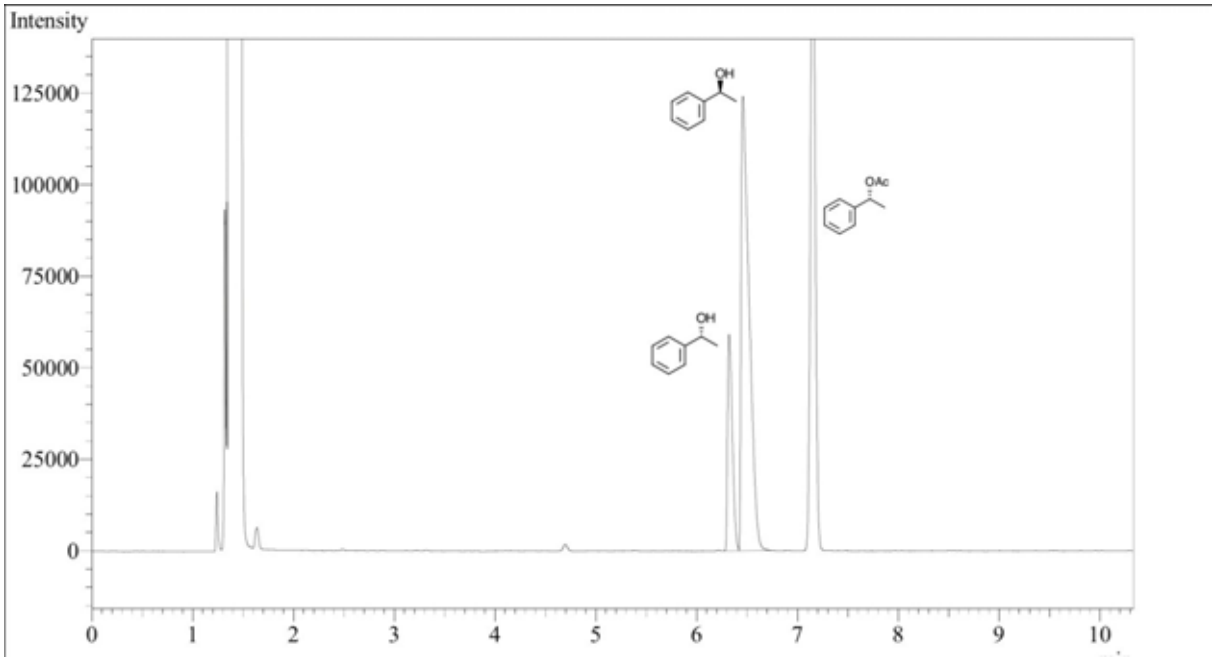

Figure S23: Kinetic resolution of (*R*,*S*)-1-Phenylethanol mediated by Novozyme 435.

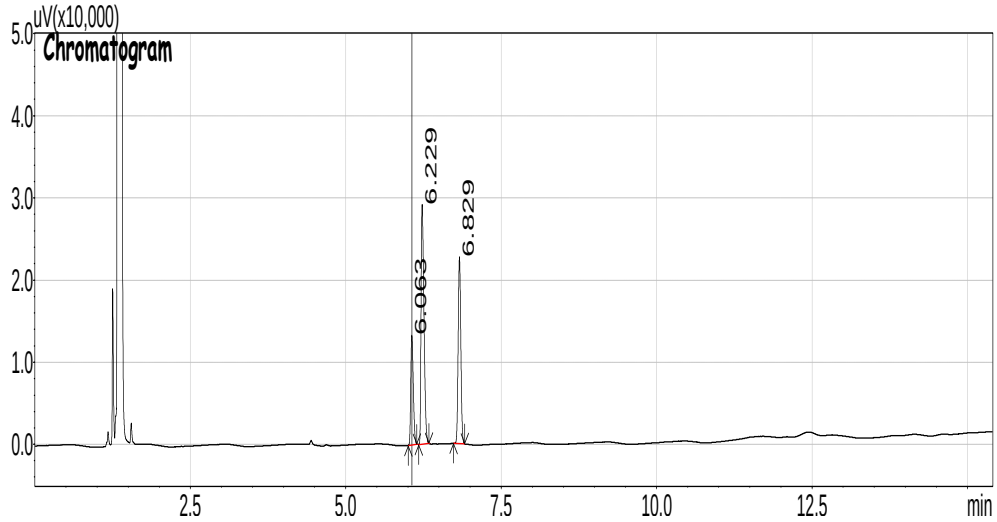

Figure S24. Kinetic resolution of (*R*,*S*)-1-Phenylethanol mediated by immobilized lipase after 2 h.

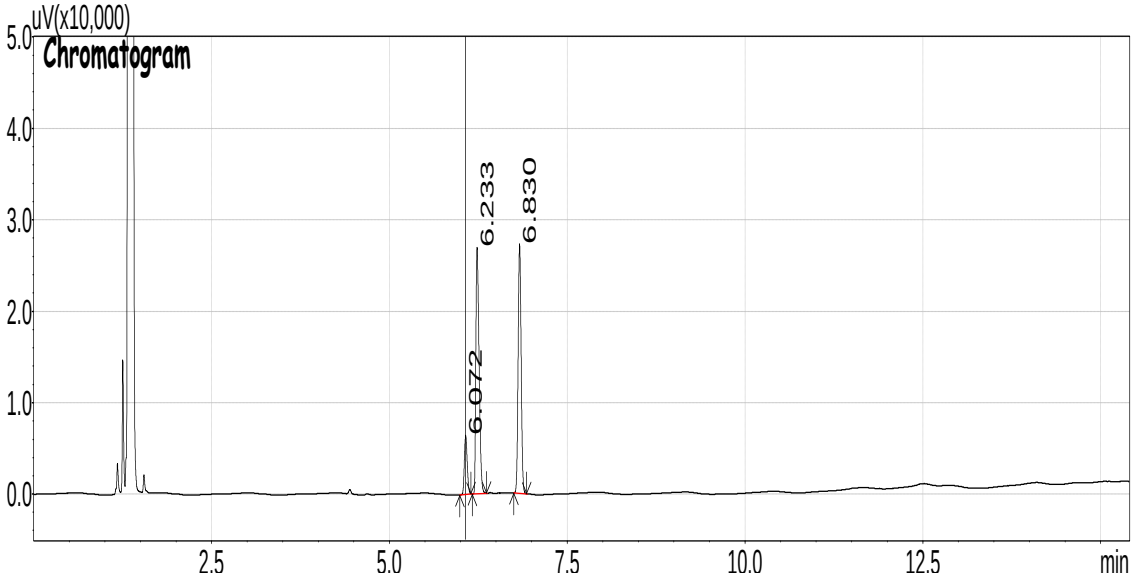

Figure S25. Kinetic resolution of (*R*,*S*)-1-Phenylethanol mediated by immobilized lipase after 4 h

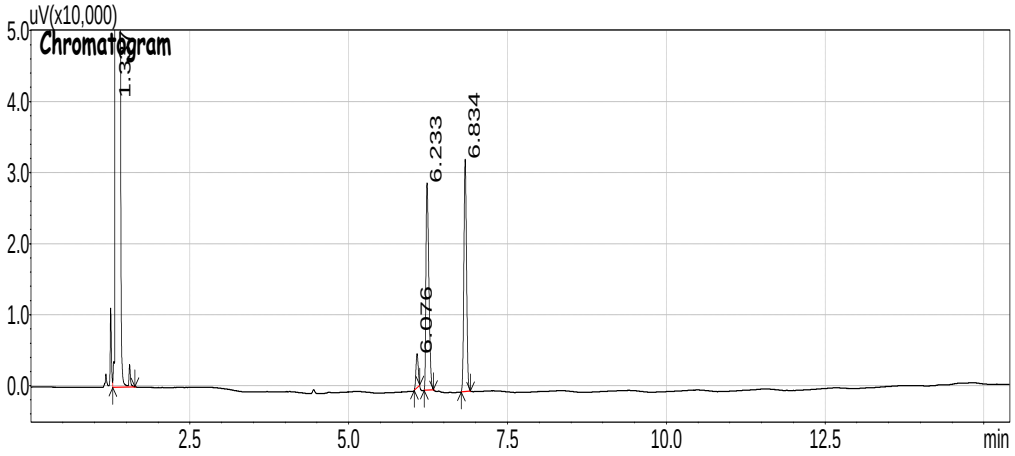

Figure S26. Kinetic resolution of (*R*,*S*)-1-Phenylethanol mediated by immobilized lipase after 5 h

8. Solid state C^{13} NMR analysis

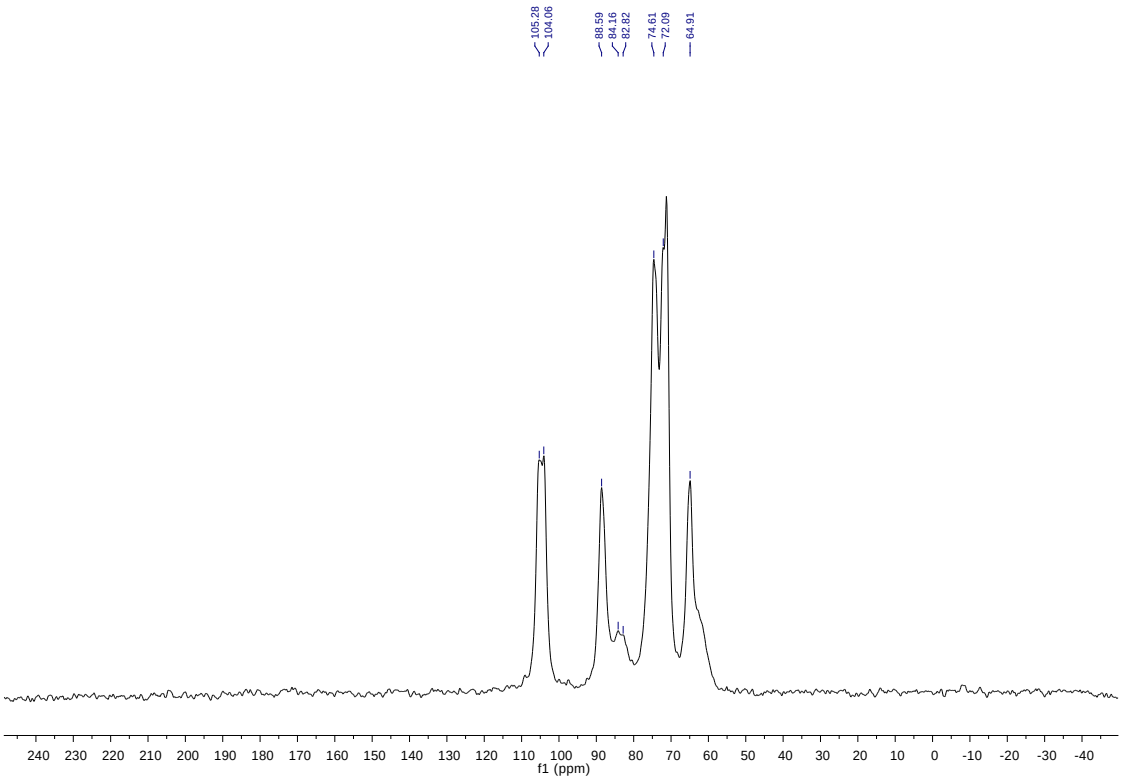

Figure S27: ^{13}C-NMR spectra of celullose.

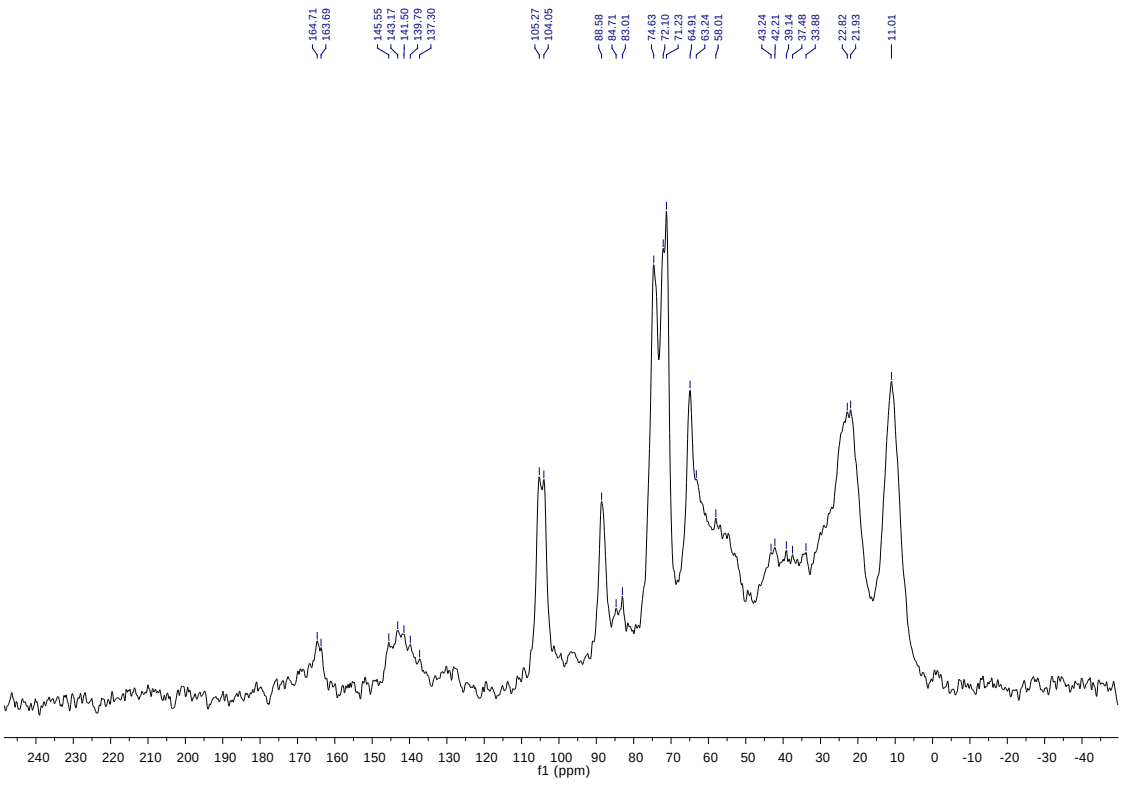

Figure S28: ^{13}C-NMR spectra of glutaraldehyde functionalized celullose.

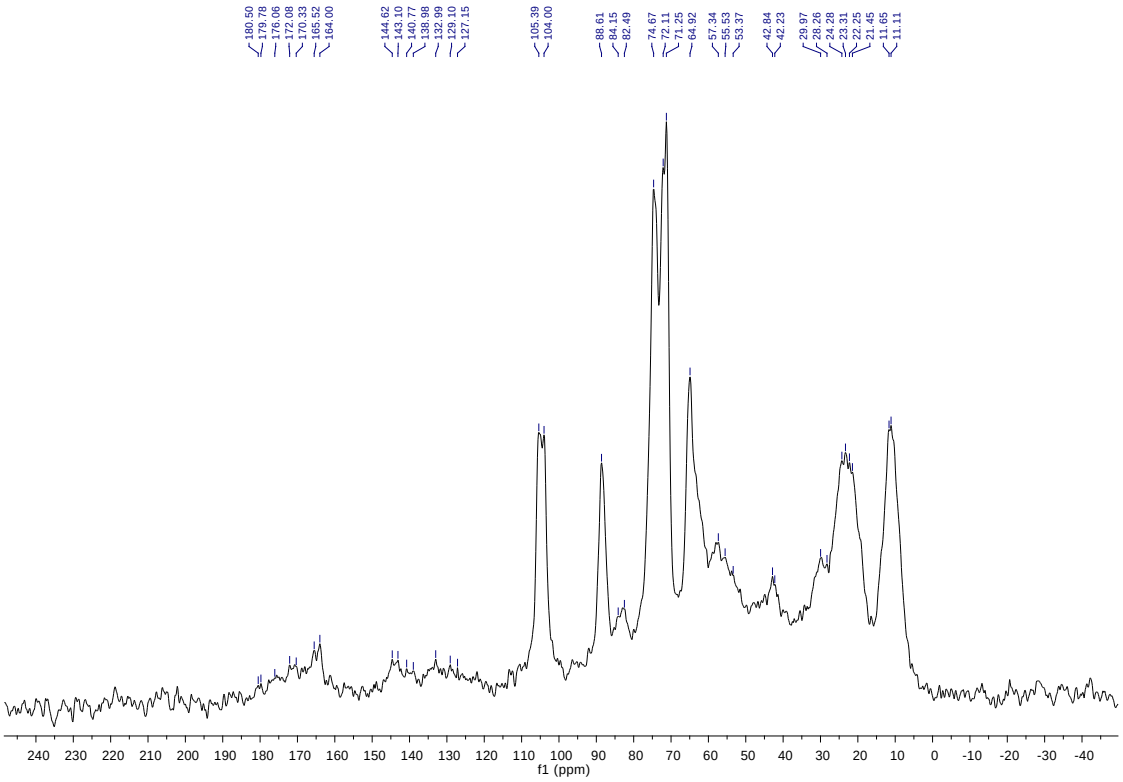

Figure S29: ^{13}C-NMR spectra of cellulose functionalized with Cal-B lipase.